Humboldt-Universität zu Berlin
Mathematisch-Naturwissenschaftliche Fakultät
Institut für Mathematik

Adaptive least-squares finite element method with optimal convergence rates

Dissertation

zur Erlangung des akademischen Grades
doctor rerum naturalium (Dr. rer. nat.)
im Fach Mathematik

eingereicht an der
Mathematisch-Naturwissenschaftlichen Fakultät
der Humboldt-Universität zu Berlin

von

M. Sc. Philipp Bringmann

Präsidentin der Humboldt-Universität zu Berlin
Prof. Dr.-Ing. Dr. Sabine Kunst

Dekan der Mathematisch-Naturwissenschaftlichen Fakultät
Prof. Dr. Elmar Kulke

Gutachter
1. Prof. Dr. Carsten Carstensen (Humboldt-Universität zu Berlin)
2. Prof. Dr. Eun-Jae Park (Yonsei University)
3. Prof. Dr. Gerhard Starke (Universität Duisburg-Essen)

Tag der mündlichen Prüfung
31. Januar 2020

Abstract

For the numerical solution of partial differential equations (PDEs) in computational fluid dynamics, solid mechanics, and various other areas of application, the least-squares finite element methods (LSFEMs) enjoy an unabated popularity. These methods base on the minimisation of the least-squares functional consisting of the squared norms of the residuals of first-order systems of PDEs. The local evaluation of the least-squares functional provides a reliable and efficient built-in a posteriori error estimator and allows for adaptive mesh-refinement.

While numerical experiments exhibit optimal convergence rates, even the proof of the plain convergence of these adaptive algorithms is not immediate. The established convergence analysis, as summarised in the axiomatic framework by Carstensen, Feischl, Page, and Praetorius (*Comp. Math. Appl.*, 67(6):1195–1253, 2014), fails for two reasons. First, the least-squares estimator lacks prefactors in terms of the mesh-size, what seemingly prevents a reduction under adaptive mesh-refinement. Second, the first-order divergence LSFEMs measure the flux or stress errors in the $H(\mathrm{div})$ norm and, thus, involve a data resolution error of the right-hand side f without a mesh-size factor. These difficulties led to a two-fold paradigm shift in the convergence analysis with rates for adaptive LSFEMs in Carstensen and Park (*SIAM J. Numer. Anal.*, 53(1):43–62, 2015) for the lowest-order discretisation of the 2D Poisson model problem with homogeneous Dirichlet boundary conditions. Accordingly, some novel explicit residual-based a posteriori error estimator accomplishes the reduction property. Furthermore, a separate marking strategy in the adaptive algorithm ensures the sufficient data resolution.

This thesis presents the generalisation of these techniques to three linear model problems, namely, the Poisson problem, the Stokes equations, and the linear elasticity problem. It verifies the axioms of adaptivity with separate marking by Carstensen and Rabus (*SIAM J. Numer. Anal.*, 55(6):2644–2665, 2017) in three spatial dimensions. The analysis covers discretisations with arbitrary polynomial degree and inhomogeneous Dirichlet and Neumann boundary conditions. Numerical experiments confirm the theoretically proven optimal convergence rates of the h-adaptive algorithm.

Zusammenfassung

Die Popularität der Least-Squares-Finiten-Elemente-Methoden (LSFEMn) zur numerischen Lösung von partiellen Differentialgleichungen in der Strömungs- und Festkörpermechanik und anderen Anwendungsgebieten ist ungebrochen. Diese Methoden basieren auf der Minimierung des Least-Squares-Funktionals, das aus den quadrierten Normen der Residuen eines Systems von partiellen Differentialgleichungen erster Ordnung besteht. Die lokale Auswertung des Least-Squares-Funktionals liefert einen zuverlässigen und effizienten Fehlerschätzer und ermöglicht die adaptive Verfeinerung des der Diskretisierung zugrundeliegenden Netzes.

Obwohl numerische Experimente für solche adaptiven Algorithmen optimale Konvergenzraten zeigen, ist bereits der theoretische Nachweis der einfachen Konvergenz nicht offensichtlich. Aus zwei Gründen versagen zudem die gängigen Methoden zum Beweis optimaler Konvergenzraten, wie sie von Carstensen, Feischl, Page und Praetorius (*Comp. Math. Appl.*, 67(6):1195–1253, 2014) axiomatisch beschrieben wurden. Zum einen fehlen den Termen des eingebauten Least-Squares-Schätzers Vorfaktoren proportional zur Netzweite. Das scheint den Beweis einer schrittweisen Reduktion der Schätzerterme zu verhindern. Zum zweiten kontrolliert das Least-Squares-Funktional den Fehler der Fluss- beziehungsweise Spannungsvariablen in der $H(\mathrm{div})$-Norm, wodurch ein Datenapproximationsfehler der rechten Seite f auftritt. Diese Schwierigkeiten führten zu einem zweifachen Paradigmenwechsel in der Analysis von Konvergenzraten adaptiver LSFEMn in Carstensen und Park (*SIAM J. Numer. Anal.*, 53(1):43–62, 2015) für das zweidimensionale Poisson-Modellproblem mit Diskretisierung niedrigster Ordnung und homogenen Dirichlet-Randdaten. Demnach erlaubt ein expliziter residuenbasierter a posteriori Fehlerschätzer den Beweis der Reduktionseigenschaft. Außerdem wird der Datenapproximationsfehler durch separiertes Markieren im adaptiven Algorithmus reduziert.

Die vorliegende Arbeit verallgemeinert diese Techniken auf die drei linearen Modellprobleme das Poisson-Problem, die Stokes-Gleichungen und das lineare Elastizitätsproblem. Die Axiome der Adaptivität mit separiertem Markieren nach Carstensen und Rabus (*SIAM J. Numer. Anal.*, 55(6):2644–2665, 2017) werden in drei Raumdimensionen nachgewiesen. Die Analysis umfasst Diskretisierungen mit beliebigem Polynomgrad sowie inhomogene Dirichlet- und Neumann-Randbedingungen. Abschließend bestätigen numerische Experimente mit dem h-adaptiven Algorithmus die theoretisch bewiesenen optimalen Konvergenzraten.

Contents

1 Introduction

Motivation. In the previous decades, the finite element method (FEM) has become a standard tool for the solution of problems in fluid and structural mechanics. Numerical simulations often form the basis for design processes in various engineering disciplines. A reliable and efficient a posteriori error estimation allows not only for a justification of the computed approximation, but also for an adaptive refinement of the underlying meshes. Adaptive mesh-refinement algorithms have been investigated since the late 1970s and some pioneering contributions include [6, 5, 105, 107]. It took about twenty years to present the first convergence proofs of adaptive FEMs [59, 84]. Eventually, the theory of nonlinear approximation paved the way to the verification of optimal convergence rates for adaptive algorithms [14, 100]. Suitable explicit residual-based a posteriori error estimators drive the local refinement and generate quasi-optimal meshes. This means, the error on the corresponding adaptive meshes differs from the error on the theoretically optimal meshes solely by a generic multiplicative constant. Figure 1.1 illustrates the relation between the optimal meshes and the adaptively computed meshes with respect to a given amount of computational effort (in terms of the number of degrees of freedom ndof).

Due to its built-in a posteriori error estimator, the least-squares finite element method (LSFEM) is a convenient choice for adaptive algorithms [12, 97, 1]. This versatile discretisation method dates back to the early 70's [21, 20] and, since then, has been established for a multitude of partial differential equations (PDEs) [17]. A naive least-squares approach minimises the squared residual of a second-order elliptic PDE. For the discretisation, this requires H^2 conforming finite elements. Therefore, the equation is usually reformulated as a first-order system of PDEs enabling the application of standard lowest-order finite elements [80, 71, 89]. The built-in estimator turned out to provide guaranteed upper error bounds and is even asymptotically exact in that the quotient of the estimator and the error converges to one [47, 103].

This thesis presents a unified convergence analysis with rates for the least-squares formulation of a generalised model problem including the author's preceding collaborative publications [26, 25, 27]. All of these publications are based on the breakthrough in [44]. The analysis at hand employs the axiomatic framework from [37, 40]. It covers conforming discretisations with arbitrary polynomial degree in an h-adaptive algorithm and includes inhomogeneous Dirichlet and Neumann boundary conditions in three spatial dimensions. While the two-dimensional case is not explicitly presented in this thesis, the publication [25] establishes optimal convergence rates for the adaptive LSFEM for the 2D Stokes equations. The author conjectures that the results in this thesis transfer to the remaining two model problems in 2D as well.

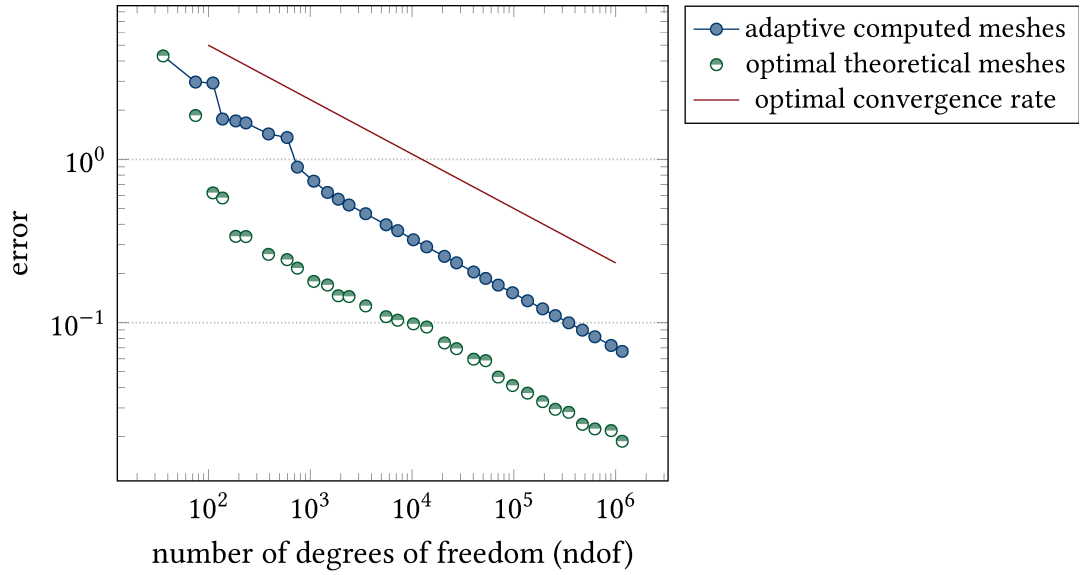

Figure 1.1: Visualisation of the errors of an adaptive algorithm and the optimal meshes. The optimal meshes provide the minimal error that can be achieved on a mesh with the given number of degrees of freedom (ndof). Both errors attain the optimal convergence rate indicated by the straight line.

Problem formulation. This thesis considers a generalised model problem on a polyhedral Lipschitz domain $\Omega \subset \mathbb{R}^3$ in three spatial dimensions, the boundary $\partial\Omega$ is locally the graph of a Lipschitz function. Some additional regularity assumptions on the boundary will be discussed below in Section 2.3. The boundary $\partial\Omega$ is subdivided into the compact Dirichlet boundary $\Gamma_D \subseteq \partial\Omega$ with positive surface measure $|\Gamma_D| > 0$ and the relatively open (possibly empty) Neumann boundary $\Gamma_N := \partial\Omega \setminus \Gamma_D$. Let $\nu : \partial\Omega \to \mathbb{R}^3$ denote the outward unit normal vector. Given a right-hand side $f : \Omega \to \mathbb{R}^3$ and the boundary data $u_D : \Gamma_D \to \mathbb{R}^3$ and $t_N : \Gamma_N \to \mathbb{R}^3$, the generalised model problem seeks $\sigma : \Omega \to \mathbb{R}^{3\times3}$ and $u : \Omega \to \mathbb{R}^3$ such that

$$\begin{aligned} f + \operatorname{div}\sigma = 0 \quad \text{and} \quad \mathcal{A}\sigma - \mathcal{S}\,\mathrm{D}\,u = 0 \quad \text{in } \Omega, \\ u = u_D \quad \text{on } \Gamma_D \quad \text{and} \quad \sigma\nu = t_N \quad \text{on } \Gamma_N. \end{aligned} \tag{1.1}$$

Some appropriate choices of bounded linear operators $\mathcal{A}, \mathcal{S} : \mathbb{R}^{3\times3} \to \mathbb{R}^{3\times3}$ are displayed in Table 1 and enable the simultaneous analysis of some first-order formulations of the Poisson model problem, the Stokes equations, and the linear elasticity problem. The operators $\mathcal{A}, \mathcal{S}$ may depend on $x \in \Omega$ as well and Section 3.1 introduces specific assumptions sufficient for the well-posedness of the resulting least-squares formulation. To obtain a discrete problem, consider a fixed polynomial degree $k \in \mathbb{N}$ and a regular triangulation $\mathcal{T}$ of Ω into closed simplices. The LSFEM minimises the least-squares functional

$$LS(f;\sigma,u) := \|f + \operatorname{div}\sigma\|^2_{L^2(\Omega)} + \|\mathcal{A}\sigma - \mathcal{S}\,\mathrm{D}\,u\|^2_{L^2(\Omega)}$$

$\mathcal{A}$	$\mathcal{S}$	Problem
id	id	Poisson model problem
dev	id	Pseudostress-velocity formulation of the Stokes equations
$\mathbb{C}^{-1}$	sym	Stress-displacement formulation in linear elasticity

Table 1.1: Various choices for the bounded linear operators in the model problem (1.1). The deviatoric part dev of a matrix, the inverted linear material law $\mathbb{C}^{-1}$, and the symmetric part sym of a matrix are defined in Section 3.2 below in (3.6)–(3.7).

in σ and u over $\Sigma^k(\mathcal{T})$ and $U^{k+1}(\mathcal{T})$, some $H(\mathrm{div},\Omega)$ and $H^1(\Omega)$ conforming finite element function spaces (up to boundary conditions).

Adaptive algorithm. The least-squares functional is a reliable and efficient a posteriori error estimator (up to boundary data oscillations). For the discrete solutions σ_{LS} and u_{LS}, the contributions on every simplex $T \in \mathcal{T}$ of the triangulation read

$$LS(f;\sigma_{\mathrm{LS}},u_{\mathrm{LS}};T) := \|f+\operatorname{div}\sigma_{\mathrm{LS}}\|^2_{L^2(T)} + \|\mathcal{A}\sigma - \mathcal{S}\,\mathrm{D}\,u_{\mathrm{LS}}\|^2_{L^2(T)}.$$

These local values can be computed using the local stiffness matrices and the coefficients of the discrete functions σ_{LS} and u_{LS}. Given some bulk parameter $0<\theta\le 1$, the Dörfler marking strategy [59] leads to a subset $\mathcal{M}\subseteq\mathcal{T}$ of (almost) minimal cardinality $|\mathcal{M}|$ with

$$\theta\, LS(f;\sigma_{\mathrm{LS}},u_{\mathrm{LS}}) \le \sum_{T\in\mathcal{M}} LS(f;\sigma_{\mathrm{LS}},u_{\mathrm{LS}};T).$$

Sorting the local values $LS(f;\sigma_{\mathrm{LS}},u_{\mathrm{LS}};T)$ allows for the computation of the subset $\mathcal{M}^*\subseteq\mathcal{T}$ of minimal cardinality, but requires suboptimal $\mathcal{O}(N\log N)$ computational complexity for the number $N=|\mathcal{T}|$ of simplices in the triangulation. An procedure of linear $\mathcal{O}(N)$ complexity from [100, Section 5] provides a subset $\mathcal{M}\subseteq\mathcal{T}$ of almost minimal cardinality with the bound

$$|\mathcal{M}| \le 2\,|\mathcal{M}^*|.$$

The adaptive algorithm for the LSFEM for the Poisson model problem in 2D employing the Dörfler marking for the least-squares functional converges Q-linearly if the bulk parameter θ is *sufficiently large* [45, Theorem 4.1]. This contrasts the established analysis [37, 40] for optimal convergence rates of adaptive algorithms, where a *sufficiently small* bulk parameter is demanded. Indeed, severe difficulties occur in the attempt of applying this analysis to the built-in least-squares estimator, which lacks prefactors in terms of the mesh-size. The alternative a posteriori error estimators proposed in [76, 30] solely control the L^2 norm of σ, but also include a contribution without such a prefactor. Up to the author's best knowledge, there is no way to circumvent the reduction of the mesh-size in the proof of the reduction of the estimator. Therefore,

this thesis introduces a novel reliable and efficient residual-based a posteriori error estimator $\eta(\mathcal{T}, \bullet) : \mathcal{T} \to [0, \infty)$ in Section 3.6. This alternative error estimator suffers the disadvantage that it requires an exact solution of the resulting linear system of the LSFEM.

The Dörfler marking provides a subset $\mathcal{M} \subseteq \mathcal{T}$ of almost minimal cardinality with, for $\eta^2(\mathcal{T}, \mathcal{M}) := \sum_{T \in \mathcal{M}} \eta^2(\mathcal{T}, T)$ and $\eta^2(\mathcal{T}) := \eta^2(\mathcal{T}, \mathcal{T})$,

$$\theta \eta^2(\mathcal{T}) \leq \eta^2(\mathcal{T}, \mathcal{M}).$$

The newest-vertex bisection (NVB) from [81, 104, 101] prevails in rate-optimal adaptive algorithms [14, 100, 37, 40]. It generates the smallest regular refinement $\widehat{\mathcal{T}}$ of $\mathcal{T}$ such that the simplices in $\mathcal{M} \subseteq \mathcal{T} \setminus \widehat{\mathcal{T}}$ are refined. For a detailed presentation of this refinement strategy, the reader is referred to Section 2.4 below.

For any discrete solution σ_{LS} and u_{LS}, the least-squares functional $LS(f; \sigma_{\mathrm{LS}}, u_{\mathrm{LS}})$ explicitly includes the squared data approximation error

$$\mu^2(\mathcal{T}) := \|(1 - \Pi_k) f\|^2_{L^2(\Omega)} \leq LS(f; \sigma_{\mathrm{LS}}, u_{\mathrm{LS}}). \tag{1.2}$$

For the data approximation of the right-hand side f, several strategies are available. In [100, Section 6], a separate routine **RHS** provides an additional refinement loop ensuring the sufficient resolution of the data f. When the error of the approximation of the variable σ is measured in the L^2 norm (instead of the full $H(\mathrm{div})$ norm), a separate Dörfler marking for oscillations of f leads to optimal convergence rates for the adaptive mixed finite element method [11]. With respect to this weaker norm, an adaptive LSFEM employing collective marking for an alternative residual-based error estimator even converges with the optimal rate [41].

This thesis employs the separate marking strategy from [46, 90, 40] to reduce the data approximation error $\mu(\mathcal{T})$. The resulting adaptive algorithm with separate marking for the least-squares finite element method (ALSFEM) reads as follows.

Input: Initial regular triangulation $\mathcal{T}_0$ of the polyhedral domain Ω into closed tetrahedra with some initial condition (cf. Section 2.4) and parameters $0 < \theta \leq 1$, $0 < \rho < 1$, and $0 < \kappa < \infty$.

for any level $\ell = 0, 1, 2, \ldots$ **do**
Solve LSFEM with respect to regular triangulation $\mathcal{T}_\ell$ for the solution (σ_ℓ, u_ℓ).
Compute $\eta(\mathcal{T}_\ell, T)$ for all $T \in \mathcal{T}_\ell$.

if CASE A $\mu^2(\mathcal{T}_\ell) \leq \kappa \eta^2(\mathcal{T}_\ell)$ **then**
Select a subset $\mathcal{M}_\ell \subseteq \mathcal{T}_\ell$ of (almost) minimal cardinality with

$$\theta \eta^2(\mathcal{T}_\ell) \leq \eta^2(\mathcal{T}_\ell, \mathcal{M}_\ell).$$

Compute smallest regular refinement $\mathcal{T}_{\ell+1}$ of $\mathcal{T}_\ell$ with $\mathcal{M}_\ell \subseteq \mathcal{T}_\ell \setminus \mathcal{T}_{\ell+1}$ by NVB.

else (**CASE B** $\kappa\eta^2(\mathcal{T}_\ell) < \mu^2(\mathcal{T}_\ell)$)
Compute an admissible refinement $\mathcal{T}_{\ell+1}$ of $\mathcal{T}_\ell$ with (almost) minimal cardinality and $\mu(\mathcal{T}_{\ell+1}) \leq \rho\mu(\mathcal{T}_\ell)$. **fi** **od**

Output: Sequence of discrete solutions $((\sigma_\ell, u_\ell) : \ell \in \mathbb{N}_0)$ and meshes $(\mathcal{T}_\ell : \ell \in \mathbb{N}_0)$.

Quasi-optimality. Any admissible refinement of the initial triangulation $\mathcal{T}_0$ by NVB generates the set $\mathbb{T}$ of admissible triangulations. The restriction to all triangulations with at most $N \in \mathbb{N}$ additional simplices leads to the finite set

$$\mathbb{T}(N) := \big\{\mathcal{T} \in \mathbb{T} : |\mathcal{T}| - |\mathcal{T}_0| \leq N\big\}.$$

The best possible error in terms of the alternative estimator η and the data approximation error μ depends on the right-hand side $f \in L^2(\Omega;\mathbb{R}^3)$ and implicitly on the exact solution $\sigma \in H(\mathrm{div},\Omega;\mathbb{R}^{3\times3})$ and $u \in H^1(\Omega;\mathbb{R}^3)$ to (1.1). It is defined by

$$E(\sigma,u,f,N) := \min_{\mathcal{T}\in\mathbb{T}(N)} \big(\eta^2(\mathcal{T}) + \mu^2(\mathcal{T})\big)^{1/2}.$$

The main result of this thesis involves the notion of a nonlinear approximation class $\mathcal{A}_s$. For any given $0 < s < \infty$, $\mathcal{A}_s$ consists of all triples $(\sigma,u,f) \in H(\mathrm{div},\Omega;\mathbb{R}^{3\times3}) \times H^1(\Omega;\mathbb{R}^3) \times L^2(\Omega;\mathbb{R}^3)$ such that $u = u_\mathrm{D}$ on Γ_D, $\sigma\nu = t_\mathrm{N}$ on Γ_N, and

$$|(\sigma,u,f)|_{\mathcal{A}_s} := \sup_{N\in\mathbb{N}} (N+1)^s E(\sigma,u,f,N) < \infty.$$

Theorem 1.1 (optimal convergence rate of ALSFEM). *There exist a maximal bulk parameter $0 < \theta_0 < 1$ and a maximal separation parameter $0 < \kappa_0 \leq \infty$ such that for all $0 < \theta < \theta_0$, for all $0 < \kappa < \kappa_0$, for all $0 < \rho < 1$, and for all $0 < s < \infty$, the output $((\sigma_\ell,u_\ell) : \ell \in \mathbb{N})$ of ALSFEM and $(\sigma,u,f) \in \mathcal{A}_s$ satisfy*

$$C_\mathrm{opt}^{-1}\,|(\sigma,u,f)|_{\mathcal{A}_s} \leq \sup_{\ell\in\mathbb{N}} \big(|\mathcal{T}_\ell| - |\mathcal{T}_0| + 1\big)^s \big(\eta^2(\mathcal{T}_\ell) + \mu^2(\mathcal{T}_\ell)\big)^{1/2} \leq C_\mathrm{opt}\,|(\sigma,u,f)|_{\mathcal{A}_s}.$$

The maximal parameters θ_0 and κ_0 depend exclusively on the initial triangulation $\mathcal{T}_0$ and the polynomial degree k, whereas the positive generic constant C_opt depends on $\mathcal{T}_0$, k, and the parameters s, ρ, θ, and κ.

The axioms of adaptivity in [37] and [40] provide a framework for the convergence analysis with rates for adaptive FEMs. For algorithms with a separate marking strategy, as the ALSFEM, this framework involves the seven axioms (A1)–(A4), (B1)–(B2), and (QM) for the proof of optimal convergence rates. The ten included positive generic constants Λ_j for $j = 1,\dots,7$, $\widehat{\Lambda}_3$, Λ_ref, and $\rho_2 < 1$ depend on the initial triangulation $\mathcal{T}_0$ and the polynomial degree $k \in \mathbb{N}_0$ in the discretisation.

The axioms (A1)–(A3), (QM), and (B2) concern an admissible refinement $\widehat{\mathcal{T}} \in \mathbb{T}(\mathcal{T})$ of an arbitrary triangulation $\mathcal{T} \in \mathbb{T}$. The distance between these triangulations is defined as some value $\delta(\widehat{\mathcal{T}}, \mathcal{T}) \geq 0$. The *stability axiom* asserts

$$|\eta(\widehat{\mathcal{T}}, \mathcal{T} \cap \widehat{\mathcal{T}}) - \eta(\mathcal{T}, \mathcal{T} \cap \widehat{\mathcal{T}})| \leq \Lambda_1 \, \delta(\widehat{\mathcal{T}}, \mathcal{T}) \tag{A1}$$

and the *reduction axiom*

$$\eta(\widehat{\mathcal{T}}, \widehat{\mathcal{T}} \setminus \mathcal{T}) \leq \rho_2 \, \eta(\mathcal{T}, \mathcal{T} \setminus \widehat{\mathcal{T}}) + \Lambda_2 \, \delta(\widehat{\mathcal{T}}, \mathcal{T}). \tag{A2}$$

The *discrete reliability axiom* postulates the existence of some set $\mathcal{T} \setminus \widehat{\mathcal{T}} \subseteq \mathcal{R} \subseteq \mathcal{T}$ of coarse simplices with $|\mathcal{R}| \leq \Lambda_{\mathrm{ref}} |\mathcal{T} \setminus \widehat{\mathcal{T}}|$ and

$$\delta^2(\widehat{\mathcal{T}}, \mathcal{T}) \leq \Lambda_3 \, \big(\eta^2(\mathcal{T}, \mathcal{R}) + \mu^2(\mathcal{T})\big) + \widehat{\Lambda}_3 \, \eta^2(\widehat{\mathcal{T}}). \tag{A3}$$

The *quasi-monotonicity axiom* on $\eta + \mu$ requires

$$\eta(\widehat{\mathcal{T}}) + \mu(\widehat{\mathcal{T}}) \leq \Lambda_7 \, \big(\eta(\mathcal{T}) + \mu(\mathcal{T})\big). \tag{QM}$$

The subsequent axioms (B1)–(B2) refer to the data approximation algorithm in Case B of the ALSFEM algorithm. The *data approximation of rate* $s > 0$ requires that, for all given tolerances $\mathrm{Tol} > 0$, there exists an admissible triangulation $\mathcal{T}_{\mathrm{Tol}} \in \mathbb{T}$ satisfying

$$|\mathcal{T}_{\mathrm{Tol}}| - |\mathcal{T}_0| \leq \Lambda_5 \, \mathrm{Tol}^{-1/(2s)} \quad \text{and} \quad \mu^2(\mathcal{T}_{\mathrm{Tol}}) \leq \mathrm{Tol}. \tag{B1}$$

The thresholding second algorithm from [15, 14] plus a completion step allows for quasi-optimal data approximation (B1) [40, Theorem 3.3] and is one possible realisation of Case B of the ALSFEM. The data approximation error μ from (1.2) satisfies the required *quasi-monotonicity*

$$\mu(\widehat{\mathcal{T}}) \leq \Lambda_6 \, \mu(\mathcal{T}). \tag{B2}$$

The *quasi-orthogonality axiom* solely concerns the outcome $(\mathcal{T}_\ell : \ell \in \mathbb{N}_0)$ of the ALSFEM algorithm and reads

$$\sum_{j=\ell}^{\infty} \delta^2(\mathcal{T}_{j+1}, \mathcal{T}_j) \leq \Lambda_4 \big(\eta^2(\mathcal{T}_\ell) + \mu^2(\mathcal{T}_\ell)\big). \tag{A4}$$

Outline. This thesis consists of six chapters. Chapter 2 deploys the theoretical background, introduces the employed notation, and provides essential tools used throughout the thesis. The subsequent Chapter 3 postulates some general assumptions on the operators $\mathcal{A}$ and $\mathcal{S}$ in the model problem (1.1) and verifies them for the three applications from Table 1. Two sections therein concern the analysis of the approximation of inhomogeneous Dirichlet and Neumann boundary data. Eventually, the chapter introduces the LSFEM as well as the alternative a posteriori error estimator for the ALSFEM algorithm. Chapter 4 is devoted to the proofs of the axioms of adaptivity. Numerical experiments for the three model problems are displayed in Chapter 5. A conclusion and outlook follows in Chapter 6. The Chapter A in the appendix documents the software `octAFEM3D` implemented for the numerical experiments.

Acknowledgement. I would like to express my deep gratitude to all my friends, family, and colleagues who supported me in one way or another during the past years of my studies. Special thanks are due to my parents and my dear grandma who always encouraged me in going my own way. Likewise, I thank my supervisor Prof. Carsten Carstensen for his steady support over the years and for guiding me through the academic world.

Since my employment as a student assistant in 2012, I enjoy the atmosphere in the numerical analysis working group at the Humboldt-Universität. It is always a place to find help in challenging questions, an honest word of advice, or just interesting discussions. Especially, I thank Fredi, Rui Ma, and Sophie for the valuable comments and corrections to this thesis, Franz and Tien for the extensive discussions on the code, and Helada and Saskia for the considerable review of the language.

Furthermore, I acknowledge the opportunity of doing research in the Deutsche Forschungsgemeinschaft (DFG) Priority Program 1748 'Reliable Simulation Techniques in Solid Mechanics. Development of Non-standard Discretization Methods, Mechanical and Mathematical Analysis' within the project 'Foundation and application of generalized mixed FEM towards nonlinear problems in solid mechanics' (CA 151/22-1). In addition, I appreciate several institutions enabling me to attend various workshops and conferences such as the Berlin Mathematical School (BMS), the Central European Network for Teaching and Research in Academic Liasion (CENTRAL), and the Oberwolfach-Leibniz-Graduate-Students program.

2 Preliminaries

The theory of Lebesgue and Sobolev spaces found the overall basis for the analysis of PDEs and their numerical solution. It is the point of departure in the first two Sections 2.1–2.2 of this chapter. The analysis of Sobolev functions with partial boundary conditions requires specific geometric assumptions on the domain which are presented in detail in Section 2.3. The notion of regular triangulations into tagged simplices is introduced in Section 2.4 and enables the definition of finite element function spaces in the subsequent Section 2.5. This chapter concludes with the two Sections 2.6–2.7 on quasi-interpolation operators preserving partial inhomogeneous boundary conditions. These operators are key tools for the analysis of discrete reliability in Section 4.3 below.

2.1 Lebesgue and Sobolev spaces

This thesis employs the standard notation for Lebesgue and Sobolev function spaces and appropriate subscripts indicate their usual norms and semi-norms. The brief description of the involved spaces given in this section will not replace a thorough study of these objects. For an overview of results on Lebesgue spaces, the reader is referred to the monograph by H. Brezis [24, Chapter 4] and, for a self-contained introduction of Lebesgue and Sobolev spaces, to the monograph by L. C. Evans and R. A. Gariepy [61, Chapter 1].

Let $(X, \mathbb{A}, \mu)$ denote a measure space and $Y \subseteq \mathbb{R}^{m\times n}$ a subspace for $m, n \in \mathbb{N}$ equipped with the Euclidian scalar products

$$a \cdot b := a^\top b \text{ for } a, b \in \mathbb{R}^m \text{ if } n = 1 \quad \text{and} \quad A : B := \operatorname{tr}(A^\top B) \text{ for } A, B \in \mathbb{R}^{m\times n}.$$

The linear space $\mathcal{L}^2(X; Y)$ consists of μ-measurable and square-integrable functions $f : X \to Y$ with bounded seminorm

$$\|f\|_{L^2(X)} := \Big(\int_X f : f \,\mathrm{d}\mu \Big)^{1/2} < \infty.$$

Since there is no ambiguity concerning the scalar product in the space Y, this space is omitted in the index of the norm for brevity. The equivalence classes of functions $f \in \mathcal{L}^2(X; Y)$ with respect to almost everywhere equality form the Hilbert space $L^2(X; Y)$ with the scalar product, for $f, g \in L^2(X; Y)$,

$$(f, g)_{L^2(X)} := \int_X f : g \,\mathrm{d}\mu.$$

Abbreviate the Lebesgue space of scalar-valued functions $L^2(X) \coloneqq L^2(X;\mathbb{R})$. Given some measurable set $A \in \mathbb{A}$ with $0 < \mu(A) < \infty$, the componentwise integral mean over A is well-defined by, for $f \in L^2(X;Y)$,

$$\fint_A f \,\mathrm{d}\mu \coloneqq \mu(A)^{-1} \int_A f \,\mathrm{d}\mu \in Y.$$

The definition of Sobolev spaces usually restricts to bounded open sets $X = \Omega \subseteq \mathbb{R}^3$ with the three-dimensional Lebesgue measure $\mathrm{d}\mu \coloneqq \mathrm{d}x$. In order to establish a meaningful notion of the restriction of Sobolev functions on the boundary $\partial\Omega$, suitable Lipschitz regularity assumptions are required. The resulting trace functions belong to Lebesgue spaces $L^2(X)$ on two-dimensional hypersurfaces $X = \Gamma \subseteq \partial\Omega$ equipped with the two-dimensional Hausdorff measure $\mathrm{d}\mu \coloneqq \mathrm{d}a$. For the detailed presentation of the geometric assumptions made in this thesis, the reader is referred to Section 2.3.

Notation 1 (measures). To keep the notation terse, the enclosing single bars $|\bullet|$ apply context-sensitively. They denote not only the modulus of real numbers, the Euclidian norm of vectors in $\mathbb{R}^3$, and the Frobenius norm of matrices in $\mathbb{R}^{3\times3}$, but also the cardinality of finite sets, the Lebesgue measure of three-dimensional Lebesgue sets, and the two-dimensional Hausdorff measure of two-dimensional surfaces.

Given any multi-index $\alpha = (\alpha_1, \alpha_2, \alpha_3) \in \mathbb{N}_0^3$ of length $|\alpha| \coloneqq \sum_{j=1}^3 \alpha_j$, let

$$\mathrm{D}^\alpha \coloneqq \frac{\partial^{|\alpha|}}{\partial x^{\alpha_1} \dots \partial x^{\alpha_3}}$$

denote the partial derivative with respect to α. Define the space of smooth functions

$$C^\infty(\Omega) \coloneqq \left\{\varphi : \mathbb{R}^3 \to \mathbb{R} \;:\; \forall \alpha \in \mathbb{N}_0^3,\ \mathrm{D}^\alpha f \text{ is continuous}\right\}$$

and its subspace of test functions with compact support $\operatorname{supp}(\bullet)$

$$C_\mathrm{c}^\infty(\Omega) \coloneqq \left\{\varphi \in C^\infty(\Omega) \;:\; \exists K \subset \Omega \text{ compact},\ \operatorname{supp}(\varphi) \subset K\right\}.$$

Analogous definitions apply for vector-valued functions in $C^\infty(\Omega;\mathbb{R}^3)$ and $C_\mathrm{c}^\infty(\Omega;\mathbb{R}^3)$ and functions being smooth up to the boundary in $C^\infty(\overline{\Omega})$ and $C_\mathrm{c}^\infty(\overline{\Omega})$. For $k \in \mathbb{N}$, the Sobolev space $H^k(\Omega)$ consists of all square-integrable Lebesgue functions $v \in L^2(\Omega)$ such that for every multi-index $\alpha \in \mathbb{N}_0^3$ with $|\alpha| \le k$ there exists some $w \in L^2(\Omega)$ with

$$(v, \mathrm{D}^\alpha \varphi)_{L^2(\Omega)} = (-1)^{|\alpha|} (w, \varphi)_{L^2(\Omega)} \quad \text{for all } \varphi \in C_\mathrm{c}^\infty(\Omega). \tag{2.1}$$

These functions are called k-times weakly differentiable and $\mathrm{D}^\alpha v \coloneqq w$ denotes their weak derivative. Equip $H^k(\Omega)$ with the Sobolev norm, for $v \in H^k(\Omega)$,

$$\|v\|_{H^k(\Omega)} \coloneqq \Big(\sum_{|\alpha| \le k} \|\mathrm{D}^\alpha v\|_{L^2(\Omega)}^2 \Big)^{1/2} < \infty.$$

Given a normed linear subspace $X \subset Y$ of a Banach space $(Y, \|\bullet\|_Y)$, let

$$\mathrm{cl}(X,Y) = \big\{ y \in Y \ : \ \exists (x_k \ : \ k \in \mathbb{N}) \subset X, \ \|x_k - y\|_Y \to 0 \text{ as } k \to \infty \big\}$$

denote the closure of X with respect to the norm of Y. The definition of the weak derivatives immediately allows for the local approximation of Sobolev functions by smooth functions on arbitrary open domains $\Omega \subseteq \mathbb{R}^3$ [61, Theorem 4.2]

$$H^1(\Omega) = \mathrm{cl}\big(C^\infty(\Omega) \cap H^1(\Omega),\, H^1(\Omega)\big).$$

Under the additional assumption that Ω is bounded and Lipschitz, it even holds that [61, Theorem 4.3]

$$H^1(\Omega) = \mathrm{cl}\big(C^\infty(\overline{\Omega}) \cap H^1(\Omega),\, H^1(\Omega)\big).$$

The definition (2.1) of weak derivatives induces weak counterparts of the differential operators from vector calculus. For $v \in H^1(\Omega)$, let $\nabla v \in L^2(\Omega;\mathbb{R}^3)$ denote the weak gradient defined by

$$(v, \operatorname{div}\varphi)_{L^2(\Omega)} = -(\nabla v, \varphi)_{L^2(\Omega)} \quad \text{for all } \varphi \in C_c^\infty(\Omega;\mathbb{R}^3).$$

Furthermore, let the space $H(\operatorname{curl},\Omega)$ consist of the functions $\beta \in L^2(\Omega;\mathbb{R}^3)$ with weak curl operator $\operatorname{curl}\beta \in L^2(\Omega;\mathbb{R}^3)$ defined by

$$(\beta, \operatorname{curl}\varphi)_{L^2(\Omega)} = (\operatorname{curl}\beta, \varphi)_{L^2(\Omega)} \quad \text{for all } \varphi \in C_c^\infty(\Omega;\mathbb{R}^3)$$

and $H(\operatorname{div},\Omega)$ of $q \in L^2(\Omega;\mathbb{R}^3)$ with weak divergence $\operatorname{div} q \in L^2(\Omega)$ defined by

$$(q, \nabla\varphi)_{L^2(\Omega)} = -(\operatorname{div} q, \varphi)_{L^2(\Omega)} \quad \text{for all } \varphi \in C_c^\infty(\Omega).$$

Equip these spaces with the graph norms

$$\|\beta\|_{H(\operatorname{curl},\Omega)} \coloneqq \big(\|\beta\|_{L^2(\Omega)}^2 + \|\operatorname{curl}\beta\|_{L^2(\Omega)}^2\big)^{1/2},$$
$$\|q\|_{H(\operatorname{div},\Omega)} \coloneqq \big(\|q\|_{L^2(\Omega)}^2 + \|\operatorname{div} q\|_{L^2(\Omega)}^2\big)^{1/2}.$$

The subspaces of non-rotational and solenoidal vector fields read

$$H(\operatorname{curl}=0,\Omega) \coloneqq \big\{ v \in H(\operatorname{curl},\Omega) \ : \ \operatorname{curl} v = 0 \text{ in } \Omega \big\},$$
$$H(\operatorname{div}=0,\Omega) \coloneqq \big\{ q \in H(\operatorname{div},\Omega) \ : \ \operatorname{div} q = 0 \text{ in } \Omega \big\}.$$

Given some regular triangulation $\mathcal{T}$ of the domain Ω into closed simplices in the sense of Section 2.4 below, define the piecewise $H(\operatorname{curl})$ and $H(\operatorname{div})$ spaces by

$$H(\operatorname{curl},\mathcal{T}) \coloneqq \big\{ v \in L^2(\Omega;\mathbb{R}^3) \ : \ \forall T \in \mathcal{T}, \ v|_T \in H(\operatorname{curl},\operatorname{int}(T)) \big\},$$
$$H(\operatorname{div},\mathcal{T}) \coloneqq \big\{ q \in L^2(\Omega;\mathbb{R}^3) \ : \ \forall T \in \mathcal{T}, \ q|_T \in H(\operatorname{div},\operatorname{int}(T)) \big\}.$$

Analogous definitions apply to vector-valued functions $v \in H^1(\Omega;\mathbb{R}^3)$ with weak Jacobian $\mathrm{D}v \in L^2(\Omega;\mathbb{R}^{3\times3})$ and matrix-valued functions $\beta \in H(\operatorname{curl},\Omega;\mathbb{R}^{3\times3})$ and $\tau \in H(\operatorname{div},\Omega;\mathbb{R}^{3\times3})$. The row-wise curl and divergence operators lead to $\operatorname{curl}\beta \in L^2(\Omega;\mathbb{R}^{3\times3})$ and $\operatorname{div}\tau \in L^2(\Omega;\mathbb{R}^{3\times3})$ with, for $j = 1,2,3$,

$$\big((\operatorname{curl}\beta)_{j1}, (\operatorname{curl}\beta)_{j2}, (\operatorname{curl}\beta)_{j3}\big) \coloneqq \operatorname{curl}(\beta_{j1}, \beta_{j2}, \beta_{j3}),$$
$$\big((\operatorname{div}\tau)_{j1}, (\operatorname{div}\tau)_{j2}, (\operatorname{div}\tau)_{j3}\big) \coloneqq \operatorname{div}(\tau_{j1}, \tau_{j2}, \tau_{j3}).$$

2.2 Boundary traces of Sobolev functions

Assume that the boundary $\partial\Omega$ of the Lipschitz domain Ω is partitioned into the compact Dirichlet boundary $\Gamma_D \subseteq \partial\Omega$ with positive surface measure $|\Gamma_D| > 0$ and the relatively open (possibly empty) Neumann boundary $\Gamma_N := \partial\Omega \setminus \Gamma_D$. For the presentation of the complete geometric assumptions on the domain and its boundary parts, the reader is referred to the subsequent Section 2.3. Given $\Gamma_X \in \{\Gamma_D, \Gamma_N\}$, the definition of Sobolev functions satisfying homogeneous boundary conditions requires the space of test functions with compact support

$$C_c^\infty(\overline{\Omega} \setminus \overline{\Gamma}_X) := \big\{\varphi \in C^\infty(\overline{\Omega}) \ : \ \exists K \subset \overline{\Omega} \text{ compact, } \operatorname{dist}(K, \Gamma_X) > 0 \text{ and } \operatorname{supp}(\varphi) \subseteq K\big\}.$$

The closure of this space under the various Sobolev norms reads

$$\begin{aligned} H^1_X(\Omega) &:= \operatorname{cl}\big(C_c^\infty(\overline{\Omega} \setminus \overline{\Gamma}_X),\, H^1(\Omega)\big), \\ H_X(\operatorname{curl}, \Omega) &:= \operatorname{cl}\big(C_c^\infty(\overline{\Omega} \setminus \overline{\Gamma}_X; \mathbb{R}^3),\, H(\operatorname{curl}, \Omega)\big), \\ H_X(\operatorname{div}, \Omega) &:= \operatorname{cl}\big(C_c^\infty(\overline{\Omega} \setminus \overline{\Gamma}_X; \mathbb{R}^3),\, H(\operatorname{div}, \Omega)\big). \end{aligned} \tag{2.2}$$

The subspaces of non-rotational and solenoidal vector fields are denoted by

$$\begin{aligned} H_X(\operatorname{curl} = 0, \Omega) &:= H_X(\operatorname{curl}, \Omega) \cap H(\operatorname{curl} = 0, \Omega), \\ H_X(\operatorname{div} = 0, \Omega) &:= H_X(\operatorname{div}, \Omega) \cap H(\operatorname{div} = 0, \Omega). \end{aligned}$$

The study of non-vanishing traces of Sobolev functions on (parts of) the boundary of Ω leads to the notion of Sobolev spaces $H^s(\Gamma_X)$ of fractional order $s \in \mathbb{R}$. The definition of $H^s(\Gamma_X)$ for non-integer order $s \notin \mathbb{Z}$ may be realised by the interpolation of Sobolev spaces of integer order and is comprehensively presented in the monograph by J. L. Lions and E. Magenes [79].

Let $\gamma : C(\overline{\Omega}) \to C(\partial\Omega)$ denote the linear trace operator with $\gamma(\varphi) := \varphi|_{\partial\Omega}$ in the classical sense for $\varphi \in C(\overline{\Omega})$. There exists a surjective extension to $\gamma : H^1(\Omega) \to H^{1/2}(\partial\Omega)$ [61, Theorem 4.6] that is bounded in the L^2 norm, for every $v \in H^1(\Omega)$,

$$\|\gamma(v)\|_{L^2(\partial\Omega)} \le C_\gamma \, \|v\|_{H^1(\Omega)}. \tag{2.3}$$

The operator γ is also naturally bounded in the minimal extension norm defined by, for $g \in H^{1/2}(\partial\Omega)$,

$$\|g\|_{H^{1/2}(\partial\Omega)} := \inf\big\{\|v\|_{H^1(\Omega)} \ : \ v \in H^1(\Omega),\ \gamma(v) = g\big\}.$$

For $v \in H^1(\Omega)$, it holds that $\|\gamma(v)\|_{H^{1/2}(\partial\Omega)} \le \|v\|_{H^1(\Omega)}$. Any other characterisation of $H^{1/2}(\partial\Omega)$ from [79] coincides. This has been established, for instance, in [85, Chapter 2, Theorem 5.1] for the half-space $\{x \in \mathbb{R}^3 \ : \ x_3 > 0\}$.

For the dual space $H^{-1/2}(\partial\Omega) := (H^{1/2}(\partial\Omega))$, the corresponding duality pairing $\langle \bullet, \bullet \rangle_{\partial\Omega}$ extends the $L^2(\partial\Omega)$ scalar product. Equip $H^{-1/2}(\partial\Omega)$ with the operator norm, for $t \in H^{-1/2}(\partial\Omega)$,

$$\|t\|_{H^{-1/2}(\partial\Omega)} := \sup\big\{\langle t, \gamma(v)\rangle_{\partial\Omega} \ : \ v \in H^1(\Omega),\ \|v\|_{H^1(\Omega)} = 1\big\}.$$

The restriction of γ to some part of the boundary Γ_X leads to the bounded and surjective trace operator $\gamma_X : H^1(\Omega) \to H^{1/2}(\Gamma_X)$ with $\gamma_X(\varphi) := \varphi|_{\Gamma_X}$ in the classical sense for $\varphi \in C(\overline{\Omega})$. The restriction is also bounded, for $v \in H^1(\Omega)$,

$$\|\gamma_X(v)\|_{L^2(\Gamma_X)} \leq C_{\gamma_X} \|v\|_{H^1(\Omega)},$$

and $\|\gamma_X(v)\|_{H^{1/2}(\Gamma_X)} \leq \|v\|_{H^1(\Omega)}$ with the minimal extension norm, for $g_X \in H^{1/2}(\Gamma_X)$,

$$\|g_X\|_{H^{1/2}(\Gamma_X)} := \inf \left\{ \|v\|_{H^1(\Omega)} \ : \ v \in H^1(\Omega),\ \gamma_X(v) = g_X \right\}.$$

The well-known Friedrichs inequality asserts the equivalence of the norms $\|\bullet\|_{H^1(\Omega)}$ and $\|\nabla \bullet\|_{L^2(\Omega)}$ on $H^1_X(\Omega)$ in the case $|\Gamma_X| > 0$.

Lemma 2.1 (Friedrichs inequality). *If Γ_X has positive surface measure $|\Gamma_X| > 0$, there exists a positive generic constant C_F such that every $v \in H^1_X(\Omega)$ satisfies*

$$\|v\|_{L^2(\Omega)} \leq C_F \|\mathrm{D}\, v\|_{L^2(\Omega)}.$$

Proof. For the proof in this general case $\Gamma_X \subset \partial\Omega$, utilise [60, Lemma B.63] with the trace operator $f := \gamma_X$ therein. □

Let $\nu : \partial\Omega \to B_1(0) := \{x \in \mathbb{R}^3 \ : \ |x| = 1\}$ denote the outward unit normal vector field on $\partial\Omega$. For $w \in H^1(\Omega)$, the surface (or tangential) gradient ∇_X for weakly differentiable functions on Γ_X can be implicitly defined [49, Equation (A.13) in Appendix A.3] by

$$\nabla w = \nabla_X w + (\nu \cdot \nabla w)\, \nu \quad \text{on } \Gamma_X. \tag{2.4}$$

This allows for the definition of the trace space

$$H^1(\Gamma_X) := \left\{ v \in L^2(\Gamma_X) \ : \ \nabla_X v \in L^2(\Gamma_X; \mathbb{R}^3) \right\}$$

employed with the norm, for $v \in H^1(\Gamma_X)$,

$$\|v\|_{H^1(\Gamma_X)} := \left(\|v\|^2_{L^2(\Gamma_X)} + \|\nabla_X v\|^2_{L^2(\Gamma_X)} \right)^{1/2}.$$

It holds that $H^1(\Gamma_X) \subset H^{1/2}(\Gamma_X)$ [49, page 276]. Throughout the thesis, the index for the boundary party Γ_X is omitted for ∇_X and its analog D_X for vector fields.

Moreover, define the trace space including partial boundary conditions and its dual space by

$$\widetilde{H}^{1/2}(\Gamma_N) := \gamma_N(H^1_D(\Omega)) \quad \text{and} \quad H^{-1/2}(\Gamma_N) := (\widetilde{H}^{1/2}(\Gamma_N))^*.$$

Let $\langle \bullet, \bullet \rangle_{\Gamma_N}$ denote the associated duality pairing extending the $L^2(\Gamma_N)$ scalar product. Equip $H^{-1/2}(\Gamma_N)$ with the norm, for $s_N \in H^{-1/2}(\Gamma_N)$,

$$\|s_N\|_{H^{-1/2}(\Gamma_N)} := \sup \left\{ \langle s_N, \gamma_N(v) \rangle_{\Gamma_N} \ : \ v \in H^1_D(\Omega),\ \|v\|_{H^1(\Omega)} = 1 \right\}.$$

The tangential trace operator $\gamma_{\mathrm{N}}^{\tan} : C(\overline{\Omega};\mathbb{R}^3) \to C(\Gamma_{\mathrm{N}})$ is defined by $\gamma_{\mathrm{N}}^{\tan}(\varphi) = \nu \times \varphi|_{\Gamma_{\mathrm{N}}}$ in the classical sense for $\varphi \in C(\overline{\Omega};\mathbb{R}^3)$. The integration by parts formula allows for a bounded extension to an operator $\gamma_{\mathrm{N}}^{\tan} : H(\operatorname{curl},\Omega) \to H^{-1/2}(\Gamma_{\mathrm{N}};\mathbb{R}^3)$, for $\beta \in H_{\mathrm{D}}(\operatorname{curl},\Omega)$ and $v \in H^1_{\mathrm{D}}(\Omega;\mathbb{R}^3)$,

$$\begin{aligned}\langle \gamma_{\mathrm{N}}^{\tan}(\beta), \gamma_{\mathrm{N}}(v)\rangle_{\Gamma_{\mathrm{N}}} &:= (\operatorname{curl}\beta, v)_{L^2(\Omega)} - (\beta, \operatorname{curl} v)_{L^2(\Omega)} \\ &= (\nu\times\beta, v)_{L^2(\partial\Omega)} = (\nu\times\beta, v)_{L^2(\Gamma_{\mathrm{N}})}.\end{aligned}$$

This extension is bounded, for $\beta \in H_{\mathrm{D}}(\operatorname{curl},\Omega)$ and $v \in H^1_{\mathrm{D}}(\Omega)$ with $\|v\|_{H^1(\Omega)} = 1$,

$$\langle \gamma_{\mathrm{N}}^{\tan}(\beta), \gamma_{\mathrm{N}}(v)\rangle \le \|\operatorname{curl}\beta\|_{L^2(\Omega)}\|v\|_{L^2(\Omega)} + \|\beta\|_{L^2(\Omega)}\|\operatorname{curl} v\|_{L^2(\Omega)} \le \sqrt{2}\|\beta\|_{H(\operatorname{curl},\Omega)}.$$

However, the operator $\gamma_{\mathrm{N}}^{\tan}$ is *not* surjective onto $H^{-1/2}(\Gamma_{\mathrm{N}};\mathbb{R}^3)$. For a precise characterisation of its range, the reader is referred to [28] as well as [83, Section 3.5.3] and [18, Section 2.1.1].

The normal trace operator $\gamma_{\mathrm{N}}^{\mathrm{nor}} : C(\overline{\Omega};\mathbb{R}^3) \to C(\Gamma_{\mathrm{N}})$ is defined by $\gamma_{\mathrm{N}}^{\mathrm{nor}}(\varphi) = \varphi\cdot\nu|_{\Gamma_{\mathrm{N}}}$ for $\varphi \in C(\overline{\Omega};\mathbb{R}^3)$ in the classical sense. The definition of $H^{-1/2}(\Gamma_{\mathrm{N}})$ allows for the natural extension of $\gamma_{\mathrm{N}}^{\mathrm{nor}}$ to the space $H_{\mathrm{D}}(\operatorname{div},\Omega)$ by the integration by parts formula, for $\tau \in H_{\mathrm{D}}(\operatorname{div},\Omega)$ and $v \in H^1_{\mathrm{D}}(\Omega)$,

$$\begin{aligned}\langle \gamma_{\mathrm{N}}^{\mathrm{nor}}(\tau), \gamma_{\mathrm{N}}(v)\rangle_{\Gamma_{\mathrm{N}}} &:= (\operatorname{div}\tau, v)_{L^2(\Omega)} + (\tau, \nabla v)_{L^2(\Omega)} \\ &= (\tau\cdot\nu, v)_{L^2(\partial\Omega)} = (\tau\cdot\nu, v)_{L^2(\Gamma_{\mathrm{N}})}.\end{aligned}$$

Hence, the extension is bounded, for $\tau \in H_{\mathrm{D}}(\operatorname{div},\Omega)$ and $v \in H^1_{\mathrm{D}}(\Omega)$ with $\|v\|_{H^1(\Omega)} = 1$,

$$\langle \gamma_{\mathrm{N}}^{\mathrm{nor}}(\tau), \gamma_{\mathrm{N}}(v)\rangle_{\Gamma_{\mathrm{N}}} \le \|\operatorname{div}\tau\|_{L^2(\Omega)}\|v\|_{L^2(\Omega)} + \|\tau\|_{L^2(\Omega)}\|\nabla v\|_{L^2(\Omega)} \le \|\tau\|_{H(\operatorname{div},\Omega)}.$$

These trace operators provide equivalent representations of the function spaces with partial homogeneous boundary conditions from (2.2)

$$\begin{aligned}H^1_{\mathrm{X}}(\Omega) &= \{v \in H^1(\Omega) \ : \ \gamma_{\mathrm{X}}(v) = 0\},\\ H_{\mathrm{X}}(\operatorname{curl},\Omega) &= \{v \in H(\operatorname{curl},\Omega) \ : \ \gamma_{\mathrm{X}}^{\tan}(v) = 0\},\\ H_{\mathrm{X}}(\operatorname{div},\Omega) &= \{v \in H(\operatorname{div},\Omega) \ : \ \gamma_{\mathrm{X}}^{\mathrm{nor}}(v) = 0\}.\end{aligned}$$

For homogeneous boundary conditions on the whole boundary $\partial\Omega$, this is a well-known result [65, Theorems 1.5, 2.6, and 2.12]. For partial boundary conditions under weakly Lipschitz regularity assumptions, this equality has been established in [9, Lemma 3.1 and Theorem 4.5].

In the context of differential forms with coefficients in terms of Sobolev functions, spaces with homogeneous boundary conditions are defined by continuous extensibility by zero outside of the domain [66, Definition 3.3]. For weakly Lipschitz domains, this notion coincides with the definition in (2.2) (cf. [77, Remark 2.2]) and allows for the application of the results in [77].

Notation 2 (traces of Sobolev functions). Throughout the thesis, equalities on the boundary $v = g$ on Γ_X for $v \in H^1(\Omega)$ and $g \in H^{1/2}(\Gamma_X)$ are always understood in the sense of traces $\gamma_X(v) = g$. Correspondingly, given $\beta \in H(\mathrm{curl}, \Omega)$, $\tau \in H(\mathrm{div}, \Omega)$, and $g \in H^{-1/2}(\Gamma_N; \mathbb{R}^3)$ (resp. $g \in H^{-1/2}(\Gamma_N)$), the expression $\nu \times \beta = g$ (resp. $\tau \cdot \nu = g$) on Γ_N stands for $\gamma_N^{\tan}(\beta) = g$ (resp. $\gamma_N^{\mathrm{nor}}(\tau) = g$).

The trace spaces and operators of $H^1(\Omega; \mathbb{R}^3)$, $H(\mathrm{curl}, \Omega; \mathbb{R}^{3\times3})$, and $H(\mathrm{div}, \Omega; \mathbb{R}^{3\times3})$ are defined analogously for every component.

2.3 Geometric assumptions

Let the subset $\Omega \subset \mathbb{R}^3$ be non-empty, bounded, open, and connected. In order to enable proper triangulations, Ω is supposed to be polyhedral. This means, its boundary $\partial\Omega$ is a C^0 manifold and the finite union of convex polygons such that the intersection of any two polygons is either empty or exactly a common vertex or edge. The boundary is subdivided into the compact Dirichlet boundary $\Gamma_D \subseteq \partial\Omega$ with positive surface measure $|\Gamma_D| > 0$ and the relatively open (possibly empty) Neumann boundary $\Gamma_N := \partial\Omega \setminus \Gamma_D$. The interface $\Gamma_I := \Gamma_D \cap \overline{\Gamma}_N$ leads to the relative interior of the Dirichlet boundary

$$\mathrm{relint}(\Gamma_D) = \Gamma_D \setminus \Gamma_I.$$

For an arbitrary 2-dimensional Lipschitz submanifold $M \subset \mathbb{R}^3$ with boundary ∂M, the relative interior of M is defined as

$$\mathrm{relint}(M) := M \setminus \partial M. \tag{2.5}$$

The definition and analysis of partial boundary data of Sobolev functions on Ω require the following assumption on the regularity of the boundary.

Assumption 1. *Assume throughout the thesis that Ω is a Lipschitz domain in that the domain lies on exactly one side of the boundary $\partial\Omega$ that is locally the graph of a Lipschitz function. Furthermore, let the interface Γ_I between the Dirichlet and Neumann boundary be piecewise affine.*

This ensures that there exist regular triangulations in Section 2.4 reflecting the partition of the boundary into a Dirichlet and a Neumann part.

Precisely, this condition can be expressed in the following way [67, Section 2]. Suppose that for every $x \in \partial\Omega$, there exists an open neighbourhood $U_x \subset \mathbb{R}^3$ of x as well as Euclidian transformations $\Phi_x : \mathbb{R}^3 \to \mathbb{R}^3$ with an orthogonal matrix $Q \in \mathbb{R}^{3\times3}$ such that $\Phi_x(y) = Q(y - x)$ for all $y \in \mathbb{R}^3$. The transformed neighbourhood can be parametrised by a Lipschitz continuous function $\phi_x : (-r_x, r_x)^2 \to (-R_x, R_x)$ for some real numbers $r_x > 0$ and $R_x > 0$ in such a way that

$$\begin{aligned}
\Phi_x(U_x \cap \Omega) &= \left\{\xi \in \mathbb{R}^3 \;:\; \xi_1, \xi_2 \in (-r_x, r_x),\ -R_x < \xi_3 < \phi_x(\xi_1, \xi_2)\right\},\\
\Phi_x(U_x \cap \partial\Omega) &= \left\{\xi \in \mathbb{R}^3 \;:\; \xi_1, \xi_2 \in (-r_x, r_x),\ \xi_3 = \phi_x(\xi_1, \xi_2)\right\},\\
\Phi_x(U_x \setminus \overline{\Omega}) &= \left\{\xi \in \mathbb{R}^3 \;:\; \xi_1, \xi_2 \in (-r_x, r_x),\ \phi_x(\xi_1, \xi_2) < \xi_3 < R_x\right\}.
\end{aligned}$$

Additionally, assume that there exists a function $\psi_x \in C((-r_x, r_x); (-r_x, r_x))$ and a finite set of points $-r_x = s_0 < \cdots < s_L = r_x$ with $\psi_x|_{(s_{\ell-1}, s_\ell)} \in P_1((s_{\ell-1}, s_\ell); (-r_x, r_x))$. Suppose that the continuous and piecewise affine function ψ_x provides the parametrisation of the interface Γ_{I}

$$\begin{aligned}
&\Phi_x(U_x \cap \operatorname{relint}(\Gamma_{\mathrm{D}})) \\
&\qquad = \big\{\xi \in \mathbb{R}^3 \ : \ \xi_1 \in (-r_x, r_x),\ -r_x < \xi_2 < \psi_x(\xi_1),\ \xi_3 = \phi_x(\xi_1, \psi_x(\xi_2))\big\}, \\
&\Phi_x(U_x \cap \Gamma_{\mathrm{I}}) = \big\{\xi \in \mathbb{R}^3 \ : \ \xi_1 \in (-r_x, r_x),\ \xi_2 = \psi_x(\xi_1),\ \xi_3 = \phi_x(\xi_1, \psi_x(\xi_2))\big\}, \\
&\Phi_x(U_x \cap \Gamma_{\mathrm{N}}) = \big\{\xi \in \mathbb{R}^3 \ : \ \xi_1 \in (-r_x, r_x),\ \psi_x(\xi_1) < \xi_2 < r_x,\ \xi_3 = \phi_x(\xi_1, \psi_x(\xi_2))\big\}.
\end{aligned}$$

The domain Ω is allowed to be multiply connected and the boundary may not be connected. Let $\Gamma_0, \dots, \Gamma_J \subseteq \partial\Omega$ for $J \in \mathbb{N}_0$ denote the $J+1$ connectivity components of $\partial\Omega$ satisfying

$$\partial\Omega = \bigcup_{j=0}^{J} \Gamma_j \quad \text{and} \quad \operatorname{dist}(\Gamma_j, \Gamma_k) > 0 \quad \text{for } j, k = 1, \dots, J \text{ with } j \neq k.$$

In particular, let Γ_0 denote the boundary of the unbounded component of $\mathbb{R}^3 \setminus \overline{\Omega}$.

The analysis of discrete reliability employs the construction of vector potentials for solenoidal vector fields satisfying partial homogeneous boundary conditions. The following Assumption 2 supposes the existence of those potentials and is established by [65, Theorem 3.4] in the case without boundary conditions.

Assumption 2. *The domain Ω and the Neumann boundary Γ_{N} are supposed to allow for the following equivalence. A vector field $\rho \in H(\operatorname{div}, \Omega)$ satisfies*

$$\begin{aligned}
&\operatorname{div} \rho = 0 \text{ in } \Omega, \quad \rho \cdot \nu = 0 \text{ on } \Gamma_{\mathrm{N}}, \quad \text{and} \\
&\int_{\Gamma_j} \rho \cdot \nu \, \mathrm{d}a = 0 \text{ for every } j = 0, \dots, J
\end{aligned} \tag{2.6}$$

if and only if there exists a vector potential $v \in H^1(\Omega; \mathbb{R}^3)$ such that

$$\rho = \operatorname{curl} v \text{ in } \Omega \quad \text{and} \quad v = 0 \text{ on } \Gamma_{\mathrm{N}}. \tag{2.7}$$

In addition, there exists a positive generic constant C_{curl} such that the following stability estimate holds

$$\|v\|_{H^1(\Omega)} \leq C_{\mathrm{curl}} \, \|\rho\|_{L^2(\Omega)}. \tag{2.8}$$

Before the Theorems 2.3–2.4 discuss sufficient geometric properties, a Helmholtz decomposition is directly derived from Assumption 2.

Theorem 2.2 (Helmholtz decomposition). *Suppose Ω and Γ_{N} satisfy Assumption 2. Given any $\tau \in H_{\mathrm{N}}(\operatorname{div}, \Omega)$, there exist $\alpha \in H^1_{\mathrm{D}}(\Omega)$ and $\beta \in H^1_{\mathrm{N}}(\Omega; \mathbb{R}^3)$ with*

$$\tau = \nabla\alpha + \operatorname{curl} \beta, \tag{2.9}$$

$$\|\nabla\alpha\|_{L^2(\Omega)} \leq C_{\mathrm{F}} \, \|\operatorname{div} \tau\|_{L^2(\Omega)}, \quad \text{and} \quad \|\beta\|_{H^1(\Omega)} \leq C_{\mathrm{curl}} \max\{1, C_{\mathrm{F}}\} \, \|\tau\|_{H(\operatorname{div},\Omega)} \tag{2.10}$$

for the Friedrichs constant C_{F} from Lemma 2.1 and C_{curl} from (2.8).

Proof. Given $\tau \in H_{\mathrm{N}}(\mathrm{div}, \Omega)$, let $\alpha \in H^1_{\mathrm{D}}(\Omega)$ solve the Poisson model problem

$$(\nabla \alpha, \nabla v)_{L^2(\Omega)} = -(\mathrm{div}\, \tau, v)_{L^2(\Omega)} \quad \text{for all } v \in H^1_{\mathrm{D}}(\Omega).$$

This and the Friedrichs inequality from Lemma 2.1 imply the stability estimate

$$\| \nabla \alpha\|^2_{L^2(\Omega)} = -(\mathrm{div}\, \tau, \alpha)_{L^2(\Omega)} \leq \| \mathrm{div}\, \tau\|_{L^2(\Omega)} \|\alpha\|_{L^2(\Omega)} \leq C_{\mathrm{F}} \| \mathrm{div}\, \tau\|_{L^2(\Omega)} \| \nabla \alpha\|_{L^2(\Omega)}.$$

Thus, $\| \nabla \alpha\|_{L^2(\Omega)} \leq C_{\mathrm{F}} \| \mathrm{div}\, \tau\|_{L^2(\Omega)}$. The integration by parts formula proves, for every test function $v \in H^1_{\mathrm{D}}(\Omega)$,

$$\begin{aligned} 0 &= -(\mathrm{div}\, \tau, v)_{L^2(\Omega)} - (\nabla \alpha, \nabla v)_{L^2(\Omega)} = (\tau - \nabla \alpha, \nabla v)_{L^2(\Omega)} \\ &= -(\mathrm{div}(\tau - \nabla \alpha), v)_{L^2(\Omega)} + ((\tau - \nabla \alpha) \cdot \nu, v)_{L^2(\Gamma_{\mathrm{N}})}. \end{aligned} \tag{2.11}$$

Since this holds also for $v \in H^1_{\mathrm{D}}(\Omega)$ with $v = 0$ on Γ_{N}, it follows that the function $\rho := \tau - \nabla \alpha \in H(\mathrm{div} = 0, \Omega)$ is divergence-free. In particular, the equality (2.11) shows, for every $v \in H^1_{\mathrm{D}}(\Omega)$,

$$0 = (\rho \cdot \nu, v)_{L^2(\Gamma_{\mathrm{N}})}.$$

Therefore, $\rho \cdot \nu = 0$ on Γ_{N} and Assumption 2 provides existence of some $\beta \in H^1_{\mathrm{N}}(\Omega; \mathbb{R}^3)$ such that $\rho = \mathrm{curl}\, \beta$. The stability estimate (2.8) in

$$\|\beta\|_{H^1(\Omega)} \leq C_{\mathrm{curl}}\, \|\rho\|_{L^2(\Omega)} \leq C_{\mathrm{curl}} \left(\|\tau\|_{L^2(\Omega)} + \| \nabla \alpha\|_{L^2(\Omega)} \right)$$

concludes the proof of (2.10). □

The necessity of the condition (2.6) is always fulfilled.

Theorem 2.3. *On every Lipschitz domain Ω, the existence of $v \in H^1(\Omega; \mathbb{R}^3)$ with* (2.7) *implies that $\rho := \mathrm{curl}\, v$ satisfies* (2.6).

Proof. For any $v \in H^1_{\mathrm{N}}(\Omega; \mathbb{R}^3) \subset H_{\mathrm{N}}(\mathrm{curl}, \Omega)$ and $\varphi \in C^\infty_{\mathrm{c}}(\overline{\Omega} \setminus \Gamma_{\mathrm{D}})$, it holds that $\mathrm{curl}\, v \in H(\mathrm{div} = 0, \Omega)$. The Green's formulas for the gradient and the curl imply

$$(\varphi, \mathrm{curl}\, v \cdot \nu)_{L^2(\Gamma_{\mathrm{N}})} = (\nabla \varphi, \mathrm{curl}\, v)_{L^2(\Omega)} = (\nabla \varphi, \nu \times v)_{L^2(\Gamma_{\mathrm{N}})} = 0.$$

This is the weak form of $(\mathrm{curl}\, v) \cdot \nu = 0$ on Γ_{N}. Hence, for every $v \in H_{\mathrm{N}}(\mathrm{curl}, \Omega)$,

$$\mathrm{curl}\, v \in H_{\mathrm{N}}(\mathrm{div} = 0, \Omega).$$

In order to guarantee the third condition in (2.6), let $\vartheta_j \in C^\infty_{\mathrm{c}}(\mathbb{R}^3)$ for $j = 0, \ldots, J$ denote smooth cut-off functions [65, proof of Theorem 3.4] with

$$0 \leq \vartheta_j \leq 1 \text{ in } \mathbb{R}^3 \quad \text{and} \quad \vartheta_j(x) = \begin{cases} 1 & \text{if } \mathrm{dist}(x, \Gamma_j) < \varepsilon, \\ 0 & \text{else.} \end{cases}$$

The functions $\rho_j := \operatorname{curl}(\vartheta_j v) \in H(\operatorname{div}=0,\Omega)$ satisfy

$$\rho_j \cdot \nu = \begin{cases} \rho \cdot \nu & \text{on } \Gamma_j, \\ 0 & \text{on } \Gamma_k \text{ for } k = 1,\dots,J \text{ with } j \neq k. \end{cases}$$

The Gauss divergence theorem concludes the proof of (2.6) in, for every $j = 0,\dots,J$,

$$\int_{\Gamma_j} \rho \cdot \nu \,\mathrm{d}a = \int_{\Gamma_j} \rho_j \cdot \nu \,\mathrm{d}a = \int_\Omega \operatorname{div} \rho_j \,\mathrm{d}x = 0. \qquad \square$$

If $\Gamma_{\mathrm{N}} = \emptyset$, the existence of a right-inverse of the curl operator, follows from [65, Theorem 3.4]. In the case of $|\Gamma_{\mathrm{N}}| > 0$ this is more involved. For instance, as in the following theorem, it requires an additional assumption on the connectivity of the Neumann boundary patches $\Gamma_{\mathrm{N},\ell}$.

Theorem 2.4. *Let the Neumann boundary*

$$\Gamma_{\mathrm{N}} = \bigcup_{\ell=1}^{L} \Gamma_{\mathrm{N},\ell}$$

consist of $L \in \mathbb{N}$ relatively open connectivity components $\Gamma_{\mathrm{N},1},\dots,\Gamma_{\mathrm{N},L} \subseteq \Gamma_{\mathrm{N}}$. If the components $\Gamma_{\mathrm{N},1},\dots,\Gamma_{\mathrm{N},L}$ are simply connected and, for all $\ell, m = 1,\dots,L$ with $\ell \neq m$,

$$\operatorname{dist}(\Gamma_{\mathrm{N},\ell}, \Gamma_{\mathrm{N},m}) > 0, \tag{2.12}$$

then Assumption 2 holds. (The distance property (2.12) *is implicitly fulfilled due to Assumption 1 and the assumptions on the parametrisation ψ_x of the interface Γ_{I} on page 16.)*

Remark 2.5. This result generalises [65, Theorem 3.4] to functions with partial homogeneous boundary conditions. The proof utilises techniques from [9, Remark 3.9] and [67, Theorem 2.3] to recover the correct boundary conditions. Both references present results similar to Theorem 2.4 including partial boundary conditions. However, [9, Theorem 3.8 with Remark 3.9] restricts to domains with connected boundary and [67, Theorem 3.2] even supposes that Ω is contractible.

Further results similar to Theorem 2.4 are presented in [3, Section 3.5] and include additional assumptions on cuts of the domain into simply connected subdomains.

Proof of Theorem 2.4. Due to Theorem 2.3, it suffices to show that, given some vector field $\rho \in H_{\mathrm{N}}(\operatorname{div},\Omega)$ satisfying (2.6), there exists a vector potential $v \in H^1_{\mathrm{N}}(\Omega;\mathbb{R}^3)$ with (2.7).

Step 1. By [67, Theorem 2.3], there exists an open bounded Lipschitz domain $\omega_{\mathrm{N}} \subset \mathbb{R}^3$ such that

$$\widetilde{\Omega} := \Omega \cup \Gamma_{\mathrm{N}} \cup \omega_{\mathrm{N}}$$

is an open bounded Lipschitz domain with $\Gamma_D \subset \partial\widetilde{\Omega}$. If required, consider suitable open subsets of ω_N in order to guarantee that ω_N can be decomposed into L open connectivity components $\omega_{N,1}, \dots, \omega_{N,L}$ each attached to the corresponding component $\Gamma_{N,1}, \dots, \Gamma_{N,L}$ of the Neumann boundary. Thus, the $\omega_{N,\ell}$ satisfy

$$\omega_N = \bigcup_{\ell=1}^{L} \omega_{N,\ell}, \quad \operatorname{dist}(\omega_{N,\ell}, \omega_{N,m}) > 0 \text{ for } \ell \neq m, \quad \text{and}$$
$$\overline{\Gamma}_{N,\ell} = \partial\Omega \cap \overline{\omega}_{N,\ell} \text{ for } \ell = 1, \dots, L.$$

The connectivity assumption on $\Gamma_{N,\ell}$ ensures that the extended patch $\omega_{N,\ell}$ is also simply connected for every $\ell = 1, \dots, L$.

Moreover, this construction results in $J+1$ connectivity components $\widetilde{\Gamma}_0, \dots, \widetilde{\Gamma}_J$ of the boundary of the extended domain $\widetilde{\Omega}$ satisfying

$$\partial\widetilde{\Omega} = \bigcup_{j=0}^{J} \widetilde{\Gamma}_j \quad \text{and} \quad \Gamma_D \cap \Gamma_j = \Gamma_D \cap \widetilde{\Gamma}_j \text{ for } j = 0, \dots, J.$$

For every $j = 0, \dots, J$, the $\widetilde{\Gamma}_j$ consists of the boundary of the extended domain at Γ_j if $|\Gamma_j \cap \Gamma_N| > 0$ and coincides with Γ_j else.

Step 2. The normal boundary condition $\rho \cdot \nu = 0$ on Γ_N allows for an extension $\widetilde{\rho} \in H(\operatorname{div}, \widetilde{\Omega})$ with

$$\widetilde{\rho}(x) = \begin{cases} \rho(x) & \text{for } x \in \Omega, \\ 0 & \text{for } x \in \omega_N. \end{cases}$$

Since $\widetilde{\rho} \cdot \nu = 0$ holds on $\partial\omega_{N,\ell} \setminus \Gamma_{N,\ell}$ for $\ell = 1, \dots, L$, the extension $\widetilde{\rho}$ satisfies, for every $j = 0, \dots, J$,

$$\int_{\widetilde{\Gamma}_j} \widetilde{\rho} \cdot \nu \, \mathrm{d}a = 0.$$

The application of [65, Theorem 3.4] provides a vector potential $\widetilde{w} \in H^1(\widetilde{\Omega}; \mathbb{R}^3)$ with

$$\widetilde{\rho} = \operatorname{curl} \widetilde{w} \quad \text{and} \quad \operatorname{div} \widetilde{w} = 0 \quad \text{in } \widetilde{\Omega}.$$

Step 3. By definition of $\widetilde{\rho}$, the restriction $w_\ell := \widetilde{w}|_{\omega_{N,\ell}}$ satisfies, for every $\ell = 1, \dots, L$,

$$\operatorname{curl} w_\ell = 0 \quad \text{in } \omega_{N,\ell}.$$

Since $\omega_{N,\ell}$ is simply connected, [65, Theorem 2.9] provides $\varphi_\ell \in H^1(\omega_{N,\ell})/\mathbb{R}$ such that

$$w_\ell = \nabla \varphi_\ell \quad \text{in } \omega_{N,\ell}.$$

The regularity of $w_\ell \in H^1(\omega_{N,\ell}; \mathbb{R}^3)$ implies that $\varphi_\ell \in H^2(\omega_{N,\ell})/\mathbb{R}$. Due to the distance $\operatorname{dist}(\omega_{N,\ell}, \omega_{N,m}) > 0$ for $\ell \neq m$, the Stein extension theorem [99, Chapter VI, Theorem 5]

and suitable cut-off functions guarantee the existence of extensions $\widetilde{\varphi}_\ell \in H^2(\widetilde{\Omega})$ such that, for every $\ell, m = 1, \dots, L$ with $\ell \neq m$,

$$\widetilde{\varphi}_\ell = \varphi_\ell \text{ in } \omega_{\mathrm{N},\ell} \quad \text{and} \quad \operatorname{dist}(\operatorname{supp}(\widetilde{\varphi}_\ell), \operatorname{supp}(\widetilde{\varphi}_m)) > 0.$$

The vector field

$$\widetilde{v} := \widetilde{w} - \sum_{\ell=1}^{L} \nabla \widetilde{\varphi}_\ell \in H^1(\widetilde{\Omega}; \mathbb{R}^3)$$

vanishes $\widetilde{v} = 0$ in every $\omega_{\mathrm{N},\ell}$ for $\ell = 1, \dots, L$. In particular, $\widetilde{v} = 0$ vanishes on every $\Gamma_{\mathrm{N},\ell}$ in the sense of traces. Thus, the restriction $v := \widetilde{v}|_\Omega \in H^1(\Omega; \mathbb{R}^3)$ satisfies

$$\rho = \operatorname{curl} v \text{ in } \Omega \quad \text{and} \quad v = 0 \text{ on } \Gamma_{\mathrm{N}}.$$

Step 4. The linear operator $\operatorname{curl} : H_1 \to H_2$ on the spaces

$$H_1 = \left\{ w \in H^1_{\mathrm{N}}(\Omega; \mathbb{R}^3) \ : \ \operatorname{div} w = 0 \right\},$$
$$H_2 = \left\{ \tau \in H_{\mathrm{N}}(\operatorname{div} = 0, \Omega) \ : \ \int_{\Gamma_j} \tau \cdot \nu \, \mathrm{d}a = 0 \text{ for } j = 0, \dots, J \right\}$$

is bounded, for every $w \in H_1$,

$$\| \operatorname{curl} w \|_{L^2(\Omega)} \leq \sqrt{2} \| \mathrm{D}\, w \|_{L^2(\Omega)} \leq \sqrt{2} \| w \|_{H^1(\Omega)}.$$

Step 3 shows that the operator $\operatorname{curl} : H_1 \to H_2$ is surjective. Thus there exists a bounded, but not necessarily linear, right-inverse of the curl operator by the Bartle-Graves theorem with some positive continuity constant C_{curl}. This concludes the proof of the stability estimate. □

2.4 Triangulations and newest-vertex bisection

Any decomposition of the polyhedral domain $\Omega \subset \mathbb{R}^3$ in this thesis is a finite set of tagged simplices T. A tagged simplex $T = (z_0, \dots, z_3; \gamma)$ consists of a tuple of vertices $z_0, \dots, z_3 \in \mathbb{R}^3$ not lying in a two-dimensional hyperplane and a type $\gamma \in \{0, 1, 2\}$. Define the domain of the tagged simplex as the convex hull $\operatorname{dom}(T) := \operatorname{conv}\{z_0, \dots, z_3\}$. Outside of this chapter, the tag γ of a simplex is not written and the tagged simplex is simply identified with its domain,

$$\partial T := \partial \operatorname{dom}(T), \quad \operatorname{int}(T) := \operatorname{int}(\operatorname{dom}(T)), \quad T \cap T' := \operatorname{dom}(T) \cap \operatorname{dom}(T'),$$
$$\operatorname{dist}(T, T') := \operatorname{dist}(\operatorname{dom}(T), \operatorname{dom}(T')), \quad v|_T := v|_{\operatorname{dom}(T)}$$

as well as the abbreviations $z \in T$ for $z \in \operatorname{dom}(T)$ and $F \subset T$ for $F \subset \operatorname{dom}(T)$.

A set $\mathcal{T}$ of (tagged) simplices is called regular triangulation of Ω if it covers the domain

$$\overline{\Omega} = \bigcup_{T \in \mathcal{T}} \operatorname{dom}(T)$$

and if any two distinct tagged simplices $T, T' \in \mathcal{T}$ with $T = (z_0, \dots, z_3; \gamma)$ and $T' = (z'_0, \dots, z'_3; \gamma')$ are either disjoint or share exactly

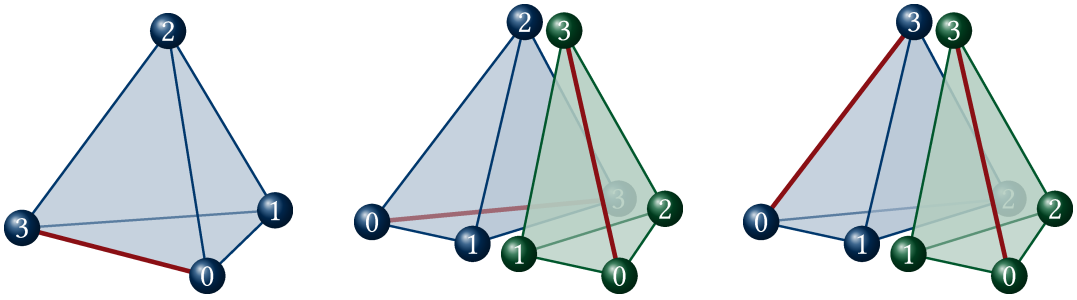

(a) Unrefined simplex T **(b)** Bisection for type 0 **(c)** Bisection for types 1, 2

Figure 2.1: Bisection rule for one simplex T with local node numbers. The thick red line indicates the refinement edge such as $\operatorname{ref}(T) = \operatorname{conv}\{z_0, z_3\}$ in (a).

- one node $T \cap T' = z_\ell = z'_m$ for some $0 \le \ell, m \le 3$, or
- one edge $T \cap T' = \operatorname{conv}\{z_{\ell_1}, z_{\ell_2}\} = \operatorname{conv}\{z'_{m_1}, z'_{m_2}\}$ for some $0 \le \ell_1 < \ell_2 \le 3$ and $0 \le m_1 < m_2 \le 3$, or
- one face $T \cap T' = \operatorname{conv}\{z_{\ell_1}, z_{\ell_2}, z_{\ell_3}\} = \operatorname{conv}\{z'_{m_1}, z'_{m_2}, z'_{m_3}\}$ for some $0 \le \ell_1 < \ell_2 < \ell_3 \le 3$ and $0 \le m_1 < m_2 < m_3 \le 3$.

In the latter case, T and T' are called neighbouring (tagged) simplices.

The NVB of any tagged simplex $T = (z_0, \dots, z_3; \gamma) \in \mathcal{T}$ generates a new node $\widetilde{z} = (z_0 + z_3)/2$ on the refinement edge $\operatorname{ref}(T) := \operatorname{conv}\{z_0, z_3\}$. The two child tagged simplices

$$(z_0, \widetilde{z}, z_1, z_2; (\gamma+1) \bmod 3) \quad \text{and} \quad \begin{cases} (z_3, \widetilde{z}, z_1, z_2; (\gamma+1) \bmod 3) & \text{if } \gamma = 1, 2, \\ (z_3, \widetilde{z}, z_2, z_1; (\gamma+1) \bmod 3) & \text{if } \gamma = 0, \end{cases}$$

are depicted in Figure 2.1 with their local node numbers. These new child simplices coincide when the bisection rule is applied to the following permutation of the tagged simplex T

$$\operatorname{perm}(T) := \begin{cases} (z_3, \widetilde{z}, z_1, z_2; 1) & \text{if } \gamma = 0, \\ (z_3, \widetilde{z}, z_2, z_1; \gamma) & \text{if } \gamma = 1, 2. \end{cases}$$

This bisection strategy stems from [81, 104] and has been analysed in [101, 64]. In combination with a closure step, it is called *refine* in [101, Section 5] and leads to the notion of one-level refinements of the triangulation $\mathcal{T}$. In order to guarantee the regularity of arbitrary refinements [101, Theorem 4.3], this refinement strategy requires the following two conditions on the initial triangulation $\mathcal{T}_0$.

(IC1) All tagged simplices $T \in \mathcal{T}_0$ share the same type γ.

(IC2) Any two neighbouring tagged simplices $T, T' \in \mathcal{T}_0$ sharing at least one refinement edge $\operatorname{ref}(T) \subset T \cap T'$ or $\operatorname{ref}(T') \subset T \cap T'$ are reflected in the sense that the ordered sequence of vertices of T or $\operatorname{perm}(T)$ coincides with that of T' on all but one position. Otherwise, any two neighbouring children of T and T' are reflected.

Additionally, assume that $\mathcal{T}_0$ resolves the decomposition of the boundary into Γ_{D} and Γ_{N}.

Such an initial regular triangulation $\mathcal{T}_0$ of tagged simplices with initial condition (IC) induces the set of all admissible triangulations

$$\begin{aligned}\mathbb{T} := \mathbb{T}(\mathcal{T}_0) := \big\{&\mathcal{T}_\ell \text{ regular triangulation of } \Omega \text{ into tagged simplices } : \\ &\exists \ell \in \mathbb{N}_0\, \exists \mathcal{T}_1, \dots, \mathcal{T}_\ell \text{ successive one-level refinements in the sense} \\ &\text{that } \mathcal{T}_{m+1} \text{ is a one-level refinement of } \mathcal{T}_m \text{ for } m = 0, \dots, \ell - 1\big\}.\end{aligned}$$

For any natural number $N \in \mathbb{N}$, set

$$\mathbb{T}(N) := \big\{\mathcal{T} \in \mathbb{T} \,:\, |\mathcal{T}| - |\mathcal{T}_0| \leq N\big\}.$$

All triangulations in this thesis are admissible, when generated with NVB. In particular, this guarantees shape-regularity of all $\mathcal{T} \in \mathbb{T}$ in the sense of [51, Section 3.2]. Furthermore, for a one-level refinement $\widehat{\mathcal{T}}$ of $\mathcal{T}$, an upper bound for the number of newly created simplices during the closure step

$$|\widehat{\mathcal{T}} \setminus \mathcal{T}| \leq C_{\mathrm{NVB}}\, |\mathcal{M}|$$

is essential for the convergence analysis with rates [14, Theorem 2.4]. For arbitrary spatial dimensions, this has been established in [101, Theorem 6.1].

For any triangulation $\mathcal{T} \in \mathbb{T}$, $\mathcal{N}$ denotes the set of nodes, $\mathcal{F}$ the set of faces, and $\mathcal{E}$ the set of edges. The corresponding sets on the boundary $\partial\Omega$ read $\mathcal{N}(\partial\Omega)$, $\mathcal{F}(\partial\Omega)$, and $\mathcal{E}(\partial\Omega)$. The elements of the complementary subsets $\mathcal{N}(\Omega)$, $\mathcal{F}(\Omega)$, and $\mathcal{E}(\Omega)$ belong to the interior Ω. For any tagged simplex $T \in \mathcal{T}$, let $\mathcal{N}(T)$ denote the set of its four nodes, $\mathcal{F}(T)$ the set of its four faces, and $\mathcal{E}(T)$ the set of its six edges. Let the set $\mathcal{F}$ of faces be subordinated to Γ_{D} and Γ_{N} in that $\mathcal{F}(\Gamma_{\mathrm{D}}) := \{F \in \mathcal{F} \,:\, F \subseteq \Gamma_{\mathrm{D}}\}$ and $\mathcal{F}(\Gamma_{\mathrm{N}}) := \{F \in \mathcal{F} \,:\, F \subseteq \overline{\Gamma}_{\mathrm{N}}\}$ partition the set $\mathcal{F}(\partial\Omega)$.

Given any subset $\omega \subseteq \Omega$ such that there exists a set of simplices $\mathcal{M} \subseteq \mathcal{T}$ satisfying

$$\overline{\omega} = \bigcup_{T \in \mathcal{M}} T,$$

let $\mathcal{T}(\omega) := \mathcal{M}$ denote the regular triangulation of ω into tagged simplices from $\mathcal{T}$.

Notation 3 (admissible refinement). Throughout the thesis, let $\mathcal{T} \in \mathbb{T}$ denote an arbitrary regular triangulation with admissible refinement $\widehat{\mathcal{T}} \in \mathbb{T}(\mathcal{T})$. Let $(\sigma_{\mathrm{LS}}, u_{\mathrm{LS}})$ and $(\widehat{\sigma}_{\mathrm{LS}}, \widehat{u}_{\mathrm{LS}})$ denote the respective discrete least-squares finite element solutions. In

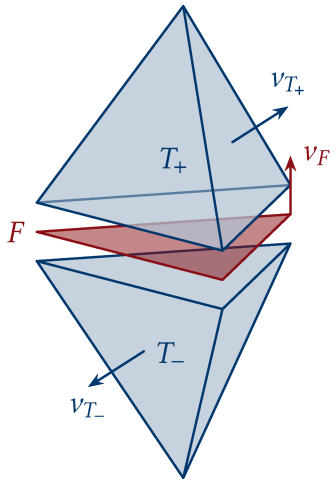

Figure 2.2: Patch $\overline{\omega}_F$ of the interior face $F \in \mathcal{F}(\Omega)$ consisting of two adjacent simplices T_+ and T_- with corresponding unit normal vector ν_F and outward unit normal vectors ν_{T_+}, ν_{T_-}.

order to indicate the relation to the refinement $\widehat{\mathcal{T}}$, the superscript $\widehat{\ }$ is applied to any set such as $\widehat{\mathcal{F}}, \widehat{\mathcal{E}}, \widehat{\mathcal{N}}$, or discrete function such as $\widehat{u}_{\mathrm{LS}}, \widehat{\tau}_{\mathrm{RT}}, \widehat{\beta}_{\mathrm{Ned}}$, or operator into discrete spaces such as $\widehat{\Pi}_{k-1}, \widehat{\mathcal{J}}_{\mathrm{D}}^{k+1}$.

Notation 4 (generic constants). Any positive generic constant $0 < C < \infty$ in the following analysis is uniformly bounded due to the shape-regularity of all $\mathcal{T} \in \mathbb{T}$. Upper case constants are identical throughout the thesis such as the constants Λ_j from the axioms of adaptivity. Lower case constants c_m for $m \in \mathbb{N}$ are solely utilised in proofs and do not vary within this scope.

Given a node $z \in \mathcal{N}$, an edge $E \in \mathcal{E}$, and a face $F \in \mathcal{F}$, define the nodal patch $\omega_z \subseteq \Omega$, the edge patch $\omega_E \subseteq \Omega$, and the face patch $\omega_F \subseteq \Omega$ by

$$\omega_z := \operatorname{int} \bigcup \{T \in \mathcal{T} \,:\, z \in T\}, \quad \omega_E := \operatorname{int} \bigcup \{T \in \mathcal{T} \,:\, E \subset T\},$$
$$\omega_F := \operatorname{int} \bigcup \{T \in \mathcal{T} \,:\, F \subset T\}.$$

For every interior face $F \in \mathcal{F}(\Omega)$, the face patch $\{T \in \mathcal{T} \,:\, F \subset T\} = \{T_+, T_-\}$ consists of exactly two adjacent simplices $T_+, T_- \in \mathcal{T}$. The index is determined by the fixed orientation of the unit normal vector ν_F of F such that $\nu_F \cdot \nu_{T_\pm} = \pm 1$ as illustrated in Figure 2.2. For every boundary face $F \in \mathcal{F}(\partial\Omega)$, the face patch $\{T \in \mathcal{T} \,:\, F \subset T\} = \{T_+\}$ consists of a unique adjacent simplex T_+.

These face patches induce the definition of tangential and normal jumps of piecewise Sobolev functions. For any piecewise function $\beta_{\mathrm{pw}} \in H(\operatorname{curl}, \mathcal{T})$, let

$$[\nu_F \times \beta_{\mathrm{pw}}]_F := \begin{cases} \nu_F \times (\beta_{\mathrm{pw}}|_{T_+}) - \nu_F \times (\beta_{\mathrm{pw}}|_{T_-}) & \text{on } F \in \mathcal{F}(\Omega) \text{ with } F = \partial T_+ \cap \partial T_-, \\ \nu_F \times (\beta_{\mathrm{pw}}|_{T_+}) & \text{on } F \in \mathcal{F}(\partial\Omega) \cap \mathcal{F}(T_+). \end{cases} \tag{2.13}$$

For any piecewise function $\tau_{\mathrm{pw}} \in H(\mathrm{div}, \mathcal{T})$, let

$$[\tau_{\mathrm{pw}} \cdot \nu_F]_F := \begin{cases} (\tau_{\mathrm{pw}}|_{T_+}) \cdot \nu_F - (\tau_{\mathrm{pw}}|_{T_-}) \cdot \nu_F & \text{on } F \in \mathcal{F}(\Omega) \text{ with } F = \partial T_+ \cap \partial T_-, \\ (\tau_{\mathrm{pw}}|_{T_+}) \cdot \nu_F & \text{on } F \in \mathcal{F}(\partial\Omega) \cap \mathcal{F}(T_+). \end{cases} \tag{2.14}$$

The analogous notation applies for matrix-valued functions in $H(\mathrm{curl}, \mathcal{T}; \mathbb{R}^{3\times 3})$ and $H(\mathrm{div}, \mathcal{T}; \mathbb{R}^{3\times 3})$.

Given any $T \in \mathcal{T}$, let $\Omega_T \subseteq \Omega$ denote the tetrahedron patch

$$\Omega_T := \mathrm{int} \bigcup \big\{ \widetilde{T} \in \mathcal{T} \ : \ \mathrm{dist}(\widetilde{T}, T) = 0 \big\}. \tag{2.15}$$

The shape-regularity of all $\mathcal{T} \in \mathbb{T}$ ensures the uniform boundedness of the positive generic overlap constant

$$C_{\mathrm{OL}}^2 := \max_{\mathcal{T}\in\mathbb{T}} \max_{T\in\mathcal{T}} |\mathcal{T}(\Omega_T)| < \infty. \tag{2.16}$$

For any natural number $n \in \mathbb{N}$, define the n-layer around a subset of simplices $\mathcal{M} \subseteq \mathcal{T}$ successively by

$$\begin{aligned} \mathcal{L}_n(\mathcal{M}) := \big\{ T \in \mathcal{T} \ : \exists T_0, \dots, T_n \in \mathcal{T} \text{ with } T_0 \in \mathcal{M}, T_n = T, \\ \text{and } \mathrm{dist}(T_m, T_{m+1}) = 0 \text{ for every } m = 0, \dots, n-1 \big\}. \end{aligned}$$

If the argument $\mathcal{M} \subseteq \mathcal{F}$ is any subset of faces, the same notation applies to n-layers of faces subordinated to the part Γ_{X} of the boundary

$$\begin{aligned} \mathcal{L}_n(\mathcal{M}, \Gamma_{\mathrm{X}}) := \big\{ F \in \mathcal{F}(\Gamma_{\mathrm{X}}) \ : \exists F_0, \dots, F_n \in \mathcal{F}(\Gamma_{\mathrm{X}}) \text{ with } F_0 \in \mathcal{M}, F_n = F, \text{and} \\ \mathrm{dist}(F_m, F_{m+1}) = 0 \text{ for every } m = 0, \dots, n-1 \big\}. \end{aligned} \tag{2.17}$$

Figure 2.3 displays examples of n-layers $\mathcal{L}_n(\mathcal{M}, \Gamma_{\mathrm{X}})$ around refined faces $\mathcal{M} = \mathcal{F} \setminus \widehat{\mathcal{F}}$ on the boundary Γ_{X}. The union of faces of such n-layers

$$\bigcup \mathcal{L}_n(\mathcal{M}, \Gamma_{\mathrm{X}}) := \bigcup \{ F \ : \ F \in \mathcal{L}_n(\mathcal{M}, \Gamma_{\mathrm{X}}) \}$$

forms a 2-dimensional Lipschitz submanifold in $\mathbb{R}^3$ with boundary.

Given a regular triangulation $\mathcal{T} \in \mathbb{T}$ and its refinement $\widehat{\mathcal{T}} \in \mathbb{T}(\mathcal{T})$, abbreviate the n-layers around the refined simplices with $\mathcal{R}_n := \mathcal{L}_n(\mathcal{T} \setminus \widehat{\mathcal{T}})$. The piecewise constant mesh-size function $h_{\mathcal{T}} \in P_0(\mathcal{T})$ is defined as the cubic root of the volume of the simplices

$$h_{\mathcal{T}}|_T := h_T := |T|^{1/3} \quad \text{for } T \in \mathcal{T}. \tag{2.18}$$

This leads to the maximal mesh-size $h_{\max} := \|h_{\mathcal{T}}\|_{L^\infty(\Omega)} > 0$.

Recall the well-known trace inequality.

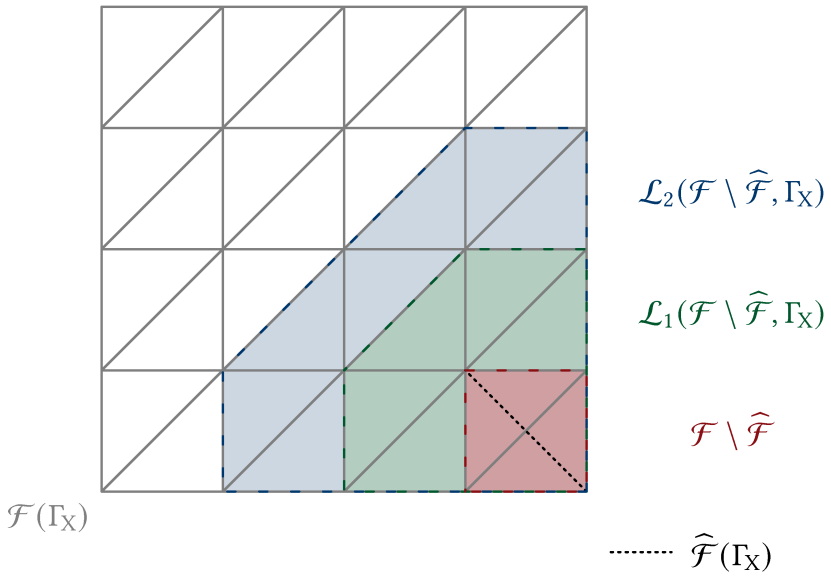

Figure 2.3: Face layers $\mathcal{L}_n(\mathcal{F} \setminus \widehat{\mathcal{F}}, \Gamma_X)$ from (2.17) for $n \in \mathbb{N}$ on the boundary part Γ_X. The square Γ_X is a subset of the boundary $\partial\Omega$ of the three-dimensional domain Ω. The dotted line indicates the bisection of boundary faces made in the refinement step from $\mathcal{F}(\Gamma_X)$ to $\widehat{\mathcal{F}}(\Gamma_X)$.

Lemma 2.6 (trace inequality). *There exists a positive generic constant C_{tr} such that for every regular triangulation $\mathcal{T} \in \mathbb{T}$ and every simplex $T \in \mathcal{T}$ with face $F \in \mathcal{F}(T)$, every $v \in H^1(\mathcal{T})$ satisfies*

$$\|v|_T\|^2_{L^2(F)} \leq C_{\mathrm{tr}} \left(|T|^{1/3} \|\nabla v\|^2_{L^2(T)} + |T|^{-1/3} \|v\|^2_{L^2(T)} \right). \tag{2.19}$$

The generic constant C_{tr} solely depends on the shape regularity of the triangulations in $\mathbb{T}$.

Proof. The shape-regularity of the triangulations $\mathcal{T} \in \mathbb{T}$ provides existence of a positive generic constant c_1 such that $\operatorname{diam}(T) \leq c_1 |T|^{1/3}$. This and the continuous trace inequality from [58, Lemma 1.49] establish

$$\|v|_T\|^2_{L^2(F)} \leq c_2 \left(2 \, \|\nabla v\|_{L^2(T)} \|v\|_{L^2(T)} + 3c_1 \, |T|^{1/3} \|v\|^2_{L^2(T)} \right).$$

Young's inequality with parameter $\alpha > 0$ shows

$$\|v|_T\|^2_{L^2(F)} \leq c_2 \left(\alpha \, |T|^{1/3} \|\nabla v\|^2_{L^2(T)} + (3c_1 + 1/\alpha) \, |T|^{-1/3} \|v\|^2_{L^2(T)} \right).$$

This concludes the proof of (2.19) with the positive generic constant

$$C_{\mathrm{tr}} := c_2 \alpha^* \quad \text{with} \quad \alpha^* := \frac{3c_1 + \sqrt{9c_1^2 + 4}}{2} = 3c_1 + \frac{1}{\alpha^*}. \qquad \square$$

2.5 Finite element discretisation

In order to define discrete subspaces of the Sobolev and Lebesgue spaces from the Sections 2.1 and 2.2, let $P_k(\mathcal{T})$ denote the space of piecewise polynomials of total degree at most $k \in \mathbb{N}_0$. The orthogonal projection of an $L^2(\Omega)$ function f onto $P_k(\mathcal{T})$ reads $\Pi_k f \in P_k(\mathcal{T})$. The componentwise projection applies for vector- or matrix-valued functions and maps onto $P_k(\mathcal{T};\mathbb{R}^3)$ or $P_k(\mathcal{T};\mathbb{R}^{3\times3})$. Recall for any face $F \in \mathcal{F}(\partial\Omega)$, that $\overline{\omega}_F \in \mathcal{T}$ denotes the unique tetrahedron with $F \subset \overline{\omega}_F$. The approximation of the boundary data $g \in L^2(\Gamma_X)$ is naturally measured in terms of the oscillations, for $\mathcal{M} \subseteq \mathcal{F}(\Gamma_X)$,

$$\operatorname{osc}^2(g,\mathcal{M}) \coloneqq \sum_{F\in\mathcal{M}} |\overline{\omega}_F|^{1/3}\, \|(1-\Pi_k)g\|^2_{L^2(F)}. \tag{2.20}$$

Throughout the thesis, fix a polynomial degree $k \in \mathbb{N}_0$. Let $S^{k+1}(\mathcal{T}) \coloneqq P_{k+1}(\mathcal{T}) \cap H^1(\Omega)$ and $S^{k+1}(\mathcal{T};\mathbb{R}^3) \coloneqq P_{k+1}(\mathcal{T};\mathbb{R}^3)\cap H^1(\Omega;\mathbb{R}^3)$ approximate the scalar- and vector-valued H^1 functions.

The discrete approximation of $H(\mathrm{div})$ functions employs the space of Raviart-Thomas functions [91, 86] with the identity mapping $\mathrm{id} : \Omega \to \mathbb{R}^3$

$$\begin{aligned} RT_k(\mathcal{T}) &\coloneqq \big\{\tau_{\mathrm{RT}} \in H(\mathrm{div},\Omega) \,:\, \forall T\in\mathcal{T}\ \exists a_T \in P_k(T;\mathbb{R}^3)\ \exists b_T \in P_k(T), \\ &\qquad\qquad \tau_{\mathrm{RT}}|_T = a_T + b_T\,\mathrm{id}\big\}, \\ RT_k(\mathcal{T};\mathbb{R}^{3\times3}) &\coloneqq \big\{\tau_{\mathrm{RT}} = (\tau_{\ell m})_{\ell,m=1,\dots,3} \in H(\mathrm{div},\Omega;\mathbb{R}^{3\times3}) \,: \\ &\qquad\qquad \forall \ell = 1,2,3,\ (\tau_{\ell1},\tau_{\ell2},\tau_{\ell3})^\top \in RT_k(\mathcal{T})\big\}. \end{aligned}$$

The $H(\mathrm{curl})$-conforming Nédélec functions of the first kind [86, 87, 65] read

$$\begin{aligned} N_k(\mathcal{T}) &\coloneqq \big\{\beta_{\mathrm{Ned}} \in H(\mathrm{curl},\Omega) \,:\, \forall T\in\mathcal{T}\ \exists a_T, b_T \in P_k(\mathcal{T};\mathbb{R}^3), \\ &\qquad\qquad \beta_{\mathrm{Ned}}|_T = a_T + b_T \times \mathrm{id}\big\}, \\ N_k(\mathcal{T};\mathbb{R}^{3\times3}) &\coloneqq \big\{\beta_{\mathrm{Ned}} = (\beta_{\ell m})_{\ell,m=1,\dots,3} \in H(\mathrm{curl},\Omega;\mathbb{R}^{3\times3}) \,: \\ &\qquad\qquad \forall \ell = 1,2,3,\ (\beta_{\ell1},\beta_{\ell2},\beta_{\ell3})^\top \in N_k(\mathcal{T})\big\}. \end{aligned}$$

For an analysis of the presented finite element function spaces, the reader is referred to the monographs [23, 19, 18]. Figure 2.4 depicts the lowest-order finite elements for the discretisation employed in this thesis.

The normal trace operator γ^{nor} from Section 2.2 is surjective from the Raviart-Thomas space $RT_k(\mathcal{T})$ onto the piecewise polynomial functions $P_k(\mathcal{F}(\partial\Omega))$ on the boundary. The following lemma asserts the existence of a discrete extension of these boundary data.

Lemma 2.7 (discrete extension in RT_k). *Given some piecewise polynomial function $t_{\mathrm{pw}} \in P_k(\mathcal{F}(\partial\Omega))$ with*

$$\fint_{\partial\Omega} t_{\mathrm{pw}}\,\mathrm{d}a = 0, \tag{2.21}$$

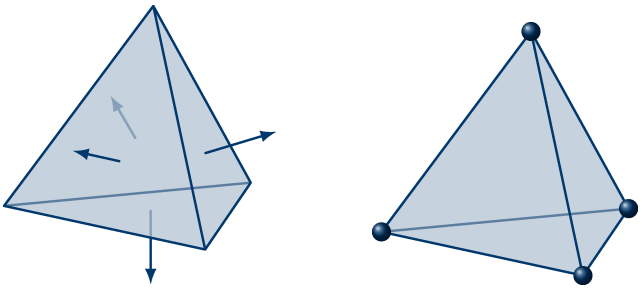

(a) RT_0 **(b)** S^1

Figure 2.4: Pictograms of lowest-order Raviart-Thomas finite elements RT_0 in (a) with 4 degrees of freedom and Courant finite elements S^1 in (b) with 4 degrees of freedom. The arrows represent the integral mean of the normal component on the corresponding face and balls symbolise the point evaluations in the vertices.

there exists a discrete extension $\rho_{\mathrm{RT}} \in RT_k(\mathcal{T})$ *with* $\operatorname{div} \rho_{\mathrm{RT}} = 0$ *in* Ω *and* $\rho_{\mathrm{RT}} \cdot \nu = t_{\mathrm{pw}}$. *Moreover, there exists a positive generic constant* C_{ext} *such that*

$$\|\rho_{\mathrm{RT}}\|_{L^2(\Omega)} \leq C_{\mathrm{ext}} \, \|t_{\mathrm{pw}}\|_{H^{-1/2}(\partial\Omega)}. \tag{2.22}$$

Proof. Since the result is proven in [2, Theorem 2.1], the proof at hand solely presents the construction of ρ_{RT} and an overview of the arguments. Let $w \in H^1(\Omega)/\mathbb{R}$ solve the Neumann problem

$$(\nabla w, \nabla v)_{L^2(\Omega)} = (t_{\mathrm{pw}}, v)_{L^2(\partial\Omega)} \quad \text{for all } v \in H^1(\Omega)/\mathbb{R}.$$

This is well-posed due to the compatibility condition (2.21). The integration by parts shows that the weak derivative $\rho := \nabla w := \mathrm{D}\, w \in H(\operatorname{div}, \Omega; \mathbb{R}^{3\times 3})$ satisfies $\operatorname{div} \rho = 0$ in Ω and $\rho\nu = t_{\mathrm{pw}}$ on $\partial\Omega$. The reduced elliptic regularity [54] of the Neumann problem ensures that $\rho \in H^{1/2+s}(\Omega; \mathbb{R}^3) \cap H(\operatorname{div}, \Omega)$ for some regularity parameter $0 < s < 1/2$. This allows for the application of the Fortin interpolation $I_{\mathrm{F}} : L^p(\Omega; \mathbb{R}^3) \cap H(\operatorname{div}, \Omega) \to RT_k(\mathcal{T})$ for $p > 2$ from [18, Example 2.5.3] to define $\rho_{\mathrm{RT}} := I_{\mathrm{F}}\rho$. The commuting diagram property of I_{F} shows

$$\operatorname{div} \rho_{\mathrm{RT}} = \operatorname{div} I_{\mathrm{F}}\rho = \Pi_k \operatorname{div} \rho = 0.$$

The definition of I_{F} [18, Equation (2.5.10)] leads to

$$\rho_{\mathrm{RT}} \cdot \nu = (I_{\mathrm{F}}\rho) \cdot \nu = \Pi_k(\rho \cdot \nu) = t_{\mathrm{pw}}.$$

The proof of the stability (2.22) is more complex and involves a localised elliptic regularity estimate and an inverse inequality for the boundary data. □

The remaining part of this section is devoted to the existence of L^2-stable vector potentials in the space of Nédélec finite element functions with homogeneous tangential boundary conditions

$$B^k_{\mathrm{N}}(\mathcal{T}) := N_k(\mathcal{T}) \cap H_{\mathrm{N}}(\operatorname{curl}, \Omega).$$

Theorem 2.8. *Suppose that Ω and Γ_N satisfy Assumption 2 from Section 2.3. Let $\mathcal{T}_0$ denote some initial triangulation with admissible refinement $\mathcal{T} \in \mathbb{T}$. Given a discrete vector field $\rho_{RT} \in RT_k(\mathcal{T})$ with $\operatorname{div} \rho_{RT} = 0$ and $\rho_{RT} \cdot \nu = 0$ on Γ_N, there exists a discrete vector potential $\beta_{Ned} \in B_N^k(\mathcal{T})$ and some vector field $\rho_{RT}^* \in RT_k(\mathcal{T}_0)$ on the initial triangulation $\mathcal{T}_0$ with $\operatorname{div} \rho_{RT}^* = 0$ in Ω and $\rho_{RT}^* \cdot \nu = 0$ on Γ_N such that*

$$\rho_{RT} = \operatorname{curl} \beta_{Ned} + \rho_{RT}^*.$$

Additionally, there exists a positive generic constant C_{Ned} such that

$$\|\beta_{Ned}\|_{H(\operatorname{curl},\Omega)} + \|\rho_{RT}^*\|_{L^2(\Omega)} \leq C_{Ned} \, \|\rho_{RT}\|_{L^2(\Omega)}. \tag{2.23}$$

Proof. Step 1. For $j = 0, \dots, J$, set the constants

$$\alpha_j := \begin{cases} \dfrac{1}{|\Gamma_j \cap \Gamma_D|} \displaystyle\int_{\Gamma_j \cap \Gamma_D} \rho_{RT} \cdot \nu \, da & \text{if } |\Gamma_j \cap \Gamma_D| > 0, \\ 0 & \text{else.} \end{cases}$$

Since the initial triangulation $\mathcal{T}_0$ resolves the partition of the boundary $\partial\Omega = \Gamma_D \cup \Gamma_N$, these constants define a piecewise constant function $\alpha_{pw}^* \in P_0(\mathcal{F}_0(\partial\Omega)) \subset H^{-1/2}(\partial\Omega)$ with respect to $\mathcal{T}_0$ by

$$\alpha_{pw}^* \equiv \alpha_j \text{ on } \Gamma_j \cap \Gamma_D \text{ for } j = 0, \dots, J \quad \text{and} \quad \alpha_{pw}^* \equiv 0 \text{ on } \Gamma_N.$$

Since $\operatorname{dist}(\Gamma_j, \Gamma_m) > 0$ for $j \neq m$, there exist smooth cut-off functions $\vartheta_j \in C^\infty(\Omega)$ for $j = 0, \dots, J$ with

$$\vartheta_j \equiv 1 \text{ on } \Gamma_j \quad \text{and} \quad \operatorname{dist}(\operatorname{supp}(\vartheta_j), \operatorname{supp}(\vartheta_m)) > 0 \text{ for } j \neq m.$$

Furthermore, define the positive generic constant

$$c_1 := \max_{j=0,\dots,J} \|\vartheta_j\|_{H^1(\Omega)},$$

that solely depends on the geometry of Ω. An integration by parts establishes

$$\int_{\Gamma_j \cap \Gamma_D} \rho_{RT} \cdot \nu \, da = (\vartheta_j, \rho_{RT} \cdot \nu)_{L^2(\partial\Omega)} = (\nabla \vartheta_j, \rho_{RT})_{L^2(\Omega)} + (\vartheta_j, \operatorname{div} \rho_{RT})_{L^2(\Omega)}.$$

The sum of this over $j = 0, \dots, J$ and the Cauchy-Schwarz inequality result in

$$\sum_{j=0}^{J} |\Gamma_j \cap \Gamma_D| \alpha_j = \sum_{j=0}^{J} \int_{\Gamma_j \cap \Gamma_D} \rho_{RT} \cdot \nu \, da \leq c_1 \, \|\rho_{RT}\|_{H(\operatorname{div},\Omega)}.$$

Another Cauchy-Schwarz inequality and the boundedness of the trace operator γ from (2.3) lead to

$$\begin{aligned}\|\alpha^*_{\mathrm{pw}}\|_{H^{-1/2}(\partial\Omega)} &= \sup\left\{\langle\alpha^*_{\mathrm{pw}}, \gamma(w)\rangle_{\partial\Omega} \ : \ w \in H^1(\Omega), \|w\|_{H^1(\Omega)} = 1\right\}\\ &\leq \sup\left\{\|\gamma(w)\|_{L^2(\partial\Omega)} \ : \ w \in H^1(\Omega), \|w\|_{H^1(\Omega)} = 1\right\} \sum_{j=0}^{J} \|\alpha_j\|_{L^2(\Gamma_{\mathrm{D}}\cap\Gamma_j)}\\ &\leq C_\gamma \sum_{j=0}^{J} |\Gamma_{\mathrm{D}} \cap \Gamma_j|\alpha_j \leq c_1 C_\gamma \, \|\rho_{\mathrm{RT}}\|_{H(\mathrm{div},\Omega)}.\end{aligned}$$

Step 2. Since $\operatorname{div}\rho_{\mathrm{RT}} = 0$ in Ω, the Gauss divergence theorem proves

$$\int_{\partial\Omega} \alpha^*_{\mathrm{pw}} \,\mathrm{d}a = \sum_{j=0}^{J} \int_{\Gamma_j\cap\Gamma_{\mathrm{D}}} \alpha_j \,\mathrm{d}a = \int_{\partial\Omega} \rho_{\mathrm{RT}} \cdot \nu \,\mathrm{d}a = \int_\Omega \operatorname{div}\rho_{\mathrm{RT}} \,\mathrm{d}x = 0.$$

Hence, Lemma 2.7 provides the existence of a discrete extension $\rho^*_{\mathrm{RT}} \in RT_k(\mathcal{T}_0)$ of α^*_{pw} on the initial triangulation such that $\operatorname{div}\rho^*_{\mathrm{RT}} = 0$ in Ω and $\rho^*_{\mathrm{RT}} \cdot \nu = \alpha^*_{\mathrm{pw}}$. The stability (2.22) shows

$$\|\rho^*_{\mathrm{RT}}\|_{H(\mathrm{div},\Omega)} \leq C_{\mathrm{ext}} \, \|\alpha^*_{\mathrm{pw}}\|_{H^{-1/2}(\partial\Omega)} \leq c_1 C_\gamma C_{\mathrm{ext}} \, \|\rho_{\mathrm{RT}}\|_{H(\mathrm{div},\Omega)}. \tag{2.24}$$

The definition of α^*_{pw} ensures, for $j = 0, \ldots, J$,

$$\int_{\Gamma_j} (\rho_{\mathrm{RT}} - \rho^*_{\mathrm{RT}}) \cdot \nu \,\mathrm{d}a = \int_{\Gamma_j\cap\Gamma_{\mathrm{D}}} (\rho_{\mathrm{RT}} - \rho^*_{\mathrm{RT}}) \cdot \nu \,\mathrm{d}a = 0.$$

The application of Assumption 2 leads to the existence of a vector potential $\beta \in H^1(\Omega;\mathbb{R}^3)$ with

$$\rho_{\mathrm{RT}} - \rho^*_{\mathrm{RT}} = \operatorname{curl}\beta \text{ in } \Omega \quad \text{and} \quad \nu \times \beta = 0 \text{ on } \Gamma_{\mathrm{N}}.$$

Moreover,

$$\|\beta\|_{H(\mathrm{curl},\Omega)} \leq \sqrt{2}\|\beta\|_{H^1(\Omega)} \leq \sqrt{2}C_{\mathrm{curl}} \, \|\rho_{\mathrm{RT}}\|_{L^2(\Omega)}. \tag{2.25}$$

Step 3. Let $\mathcal{P}_{\mathrm{Ned}} : L^2(\Omega;\mathbb{R}^3) \to B^k_{\mathrm{N}}(\mathcal{T})$ and $\mathcal{P}_{\mathrm{RT}} : L^2(\Omega;\mathbb{R}^3) \to RT_k(\mathcal{T}) \cap H_{\mathrm{N}}(\mathrm{div},\Omega)$ denote the projections from [77, Theorem 1.1] with the commuting diagram property

$$\begin{array}{ccc} H(\mathrm{curl},\Omega) & \xrightarrow{\mathrm{curl}} & H(\mathrm{div},\Omega) \\ \downarrow{\scriptstyle \mathcal{P}_{\mathrm{Ned}}} & & \downarrow{\scriptstyle \mathcal{P}_{\mathrm{RT}}} \\ N_k(\mathcal{T}) & \xrightarrow{\mathrm{curl}} & RT_k(\mathcal{T}) \end{array}.$$

These operators preserve partial homogeneous boundary conditions in that the equation $\nu \times \beta = 0$ on Γ_{N} implies that $\beta_{\mathrm{Ned}} := \mathcal{P}_{\mathrm{Ned}}\beta$ satisfies $\nu \times \beta_{\mathrm{Ned}} = 0$ on Γ_{N}. Their

pointwise invariance property $\mathcal{P}_{\mathrm{RT}} q_{\mathrm{RT}} = q_{\mathrm{RT}}$ for all $q_{\mathrm{RT}} \in RT_k(\mathcal{T}) \cap H_{\mathrm{N}}(\mathrm{div}, \Omega)$ and the commuting diagram property lead to

$$\operatorname{curl} \beta_{\mathrm{Ned}} = \operatorname{curl} \mathcal{P}_{\mathrm{Ned}} \beta = \mathcal{P}_{\mathrm{RT}}(\rho_{\mathrm{RT}} - \rho_{\mathrm{RT}}^*) = \rho_{\mathrm{RT}} - \rho_{\mathrm{RT}}^*.$$

Further, the operators satisfy the L^2 stability estimates [77, Theorem 6.3] with some positive generic constant c_2, for all $q \in L^2(\Omega; \mathbb{R}^3)$,

$$\|\mathcal{P}_{\mathrm{Ned}} q\|_{L^2(\Omega)} \leq c_2 \, \|q\|_{L^2(\Omega)} \quad \text{and} \quad \|\mathcal{P}_{\mathrm{RT}} q\|_{L^2(\Omega)} \leq c_2 \, \|q\|_{L^2(\Omega)}.$$

The positive generic constant c_2 solely depends on the polynomial degree $k \in \mathbb{N}_0$, the geometric properties of Ω and Γ_{N}, and the initial triangulation $\mathcal{T}_0$. The commuting diagram property immediately implies the $H(\mathrm{curl})$ stability of $\mathcal{P}_{\mathrm{Ned}}$, for all $q \in H(\mathrm{curl}, \Omega)$,

$$\|\operatorname{curl} \mathcal{P}_{\mathrm{Ned}} q\|_{L^2(\Omega)} = \|\mathcal{P}_{\mathrm{RT}} \operatorname{curl} q\|_{L^2(\Omega)} \leq c_2 \, \|\operatorname{curl} q\|_{L^2(\Omega)}.$$

In particular, (2.25) shows

$$\|\beta_{\mathrm{Ned}}\|_{H(\mathrm{curl},\Omega)} \leq c_2 \, \|\beta\|_{H(\mathrm{curl},\Omega)}. \leq \sqrt{2} C_{\mathrm{curl}} c_3 \, \|\rho_{\mathrm{RT}}\|_{L^2(\Omega)}$$

This and (2.24) conclude the proof of the stability (2.23) with the positive generic constant $C_{\mathrm{Ned}} := c_1 C_\gamma C_{\mathrm{ext}} + \sqrt{2} C_{\mathrm{curl}} c_2$. □

2.6 Scott-Zhang quasi-interpolation operator

This section introduces two modifications of the Scott-Zhang quasi-interpolation operator from [96] and presents their entire construction. The first operator $\mathcal{J}_{\mathrm{X}}^{k+1} : H^1(\Omega) \to S^{k+1}(\mathcal{T})$ preserves polynomial boundary conditions up to degree $k+1$ on one part $\Gamma_{\mathrm{X}} \in \{\Gamma_{\mathrm{D}}, \Gamma_{\mathrm{N}}\}$ of the boundary and enables the interpolation of the given Dirichlet boundary data as described in Section 3.3. For any admissible refinement $\widehat{\mathcal{T}} \in \mathbb{T}(\mathcal{T})$ of $\mathcal{T} \in \mathbb{T}$, the second operator $\mathcal{K}_{\mathrm{X}}^{k+1} : S^{k+1}(\widehat{\mathcal{T}}) \to S^{k+1}(\mathcal{T})$ allows for the preservation of the values on the unrefined simplices $\widehat{\mathcal{T}} \cap \mathcal{T}$ and is solely employed in the analysis of the discrete reliability in Section 4.2 below. Throughout the thesis, $\mathcal{J}_{\mathrm{X}}^{k+1}$ or $\mathcal{K}_{\mathrm{X}}^{k+1}$ act componentwise when applied to vector fields $w \in H^1(\Omega; \mathbb{R}^3)$.

The definition the Scott-Zhang quasi-interpolation of some $v \in H^1(\Omega)$ proceeds as follows. Let $(\phi_m \ : \ m = 1, \dots, M)$ for $M := \dim(S^{k+1}(\mathcal{T}))$ denote the nodal basis functions of $S^{k+1}(\mathcal{T})$ with associated nodes $\mathcal{I}_{k+1} := (a_m \in \overline{\Omega} \ : \ m = 1, \dots, M)$ such that

$$\phi_m(a_n) = \delta_{mn} := \begin{cases} 1 & \text{if } m = n, \\ 0 & \text{else.} \end{cases}$$

In particular, $\mathcal{I}_1 = \mathcal{N}$ or $\mathcal{I}_2 = \mathcal{N} \cup \{\mathrm{mid}(E) \ : \ E \in \mathcal{E}\}$. The local definition of the coefficients of the nodal basis functions in [96, Section 2] are determined by a weighted integral of v over some two- or three-dimensional closed simplex S_m. The choice of

S_m depends on the location of the node a_m and allows to impose some additional properties on the quasi-interpolation.

If $a_m \in \operatorname{int}(T)$ belongs to some simplex $T \in \mathcal{T}$, set $S_m := T$. If $a_m \in \operatorname{relint}(F)$ belongs to the relative interior of some face $F \in \mathcal{F}$, set $S_m := F$. Any other a_m belongs to some edge or is the vertex of a simplex and the choice of S_m is subject to one of the following conditions.

Condition 1. Fix one part $\Gamma_X \in \{\Gamma_D, \Gamma_N\}$ of the boundary. For any node $a_m \in \mathcal{N}$ or $a_m \in E$ on some edge $E \in \mathcal{E}$, if $a_m \in \overline{\Gamma}_X$ belongs to this part Γ_X, choose some subordinated face $S_m \in \mathcal{F}(\Gamma_X)$ with $a_m \in S_m$. Any remaining S_m can be chosen arbitrarily.

This condition constitutes the operator $\mathcal{J}_X^{k+1}$ in Definition 2.9 below [4, Section 3.1].

Condition 2. Fix one part $\Gamma_X \in \{\Gamma_D, \Gamma_N\}$ of the boundary and one admissible refinement $\widehat{\mathcal{T}} \in \mathbb{T}(\mathcal{T})$ of $\mathcal{T}$. For any node $a_m \in \mathcal{N}$ or $a_m \in E$ on some edge $E \in \mathcal{E}$, if $a_m \in T$ belongs to some unrefined $T \in \widehat{\mathcal{T}} \cap \mathcal{T}$, choose some unrefined face $S_m \in \widehat{\mathcal{F}} \cap \mathcal{F}$ with $a_m \in S_m$. If this is not possible (in the case that any $F \in \mathcal{F}$ with $a_m \in F$ has been refined) and $a_m \in \overline{\Gamma}_X$, choose $S_m \in \mathcal{F}(\Gamma_X)$ with $a_m \in S_m$. Any remaining S_m can be chosen arbitrarily.

This condition leads to the operator $\mathcal{K}_X^{k+1}$ in Definition 2.10 below [48, Section 3.2].

For every $m = 1, \dots, M$, let the functions $(\phi_{m,n} \in P_{k+1}(S_m) \ : \ n = 1, \dots, N_m)$ for $N_m := \dim(P_{k+1}(S_m))$ denote the canonical nodal basis of $P_{k+1}(S_m)$. Without loss of generality, $\phi_{m,1} = \phi_m|_{S_m}$. Define $(\psi_{m,n} \in P_{k+1}(S_m) \ : \ n = 1, \dots, N_j)$ as the Riesz representatives in the Hilbert space $P_{k+1}(S_m) \subset L^2(S_m)$ of the point evaluations in the nodes $\mathcal{I}_{k+1} \cap S_m$, for $n, \nu = 1, \dots, N_m$,

$$(\psi_{m,n}, \phi_{m,\nu})_{L^2(S_m)} = \delta_{n\nu}.$$

For $\psi_m := \psi_{m,1}$ and $m, n = 1, \dots, M$, it holds that

$$(\psi_m, \phi_n)_{L^2(S_m)} = \delta_{mn}. \tag{2.26}$$

Definition 2.9. Given any part $\Gamma_X \in \{\Gamma_D, \Gamma_N\}$ of the boundary and some $v \in H^1(\Omega)$, let the choice of the domains S_m meet the Condition 1 and define $\mathcal{J}_X^{k+1} v$ by nodal interpolation of the values at $a_m \in \mathcal{I}_{k+1}$ with

$$(\mathcal{J}_X^{k+1} v)(a_m) = (\psi_m, v)_{L^2(S_m)}.$$

Definition 2.10. Given any admissible refinement $\widehat{\mathcal{T}} \in \mathbb{T}(\mathcal{T})$ of $\mathcal{T}$, any part $\Gamma_X \in \{\Gamma_D, \Gamma_N\}$ of the boundary, and some $\widehat{v}_C \in S^{k+1}(\widehat{\mathcal{T}})$, let the choice of the domains S_m meet the Condition 2 and define $\mathcal{K}_X^{k+1} \widehat{v}_C$ by nodal interpolation of the values in $a_m \in \mathcal{I}_{k+1}$ with

$$(\mathcal{K}_X^{k+1} \widehat{v}_C)(a_m) = (\psi_m, \widehat{v}_C)_{L^2(S_m)}$$

Remark 2.11. The Definition 2.10 applies to discrete functions $\widehat{v}_C$ with respect to some refinement $\widehat{\mathcal{T}} \in \mathbb{T}(\mathcal{T})$. This defines a class of operators $\mathcal{K}_X^{k+1}(\widehat{\mathcal{T}}, \mathcal{T}) : S^{k+1}(\widehat{\mathcal{T}}) \to S^{k+1}(\mathcal{T})$ whereas $\mathcal{J}_X^{k+1}(\mathcal{T})$ solely depends on $\mathcal{T}$. To emphasize this difference, the two operators are distinguished in this thesis, although $\mathcal{K}_X^{k+1}$ has similar properties to $\mathcal{J}_X^{k+1}$ due to the following lemma. However, all dependencies on the triangulations are omitted.

Recall the positive generic constant C_{OL} from (2.16).

Lemma 2.12. *The two modifications, $\mathcal{J} = \mathcal{J}_X^{k+1}$ and $\mathcal{J} = \mathcal{K}_X^{k+1}$, of the Scott-Zhang quasi-interpolation operator satisfy*

(a) the pointwise invariance property, for all $v_C \in S^{k+1}(\mathcal{T})$, $\mathcal{J} v_C = v_C$,

(b) the local stability and the first-order approximation property with a positive generic constant C_{SZ} such that, for all $v \in H^1(\Omega)$ and $T \in \mathcal{T}$,

$$\| \nabla(1 - \mathcal{J})v\|_{L^2(T)} + \|h_T^{-1}(1 - \mathcal{J})v\|_{L^2(T)} \leq C_{SZ} \| \nabla v\|_{L^2(\Omega_T)}$$

with the tetrahedron patch Ω_T from (2.15)*,*

(c) the global stability and the first-order approximation property, for all $v \in H^1(\Omega)$,

$$\| \nabla(1 - \mathcal{J})v\|_{L^2(\Omega)} + \|h_{\mathcal{T}}^{-1}(1 - \mathcal{J})v\|_{L^2(\Omega)} \leq C_{OL}C_{SZ} \| \nabla v\|_{L^2(\Omega)},$$

(d) the H^1 stability, for all $v \in H^1(\Omega)$,

$$\|\mathcal{J} v\|_{H^1(\Omega)} \leq (1 + \max\{1, h_{\max}\}C_{OL}C_{SZ}) \|v\|_{H^1(\Omega)},$$

(e) the preservation of polynomial boundary data on Γ_X, i.e., if there exists some $v_C \in S^{k+1}(\mathcal{F}(\Gamma_X))$ with $v = v_C$ on Γ_X, then $\mathcal{J} v = v_C$ on Γ_X; in particular, $\mathcal{J}$ preserves homogeneous boundary conditions.

Moreover, for any admissible refinement $\widehat{\mathcal{T}} \in \mathbb{T}(\mathcal{T})$ of $\mathcal{T}$, every $\widehat{v}_C \in S^{k+1}(\widehat{\mathcal{T}})$ satisfies that

(f) the approximation error $(1 - \mathcal{J}_X^{k+1})\widehat{v}_C|_T = 0$ vanishes on every $T \in \mathcal{T} \setminus \mathcal{R}_1$,

(g) in particular, the approximation error $(1 - \mathcal{J}_X^{k+1})\widehat{v}_C|_F = 0$ vanishes on every $F \in \mathcal{F}(\Gamma_X) \setminus \mathcal{L}_1(\mathcal{F} \setminus \widehat{\mathcal{F}}, \Gamma_X)$,

(h) the approximation error $(1 - \mathcal{K}_X^{k+1})\widehat{v}_C|_T = 0$ even vanishes on every $T \in \widehat{\mathcal{T}} \cap \mathcal{T}$.

Proof. The pointwise invariance property (a) has been shown in [96, Equation (2.18)] and the local stability and first order approximation estimate (b) in [96, Theorem 3.1]

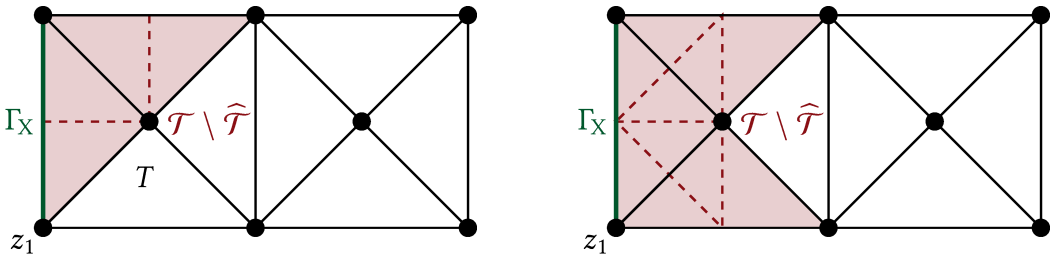

(a) Case 1 **(b)** Case 2

Figure 2.5: In two spatial dimensions, one has to choose an edge $S_m = E$ for the interpolation node $a_m = z_1 \in \mathcal{N}$. To define the value of $\mathcal{K}_X^{k+1}\widehat{v}_C(z_1)$ in Case 1, any of the two edges $E \in \mathcal{E}(T)$ of triangle T with $z_1 \in E$ can be chosen and polynomial boundary conditions are preserved. In Case 2, Condition 2 requires $E \in \mathcal{E}(\Gamma_X)$ and polynomial boundary conditions are preserved as well.

and [96, Equation (4.3)]. This and the finite overlap of the patches Ω_T immediately imply (c). The H^1 stability (d) follows from (c) in

$$\begin{aligned}\min\{1, h_{\max}^{-1}\}\|(1 - \mathcal{J}^{k+1})v\|_{H^1(\Omega)} &\leq \|\nabla(1 - \mathcal{J}^{k+1})v\|_{L^2(\Omega)} + \|h_{\mathcal{T}}^{-1}(1 - \mathcal{J}^{k+1})v\|_{L^2(\Omega)} \\ &\leq C_{OL}C_{SZ}\,\|\nabla v\|_{L^2(\Omega)}\end{aligned}$$

in combination with the equality $\min\{1, h_{\max}^{-1}\}^{-1} = \max\{1, h_{\max}\}$ and the triangle inequality.

For the operator $\mathcal{J}_X^{k+1}$, property (e) is ensured by Condition 1 and (2.26) in

$$(\mathcal{J}_X^{k+1}v)(a_m) = (\psi_m, v_C)_{L^2(S_m)} = v_C(a_m).$$

However, for the operator $\mathcal{K}_X^{k+1}$, if $a_m \in \overline{\Gamma}_X$ and $a_m \in T$ belongs to some $T \in \widehat{\mathcal{T}} \cap \mathcal{T}$, Condition 2 and the property (2.26) lead to

$$(\mathcal{K}_X^{k+1}\widehat{v}_C)(a_m) = (\psi_m, \widehat{v}_C)_{L^2(S_m)} = \widehat{v}_C(a_m).$$

If $a_m \in \overline{\Gamma}_X$ and if there exists no $T \in \widehat{\mathcal{T}} \cap \mathcal{T}$ with $a_m \in T$, then Condition 2 and $\widehat{v}_C = v_C$ on Γ_X ensure that

$$(\mathcal{K}_X^{k+1}\widehat{v}_C)(a_m) = (\psi_m, \widehat{v}_C)_{L^2(\Omega)} = 0.$$

Thus, $\mathcal{K}_X^{k+1}$ satisfies (e) as well. Figure 2.5 illustrates the critical cases for the definition of the value of $\mathcal{K}_X^{k+1}\widehat{v}_C$ on the boundary Γ_X in 2D.

The locality (f) follows from the fact that, for any $a_m \in T$ with $T \in \mathcal{T} \setminus \mathcal{R}_1$, the simplex $S_m \in \mathcal{T}$ or the face $S_m \in \mathcal{F}$ belong to the coarse triangulation $\mathcal{T}$. Thus, (2.26) shows

$$(\mathcal{J}_X^{k+1}\widehat{v}_C)(a_m) = (\psi_m, \widehat{v}_C)_{L^2(S_m)} = \widehat{v}_C(a_m). \tag{2.27}$$

Since the value $(\mathcal{J}_X^{k+1}\widehat{v}_C)(a_m)$ solely depends on the values of $\widehat{v}_C$ on Γ_D, this also establishes (g). For $\mathcal{K}_X^{k+1}$, Condition 2 ensures that (2.27) even holds for $a_m \in T$ with $T \in \widehat{\mathcal{T}} \cap \mathcal{T}$. □

2.7 Boundary preserving quasi-interpolation operators

This section presents two quasi-interpolation operators for Nédélec finite element functions with homogeneous tangential boundary conditions on Γ_N in the space $B^k_N(\mathcal{T})$. Every operator acts componentwise when applied to matrix-valued functions.

The quasi-interpolation operator $\mathcal{S}_{\mathrm{Ned}} : H_N(\mathrm{curl}, \Omega) \to B^0_N(\mathcal{T})$ from [93, Theorem 1] preserves homogeneous boundary conditions, but has been established solely for the lowest-order case. The following theorem summarises its main properties.

Theorem 2.13. *Given $\beta \in H_N(\mathrm{curl}, \Omega)$, there exists $\phi \in H^1_N(\Omega)$ and $z \in H^1_N(\Omega; \mathbb{R}^3)$ such that the following regular split of the quasi-interpolation error holds*

$$(1 - \mathcal{S}_{\mathrm{Ned}})\beta = z + \nabla \phi \tag{2.28}$$

The local approximation error estimate involves the positive generic constant C_{Sch}, for every $T \in \mathcal{T}$,

$$\begin{aligned} \|h_{\mathcal{T}}^{-1} z\|_{L^2(T)} + \|\mathrm{D}\, z\|_{L^2(T)} &\leq C_{\mathrm{Sch}} \,\|\mathrm{curl}\, \beta\|_{L^2(\Omega_T)}, \\ \|h_{\mathcal{T}}^{-1} \phi\|_{L^2(T)} + \|\nabla \phi\|_{L^2(T)} &\leq C_{\mathrm{Sch}} \,\|\beta\|_{L^2(\Omega_T)}. \end{aligned} \tag{2.29}$$

In particular,

$$\beta|_{\Omega_T} = 0 \quad \textit{implies} \quad \mathcal{S}_{\mathrm{Ned}}\beta|_T = (1 - \mathcal{S}_{\mathrm{Ned}})\beta|_T = 0. \tag{2.30}$$

Proof. The regular split (2.28) with partial homogeneous boundary conditions and the estimates (2.29) have been proven in [93, Theorem 1]. The operator is defined locally in that values of $\mathcal{S}_{\mathrm{Ned}}\beta$ on a simplex $T \in \mathcal{T}$ solely depend on the values of $\beta \in H_N(\mathrm{curl}, \Omega)$ on the tetrahedron patch Ω_T from (2.15). The implication (2.30) follows from the combination of the two local estimates in (2.29). □

Let $\widehat{\mathcal{T}} \in \mathbb{T}(\mathcal{T})$ denote an admissible refinement of $\mathcal{T} \in \mathbb{T}$ and apply Notation 3 from page 22. Recall the definition of $\mathcal{R}_\ell$ from Section 2.4. The following theorem asserts the existence of a stable local projection as introduced by [106, Theorem 4.1] for Nédélec functions with homogeneous tangential boundary conditions on Γ_N.

Theorem 2.14. *There exists a quasi-interpolation operator $Q_{\mathrm{Ned}} : B^k_N(\widehat{\mathcal{T}}) \to B^k_N(\mathcal{T})$ such that, for all $\widehat{\beta}_{\mathrm{Ned}} \in B^k_N(\widehat{\mathcal{T}})$,*

(i) $(1 - Q_{\mathrm{Ned}})\widehat{\beta}_{\mathrm{Ned}} \equiv 0$ *in every* $T \in \mathcal{T} \setminus \mathcal{R}_2$,

(ii) $\|(1 - Q_{\mathrm{Ned}})\widehat{\beta}_{\mathrm{Ned}}\|_{H(\mathrm{curl},\Omega)} \leq C_{\mathrm{qi}} \,\|\widehat{\beta}_{\mathrm{Ned}}\|_{H(\mathrm{curl},\Omega)}$.

The proof of Theorem 2.14 follows the strategy from [106] to construct Q_{Ned}, while it employs a boundary-aware discrete regular decomposition from [70] and the boundary data preserving quasi-interpolation operator $\mathcal{S}_{\mathrm{Ned}}$ from Theorem 2.13. It requires several operators introduced in the following lemmas.

Lemma 2.15. *There exists a cut-off operator* $\chi_R : B^k_{\mathrm{N}}(\widehat{\mathcal{T}}) \to B^k_{\mathrm{N}}(\widehat{\mathcal{T}})$ *with*

$$\chi_R\widehat{\beta}_{\mathrm{Ned}}|_K = 0 \text{ for all } K \in \mathcal{T} \setminus \mathcal{R}_1 \quad \text{and} \quad \chi_R\widehat{\beta}_{\mathrm{Ned}}|_T = \widehat{\beta}_{\mathrm{Ned}}|_T \text{ for all } T \in \mathcal{T} \setminus \widehat{\mathcal{T}}. \tag{2.31}$$

If $\widehat{\beta}_{\mathrm{Ned}} \in B^k_{\mathrm{N}}(\widehat{\mathcal{T}})$ *satisfies* $\|h_{\mathcal{T}}^{-1}\widehat{\beta}_{\mathrm{Ned}}\|_{L^2(\Omega)} \leq C_{\mathrm{freq}} \|\widehat{\beta}_{\mathrm{Ned}}\|_{H(\mathrm{curl},\Omega)}$*, then the stability estimate*

$$\|\chi_R\widehat{\beta}_{\mathrm{Ned}}\|_{H(\mathrm{curl},\Omega)} \leq C_{\mathrm{cut}} \|\widehat{\beta}_{\mathrm{Ned}}\|_{H(\mathrm{curl},\Omega)} \tag{2.32}$$

holds with a positive generic constant C_{cut}.

Proof. Let $\widehat{b}_1, \dots, \widehat{b}_M \in B^k_{\mathrm{N}}(\widehat{\mathcal{T}})$ denote the canonical basis functions of $B^k_{\mathrm{N}}(\widehat{\mathcal{T}})$ with $M = \dim(B^k_{\mathrm{N}}(\widehat{\mathcal{T}}))$. Define the index set

$$R := \big\{m = 1, \dots, M \ : \ \widehat{b}_m \notin B^k_{\mathrm{N}}(\mathcal{T})\big\}.$$

Following [106, Section 4.1.1], define

$$\chi_R\widehat{\beta}_{\mathrm{Ned}} := \sum_{m\in R} \alpha_m \widehat{b}_m \quad \text{for all } \widehat{\beta}_{\mathrm{Ned}} = \sum_{m=1}^{M} \alpha_m \widehat{b}_m.$$

This ensures the locality (2.31). The operator χ_R preserves boundary conditions in that $\nu \times \widehat{\beta}_{\mathrm{Ned}} = 0$ on Γ_{N} implies $\nu \times (\chi_R\widehat{\beta}_{\mathrm{Ned}}) = 0$ on Γ_{N}. The L^2 stability of χ_R [69, Section 3.6, Equation (3.37)] reads

$$\|\chi_R\widehat{\beta}_{\mathrm{Ned}}\|_{L^2(\Omega)} \leq c_1 \|\widehat{\beta}_{\mathrm{Ned}}\|_{L^2(\Omega)} \quad \text{for all } \widehat{\beta}_{\mathrm{Ned}} \in B^k_{\mathrm{N}}(\widehat{\mathcal{T}}).$$

An inverse estimate [60, Section 1.7] leads to a positive generic constant c_2 with

$$\|\chi_R\widehat{\beta}_{\mathrm{Ned}}\|_{H(\mathrm{curl},\Omega)} \leq c_2 \|h_{\mathcal{T}}^{-1}\chi_R\widehat{\beta}_{\mathrm{Ned}}\|^2_{L^2(\Omega)}.$$

The combination of the two previously displayed formulas proves the stability estimate (2.32) with positive generic constant $C_{\mathrm{cut}} := c_1c_2C_{\mathrm{freq}}$ [106, Section 4.1.1], for every $\widehat{\beta}_{\mathrm{Ned}} \in B^k_{\mathrm{N}}(\mathcal{T})$ with $\|h_{\mathcal{T}}^{-1}\widehat{\beta}_{\mathrm{Ned}}\|_{L^2(\Omega)} \leq C_{\mathrm{freq}} \|\widehat{\beta}_{\mathrm{Ned}}\|_{H(\mathrm{curl},\Omega)}$,

$$\|\chi_R\widehat{\beta}_{\mathrm{Ned}}\|_{H(\mathrm{curl},\Omega)} \leq c_1c_2 \|h_{\mathcal{T}}^{-1}\widehat{\beta}_{\mathrm{Ned}}\|_{L^2(\Omega)} \leq c_1c_2C_{\mathrm{freq}} \|\widehat{\beta}_{\mathrm{Ned}}\|_{H(\mathrm{curl},\Omega)}. \qquad \square$$

The piecewise polynomial and globally H^1 functions in $S^{k+1}(\mathcal{T})$ do not possess any jumps and, thus, are globally continuous. They satisfy the following slightly stronger regularity property.

Lemma 2.16. *For any* $0 < s < 1/2$, $S^{k+1}(\mathcal{T}) \subset H^{1+s}(\Omega)$.

Proof. This result is an immediate consequence of [73, Lemma 1] stating that piecewise smooth functions are H^s multipliers for $s < 1/2$. It is based on the characterisation of H^s regularity from [79, Theorem 10.2 in Chapter 1.10.2].

For arbitrary $v_C \in S^{k+1}(\mathcal{T})$, any component $g_j \in P_k(\mathcal{T})$ of its gradient $(g_1, g_2, g_3)^\top := \nabla v_C$ can be represented in the form

$$g_j = \sum_{T \in \mathcal{T}} \chi_T p_T$$

with bounded Lipschitz continuous functions $p_T \in C^{0,1}(\Omega)$ satisfying $p_T|_T \in P_k(T)$. Since the constant function $1 \in H^s(\Omega)$, [73, Lemma 1] implies $g_j\, 1 = g_j \in H^s(\Omega)$. □

The required discrete regular decomposition in the proof of Theorem 2.14 involves the following strictly local and continuous interpolation operator $\mathcal{H}_{\mathrm{Ned}}$ from [70, Section 4.1.4].

Lemma 2.17. *There exists a linear and bounded operator $\mathcal{H}_{\mathrm{Ned}} : H^{1+s}(\Omega;\mathbb{R}^3) \to N_k(\mathcal{T})$ such that $\mathcal{H}_{\mathrm{Ned}}$ is well-defined for any $s > 0$ and it holds that, for all $v_C \in S^{k+1}(\mathcal{T};\mathbb{R}^3)$,*

$$\|\mathcal{H}_{\mathrm{Ned}} v_C\|_{H(\mathrm{curl},\Omega)} \leq C_{\mathrm{HP}}\, \|v_C\|_{H(\mathrm{curl},\Omega)} \tag{2.33}$$

with a positive generic constant C_{HP} depending on $s > 0$. The operator $\mathcal{H}_{\mathrm{Ned}}$ preserves boundary conditions in that the image of $H^{1+s}(\Omega;\mathbb{R}^3) \cap H_{\mathrm{N}}(\mathrm{curl},\Omega)$ is $B^k_{\mathrm{N}}(\mathcal{T})$,

$$\mathcal{H}_{\mathrm{Ned}}\big(H^{1+s}(\Omega;\mathbb{R}^3) \cap H_{\mathrm{N}}(\mathrm{curl},\Omega)\big) = B^k_{\mathrm{N}}(\mathcal{T}).$$

Every $v, w \in H^{1+s}(\Omega,\mathbb{R}^3)$ and $T \in \mathcal{T}$ satisfy that

$$(v - w)|_T = 0 \quad \textit{implies} \quad (\mathcal{H}_{\mathrm{Ned}} v - \mathcal{H}_{\mathrm{Ned}} w)|_T = 0. \tag{2.34}$$

Proof. There exists some linear and bounded operator $\mathcal{H}_{\mathrm{RT}} : H^{1/2+s}(\Omega;\mathbb{R}^3) \to RT_k(\mathcal{T})$ such that $\mathcal{H}_{\mathrm{Ned}}$ satisfies the commuting diagram property [70, Lemma 4.7]

$$\begin{array}{ccc} C^\infty(\overline{\Omega}) & \xrightarrow{\mathrm{curl}} & C^\infty(\overline{\Omega}) \\ \big\downarrow{\scriptstyle \mathcal{H}_{\mathrm{Ned}}} & & \big\downarrow{\scriptstyle \mathcal{H}_{\mathrm{RT}}} \\ N_k(\mathcal{T}) & \xrightarrow{\mathrm{curl}} & RT_k(\mathcal{T}) \end{array}.$$

The space $RT_k(\mathcal{T})$ is pointwise invariant under $\mathcal{H}_{\mathrm{RT}}$ in the sense that $\mathcal{H}_{\mathrm{RT}}\rho_{\mathrm{RT}} = \rho_{\mathrm{RT}}$ for all $\rho_{\mathrm{RT}} \in RT_k(\mathcal{T})$ [70, this result is the projection property from Lemma 4.7].

Due to Lemma 2.16, the operator $\mathcal{H}_{\mathrm{Ned}}$ is well-defined on $S^{k+1}(\mathcal{T};\mathbb{R}^3)$ [70, Equation (4.92)]. For $v_C \in S^{k+1}(\mathcal{T};\mathbb{R}^3)$, $\operatorname{curl} v_C \in P_k(\mathcal{T};\mathbb{R}^3)$ and $\operatorname{div}\operatorname{curl} v_C = 0$ imply $\operatorname{curl} v_C \in RT_k(\mathcal{T})$. This shows, for any $T \in \mathcal{T}$,

$$\|\operatorname{curl}(1 - \mathcal{H}_{\mathrm{Ned}}) v_C\|_{L^2(T)} = \|(1 - \mathcal{H}_{\mathrm{RT}}) \operatorname{curl} v_C\|_{L^2(T)} = 0. \tag{2.35}$$

Since $\operatorname{curl} v_C \in P_k(\mathcal{T};\mathbb{R}^3)$, the estimate from [70, Lemma 4.16] leads to the existence of a positive generic constant c_1 depending on the polynomial degree k and satisfying, for all $T \in \mathcal{T}$ and $v_C \in S^{k+1}(\Omega;\mathbb{R}^3)$,

$$\|(1 - \mathcal{H}_{\mathrm{Ned}}) v_C\|_{L^2(T)} \leq c_1 h_T\, \|\mathrm{D}\, v_C\|_{L^2(T)}.$$

An inverse estimate [60, Section 1.7] with some positive generic constant c_2 leads to

$$\|(1-\mathcal{H}_{\mathrm{Ned}})v_{\mathrm{C}}\|_{L^2(T)} \leq c_1c_2\,\|v_{\mathrm{C}}\|_{L^2(T)}.$$

The combination of this with (2.35) and a triangle inequality prove the stability (2.33) with the positive generic constant $C_{\mathrm{HP}} := 1 + c_1c_2$. The preservation of homogeneous tangential boundary conditions has been established in [70, Equation (4.94)]. Finally, the strict locality from [70, Lemma 4.8] shows the implication (2.34). □

Proof of Theorem 2.14. Step 1. Given any $\widehat{\beta}_{\mathrm{Ned}} \in B^k_{\mathrm{N}}(\widehat{\mathcal{T}})$, the discrete regular decomposition from [70, Theorem 1.3] with respect to the triangulation $\widehat{\mathcal{T}}$ leads to some $\widehat{v}_{\mathrm{C}} \in S^{k+1}(\widehat{\mathcal{T}};\mathbb{R}^3)$ with $\widehat{v}_{\mathrm{C}} = 0$ on Γ_{N}, $\widehat{\phi}_{\mathrm{C}} \in S^{k+1}(\widehat{\mathcal{T}})$ with $\widehat{\phi}_{\mathrm{C}} = 0$ on Γ_{N}, and the remainder $\widetilde{\beta}_{\mathrm{Ned}} \in B^k_{\mathrm{N}}(\widehat{\mathcal{T}})$ for the decomposition

$$\widehat{\beta}_{\mathrm{Ned}} = \widehat{\mathcal{H}}_{\mathrm{Ned}}\widehat{v}_{\mathrm{C}} + \nabla\,\widehat{\phi}_{\mathrm{C}} + \widetilde{\beta}_{\mathrm{Ned}}$$

The functions $\widehat{v}_{\mathrm{C}}$, $\widehat{\phi}_{\mathrm{C}}$, and $\widetilde{\beta}_{\mathrm{Ned}}$ satisfy the stability estimates

$$\begin{aligned}\|\widehat{v}_{\mathrm{C}}\|_{L^2(\Omega)} + \|\nabla\,\widehat{\phi}_{\mathrm{C}}\|_{L^2(\Omega)} &\leq c_1\,\|\widehat{\beta}_{\mathrm{Ned}}\|_{L^2(\Omega)},\\ \|\mathrm{D}\,\widehat{v}_{\mathrm{C}}\|_{L^2(\Omega)} + \|h_{\mathcal{T}}^{-1}\widetilde{\beta}_{\mathrm{Ned}}\|_{L^2(\Omega)} &\leq c_2\,\|\widehat{\beta}_{\mathrm{Ned}}\|_{H(\mathrm{curl},\Omega)}.\end{aligned} \tag{2.36}$$

Recall the Scott-Zhang quasi-interpolation operator $\mathcal{K}^{k+1}_{\mathrm{N}}$ from Definition 2.10 with respect to the part Γ_{N} of the boundary. Following [106, Section 4.4], define

$$Q_{\mathrm{Ned}}\widehat{\beta}_{\mathrm{Ned}} := \mathcal{H}_{\mathrm{Ned}}\mathcal{K}^{k+1}_{\mathrm{N}}\widehat{v}_{\mathrm{C}} + \nabla\,\mathcal{K}^{k+1}_{\mathrm{N}}\widehat{\phi}_{\mathrm{C}} + \mathcal{S}_{\mathrm{Ned}}\chi_R\widetilde{\beta}_{\mathrm{Ned}} + (1-\chi_R)\widetilde{\beta}_{\mathrm{Ned}} \in N_k(\mathcal{T}).$$

Step 2. Since $\mathcal{K}^{k+1}_{\mathrm{N}}\widehat{v}_{\mathrm{C}}$ and $\mathcal{K}^{k+1}_{\mathrm{N}}\widehat{\phi}_{\mathrm{C}}$ satisfy homogeneous tangential boundary conditions on Γ_{N},

$$\nu \times \left(\mathcal{H}_{\mathrm{Ned}}\mathcal{K}^{k+1}_{\mathrm{N}}\widehat{v}_{\mathrm{C}} + \nabla\,\mathcal{K}^{k+1}_{\mathrm{N}}\widehat{\phi}_{\mathrm{C}}\right) = 0 \quad \text{on } \Gamma_{\mathrm{N}}.$$

The operators χ_R, $1-\chi_R$, and $\mathcal{S}_{\mathrm{N}}$ preserve homogeneous boundary conditions and, therefore,

$$\nu \times \left(\mathcal{S}_{\mathrm{N}}\chi_R\widetilde{\beta}_{\mathrm{N}} + (1-\chi_R)\widetilde{\beta}_{\mathrm{N}}\right) = 0 \quad \text{on } \Gamma_{\mathrm{N}}.$$

Consequently, $\nu \times Q_{\mathrm{Ned}}\widehat{\beta}_{\mathrm{Ned}} = 0$ on Γ_{N}.

Step 3. The quasi-interpolation error reads

$$(1-Q_{\mathrm{Ned}})\widehat{\beta}_{\mathrm{Ned}} = (\widehat{\mathcal{H}}_{\mathrm{Ned}} - \mathcal{H}_{\mathrm{Ned}}\mathcal{K}^{k+1}_{\mathrm{N}})\widehat{v}_{\mathrm{C}} + \nabla(1-\mathcal{K}^{k+1}_{\mathrm{N}})\widehat{\phi}_{\mathrm{C}} + (1-\mathcal{S}_{\mathrm{Ned}})\chi_R\widetilde{\beta}_{\mathrm{Ned}}.$$

The careful definition of the Scott-Zhang quasi-interpolation $\mathcal{K}^{k+1}_{\mathrm{N}}$ in Section 2.6 ensures that $(1-\mathcal{K}^{k+1}_{\mathrm{N}})\widehat{v}_{\mathrm{C}}|_K = 0$ and $(1-\mathcal{K}^{k+1}_{\mathrm{N}})\widehat{\phi}_{\mathrm{C}}|_K = 0$ vanish on any unrefined simplex $K \in \mathcal{T}\cap\widehat{\mathcal{T}}$. Hence, the implication (2.34) shows that $(\widehat{\mathcal{H}}_{\mathrm{Ned}} - \mathcal{H}_{\mathrm{Ned}}\mathcal{K}^{k+1}_{\mathrm{N}})v_{\mathrm{C}}|_K = 0$ vanishes on any unrefined simplex $K \in \mathcal{T}\cap\widehat{\mathcal{T}}$ as well.

By definition of the cut-off operator χ_R from Lemma 2.15, $(\chi_R\widetilde{\beta}_{\mathrm{Ned}})|_T = 0$ vanishes on any $T \in \mathcal{T} \setminus \mathcal{R}_1$. This and (2.30) show that $((1-\mathcal{S}_{\mathrm{Ned}})\chi_R\widetilde{\beta}_{\mathrm{Ned}})|_T = 0$ vanishes on any $T \in \mathcal{T} \setminus \mathcal{R}_2$. Since $\mathcal{T} \setminus \mathcal{R}_2 \subseteq \mathcal{T} \setminus \mathcal{R}_1 \subseteq \mathcal{T} \cap \widehat{\mathcal{T}}$, it follows that $((1-\mathcal{Q}_{\mathrm{Ned}})\widehat{\beta}_{\mathrm{Ned}})|_T = 0$ on any $T \in \mathcal{T} \setminus \mathcal{R}_2$.

Step 4. The triangle inequality and the stability estimate (2.33) show

$$\|(\widehat{\mathcal{H}}_{\mathrm{Ned}} - \mathcal{H}_{\mathrm{Ned}}\mathcal{K}_{\mathrm{N}}^{k+1})\widehat{v}_{\mathrm{C}}\|_{H(\mathrm{curl},\Omega)} \leq C_{\mathrm{HP}} \left(\|\widehat{v}_{\mathrm{C}}\|_{H(\mathrm{curl},\Omega)} + \|\mathcal{K}_{\mathrm{N}}^{k+1}\widehat{v}_{\mathrm{C}}\|_{H(\mathrm{curl},\Omega)}\right).$$

The estimate $\|\operatorname{curl}\widehat{v}_{\mathrm{C}}\|_{L^2(\Omega)} \leq \sqrt{2}\|\mathrm{D}\,\widehat{v}_{\mathrm{C}}\|_{L^2(\Omega)}$ and Lemma 2.12 (d) lead to

$$\|(\widehat{\mathcal{H}}_{\mathrm{Ned}} - \mathcal{H}_{\mathrm{Ned}}\mathcal{K}_{\mathrm{N}}^{k+1})\widehat{v}_{\mathrm{C}}\|_{H(\mathrm{curl},\Omega)} \leq C_{\mathrm{HP}}\sqrt{2}(2+\max\{1,h_{\max}\}C_{\mathrm{OL}}C_{\mathrm{SZ}})\,\|\widehat{v}_{\mathrm{C}}\|_{H^1(\Omega)}.$$

Hence, the stability estimates from (2.36) result in

$$\begin{aligned}&\|(\widehat{\mathcal{H}}_{\mathrm{Ned}} - \mathcal{H}_{\mathrm{Ned}}\mathcal{K}_{\mathrm{N}}^{k+1})\widehat{v}_{\mathrm{C}}\|_{H(\mathrm{curl},\Omega)}\\ &\quad\leq C_{\mathrm{HP}}\sqrt{2}(2+\max\{1,h_{\max}\}C_{\mathrm{OL}}C_{\mathrm{SZ}})(c_1+c_2)\,\|\widehat{\beta}_{\mathrm{Ned}}\|_{H(\mathrm{curl},\Omega)}.\end{aligned}$$

Moreover, the stability from Lemma 2.12 (c) and the estimate (2.36) prove

$$\|\nabla(1-\mathcal{K}_{\mathrm{N}}^{k+1})\widehat{\phi}_{\mathrm{C}}\|_{H(\mathrm{curl},\Omega)} \leq C_{\mathrm{OL}}C_{\mathrm{SZ}}\,\|\nabla\widehat{\phi}_{\mathrm{C}}\|_{L^2(\Omega)} \leq C_{\mathrm{OL}}C_{\mathrm{SZ}}c_1\,\|\widehat{\beta}_{\mathrm{Ned}}\|_{L^2(\Omega)}.$$

The sum of the local stability (2.29) over all $T \in \mathcal{T}$ leads to, for all $\beta \in H_{\mathrm{N}}(\mathrm{curl},\Omega)$,

$$\|(1-\mathcal{S}_{\mathrm{Ned}})\beta\|_{H(\mathrm{curl},\Omega)} \leq \max\{1,h_{\max}\}\,C_{\mathrm{OL}}C_{\mathrm{Sch}}\,\|\beta\|_{H(\mathrm{curl},\Omega)}.$$

Since $\|h_{\mathcal{T}}^{-1}\widetilde{\beta}_{\mathrm{Ned}}\|_{L^2(\Omega)} \leq c_2\,\|\widehat{\beta}_{\mathrm{Ned}}\|_{H(\mathrm{curl},\Omega)}$, this for $\beta = \widetilde{\beta}_{\mathrm{Ned}}$ and (2.32) verify

$$\|(1-\mathcal{S}_{\mathrm{Ned}})\chi_R\widetilde{\beta}_{\mathrm{Ned}}\|_{H(\mathrm{curl},\Omega)} \leq \max\{1,h_{\max}\}C_{\mathrm{OL}}C_{\mathrm{Sch}}C_{\mathrm{cut}}\,\|\widetilde{\beta}_{\mathrm{Ned}}\|_{H(\mathrm{curl},\Omega)}.$$

The combination of the three previously displayed formulas proves assertion (ii) with the positive stability constant

$$\begin{aligned}C_{\mathrm{qi}} \coloneqq\ & C_{\mathrm{HP}}\sqrt{2}(2+\max\{1,h_{\max}\}C_{\mathrm{OL}}C_{\mathrm{SZ}})(c_1+c_2)\\ &+ C_{\mathrm{OL}}C_{\mathrm{SZ}}c_1 + \max\{1,h_{\max}\}C_{\mathrm{OL}}C_{\mathrm{Sch}}C_{\mathrm{cut}}.\end{aligned}$$

□

3 Adaptive least-squares finite element method

This chapter introduces the LSFEM and the alternative a posteriori error estimation. To this end, the first Section 3.1 presents the generalised first-order system and formulates assumptions on the involved operators. Those assumptions guarantee well-posedness of the resulting LSFEM as well as the convergence analysis of the adaptive scheme. Subsequently, they are verified for the three model problems in Section 3.2.

The discrete solutions to the LSFEM have to explicitly satisfy some discrete boundary conditions. The Sections 3.3–3.4 present the approximation of the given boundary conditions in the appropriate spaces. Some extensions of the approximation errors on the boundary are required to remedy the lack of the Galerkin orthogonality in the case of inhomogeneous boundary data. The reader may skip both sections when the main interest is on homogeneous boundary conditions.

The Section 3.5 states the LSFEM and analyses its well-posedness based on the assumptions from Section 3.1. Furthermore, it verifies a posteriori estimates for the built-in error estimator. Eventually, the Section 3.6 introduces the a posteriori error estimator and the data approximation error for the ALSFEM algorithm from page 4.

3.1 Generalised model problem

This thesis investigates the LSFEM for the solution of a generalised model problem. It includes two bounded linear, not necessarily self-adjoint, operators $\mathcal{A}, \mathcal{S} : L^2(\Omega;\mathbb{R}^{3\times3}) \to L^2(\Omega;\mathbb{R}^{3\times3})$. They serve as the generalisation of the operators from the three model problems listed in Table 1 on page 3.

The assumptions on the linear operators $\mathcal{A}$ and $\mathcal{S}$ involve the seven positive generic constants $C_{\mathcal{A}}$, C_{tdd}, C_{En}, $C_{\mathcal{S}}$, C_{K}, C_{inv}, and C_{dti}. Throughout the thesis, suppose that

(W1) $\|\mathcal{A}\tau\|_{L^2(\Omega)} \leq C_{\mathcal{A}} \|\tau\|_{L^2(\Omega)}$ for all $\tau \in L^2(\Omega;\mathbb{R}^{3\times3})$,

(W2) $\|\tau\|^2_{L^2(\Omega)} \leq C_{\mathrm{tdd}} \big((\mathcal{A}\tau,\tau)_{L^2(\Omega)} + \|\operatorname{div}\tau\|^2_{L^2(\Omega)}\big)$ for all $\tau \in \Sigma_{\mathrm{N}}$,

(W3) $(\mathcal{S}\,\mathrm{D}\,v,\tau)_{L^2(\Omega)} \leq C_{\mathrm{En}} \big(\|\mathcal{A}\tau - \mathcal{S}\,\mathrm{D}\,v\|_{L^2(\Omega)} + \|\operatorname{div}\tau\|_{L^2(\Omega)}\big)\|\mathcal{S}\,\mathrm{D}\,v\|_{L^2(\Omega)}$ for all $\tau \in \Sigma_{\mathrm{N}}$ and $v \in U_{\mathrm{D}}$.

The second assumption (W2) generalises the well-known tr-dev-div inequality established in a general setting in [8, Theorem 3.1].

Since $\mathcal{S}\,\mathrm{D}$ might be the gradient or its symmetric part, $\|\mathcal{S}\,\mathrm{D}\,\bullet\|_{L^2(\Omega)}$ is the natural energy norm on $H^1_{\mathrm{D}}(\Omega;\mathbb{R}^3)$. In particular, it measures the strain tensor in the case of linear elasticity. Thus, the following boundedness of the operator $\mathcal{S}$

(W4) $\|\mathcal{S}\tau\|_{L^2(\Omega)} \leq C_{\mathcal{S}}\,\|\tau\|_{L^2(\Omega)}$ for all $\tau \in L^2(\Omega;\mathbb{R}^{3\times 3})$

and the abstract Korn inequality

(W5) $\|\mathrm{D}\,v\|_{L^2(\Omega)} \leq C_{\mathrm{K}}\,\|\mathcal{S}\,\mathrm{D}\,v\|_{L^2(\Omega)}$ for all $v \in H^1_{\mathrm{D}}(\Omega;\mathbb{R}^3)$

are assumed as well.

Let $\mathcal{A}^*, \mathcal{S}^* : L^2(\Omega;\mathbb{R}^{3\times 3}) \to L^2(\Omega;\mathbb{R}^{3\times 3})$ denote the adjoint operators to $\mathcal{A}, \mathcal{S}$. For every admissible triangulation $\mathcal{T} \in \mathbb{T}$ and piecewise polynomial functions $\tau_{\mathrm{pw}} \in P_{k+1}(\mathcal{T};\mathbb{R}^{3\times 3})$ and $v_{\mathrm{pw}} \in P_{k+1}(\mathcal{T};\mathbb{R}^{3\times 3})$, suppose that

$$\begin{aligned} &\mathcal{S}^*(\mathcal{A}\tau_{\mathrm{pw}} - \mathcal{S}\,\mathrm{D}\,v_{\mathrm{pw}}) \in H(\mathrm{div},\mathcal{T};\mathbb{R}^{3\times 3}),\\ &\mathcal{A}^*(\mathcal{A}\tau_{\mathrm{pw}} - \mathcal{S}\,\mathrm{D}\,v_{\mathrm{pw}}) \in H(\mathrm{curl},\mathcal{T};\mathbb{R}^{3\times 3}). \end{aligned} \tag{3.1}$$

Additionally, assume the following abstract inverse estimates, for $T \in \mathcal{T}$,

(W6) $|T|^{1/3}\|\,\mathrm{div}\,\mathcal{S}^*(\mathcal{A}\tau_{\mathrm{pw}} - \mathcal{S}\,\mathrm{D}\,v_{\mathrm{pw}})\|_{L^2(T)} \leq C_{\mathrm{inv}}\,\|\mathcal{S}^*(\mathcal{A}\tau_{\mathrm{pw}} - \mathcal{S}\,\mathrm{D}\,v_{\mathrm{pw}})\|_{L^2(T)}$,

(W7) $|T|^{1/3}\|\,\mathrm{curl}\,\mathcal{A}^*(\mathcal{A}\tau_{\mathrm{pw}} - \mathcal{S}\,\mathrm{D}\,v_{\mathrm{pw}})\|_{L^2(T)} \leq C_{\mathrm{inv}}\,\|\mathcal{A}^*(\mathcal{A}\tau_{\mathrm{pw}} - \mathcal{S}\,\mathrm{D}\,v_{\mathrm{pw}})\|_{L^2(T)}$.

Due to the regularity (3.1), the normal trace $(\mathcal{S}^*(\mathcal{A}\tau_{\mathrm{pw}} - \mathcal{S}\,\mathrm{D}\,v_{\mathrm{pw}}))|_T\,\nu_F$ and the tangential trace $\nu_F \times (\mathcal{A}^*(\mathcal{A}\tau_{\mathrm{pw}} - \mathcal{S}\,\mathrm{D}\,v_{\mathrm{pw}}))|_T$ exist on every face $F \in \mathcal{F}(T)$ of $T \in \mathcal{T}$ in the sense of Section 2.2. Further, let every $\tau_{\mathrm{pw}} \in P_{k+1}(\mathcal{T};\mathbb{R}^{3\times 3})$, $v_{\mathrm{pw}} \in P_{k+1}(\mathcal{T};\mathbb{R}^3)$, and $T \in \mathcal{T}$ with $F \in \mathcal{F}(T)$ satisfy the abstract discrete trace inequalities

(W8) $|T|^{1/6}\|(\mathcal{S}^*(\mathcal{A}\tau_{\mathrm{pw}} - \mathcal{S}\,\mathrm{D}\,v_{\mathrm{pw}}))|_T\;\nu_F\|_{L^2(F)} \leq C_{\mathrm{dti}}\,\|\mathcal{A}\tau_{\mathrm{pw}} - \mathcal{S}\,\mathrm{D}\,v_{\mathrm{pw}}\|_{L^2(T)}$,

(W9) $|T|^{1/6}\|\nu_F \times (\mathcal{A}^*(\mathcal{A}\tau_{\mathrm{pw}} - \mathcal{S}\,\mathrm{D}\,v_{\mathrm{pw}}))|_T\|_{L^2(F)} \leq C_{\mathrm{dti}}\,\|\mathcal{A}\tau_{\mathrm{pw}} - \mathcal{S}\,\mathrm{D}\,v_{\mathrm{pw}}\|_{L^2(T)}$.

Remark 3.1. The assumptions (W1) and (W4) imply that the adjoint operators $\mathcal{A}^*, \mathcal{S}^*$ to $\mathcal{A}, \mathcal{S}$ are as well bounded with the same generic constant, for every $\tau \in L^2(\Omega;\mathbb{R}^{3\times 3})$,

$$\|\mathcal{A}^*\tau\|_{L^2(\Omega)} \leq C_{\mathcal{A}}\,\|\tau\|_{L^2(\Omega)} \quad \text{and} \quad \|\mathcal{S}^*\tau\|_{L^2(\Omega)} \leq C_{\mathcal{S}}\,\|\tau\|_{L^2(\Omega)}. \tag{3.2}$$

Given $|\Gamma_{\mathrm{N}}| > 0$ and the Neumann boundary conditions $t_{\mathrm{N}} \in L^2(\Gamma_{\mathrm{N}};\mathbb{R}^3)$, define the space

$$\Sigma := \big\{\tau \in H(\mathrm{div},\Omega;\mathbb{R}^{3\times 3}) \;:\; \tau\cdot\nu = t_{\mathrm{N}} \text{ on } \Gamma_{\mathrm{N}}\big\}.$$

For $|\Gamma_{\mathrm{N}}| = 0$, let

$$\Sigma := \Big\{\tau \in H(\mathrm{div},\Omega;\mathbb{R}^{3\times 3}) \;:\; \fint_\Omega \mathrm{tr}\,\tau\,\mathrm{d}x = 0\Big\}.$$

The test functions belong to the corresponding space with homogeneous normal boundary conditions

$$\Sigma_{\mathrm{N}} \coloneqq \begin{cases} H_{\mathrm{N}}(\operatorname{div}, \Omega; \mathbb{R}^{3\times 3}) & \text{if } |\Gamma_{\mathrm{N}}| > 0, \\ \Sigma & \text{else.} \end{cases}$$

For the Dirichlet boundary conditions $u_{\mathrm{D}} \in H^1(\Gamma_{\mathrm{D}}; \mathbb{R}^3)$, define the space

$$U \coloneqq \left\{ v \in H^1(\Omega; \mathbb{R}^3) \;:\; v = u_{\mathrm{D}} \text{ on } \Gamma_{\mathrm{D}} \right\}$$

and for the test functions

$$U_{\mathrm{D}} \coloneqq H^1_{\mathrm{D}}(\Omega; \mathbb{R}^3).$$

Given a right-hand side $f \in L^2(\Omega; \mathbb{R}^3)$, the linear model problem seeks $\sigma \in \Sigma$ and $u \in U$ such that

$$f + \operatorname{div} \sigma = 0 \quad \text{and} \quad \mathcal{A}\sigma - \mathcal{S}\,\mathrm{D}\,u = 0 \quad \text{in } \Omega. \tag{3.3}$$

This formulation and the definition of the spaces Σ and U remain meaningful for less regular boundary data $t_{\mathrm{N}} \in H^{-1/2}(\Gamma_{\mathrm{N}}; \mathbb{R}^3)$ and $u_{\mathrm{D}} \in H^{1/2}(\Gamma_{\mathrm{D}}; \mathbb{R}^3)$. However, the a posteriori analysis of FEMs with approximated inhomogeneous boundary data usually incorporates additional regularity assumptions [7, 4]. The assumptions $t_{\mathrm{N}} \in L^2(\Gamma_{\mathrm{N}}; \mathbb{R}^3)$ and $u_{\mathrm{D}} \in H^1(\Gamma_{\mathrm{D}}; \mathbb{R}^3)$ in this thesis allow for suitable approximation error estimates in the Sections 3.3–3.4 below.

3.2 Application to the three model problems

This section verifies the assumptions (W1)–(W9) for the three model problems from Table 1 on page 3.

The Laplace operator Δ acts on each of the three components in the vector-valued Poisson model problem

$$-\Delta u = f \text{ in } \Omega, \quad u = u_{\mathrm{D}} \text{ on } \Gamma_{\mathrm{D}}, \quad \text{and} \quad \mathrm{D}\,u\,\nu = t_{\mathrm{N}} \text{ on } \Gamma_{\mathrm{N}}.$$

The introduction of the flux variable $\sigma \coloneqq \mathrm{D}\,u$ leads to an equivalent first-order system of PDEs with the identity id on $L^2(\Omega; \mathbb{R}^{3\times 3})$ for $\mathcal{A} \coloneqq \mathrm{id}$ and $\mathcal{S} \coloneqq \mathrm{id}$ in the equations (3.3). The corresponding least-squares formulation from [80, 71] minimises

$$LS(f; \sigma, u) \coloneqq \|f + \operatorname{div} \sigma\|^2_{L^2(\Omega)} + \|\sigma - \mathrm{D}\,u\|^2_{L^2(\Omega)}.$$

Lemma 3.2. *In the case of the Poisson model problem, the operators $\mathcal{A} = \mathcal{S} = \mathrm{id}$ satisfy the assumptions (W1)–(W9).*

Proof. For $\mathcal{A} = \mathcal{S} = \mathrm{id}$, the assumptions (W1)–(W2) and (W4)–(W5) are trivial with the positive generic constants $C_{\mathcal{A}} = C_{\mathrm{tdd}} = C_{\mathcal{S}} = C_{\mathrm{K}} = 1$.

For $\tau \in \Sigma_{\mathrm{N}}$, the Helmholtz decomposition (2.9) from Theorem 2.2 applied to the three components guarantees the existence of $\alpha \in H^1_{\mathrm{D}}(\Omega;\mathbb{R}^3)$ and $\beta \in H^1_{\mathrm{N}}(\Omega;\mathbb{R}^{3\times 3})$ with $\tau = \mathrm{D}\,\alpha + \operatorname{curl}\beta$. The stability estimate $\|\mathrm{D}\,\alpha\|_{L^2(\Omega)} \leq C_{\mathrm{F}}\,\|\operatorname{div}\tau\|_{L^2(\Omega)}$ from (2.10) shows

$$(\mathrm{D}\,v,\tau)_{L^2(\Omega)} = (\mathrm{D}\,v,\mathrm{D}\,\alpha)_{L^2(\Omega)} \leq \|\mathrm{D}\,v\|_{L^2(\Omega)}\|\mathrm{D}\,\alpha\|_{L^2(\Omega)} \leq C_{\mathrm{F}}\,\|\mathrm{D}\,v\|_{L^2(\Omega)}\|\operatorname{div}\tau\|_{L^2(\Omega)}$$

and concludes the proof of (W3) with $C_{\mathrm{En}} = C_{\mathrm{F}}$ in the case of the Poisson model problem

For the self-adjoint operators $\mathcal{A} = \mathcal{A}^* = \mathcal{S} = \mathcal{S}^* = \mathrm{id}$ and the abbreviation $\rho_{\mathrm{pw}} := \tau_{\mathrm{pw}} - \mathrm{D}\,v_{\mathrm{pw}} \in P_{k+1}(\mathcal{T};\mathbb{R}^{3\times 3})$, it holds that $\mathcal{S}^*\rho_{\mathrm{pw}} = \mathcal{A}^*\rho_{\mathrm{pw}} = \rho_{\mathrm{pw}}$. A standard inverse estimate [60, Section 1.7] shows, for a positive generic constant c_{inv},

$$\|\mathrm{D}\,\rho_{\mathrm{pw}}\|^2_{L^2(T)} \leq c^2_{\mathrm{inv}}\,|T|^{-2/3}\|\rho_{\mathrm{pw}}\|^2_{L^2(T)}. \tag{3.4}$$

This immediately implies the assumptions (W6)–(W7) with the positive generic constant $C_{\mathrm{inv}} := \sqrt{2}c_{\mathrm{inv}}$.

Recall from Notation 1 on page 10 that $|M|$ denotes the Frobenius norm when applied to matrices $M \in \mathbb{R}^{3\times 3}$. Given any $T \in \mathcal{T}$ and $F \in \mathcal{F}(T)$ with unit normal vector ν_F satisfying $|\nu_F| = 1$, an elementary relation between the row-wise scalar product and cross product reads, for all $M \in \mathbb{R}^{3\times 3}$,

$$|M\nu_F|^2 + |\nu_F \times M|^2 = |M|^2.$$

Hence,

$$\|\rho_{\mathrm{LS}}|_T\,\nu_F\|^2_{L^2(F)} + \|\nu_F \times \rho_{\mathrm{LS}}|_T\|^2_{L^2(F)} = \|\rho_{\mathrm{LS}}|_T\|^2_{L^2(F)}. \tag{3.5}$$

This and the trace inequality from Lemma 2.6 applied to each of the nine components prove

$$\|\rho_{\mathrm{pw}}|_T\,\nu_F\|^2_{L^2(F)} + \|\nu_F \times \rho_{\mathrm{pw}}|_T\|^2_{L^2(F)} \leq C_{\mathrm{tr}}\left(|T|^{1/3}\|\mathrm{D}\,\rho_{\mathrm{pw}}\|^2_{L^2(T)} + |T|^{-1/3}\|\rho_{\mathrm{pw}}\|^2_{L^2(T)}\right).$$

The inverse estimate (3.4) leads to

$$\|\rho_{\mathrm{pw}}|_T\,\nu_F\|^2_{L^2(F)} + \|\nu_F \times \rho_{\mathrm{pw}}|_T\|^2_{L^2(F)} \leq C_{\mathrm{tr}}(1 + c^2_{\mathrm{inv}})\,|T|^{-1/3}\|\rho_{\mathrm{pw}}\|^2_{L^2(T)}.$$

The square root of this estimate concludes the proof of (W8)–(W9) with the positive generic constant $C_{\mathrm{dti}} := (C_{\mathrm{tr}}(1 + c^2_{\mathrm{inv}}))^{1/2}$. □

Define the deviatoric (or trace-free) part $\operatorname{dev} : L^2(\Omega;\mathbb{R}^{3\times 3}) \to L^2(\Omega;\mathbb{R}^{3\times 3})$, for $\tau \in L^2(\Omega;\mathbb{R}^{3\times 3})$,

$$\operatorname{dev}\tau := \tau - \frac{1}{3}\operatorname{tr}\tau\, I_{3\times 3}. \tag{3.6}$$

Let $\Gamma_N = \emptyset$. Given the Stokes equations

$$-\Delta u + \nabla p = f \quad \text{and} \quad \operatorname{div} u = 0 \quad \text{in } \Omega,$$

the pseudostress variable $\sigma := \mathrm{D}\, u - pI_{3\times 3}$ leads to the equivalent first-order system of PDEs from [32]

$$f + \operatorname{div} \sigma = 0 \quad \text{and} \quad \operatorname{dev} \sigma - \mathrm{D}\, u = 0 \quad \text{in } \Omega.$$

For the choice of $\mathcal{A} := \operatorname{dev}$ and $\mathcal{S} := \mathrm{id}$, this is (3.3).

Alternative least-squares formulations beyond the scope of this thesis include other additional variables such as the velocity-vorticity-pressure formulation [72], the velocity-stress-pressure formulation [16], and the velocity-velocity gradient-pressure formulation [29]. For a comprehensive presentation of the corresponding least-squares discretisations, the reader is referred to [17].

Lemma 3.3. *In the case of the Stokes equations,* $\mathcal{A} = \operatorname{dev}$ *and* $\mathcal{S} = \mathrm{id}$ *satisfy the assumptions (W1)–(W9).*

Proof. For the projections $\mathcal{A} = \operatorname{dev}$ and $\mathcal{S} = \mathrm{id}$, the assumptions (W1) and (W4)–(W5) are trivial with the positive generic constants $C_{\mathcal{A}} = C_{\mathcal{S}} = C_{\mathrm{K}} = 1$.

Since $|\Gamma_N| = 0$, every $\tau \in \Sigma_N$ satisfies

$$\fint_\Omega \operatorname{tr}(\tau)\, \mathrm{d}x = 0.$$

Hence, the tr-dev-div inequality [18, Proposition 9.1.1] implies the assumption (W2) in the case of the Stokes equation

$$\|\operatorname{tr}\tau\|^2_{L^2(\Omega)} \leq C_{\mathrm{tdd}} \left(\|\operatorname{dev}\tau\|^2_{L^2(\Omega)} + \|\operatorname{div}\tau\|^2_{L^2(\Omega)} \right).$$

The proof of (W3) again employs the Helmholtz decomposition (2.9) from Theorem 2.2 and follows verbatim the proof of Lemma 3.2 with the positive generic constant $C_{\mathrm{En}} := C_{\mathrm{F}}$.

The self-adjoint operators $\mathcal{A} = \mathcal{A}^* = \operatorname{dev}$ and $\mathcal{S} = \mathcal{S}^* = \mathrm{id}$ do not depend on $x \in \Omega$ and, thus, map arguments from $P_{k+1}(\mathcal{T}; \mathbb{R}^{3\times 3})$ to $P_{k+1}(\mathcal{T}; \mathbb{R}^{3\times 3})$. Consequently, the assumptions (W6)–(W7) follow from the inverse estimate (3.4) with the positive generic constant $C_{\mathrm{inv}} := \sqrt{2} c_{\mathrm{inv}}$.

For $\rho_{\mathrm{pw}} := \operatorname{dev}\tau_{\mathrm{pw}} - \mathrm{D}\, v_{\mathrm{pw}} \in P_{k+1}(\mathcal{T}; \mathbb{R}^{3\times 3})$, a direct calculation with the row-wise cross product as in the proof of Lemma 3.2 leads to

$$\begin{aligned} \|\rho_{\mathrm{pw}}|_T\, \nu_F\|^2_{L^2(F)} + \|\nu_F \times \rho_{\mathrm{pw}}|_T\|^2_{L^2(F)} &= \|\rho_{\mathrm{pw}}|_T\|^2_{L^2(F)}, \\ \|(\operatorname{dev}\rho_{\mathrm{pw}})|_T\, \nu_F\|^2_{L^2(F)} + \|\nu_F \times (\operatorname{dev}\rho_{\mathrm{pw}})|_T\|^2_{L^2(F)} &= \|(\operatorname{dev}\rho_{\mathrm{pw}})|_T\|^2_{L^2(F)}. \end{aligned}$$

This and the trace inequality (2.19) from Lemma 2.6 lead to

$$\|\rho_{\mathrm{pw}}|_T\, \nu_F\|_{L^2(F)}^2 \leq C_{\mathrm{tr}}\left(|T|^{1/3}\|\,\mathrm{D}\,\rho_{\mathrm{pw}}\|_{L^2(T)}^2 + |T|^{-1/3}\|\rho_{\mathrm{pw}}\|_{L^2(T)}^2\right),$$
$$\|\nu_F \times (\operatorname{dev}\rho_{\mathrm{pw}})|_T\|_{L^2(F)}^2 \leq C_{\mathrm{tr}}\left(|T|^{1/3}\|\,\mathrm{D}(\operatorname{dev}\rho_{\mathrm{pw}})\|_{L^2(T)}^2 + |T|^{-1/3}\|\operatorname{dev}\rho_{\mathrm{pw}}\|_{L^2(T)}^2\right).$$

The inverse estimate (3.4) and the boundedness of the deviatoric part conclude the proof of the assumptions (W8)–(W9) with the constant $C_{\mathrm{dti}} := (C_{\mathrm{tr}}(1 + c_{\mathrm{inv}}^2))^{1/2}$. □

Let $\mathcal{S} : L^2(\Omega;\mathbb{R}^{3\times3}) \to L^2(\Omega;\mathbb{R}^{3\times3})$ denote the symmetric part of a matrix-valued function, for $\tau \in L^2(\Omega;\mathbb{R}^{3\times3})$,

$$\mathcal{S}\tau := \operatorname{sym}\tau = \frac{1}{2}(\tau + \tau^\top). \tag{3.7}$$

and $\varepsilon(u) := \operatorname{sym}\mathrm{D}\,u$ the strain tensor of the displacement $u \in H^1(\Omega;\mathbb{R}^3)$. For the two Lamé parameters $\lambda, \mu > 0$, the fourth-order tensor $\mathbb{C} : \mathbb{R}^{3\times3} \to \mathbb{R}^{3\times3}$ with $\mathbb{C}M := 2\mu M + \lambda(\operatorname{tr}M)I_{3\times3}$ for all $M \in \mathbb{R}^{3\times3}$ defines the isotropic material law in the equations of linear elasticity

$$-\operatorname{div}(\mathbb{C}\varepsilon(u)) = f \text{ in } \Omega, \quad u = u_{\mathrm{D}} \text{ on } \Gamma_{\mathrm{D}}, \quad \text{and} \quad (\mathbb{C}\varepsilon(u))\,\nu = t_{\mathrm{N}} \text{ on } \Gamma_{\mathrm{N}}.$$

The inverse of $\mathbb{C}$ defines the operator $\mathcal{A} : L^2(\Omega;\mathbb{R}^{3\times3}) \to L^2(\Omega;\mathbb{R}^{3\times3})$, for $\tau \in L^2(\Omega;\mathbb{R}^{3\times3})$,

$$\mathcal{A}\tau := \mathbb{C}^{-1}\tau = \frac{1}{2\mu}\Big(\tau - \frac{\lambda}{3\lambda + 2\mu}(\operatorname{tr}\tau)I_{3\times3}\Big). \tag{3.8}$$

The introduction of the stress variable $\sigma := \mathbb{C}\varepsilon(u)$ leads to an equivalent first-order system of PDEs. The resulting least-squares formulation of the linear elasticity problem from [34] reads

$$LS(f;\sigma,u) := \|f + \operatorname{div}\sigma\|_{L^2(\Omega)}^2 + \|\mathbb{C}^{-1}\sigma - \varepsilon(u)\|_{L^2(\Omega)}^2$$

and provides a locking-free discretisation. Alternative formulations beyond the scope of this thesis employ a different scaling with the material tensor $\mathbb{C}$ [33, 31] or are based on other equivalent first-order systems such as the displacement-displacement gradient formulation [75], the displacement-displacement gradient-pressure formulation [29], and the stress-displacement-rotation(-pressure) formulation [13]. Further methods include an additional residual to weakly impose the symmetry of the stresses for an improved momentum balance [94, 98].

Lemma 3.4. *In the case of the linear elasticity problem, $\mathcal{A} = \mathbb{C}^{-1}$ and $\mathcal{S} = \operatorname{sym}$ satisfy the assumptions (W1)–(W9) with λ-independent generic constants.*

Proof. A direct calculation from [34, proof of Theorem 3.1] proves the assumption (W1), for $\tau \in L^2(\Omega;\mathbb{R}^{3\times3})$,

$$\|\mathbb{C}^{-1}\tau\|_{L^2(\Omega)} \leq \frac{1}{2\mu}\,\|\tau\|_{L^2(\Omega)}.$$

The boundedness (W4) of the projection sym is trivial with generic constant $C_{\mathcal{S}} = 1$. Since $|\Gamma_{\mathrm{D}}| > 0$, the assumption (W5) follows from the standard Korn inequality [52, Theorem 6.3-4].

For both cases, $|\Gamma_{\mathrm{N}}| = 0$ and $|\Gamma_{\mathrm{N}}| > 0$, the subspace $\Sigma_{\mathrm{N}} \subset H(\mathrm{div}, \Omega; \mathbb{R}^{3\times3})$ does not contain the constant identity tensor $\tau \equiv I_{3\times3}$ and, thus, there exists a positive generic constant c_1 such that $\tau \in \Sigma_{\mathrm{N}}$ satisfies [38, Lemma 4.2]

$$\|\operatorname{tr}\tau\|^2_{L^2(\Omega)} \leq c_1 \left(\|\operatorname{dev}\tau\|^2_{L^2(\Omega)} + \|\operatorname{div}\tau\|^2_{L^2(\Omega)}\right).$$

For $\mathcal{A} = \mathbb{C}^{-1}$, this implies the assumption (W2) using

$$\begin{aligned}
\|\operatorname{dev}\tau\|^2_{L^2(\Omega)} &= (\operatorname{dev}\tau, \tau)_{L^2(\Omega)} = 2\mu(\mathbb{C}^{-1}\tau, \operatorname{dev}\tau)_{L^2(\Omega)} \\
&\leq 2\mu(\mathbb{C}^{-1}\tau, \operatorname{dev}\tau)_{L^2(\Omega)} + \left(1 - \frac{3\lambda}{3\lambda + 2\mu}\right)\|\operatorname{tr}\tau\|^2_{L^2(\Omega)} \\
&= 2\mu(\mathbb{C}^{-1}\tau, \operatorname{dev}\tau)_{L^2(\Omega)} + 2\mu(\operatorname{tr}\mathbb{C}^{-1}\tau, \operatorname{tr}\tau)_{L^2(\Omega)} \\
&= 2\mu(\mathbb{C}^{-1}\tau, \operatorname{dev}\tau)_{L^2(\Omega)} + \frac{2\mu}{3}(\mathbb{C}^{-1}\tau, (\operatorname{tr}\tau)I_{3\times3})_{L^2(\Omega)} \\
&= 2\mu(\mathbb{C}^{-1}\tau, \tau)_{L^2(\Omega)}.
\end{aligned}$$

The resulting positive generic constant $C_{\mathrm{tdd}} := 2\mu c_1$ is independent of the Lamé parameter λ.

For $\mathcal{S} = \mathrm{sym}$, an integration by parts and the orthogonality of the projection sym show

$$\begin{aligned}
(\varepsilon(v), \tau)_{L^2(\Omega)} &= (\mathrm{D}\, v, \operatorname{sym}\tau)_{L^2(\Omega)} = (\mathrm{D}\, v, \tau)_{L^2(\Omega)} + (\mathrm{D}\, v, (1 - \mathrm{sym})\tau)_{L^2(\Omega)} \\
&= -(v, \operatorname{div}\tau)_{L^2(\Omega)} + 2\mu(\mathrm{D}\, v, (1 - \mathrm{sym})\,\mathbb{C}^{-1}\tau)_{L^2(\Omega)} \\
&= -(v, \operatorname{div}\tau)_{L^2(\Omega)} + 2\mu(\mathrm{D}\, v, (1 - \mathrm{sym})(\mathbb{C}^{-1}\tau - \varepsilon(v)))_{L^2(\Omega)}.
\end{aligned}$$

The Cauchy-Schwarz inequality and the Friedrichs inequality from Lemma 2.1 yield

$$(\varepsilon(v), \tau)_{L^2(\Omega)} \leq \left(C_{\mathrm{F}}\,\|\operatorname{div}\tau\|_{L^2(\Omega)} + 2\mu\,\|\mathbb{C}^{-1}\tau - \varepsilon(v)\|_{L^2(\Omega)}\right)\|\mathrm{D}\, v\|_{L^2(\Omega)}.$$

This and the already proven assumption (W5) with the positive generic constant C_{K} conclude the proof of the estimate (W3) with the constant $C_{\mathrm{En}} = C_{\mathrm{K}} \max\{C_{\mathrm{F}}, 2\mu\}$ independent of the Lamé parameter λ.

The self-adjoint operators $\mathcal{A} = \mathcal{A}^* = \mathbb{C}^{-1}$ and $\mathcal{S} = \mathcal{S}^* = \mathrm{sym}$ do not depend on $x \in \Omega$ and, thus, map arguments from $P_{k+1}(\mathcal{T}; \mathbb{R}^{3\times3})$ to $P_{k+1}(\mathcal{T}; \mathbb{R}^{3\times3})$. Consequently, the assumptions (W6)–(W7) follow from the inverse estimate (3.4) with the positive generic constant $C_{\mathrm{inv}} := \sqrt{2}c_{\mathrm{inv}}$.

For $\rho_{\mathrm{pw}} := \mathbb{C}^{-1}\tau_{\mathrm{pw}} - \varepsilon(v_{\mathrm{pw}}) \in P_{k+1}(\mathcal{T}; \mathbb{R}^{3\times3})$, proceed as in the proof of Lemma 3.2 to establish

$$\begin{aligned}
\|(\operatorname{sym}\rho_{\mathrm{pw}})|_T\,\nu_F\|^2_{L^2(F)} + \|\nu_F \times (\operatorname{sym}\rho_{\mathrm{pw}})|_T\|^2_{L^2(F)} &= \|(\operatorname{sym}\rho_{\mathrm{pw}})|_T\|^2_{L^2(F)}, \\
\|(\mathbb{C}^{-1}\rho_{\mathrm{pw}})|_T\,\nu_F\|^2_{L^2(F)} + \|\nu_F \times (\mathbb{C}^{-1}\rho_{\mathrm{pw}})|_T\|^2_{L^2(F)} &= \|(\mathbb{C}^{-1}\rho_{\mathrm{pw}})|_T\|^2_{L^2(F)}.
\end{aligned}$$

This and the trace inequality (2.19) from Lemma 2.6 show

$$\|(\operatorname{sym}\rho_{\mathrm{pw}})|_T\,\nu_F\|^2_{L^2(F)} \le C_{\mathrm{tr}}\left(|T|^{1/3}\|\,\mathrm{D}(\operatorname{sym}\rho_{\mathrm{pw}})\|^2_{L^2(T)} + |T|^{-1/3}\|(\operatorname{sym}\rho_{\mathrm{pw}})\|^2_{L^2(T)}\right),$$
$$\|\nu_F \times (\mathbb{C}^{-1}\rho_{\mathrm{pw}})|_T\|^2_{L^2(F)} \le C_{\mathrm{tr}}\left(|T|^{1/3}\|\,\mathrm{D}(\mathbb{C}^{-1}\rho_{\mathrm{pw}})\|^2_{L^2(T)} + |T|^{-1/3}\|\mathbb{C}^{-1}\rho_{\mathrm{pw}}\|^2_{L^2(T)}\right).$$

The inverse estimate (3.4) and the boundedness of the symmetric part and the material tensor $\mathbb{C}^{-1}$ in

$$\|\operatorname{sym}\rho_{\mathrm{pw}}\|^2_{L^2(T)} \le \|\rho_{\mathrm{pw}}\|^2_{L^2(T)} \quad \text{and} \quad \|\mathbb{C}^{-1}\rho_{\mathrm{pw}}\|^2_{L^2(T)} \le \frac{1}{4\mu^2}\,\|\rho_{\mathrm{pw}}\|^2_{L^2(T)}$$

conclude the proof the assumptions (W8)–(W9) with the λ-independent constant $C_{\mathrm{dti}} := \max\{1, 1/(2\mu)\}(C_{\mathrm{tr}}(1 + c^2_{\mathrm{inv}}))^{1/2}$. □

Remark 3.5. All arguments in the proof of Lemma 3.4 can be employed element-wise for $T \in \mathcal{T}$. Therefore, they apply to problems with composite materials if the piecewise constant Lamé parameters are resolved by the initial triangulation $\mathcal{T}_0$.

3.3 Approximation of Dirichlet boundary data

For the approximation of inhomogeneous Dirichlet boundary data $u_{\mathrm{D}} \in H^1(\Gamma_{\mathrm{D}};\mathbb{R}^3)$, the Scott-Zhang quasi-interpolation operator $\mathcal{J}^{k+1}_{\mathrm{D}}$ from Section 2.6 is employed [92, 4]. The Condition 1 with respect to Γ_{D} ensures that the values of the quasi-interpolation at the interpolation nodes $a_j \in \mathcal{I}_{k+1} \cap \Gamma_{\mathrm{D}}$ on the Dirichlet boundary solely depend on integrals of u_{D} over boundary faces $F \in \mathcal{F}(\Gamma_{\mathrm{D}})$. Since $u_{\mathrm{D}} \in H^1(\Gamma_{\mathrm{D}};\mathbb{R}^3)$, this is well-defined. Formally, the construction follows [4, Section 3.2]. Given a regular triangulation $\mathcal{T} \in \mathbb{T}$ in the sense of Section 2.4, let $\bar{u}_{\mathrm{D}} \in H^1(\Omega;\mathbb{R}^3)$ denote *any* extension of u_{D} on Ω with $\bar{u}_{\mathrm{D}} = u_{\mathrm{D}}$ on Γ_{D} and regard $\widetilde{\mathcal{J}}^{k+1}_{\mathrm{D}} : H^{1/2}(\Gamma_{\mathrm{D}};\mathbb{R}^3) \to S^{k+1}(\mathcal{F}(\Gamma_{\mathrm{D}});\mathbb{R}^3)$ with $\widetilde{\mathcal{J}}^{k+1}_{\mathrm{D}} u_{\mathrm{D}} := \gamma_{\mathrm{D}}(\mathcal{J}^{k+1}_{\mathrm{D}}\bar{u}_{\mathrm{D}})$ as an approximation of the Dirichlet boundary data. For the ease of the notation, the operator $\widetilde{\mathcal{J}}^{k+1}_{\mathrm{D}}$ is again denoted by $\mathcal{J}^{k+1}_{\mathrm{D}}$. Let $\mathrm{D}\,u_{\mathrm{D}}$ abbreviate the surface gradient $\mathrm{D}_{\mathrm{X}}\,u_{\mathrm{D}}$ from from (2.4).

The following lemma asserts the well-known surjectivity of the trace operator γ_{D}. It is proved here for the sake of explicit stability constants. Recall Notation 3 from page 22 for a triangulation $\mathcal{T} \in \mathbb{T}$ and its admissible refinement $\widehat{\mathcal{T}} \in \mathbb{T}(\mathcal{T})$.

Lemma 3.6 (Dirichlet boundary data extension). *There exists some extension $w \in H^1(\Omega;\mathbb{R}^3)$ with*

$$w = (1 - \mathcal{J}^{k+1}_{\mathrm{D}})u_{\mathrm{D}} \text{ on } \Gamma_{\mathrm{D}} \quad \text{and} \quad \|\,\mathrm{D}\,w\|_{L^2(\Omega)} \le \|(1 - \mathcal{J}^{k+1}_{\mathrm{D}})u_{\mathrm{D}}\|_{H^{1/2}(\Gamma_{\mathrm{D}})}. \tag{3.9}$$

For the overlap constant C_{OL} and the stability constant C_{SZ} of the Scott-Zhang operator from Lemma 2.12 (c), there exists some discrete extension $\widehat{w}_{\mathrm{C}} \in S^{k+1}(\widehat{\mathcal{T}};\mathbb{R}^3)$ satisfying

$$\begin{aligned} \widehat{w}_{\mathrm{C}} &= (\widehat{\mathcal{J}}^{k+1}_{\mathrm{D}} - \mathcal{J}^{k+1}_{\mathrm{D}})u_{\mathrm{D}} \text{ on } \Gamma_{\mathrm{D}} \quad \text{and} \\ \|\,\mathrm{D}\,\widehat{w}_{\mathrm{C}}\|_{L^2(\Omega)} &\le C_{\mathrm{OL}}C_{\mathrm{SZ}}\,\|(\widehat{\mathcal{J}}^{k+1}_{\mathrm{D}} - \mathcal{J}^{k+1}_{\mathrm{D}})u_{\mathrm{D}}\|_{H^{1/2}(\Gamma_{\mathrm{D}})}. \end{aligned} \tag{3.10}$$

Proof. Step 1. Abbreviate $y := (1 - \mathcal{J}_{\mathrm{D}}^{k+1})u_{\mathrm{D}} \in H^1(\Gamma_{\mathrm{D}};\mathbb{R}^3)$ and let $w \in H^1(\Omega;\mathbb{R}^3)$ solve the Dirichlet problem

$$(\mathrm{D}\, w, \mathrm{D}\, v)_{L^2(\Omega)} + (w, v)_{L^2(\Omega)} = 0 \text{ for all } v \in H^1_{\mathrm{D}}(\Omega;\mathbb{R}^3) \quad \text{and} \quad w = y \text{ on } \Gamma_{\mathrm{D}}.$$

The weak solution w solves the minimisation problem

$$\begin{aligned}\|w\|_{H^1(\Omega)} &= \min\left\{\|z\|_{H^1(\Omega)} \,:\, z \in H^1(\Omega;\mathbb{R}^3) \text{ with } z = y \text{ on } \Gamma_{\mathrm{D}}\right\}\\ &= \|y\|_{H^{1/2}(\Gamma_{\mathrm{D}})} = \|(1 - \mathcal{J}_{\mathrm{D}}^{k+1})u_{\mathrm{D}}\|_{H^{1/2}(\Gamma_{\mathrm{D}})}\end{aligned}$$

and satisfies (3.9).

Step 2. The application of Step 1 leads to $\widetilde{w} \in H^1(\Omega;\mathbb{R}^3)$ with

$$\widetilde{w} = (\widehat{\mathcal{J}}_{\mathrm{D}}^{k+1} - \mathcal{J}_{\mathrm{D}}^{k+1})u_{\mathrm{D}} \text{ on } \Gamma_{\mathrm{D}} \quad \text{and} \quad \|\mathrm{D}\,\widetilde{w}\|_{L^2(\Omega)} \le \|(\widehat{\mathcal{J}}_{\mathrm{D}}^{k+1} - \mathcal{J}_{\mathrm{D}}^{k+1})u_{\mathrm{D}}\|_{H^{1/2}(\Gamma_{\mathrm{D}})}.$$

The Scott-Zhang quasi-interpolation $\widehat{w}_{\mathrm{C}} := \widehat{\mathcal{J}}_{\mathrm{D}}^{k+1}\widetilde{w}$ preserves polynomial boundary data on Γ_{D} with respect to the triangulation $\widehat{\mathcal{T}}$ by Lemma 2.12 (e). Thus, $\widehat{w}_{\mathrm{C}} = (\widehat{\mathcal{J}}_{\mathrm{D}}^{k+1} - \mathcal{J}_{\mathrm{D}}^{k+1})u_{\mathrm{D}}$ on Γ_{D} and the global stability from Lemma 2.12 (c) holds

$$\|\mathrm{D}\,\widehat{w}_{\mathrm{C}}\|_{L^2(\Omega)} \le C_{\mathrm{OL}}C_{\mathrm{SZ}}\,\|\mathrm{D}\,\widetilde{w}\|_{L^2(\Omega)}.$$

The combination of the two previously displayed formulas proves (3.10). □

The approximation of the Dirichlet data is naturally measured in terms of the boundary oscillations from (2.20) evaluated for the surface gradient of u_{D}

$$\mathrm{osc}^2(\mathrm{D}\,u_{\mathrm{D}}, \mathcal{F}(\Gamma_{\mathrm{D}})) := \sum_{F\in\mathcal{F}(\Gamma_{\mathrm{D}})} |\omega_F|^{1/3}\|(1 - \Pi_k)\,\mathrm{D}\,u_{\mathrm{D}}\|^2_{L^2(F)}.$$

The following results require the additional regularity $u_{\mathrm{D}} \in H^1(\Gamma_{\mathrm{D}};\mathbb{R}^3)$ to control the boundary data approximation errors from (3.9)–(3.10) in Lemma 3.6 in terms of the oscillations.

Lemma 3.7. *There exists a positive generic constant C_{D1} such that every $u_{\mathrm{D}} \in H^1(\Gamma_{\mathrm{D}};\mathbb{R}^3)$ satisfies*

$$\|(1 - \mathcal{J}_{\mathrm{D}}^{k+1})u_{\mathrm{D}}\|_{H^{1/2}(\Gamma_{\mathrm{D}})} \le C_{\mathrm{D1}}\ \mathrm{osc}(\mathrm{D}\,u_{\mathrm{D}}, \mathcal{F}(\Gamma_{\mathrm{D}})).$$

Proof. Since the Scott-Zhang quasi-interpolation operator $\mathcal{J}_{\mathrm{D}}^{k+1}$ is an $H^{1/2}$-stable operator and $u_{\mathrm{D}} \in H^1(\Gamma_{\mathrm{D}};\mathbb{R}^3)$, [74, Theorem 4] applies and proves the existence of a positive generic constant c_1 with

$$\|(1 - \mathcal{J}_{\mathrm{D}}^{k+1})u_{\mathrm{D}}\|_{H^{1/2}(\Gamma_{\mathrm{D}})} \le c_1\|h_{\mathcal{T}}^{1/2}\,\mathrm{D}((1 - \mathcal{J}_{\mathrm{D}}^{k+1})u_{\mathrm{D}})\|_{L^2(\Gamma_{\mathrm{D}})}.$$

The localisation of the estimate

$$\|\mathrm{D}((1 - \mathcal{J}_{\mathrm{D}}^{k+1})u_{\mathrm{D}})\|_{L^2(\Gamma_{\mathrm{D}})} \le c_2\|(1 - \Pi_k)\,\mathrm{D}\,u_{\mathrm{D}}\|_{L^2(\Gamma_{\mathrm{D}})}$$

from [4, Proposition 3.1] with some factor $h_{\mathcal{T}}$ inside concludes the proof. □

Recall the notation for n-layers $\mathcal{L}_n$ around faces from page 24.

Lemma 3.8. *There exists a positive generic constant $C_{\mathrm{D}2}$ such that every $u_{\mathrm{D}} \in H^1(\Gamma_{\mathrm{D}};\mathbb{R}^3)$ satisfies*

$$\|(\widehat{\mathcal{J}}_{\mathrm{D}}^{k+1} - \mathcal{J}_{\mathrm{D}}^{k+1})u_{\mathrm{D}}\|^2_{H^{1/2}(\Gamma_{\mathrm{D}})} \leq C_{\mathrm{D}2}\ \operatorname{osc}^2(\mathrm{D}\,u_{\mathrm{D}}, \mathcal{L}_5(\mathcal{F}\setminus\widehat{\mathcal{F}},\Gamma_{\mathrm{D}})). \tag{3.11}$$

Proof. Since the estimate has been shown in [4, proof of Proposition 6.1, from line 7 on page 1227 to line 19 on page 1228], the proof at hand solely gives an overview of the arguments. The locality of the Scott-Zhang quasi-interpolation operator from Lemma 2.12 (g) ensures that

$$(\widehat{\mathcal{J}}_{\mathrm{D}}^{k+1} - \mathcal{J}_{\mathrm{D}}^{k+1})u_{\mathrm{D}}|_F = 0 \quad \text{on every } F \in \mathcal{F}(\Gamma_{\mathrm{D}}) \setminus \mathcal{L}_1(\mathcal{F}\setminus\widehat{\mathcal{F}},\Gamma_{\mathrm{D}}).$$

The remaining surface $S_{\mathrm{D},1} := \operatorname{relint}\bigcup\mathcal{L}_1(\mathcal{F}\setminus\widehat{\mathcal{F}},\Gamma_{\mathrm{D}})$ is the relative interior from (2.5) of the union of all the faces in $\mathcal{L}_1(\mathcal{F}\setminus\widehat{\mathcal{F}},\Gamma_{\mathrm{D}})$ on the Dirichlet boundary. The estimation of $\|(\widehat{\mathcal{J}}_{\mathrm{D}}^{k+1}-\mathcal{J}_{\mathrm{D}}^{k+1})u_{\mathrm{D}}\|_{H^{1/2}(\Gamma_{\mathrm{D}})}$ on $S_{\mathrm{D},1}$ employs a localisation technique from [39, Section 3]. For all $F \in \mathcal{F}(\Gamma_{\mathrm{D}})$ with patch $S_F := \operatorname{relint}\bigcup\mathcal{L}_1(\{F\},\Gamma_{\mathrm{D}})$, [4, Proposition 3.1] shows

$$\|(1-\Pi_k)\,\mathrm{D}\,u_{\mathrm{D}}\|_{L^2(F)} \leq \|\,\mathrm{D}((1-\mathcal{J}_{\mathrm{X}}^{k+1})u_{\mathrm{D}})\|_{L^2(F)} \leq c_1\,\|(1-\Pi_k)\,\mathrm{D}\,u_{\mathrm{D}}\|_{L^2(S_F)}.$$

This plus the stability and approximation property of the Scott-Zhang operator on the boundary [4, Equations (3.7)–(3.9)] lead to the estimate (3.11) in the third displayed formula on [4, page 1228]. □

3.4 Approximation of Neumann boundary data

Given a regular triangulation $\mathcal{T} \in \mathbb{T}$ with the set of Neumann boundary faces $\mathcal{F}(\Gamma_{\mathrm{N}})$, approximate inhomogeneous boundary values $t_{\mathrm{N}} \in L^2(\Gamma_{\mathrm{N}};\mathbb{R}^3) \subset H^{-1/2}(\Gamma_{\mathrm{N}};\mathbb{R}^3)$ by the $L^2(\Gamma_{\mathrm{N}})$ orthogonal projection $\Pi_k t_{\mathrm{N}}$ onto the piecewise polynomials $P_k(\mathcal{F}(\Gamma_{\mathrm{N}});\mathbb{R}^3)$ with

$$\|t_{\mathrm{N}} - \Pi_k t_{\mathrm{N}}\|_{L^2(\Gamma_{\mathrm{N}})} = \inf\left\{\|t_{\mathrm{N}} - s_{\mathrm{pw}}\|_{L^2(\Gamma_{\mathrm{N}})} \ :\ s_{\mathrm{pw}} \in P_k(\mathcal{F}(\Gamma_{\mathrm{N}});\mathbb{R}^3)\right\}.$$

The analysis of the approximation error

$$(1-\Pi_k)t_{\mathrm{N}} \perp P_k(\mathcal{F}(\Gamma_{\mathrm{N}});\mathbb{R}^3)$$

involves the extension $\widetilde{t_{\mathrm{N}}} \in L^2(\partial\Omega;\mathbb{R}^3)$ by zero

$$\widetilde{t_{\mathrm{N}}}(x) := \begin{cases} t_{\mathrm{N}}(x) & \text{if } x \in \Gamma_{\mathrm{N}}, \\ 0 & \text{else.} \end{cases}$$

This leads to an approximation error $(1-\Pi_k)\widetilde{t_{\mathrm{N}}} \in L^2(\partial\Omega)$ on the whole boundary with $(1-\Pi_k)\widetilde{t_{\mathrm{N}}} = 0$ on Γ_{D}.

The following lemma asserts the well-known surjectivity of the normal trace operator $\gamma_{\mathrm{N}}^{\mathrm{nor}}$ from Section 2.2 and allows for an $H(\mathrm{div})$-stable extension of the Neumann boundary data approximation error inside the domain. It is proved here for the sake of explicit stability constants. Let $\widehat{\mathcal{T}} \in \mathbb{T}(\mathcal{T})$ denote an admissible refinement of the regular triangulation $\mathcal{T} \in \mathbb{T}$ with Notation 3 from page 22. Recall the Friedrichs constant C_{F} from Lemma 2.1 and the stability constant C_{ext} from Lemma 2.7.

Lemma 3.9 (Neumann boundary data extension). *Given $t_{\mathrm{N}} \in L^2(\Gamma_{\mathrm{N}};\mathbb{R}^3)$, there exists some divergence-free extension $\xi \in H(\mathrm{div}=0,\Omega;\mathbb{R}^{3\times3})$ with*

$$\xi\nu = (1-\Pi_k)\widetilde{t}_{\mathrm{N}} \text{ on } \partial\Omega \quad \text{and} \quad \|\xi\|_{L^2(\Omega)} \leq (1+C_{\mathrm{F}}^2)\,\|(1-\Pi_k)\widetilde{t}_{\mathrm{N}}\|_{H^{-1/2}(\partial\Omega)}. \tag{3.12}$$

There exists some discrete divergence-free extension $\widehat{\xi}_{\mathrm{RT}} \in RT_k(\widehat{\mathcal{T}};\mathbb{R}^{3\times3}) \cap H(\mathrm{div}=0,\Omega;\mathbb{R}^{3\times3})$ with

$$\widehat{\xi}_{\mathrm{RT}}\nu = (\widehat{\Pi}_k-\Pi_k)\widetilde{t}_{\mathrm{N}} \text{ on } \partial\Omega \quad \text{and} \quad \|\widehat{\xi}_{\mathrm{RT}}\|_{L^2(\Omega)} \leq C_{\mathrm{ext}}\,\|(\widehat{\Pi}_k-\Pi_k)\widetilde{t}_{\mathrm{N}}\|_{H^{-1/2}(\partial\Omega)}. \tag{3.13}$$

Proof. Step 1. Let $w \in H^1(\Omega;\mathbb{R}^3)/\mathbb{R}^3$ solve the Neumann problem

$$(\mathrm{D}\,w,\mathrm{D}\,v)_{L^2(\Omega)} = \big(v,(1-\Pi_k)t_{\mathrm{N}}\big)_{L^2(\partial\Omega)} \quad \text{for all } v \in H^1(\Omega;\mathbb{R}^3)/\mathbb{R}^3. \tag{3.14}$$

The integration by parts shows that its weak derivative $\xi := \mathrm{D}\,w \in H(\mathrm{div},\Omega;\mathbb{R}^{3\times3})$ satisfies $\mathrm{div}\,\xi = 0$ and $\xi\nu = (1-\Pi_k)t_{\mathrm{N}}$ on $\partial\Omega$. The stability of this boundary value problem follows from the Friedrichs inequality from Lemma 2.1 and (3.14) in

$$\frac{1}{(1+C_{\mathrm{F}}^2)}\,\|w\|_{H^1(\Omega)}^2 \leq \|\mathrm{D}\,w\|_{L^2(\Omega)}^2 = (\mathrm{D}\,w,\mathrm{D}\,w)_{L^2(\Omega)} = \big(w,(1-\Pi_k)t_{\mathrm{N}}\big)_{L^2(\Gamma_{\mathrm{N}})}.$$

The division by $\|w\|_{H^1(\Omega)}$ and the estimate by the supremum over $H^1(\Omega;\mathbb{R}^3)\setminus\{0\}$ lead to

$$\|\xi\|_{H(\mathrm{div},\Omega)} = \|\mathrm{D}\,w\|_{L^2(\Omega)} \leq \|w\|_{H^1(\Omega)} \leq (1+C_{\mathrm{F}}^2)\,\|(1-\Pi_k)t_{\mathrm{N}}\|_{H^{-1/2}(\Gamma_{\mathrm{N}})}.$$

Step 2. By definition of the $L^2(\partial\Omega)$-orthogonal projection $\widehat{\Pi}_k$, the function $\widehat{t}_{\mathrm{pw}} := (\widehat{\Pi}_k-\Pi_k)\widetilde{t}_{\mathrm{N}} \in P_k(\widehat{\mathcal{F}}(\partial\Omega);\mathbb{R}^3)$ satisfies

$$\fint_{\partial\Omega} \widehat{t}_{\mathrm{pw}}\,\mathrm{d}a = \fint_{\Gamma_{\mathrm{N}}} (\widehat{\Pi}_k-\Pi_k)\widetilde{t}_{\mathrm{N}}\,\mathrm{d}a = 0.$$

Hence, Lemma 2.7 applied to every component with respect to the fine triangulation $\widehat{\mathcal{T}}$ guarantees the existence of some discrete extension $\widehat{\rho}_{\mathrm{RT}} \in RT_k(\widehat{\mathcal{T}};\mathbb{R}^{3\times3})$ such that $\mathrm{div}\,\widehat{\rho}_{\mathrm{RT}} = 0$ in Ω and $\widehat{\rho}_{\mathrm{RT}}\nu = \widehat{t}_{\mathrm{pw}} = (\widehat{\Pi}_k-\Pi_k)\widetilde{t}_{\mathrm{N}}$ on $\partial\Omega$. The stability (2.22) reads

$$\|\widehat{\xi}_{\mathrm{RT}}\|_{L^2(\Omega)} \leq C_{\mathrm{ext}}\,\|(\widehat{\Pi}_k-\Pi_k)t_{\mathrm{N}}\|_{H^{-1/2}(\partial\Omega)}$$

and concludes the proof of (3.13). □

The approximation of the boundary data is naturally measured in terms of the oscillations

$$\operatorname{osc}^2(t_{\mathrm{N}}, \mathcal{F}(\Gamma_{\mathrm{N}})) \coloneqq \sum_{F\in\mathcal{F}(\Gamma_{\mathrm{N}})} |\omega_F|^{1/3} \|(1-\Pi_k)t_{\mathrm{N}}\|^2_{L^2(F)}.$$

The following two results require the additional regularity $t_{\mathrm{N}} \in L^2(\Omega;\mathbb{R}^3)$ to control the boundary data approximation error from Lemma 3.9 in terms of the oscillations.

Lemma 3.10. *There exists a positive generic constant C_{N} such that the extension $\widetilde{t}_{\mathrm{N}} \in L^2(\partial\Omega;\mathbb{R}^3)$ by zero of any $t_{\mathrm{N}} \in L^2(\Gamma_{\mathrm{N}};\mathbb{R}^3)$ satisfies*

$$\|(1-\Pi_k)\widetilde{t}_{\mathrm{N}}\|_{H^{-1/2}(\partial\Omega)} \leq C_{\mathrm{N}}\ \operatorname{osc}(t_{\mathrm{N}}, \mathcal{F}(\Gamma_{\mathrm{N}})).$$

Proof. Recall for any face $F \in \mathcal{F}(\Gamma_{\mathrm{N}})$ of surface measure $|F|$, that $\overline{\omega}_F \in \mathcal{T}$ denotes the unique tetrahedron with $F \in \mathcal{F}(\overline{\omega}_F)$ of volume $|\omega_F|$ and diameter $\operatorname{diam}(\omega_F)$. Since $(1-\Pi_k)\widetilde{t}_{\mathrm{N}} \in L^2(\partial\Omega;\mathbb{R}^3)$ and the duality bracket $\langle \bullet, \bullet\rangle_{\partial\Omega}$ for the dual space $H^{-1/2}(\partial\Omega;\mathbb{R}^3)$ of $H^{1/2}(\partial\Omega;\mathbb{R}^3)$ extends the $L^2(\partial\Omega)$ scalar product,

$$\big\langle (1-\Pi_k)\widetilde{t}_{\mathrm{N}}, v\big\rangle_{\partial\Omega} = \big((1-\Pi_k)\widetilde{t}_{\mathrm{N}}, v\big)_{L^2(\partial\Omega)} = \big((1-\Pi_k)t_{\mathrm{N}}, v\big)_{L^2(\Gamma_{\mathrm{N}})}.$$

The supremum of this over $v \in H^1(\Omega;\mathbb{R}^3)$ with norm $\|v\|_{H^1(\Omega)} = 1$ results in the operator norm $\|\bullet\|_{H^{-1/2}(\partial\Omega)}$ on the space $H^{-1/2}(\partial\Omega;\mathbb{R}^3)$. Hence, it suffices for any $v \in H^1_{\mathrm{D}}(\Omega;\mathbb{R}^3)$ with $\|v\|_{H^1(\Omega)} = 1$ to prove the estimate

$$\big((1-\Pi_k)t_{\mathrm{N}}, v\big)_{L^2(\Gamma_{\mathrm{N}})} \leq C_{\mathrm{N}}\ \operatorname{osc}(t_{\mathrm{N}}, \mathcal{F}(\Gamma_{\mathrm{N}})). \tag{3.15}$$

Given any such v, let $v_F \coloneqq \fint_{\omega_F} v\,\mathrm{d}x$ be the integral mean of v on the face-patch ω_F of $F \in \mathcal{F}(\Gamma_{\mathrm{N}})$. The Poincaré inequality including the Payne-Weinberger constant from [88, Section 4] with a corrected proof in [10, Theorem 3.2] verifies

$$\|v - v_F\|_{L^2(\omega_F)} \leq \frac{\operatorname{diam}(\omega_F)}{\pi}\, \|\,\mathrm{D}\, v\|_{L^2(\omega_F)}. \tag{3.16}$$

Since $\fint_F (1-\Pi_k)t_{\mathrm{N}}\,\mathrm{d}a = 0$ for every $F \in \mathcal{F}(\Gamma_{\mathrm{N}})$, Cauchy-Schwarz inequalities in $L^2(F)$ and in $\mathbb{R}^{|\mathcal{F}(\Gamma_{\mathrm{N}})|}$ show for the left-hand side in (3.15) that

$$\begin{aligned}
\big((1-\Pi_k)t_{\mathrm{N}}, v\big)_{L^2(\Gamma_{\mathrm{N}})} &= \sum_{F\in\mathcal{F}(\Gamma_{\mathrm{N}})} \big((1-\Pi_k)t_{\mathrm{N}}, v - v_F\big)_{L^2(F)} \\
&\leq \sum_{F\in\mathcal{F}(\Gamma_{\mathrm{N}})} |\omega_F|^{1/6} \|(1-\Pi_k)t_{\mathrm{N}}\|_{L^2(F)}\ |\omega_F|^{-1/6}\|v - v_F\|_{L^2(F)} \\
&\leq \operatorname{osc}(t_{\mathrm{N}}, \mathcal{F}(\Gamma_{\mathrm{N}})) \sqrt{\sum_{F\in\mathcal{F}(\Gamma_{\mathrm{N}})} |\omega_F|^{-1/3}\|v - v_F\|^2_{L^2(F)}}.
\end{aligned}$$

The trace identity for $g := |v - v_F|^2 \in W^{1,1}(\omega_F)$ on the tetrahedron $\overline{\omega}_F =: \operatorname{conv}\{F, P_F\}$ reads [42, Lemma 2.6]

$$\begin{aligned}|F|^{-1}\|v - v_F\|^2_{L^2(F)} &= \fint_F g(x)\,\mathrm{d}a = \fint_{\omega_F} g(x)\,\mathrm{d}x + \frac{1}{3}\fint_{\omega_F}(x - P_F)\cdot\nabla g(x)\,\mathrm{d}x\\ &\le |\omega_F|^{-1}\|v - v_F\|^2_{L^2(\omega_F)} + 2\frac{\operatorname{diam}(\omega_F)}{3|\omega_F|}\,\|v - v_F\|_{L^2(\omega_F)}\|\,\mathrm{D}\,v\|_{L^2(\omega_F)}.\end{aligned}$$

This and (3.16) prove

$$\|v - v_F\|^2_{L^2(F)} \le \frac{|F|\operatorname{diam}(\omega_F)^2}{\pi|\omega_F|}\Big(\frac{2}{3} + \frac{1}{\pi}\Big)\,\|\,\mathrm{D}\,v\|^2_{L^2(\omega_F)}.$$

With the positive generic constant

$$C_{\mathrm{N}}^2 := \frac{4}{\pi}\Big(\frac{2}{3} + \frac{1}{\pi}\Big)\max_{F\in\mathcal{F}(\Gamma_{\mathrm{N}})}|F|\,\operatorname{diam}(\omega_F)^2|\omega_F|^{-4/3},$$

the weighted sum of all those contributions reads

$$\sum_{F\in\mathcal{F}(\Gamma_{\mathrm{N}})}|\omega_F|^{-1/3}\|v - v_F\|^2_{L^2(F)} \le \frac{C_{\mathrm{N}}^2}{4}\sum_{F\in\mathcal{F}(\Gamma_{\mathrm{N}})}\|\,\mathrm{D}\,v\|^2_{L^2(\omega_F)}.$$

The finite overlap of the family $(\omega_F : F \in \mathcal{F}(\Gamma_{\mathrm{N}}))$ shows that the last term in the previously displayed equation is controlled by $C_{\mathrm{N}}^2\,\|\,\mathrm{D}\,v\|_{L^2(\Omega)} \le C_{\mathrm{N}}^2$. The combination with (3.15) concludes the proof. □

Corollary 3.11. *It holds that*

$$\|(\widehat{\Pi}_k - \Pi_k)\widetilde{t}_{\mathrm{N}}\|_{H^{-1/2}(\partial\Omega)} \le C_{\mathrm{N}}\,\operatorname{osc}(t_{\mathrm{N}}, \mathcal{F}(\Gamma_{\mathrm{N}})\setminus\widehat{\mathcal{F}}(\Gamma_{\mathrm{N}})). \tag{3.17}$$

Proof. The estimate is a direct consequence of Lemma 3.10 applied to $\widehat{\Pi}_k t_{\mathrm{N}}$ and the Pythagoras theorem exploiting the orthogonality of the projection Π_k. This leads to

$$\begin{aligned}\|(\widehat{\Pi}_k - \Pi_k)\widetilde{t}_{\mathrm{N}}\|^2_{H^{-1/2}(\partial\Omega)} &= \|(1 - \Pi_k)\widehat{\Pi}_k\widetilde{t}_{\mathrm{N}}\|^2_{H^{-1/2}(\partial\Omega)}\\ &\le C_{\mathrm{N}}^2\sum_{F\in\mathcal{F}(\Gamma_{\mathrm{N}})}|\omega_F|^{1/3}\|(\widehat{\Pi}_k - \Pi_k)t_{\mathrm{N}}\|^2_{L^2(F)}\\ &= C_{\mathrm{N}}^2\sum_{F\in\mathcal{F}(\Gamma_{\mathrm{N}})}|\omega_F|^{1/3}\big(\|(1 - \Pi_k)t_{\mathrm{N}}\|^2_{L^2(F)} - \|(1 - \widehat{\Pi}_k)t_{\mathrm{N}}\|^2_{L^2(F)}\big).\end{aligned}$$

Since $(\widehat{\Pi}_k - \Pi_k)t_{\mathrm{N}}|_F = 0$ vanishes on every $F \in \widehat{\mathcal{F}}(\Gamma_{\mathrm{N}})\cap\mathcal{F}(\Gamma_{\mathrm{N}})$ and $-\|(1-\widehat{\Pi}_k)t_{\mathrm{N}}\|^2_{L^2(F)} \le 0$ for $F \in \mathcal{F}(\Gamma_{\mathrm{N}})\setminus\widehat{\mathcal{F}}(\Gamma_{\mathrm{N}})$ on the right-hand side, this proves (3.17). □

3.5 Least-squares formulation

Let $\mathcal{T} \in \mathbb{T}$ denote an admissible triangulation in the sense of Section 2.4. Approximate the Neumann boundary data t_N with the L^2-orthogonal projection $\Pi_k t_N$ onto the piecewise polynomials $P_k(\mathcal{T};\mathbb{R}^3)$ from Section 3.4. Choose the Raviart-Thomas finite element functions

$$\Sigma^k(\mathcal{T}) := \big\{\tau_{RT} \in RT_k(\mathcal{T};\mathbb{R}^{3\times3}) \ : \ \tau_{RT}\cdot\nu = \Pi_k t_N \text{ on } \Gamma_N\big\}$$

for the discretisation of Σ. If $\Gamma_N = \emptyset$, then $\Sigma^k(\mathcal{T}) := RT_k(\mathcal{T};\mathbb{R}^{3\times3}) \cap \Sigma$ is a discrete conforming subspace. Approximate the Dirichlet boundary data u_D with the Scott-Zhang quasi-interpolation $\mathcal{J}_D^{k+1}u_D$ as described in Section 3.3. For the discretisation of U, choose

$$U^{k+1}(\mathcal{T}) := \big\{v_C \in S^{k+1}(\mathcal{T};\mathbb{R}^3) \ : \ v_C = \mathcal{J}_D^{k+1}u_D \text{ on } \Gamma_D\big\}.$$

The corresponding discrete spaces with homogeneous boundary conditions for the test functions read

$$\begin{aligned}\Sigma_N^k(\mathcal{T}) &:= \big\{\tau_{RT} \in RT_k(\mathcal{T};\mathbb{R}^{3\times3}) \ : \ \tau_{RT}\cdot\nu \equiv 0 \text{ on } \Gamma_N\big\} \subset \Sigma_N,\\ U_D^{k+1}(\mathcal{T}) &:= \big\{v_C \in S^{k+1}(\mathcal{T};\mathbb{R}^3) \ : \ v_C \equiv 0 \text{ on } \Gamma_D\big\} \subset U_D.\end{aligned}$$

The least-squares formulation involves the symmetric and bilinear form

$$\begin{aligned}\mathcal{B} &: (H(\operatorname{div},\Omega;\mathbb{R}^{3\times3}) \times H^1(\Omega;\mathbb{R}^3)) \times (H(\operatorname{div},\Omega;\mathbb{R}^{3\times3}) \times H^1(\Omega;\mathbb{R}^3)) \to \mathbb{R},\\ \mathcal{B}(\sigma,u;\tau,v) &:= (\operatorname{div}\sigma,\operatorname{div}\tau)_{L^2(\Omega)} + (\mathcal{A}\sigma - \mathcal{S}\,\mathrm{D}\,u, \mathcal{A}\tau - \mathcal{S}\,\mathrm{D}\,v)_{L^2(\Omega)}.\end{aligned}$$

The LSFEM seeks $(\sigma_{LS},u_{LS}) \in \Sigma^k(\mathcal{T}) \times U^{k+1}(\mathcal{T})$ such that, for all $\tau_{LS} \in \Sigma_N^k(\mathcal{T})$ (or $\tau_{LS} \in \Sigma^k(\mathcal{T})$ in the case of $\Gamma_N = \emptyset$) and $v_{LS} \in U_D^{k+1}(\mathcal{T})$,

$$\mathcal{B}(\sigma_{LS},u_{LS};\tau_{LS},v_{LS}) = -(f,\operatorname{div}\tau_{LS})_{L^2(\Omega)}. \tag{3.18}$$

The solution (σ_{LS},u_{LS}) is the unique discrete minimiser of the least-squares functional

$$LS(f;\sigma_{LS},u_{LS}) := \|f + \operatorname{div}\sigma_{LS}\|_{L^2(\Omega)}^2 + \|\mathcal{A}\sigma_{LS} - \mathcal{S}\,\mathrm{D}\,u_{LS}\|_{L^2(\Omega)}^2.$$

The existence and uniqueness of the minimiser follows from well-known fundamental equivalences asserting the ellipticity of the bilinear form $\mathcal{B}$. Due to the Lemmas 3.2–3.4, the following theorem applies for all three model problems at hand. It solely requires the first three assumptions (W1)–(W3) from Section 3.1.

Theorem 3.12 (fundamental equivalence). *The assumptions (W1)–(W3) imply the existence of the positive generic constants* $C_{bdd} := 1 + C_{\mathcal{A}}^2$ *and*

$$\begin{aligned}C_{ell} := \max\big\{&4 + 2C_{tdd}^2\big(8 + C_{tdd} + 2C_{\mathcal{A}}^2(C_{tdd} + 8C_{\mathcal{A}}^2C_{En}^2)(1 + 4C_{tdd}^2)\big),\\ &1 + 4C_{tdd}\big(1 + 2C_{\mathcal{A}}^2(1 + 4C_{\mathcal{A}}^2C_{tdd}C_{En}^2)(1 + 4C_{tdd}^2)\big)\big\}\end{aligned} \tag{3.19}$$

such that, for all $\tau \in \Sigma_{\mathrm{N}}$ *and* $v \in U_{\mathrm{D}}$,

$$LS(0;\tau,v) \leq C_{\mathrm{bdd}} \left(\|\tau\|^2_{H(\mathrm{div},\Omega)} + \|\mathcal{S}\,\mathrm{D}\,v\|^2_{L^2(\Omega)} \right), \tag{3.20}$$

$$\|\tau\|^2_{H(\mathrm{div},\Omega)} + \|\mathcal{S}\,\mathrm{D}\,v\|^2_{L^2(\Omega)} \leq C_{\mathrm{ell}}\, LS(0;\tau,v). \tag{3.21}$$

This equivalence is well-known for the three model problems at hand. In particular, it generalises the results for the Poisson model problem [71, Lemma 4.3], the Stokes problem [32, Theorem 4.2], and the linear elasticity problem [34, Theorem 3.1]. The purpose of Theorem 3.12 is to underline its generality.

Proof of Theorem 3.12. Step 1. The triangle inequality and Young's inequality for any parameter $\alpha > 0$ yield

$$\begin{aligned} LS(0;\tau,v) &= \|\operatorname{div}\tau\|^2_{L^2(\Omega)} + \|\mathcal{A}\tau - \mathcal{S}\,\mathrm{D}\,v\|^2_{L^2(\Omega)} \\ &\leq \|\operatorname{div}\tau\|^2_{L^2(\Omega)} + (1+\alpha)\,\|\mathcal{A}\tau\|^2_{L^2(\Omega)} + (1+1/\alpha)\,\|\mathcal{S}\,\mathrm{D}\,v\|^2_{L^2(\Omega)}. \end{aligned}$$

The boundedness of $\mathcal{A}$ from the assumption (W1) concludes the proof of the boundedness

$$LS(0;\tau,v) \leq C_{\mathrm{bdd}}(\alpha) \left(\|\tau\|^2_{H(\mathrm{div},\Omega)} + \|\mathcal{S}\,\mathrm{D}\,v\|^2_{L^2(\Omega)} \right)$$

with $C_{\mathrm{bdd}}(\alpha) := \max\{(1+\alpha)C^2_{\mathcal{A}}, (1+1/\alpha)\}$. This parameter attains its minimum

$$C_{\mathrm{bdd}} := C_{\mathrm{bdd}}(\alpha^*) = 1 + C^2_{\mathcal{A}} \quad \text{for} \quad \alpha^* = \frac{1}{C^2_{\mathcal{A}}}.$$

Step 2. The proof of the ellipticity departs with the triangle inequality and the boundedness (W1) to show

$$\|\mathcal{S}\,\mathrm{D}\,v\|^2_{L^2(\Omega)} \leq 2\,\|\mathcal{A}\tau - \mathcal{S}\,\mathrm{D}\,v\|^2_{L^2(\Omega)} + 2C^2_{\mathcal{A}}\,\|\tau\|^2_{L^2(\Omega)}.$$

The abstract tr-dev-div inequality from (W2) establishes

$$\|\mathcal{S}\,\mathrm{D}\,v\|^2_{L^2(\Omega)} \leq 2\,\|\mathcal{A}\tau - \mathcal{S}\,\mathrm{D}\,v\|^2_{L^2(\Omega)} + 2C^2_{\mathcal{A}} C_{\mathrm{tdd}} \left(\|\operatorname{div}\tau\|^2_{L^2(\Omega)} + (\mathcal{A}\tau,\tau)_{L^2(\Omega)} \right). \tag{3.22}$$

In order to estimate the last term on the right-hand side, utilise the Cauchy-Schwarz inequality and, again, the abstract tr-dev-div inequality (W2) to prove

$$\begin{aligned} (\mathcal{A}\tau,\tau)_{L^2(\Omega)} &= (\mathcal{A}\tau - \mathcal{S}\,\mathrm{D}\,v,\tau)_{L^2(\Omega)} + (\mathcal{S}\,\mathrm{D}\,v,\tau)_{L^2(\Omega)} \\ &\leq C_{\mathrm{tdd}}\,\|\mathcal{A}\tau - \mathcal{S}\,\mathrm{D}\,v\|_{L^2(\Omega)} \big((\mathcal{A}\tau,\tau)_{L^2(\Omega)} + \|\operatorname{div}\tau\|^2_{L^2(\Omega)} \big)^{1/2} \\ &\quad + (\mathcal{S}\,\mathrm{D}\,v,\tau)_{L^2(\Omega)} \\ &\leq \frac{C^2_{\mathrm{tdd}}}{2}\,\|\mathcal{A}\tau - \mathcal{S}\,\mathrm{D}\,v\|^2_{L^2(\Omega)} + \frac{1}{2}\,(\mathcal{A}\tau,\tau)_{L^2(\Omega)} + \frac{1}{2}\,\|\operatorname{div}\tau\|^2_{L^2(\Omega)} \\ &\quad + (\mathcal{S}\,\mathrm{D}\,v,\tau)_{L^2(\Omega)} \end{aligned}$$

with Young's inequality in the last step. The absorption of the term $(\mathcal{A}\tau, \tau)_{L^2(\Omega)}$ on the left-hand side results in

$$(\mathcal{A}\tau, \tau)_{L^2(\Omega)} \leq C_{\mathrm{tdd}}^2 \, \|\mathcal{A}\tau - \mathcal{S}\,\mathrm{D}\, v\|_{L^2(\Omega)}^2 + \|\operatorname{div}\tau\|_{L^2(\Omega)}^2 + 2\,(\mathcal{S}\,\mathrm{D}\, v, \tau)_{L^2(\Omega)}. \tag{3.23}$$

The estimate (W3) and Young's inequality with parameter $\alpha > 0$ provide

$$(\mathcal{S}\,\mathrm{D}\, v, \tau)_{L^2(\Omega)} \leq \frac{C_{\mathrm{En}}^2}{\alpha} \, \|\mathcal{A}\tau - \mathcal{S}\,\mathrm{D}\, v\|_{L^2(\Omega)}^2 + \frac{C_{\mathrm{En}}^2}{\alpha} \, \|\operatorname{div}\tau\|_{L^2(\Omega)}^2 + \frac{\alpha}{2} \, \|\mathcal{S}\,\mathrm{D}\, v\|_{L^2(\Omega)}^2.$$

The combination of this with (3.23) in (3.22) yields

$$\begin{aligned}
\|\mathcal{S}\,\mathrm{D}\, v\|_{L^2(\Omega)}^2 &\leq 2(1 + C_{\mathcal{A}}^2 C_{\mathrm{tdd}}^3) \, \|\mathcal{A}\tau - \mathcal{S}\,\mathrm{D}\, v\|_{L^2(\Omega)}^2 + 4C_{\mathcal{A}}^2 C_{\mathrm{tdd}} \, \|\operatorname{div}\tau\|_{L^2(\Omega)}^2 \\
&\quad + 4C_{\mathcal{A}}^2 C_{\mathrm{tdd}} \, (\mathcal{S}\,\mathrm{D}\, v, \tau)_{L^2(\Omega)} \\
&\leq 2\big(1 + C_{\mathcal{A}}^2 C_{\mathrm{tdd}} (C_{\mathrm{tdd}}^2 + 2C_{\mathrm{En}}^2/\alpha)\big) \, \|\mathcal{A}\tau - \mathcal{S}\,\mathrm{D}\, v\|_{L^2(\Omega)}^2 \\
&\quad + 4C_{\mathcal{A}}^2 C_{\mathrm{tdd}} (1 + C_{\mathrm{En}}^2/\alpha) \, \|\operatorname{div}\tau\|_{L^2(\Omega)}^2 + 2C_{\mathcal{A}}^2 C_{\mathrm{tdd}} \alpha \, \|\mathcal{S}\,\mathrm{D}\, v\|_{L^2(\Omega)}^2.
\end{aligned}$$

Eventually, for $\alpha = 1/(4C_{\mathcal{A}}^2 C_{\mathrm{tdd}})$, another absorption of the term $\|\mathcal{S}\,\mathrm{D}\, v\|_{L^2(\Omega)}^2$ on the left-hand side leads to

$$\|\mathcal{S}\,\mathrm{D}\, v\|_{L^2(\Omega)}^2 \leq c_1 \, \|\mathcal{A}\tau - \mathcal{S}\,\mathrm{D}\, v\|_{L^2(\Omega)}^2 + c_2 \, \|\operatorname{div}\tau\|_{L^2(\Omega)}^2. \tag{3.24}$$

with the positive generic constants

$$c_1 := 4\big(1 + C_{\mathcal{A}}^2 C_{\mathrm{tdd}}^2 (C_{\mathrm{tdd}} + 8C_{\mathcal{A}}^2 C_{\mathrm{En}}^2)\big) \quad \text{and} \quad c_2 := 8C_{\mathcal{A}}^2 C_{\mathrm{tdd}} (1 + 4C_{\mathcal{A}}^2 C_{\mathrm{tdd}} C_{\mathrm{En}}^2).$$

Step 3. The estimate of the remaining term $\|\tau\|_{H(\operatorname{div},\Omega)}^2$ employs the assumption (W2), the estimate (3.23), and the Cauchy-Schwarz inequality to verify

$$\begin{aligned}
\|\tau\|_{L^2(\Omega)}^2 &\leq C_{\mathrm{tdd}} \, \|\operatorname{div}\tau\|_{L^2(\Omega)}^2 + C_{\mathrm{tdd}} \, (\mathcal{A}\tau, \tau)_{L^2(\Omega)} \\
&\leq C_{\mathrm{tdd}}^3 \, \|\mathcal{A}\tau - \mathcal{S}\,\mathrm{D}\, v\|_{L^2(\Omega)}^2 + 2C_{\mathrm{tdd}} \, \|\operatorname{div}\tau\|_{L^2(\Omega)}^2 + 2C_{\mathrm{tdd}} \, \|\mathcal{S}\,\mathrm{D}\, v\|_{L^2(\Omega)} \|\tau\|_{L^2(\Omega)}.
\end{aligned}$$

Young's inequality with parameter $\alpha = 1/2$ allows for an absorption of the last term. The resulting estimate reads

$$\|\tau\|_{L^2(\Omega)}^2 \leq 2C_{\mathrm{tdd}}^3 \, \|\mathcal{A}\tau - \mathcal{S}\,\mathrm{D}\, v\|_{L^2(\Omega)}^2 + 4C_{\mathrm{tdd}} \, \|\operatorname{div}\tau\|_{L^2(\Omega)}^2 + 4C_{\mathrm{tdd}}^2 \, \|\mathcal{S}\,\mathrm{D}\, v\|_{L^2(\Omega)}^2.$$

This and (3.24) show

$$\|\tau\|_{H(\operatorname{div},\Omega)}^2 \leq 2C_{\mathrm{tdd}}^2 (C_{\mathrm{tdd}} + 2c_1) \, \|\mathcal{A}\tau - \mathcal{S}\,\mathrm{D}\, v\|_{L^2(\Omega)}^2 + \big(1 + 4C_{\mathrm{tdd}}(1 + C_{\mathrm{tdd}} c_2)\big) \, \|\operatorname{div}\tau\|_{L^2(\Omega)}^2.$$

Step 4. The combination of the Steps 2 and 3 concludes the proof of the ellipticity with the positive generic constant

$$C_{\mathrm{ell}} := \max\big\{c_1 + 2C_{\mathrm{tdd}}^2 (C_{\mathrm{tdd}} + 2c_1), c_2 + \big(1 + 4C_{\mathrm{tdd}}(1 + C_{\mathrm{tdd}} c_2)\big)\big\}.$$

The insertion of c_1 and c_2 and the simplification of the terms result in the constant from (3.19). □

Remark 3.13. The proof of well-posedness in Theorem 3.12 is very general and does not employ the linearity of the operators $\mathcal{A}$ and $\mathcal{S}$. It applies to nonlinear problems as well.

Remark 3.14. The analysis in Section 3.2 reveals that the positive constant C_{En} in the assumption (W3) and, thus, also the ellipticity constant C_{ell} depend on the Friedrichs constant C_{F}. In particular, they scale with the diameter of the domain Ω. This is a common criticism on least-squares methods. However, the reader is referred to [25, Section 3] for a remedy and a scaling of the residuals with an ellipticity constant independent of $\operatorname{diam}(\Omega)$ in the case of the Stokes problem in 2D.

Remark 3.15. Another scaling issue is addressed in [95] in the context of a time-dependent linear elasticity problem. For the corresponding static formulation at hand, this results in the weighted least-squares functional

$$\widetilde{LS}(f;\sigma,u) := \big\|\frac{1}{\sqrt{E}}(f+\operatorname{div}\sigma)\big\|^2_{L^2(\Omega)} + \|\mathbb{C}^{-1}\sigma-\varepsilon(u)\|^2_{L^2(\Omega)},$$

where E denotes the Young's modulus. The weights are chosen in a way such that the L^2 norms measure dimensionless residuals.

The remaining part of this section is devoted to the proof of the standard a posteriori error estimates involving the boundary oscillations from (2.20). For the surface gradient $\mathrm{D}\,u_{\mathrm{D}}$ of the Dirichlet boundary data from (2.4), abbreviate the oscillation terms with

$$\eta^2_{\mathrm{osc}}(\mathcal{T}) := \operatorname{osc}^2(\mathrm{D}\,u_{\mathrm{D}},\mathcal{F}(\Gamma_{\mathrm{D}})) + \operatorname{osc}^2(t_{\mathrm{N}},\mathcal{F}(\Gamma_{\mathrm{N}})). \tag{3.25}$$

Theorem 3.16 (a posteriori estimates). *Given the assumptions (W1)–(W4), there exist positive generic constants C_{LS1} and C_{LS2} such that the exact solution $\sigma\in\Sigma$ and $u\in U$ to* (3.3) *and any $\tau_{\mathrm{RT}}\in\Sigma^k(\mathcal{T})$ and $v_{\mathrm{C}}\in U^{k+1}(\mathcal{T})$ satisfy*

$$\|\sigma-\tau_{\mathrm{RT}}\|^2_{H(\operatorname{div},\Omega)} + \|\mathcal{S}\,\mathrm{D}(u-v_{\mathrm{C}})\|^2_{L^2(\Omega)} \le C_{\mathrm{LS1}}\big(LS(f;\tau_{\mathrm{RT}},v_{\mathrm{C}}) + \eta^2_{\mathrm{osc}}(\mathcal{T})\big), \tag{3.26}$$

$$LS(f;\tau_{\mathrm{RT}},v_{\mathrm{C}}) \le C_{\mathrm{LS2}}\big(\|\sigma-\tau_{\mathrm{RT}}\|^2_{H(\operatorname{div},\Omega)} + \|\mathcal{S}\,\mathrm{D}(u-v_{\mathrm{C}})\|^2_{L^2(\Omega)} + \eta^2_{\mathrm{osc}}(\mathcal{T})\big). \tag{3.27}$$

Remark 3.17. Since Theorem 3.16 applies to arbitrary $\tau_{\mathrm{RT}}\in\Sigma^k(\mathcal{T})$ and $v_{\mathrm{C}}\in U^{k+1}(\mathcal{T})$, the least-squares functional $LS(f;\tau_{\mathrm{RT}},v_{\mathrm{C}})$ allows for a posteriori error estimation even in the case of an inexact solution of the linear system, for instance, by an iterative solver.

Proof of Theorem 3.16. Step 1. Let σ and u solve the first-order system (3.3) and $\tau_{\mathrm{RT}}\in\Sigma^k(\mathcal{T})$ and $v_{\mathrm{C}}\in U^{k+1}(\mathcal{T})$ be arbitrary. The boundary data of the respective differences read

$$u-v_{\mathrm{C}} = (1-\mathcal{J}_{\mathrm{D}}^{k+1})u_{\mathrm{D}} \text{ on } \Gamma_{\mathrm{D}} \quad\text{and}\quad (\sigma-\tau_{\mathrm{RT}})\nu = (1-\Pi_k)t_{\mathrm{N}} \text{ on } \Gamma_{\mathrm{N}}$$

and do not vanish in general. Since Theorem 3.12 solely applies to functions with homogeneous boundary conditions, its application requires suitable extensions of the boundary data approximation errors from the Sections 3.3–3.4.

The extension $w \in H^1(\Omega;\mathbb{R}^3)$ from Lemma 3.6 satisfies $w = (1 - \mathcal{J}_{\mathrm{D}}^{k+1})u_{\mathrm{D}}$ on Γ_{D} and

$$\|\mathrm{D}\, w\|_{L^2(\Omega)}^2 \leq \|(1 - \mathcal{J}_{\mathrm{D}}^{k+1})u_{\mathrm{D}}\|_{H^{1/2}(\Gamma_{\mathrm{D}})}^2.$$

Consequently, Lemma 3.7 implies

$$\|\mathrm{D}\, w\|_{L^2(\Omega)}^2 \leq C_{\mathrm{D1}}^2 \ \mathrm{osc}^2(\mathrm{D}\, u_{\mathrm{D}}, \mathcal{F}(\Gamma_{\mathrm{D}})).$$

This and the boundedness of the operator $\mathcal{S}$ from (W4) prove

$$\|\mathcal{S}\,\mathrm{D}\, w\|_{L^2(\Omega)}^2 \leq C_{\mathcal{S}}^2 C_{\mathrm{D1}}^2 \ \mathrm{osc}^2(\mathrm{D}\, u_{\mathrm{D}}, \mathcal{F}(\Gamma_{\mathrm{D}})). \tag{3.28}$$

The extension $\xi \in H(\mathrm{div} = 0, \Omega;\mathbb{R}^{3\times 3})$ from Lemma 3.9 satisfies $\xi\nu = (1 - \Pi_{\mathrm{N}})t_{\mathrm{N}}$ on Γ_{N} and

$$\|\xi\|_{L^2(\Omega)}^2 \leq (1 + C_{\mathrm{F}}^2)^2 \, \|(1 - \Pi_k)\widetilde{t}_{\mathrm{N}}\|_{H^{-1/2}(\partial\Omega)}^2.$$

Thus, Lemma 3.10 shows

$$\|\xi\|_{L^2(\Omega)}^2 \leq (1 + C_{\mathrm{F}}^2)^2 C_{\mathrm{N}}^2 \ \mathrm{osc}^2(t_{\mathrm{N}}, \mathcal{F}(\Gamma_{\mathrm{N}})). \tag{3.29}$$

The triangle inequality, the boundedness of the operator $\mathcal{A}$ from (W1), and the estimates (3.28)–(3.29) lead to

$$\begin{aligned}\|\mathcal{A}\xi - \mathcal{S}\,\mathrm{D}\, w\|_{L^2(\Omega)}^2 \leq{}& 2C_{\mathcal{A}}^2(1 + C_{\mathrm{F}}^2)^2 C_{\mathrm{N}}^2 \ \mathrm{osc}^2(t_{\mathrm{N}}, \mathcal{F}(\Gamma_{\mathrm{N}})) \\ &+ 2C_{\mathcal{S}}^2 C_{\mathrm{D1}}^2 \ \mathrm{osc}^2(\mathrm{D}\, u_{\mathrm{D}}, \mathcal{F}(\Gamma_{\mathrm{N}})).\end{aligned} \tag{3.30}$$

The abbreviations $\tau_{\mathrm{N}} := \sigma - \tau_{\mathrm{RT}} - \xi \in \Sigma_{\mathrm{N}}$ and $v_{\mathrm{D}} := u - v_{\mathrm{C}} - w \in U_{\mathrm{D}}$ satisfy homogeneous boundary conditions.

Step 2. Since σ and u are exact solutions to the first-order system (3.3), it holds that

$$\begin{aligned}LS(0;\tau_{\mathrm{N}}, v_{\mathrm{D}}) &= \|\,\mathrm{div}\,\tau_{\mathrm{N}}\|_{L^2(\Omega)}^2 + \|\mathcal{A}\tau_{\mathrm{N}} - \mathcal{S}\,\mathrm{D}\, v_{\mathrm{D}}\|_{L^2(\Omega)}^2 \\ &= \|f + \mathrm{div}(\tau_{\mathrm{RT}} - \xi)\|_{L^2(\Omega)}^2 + \|\mathcal{A}(\tau_{\mathrm{RT}} - \xi) - \mathcal{S}\,\mathrm{D}(v_{\mathrm{C}} + w)\|_{L^2(\Omega)}^2.\end{aligned}$$

This and $\mathrm{div}\,\xi = 0$ imply

$$\begin{aligned}LS(0;\tau_{\mathrm{N}}, v_{\mathrm{D}}) = LS(f;\tau_{\mathrm{RT}}, v_{\mathrm{C}}) &+ 2\,(\mathcal{A}\tau_{\mathrm{RT}} - \mathcal{S}\,\mathrm{D}\, v_{\mathrm{C}}, \mathcal{A}\xi - \mathcal{S}\,\mathrm{D}\, w)_{L^2(\Omega)} \\ &+ \|\mathcal{A}\xi - \mathcal{S}\,\mathrm{D}\, w\|_{L^2(\Omega)}^2.\end{aligned} \tag{3.31}$$

Step 3. The proof of the reliability of the least-squares functional departs with the triangle inequality and Young's inequality to show

$$\begin{aligned}&\|\sigma - \tau_{\mathrm{RT}}\|_{H(\mathrm{div},\Omega)}^2 + \|\mathcal{S}\,\mathrm{D}(u - v_{\mathrm{C}})\|_{L^2(\Omega)}^2 \\ &\qquad\leq 2\big(\|\tau_{\mathrm{N}}\|_{H(\mathrm{div},\Omega)}^2 + \|\mathcal{S}\,\mathrm{D}\, v_{\mathrm{D}}\|_{L^2(\Omega)}^2 + \|\xi\|_{L^2(\Omega)}^2 + \|\mathcal{S}\,\mathrm{D}\, w\|_{L^2(\Omega)}^2\big).\end{aligned}$$

The ellipticity (3.21) of the least-squares functional from Theorem 3.12 proves

$$\|\tau_{\mathrm{N}}\|^2_{H(\mathrm{div},\Omega)} + \|\mathcal{S}\,\mathrm{D}\,v_{\mathrm{D}}\|^2_{L^2(\Omega)} \leq C_{\mathrm{ell}}\,LS(0;\tau_{\mathrm{N}},v_{\mathrm{D}}).$$

The combination of the two previously displayed formulas leads to

$$\|\sigma-\tau_{\mathrm{RT}}\|^2_{L^2(\Omega)} + \|\mathcal{S}\,\mathrm{D}(u-v_{\mathrm{C}})\|^2_{L^2(\Omega)} \leq 2\,\big(C_{\mathrm{ell}}\,LS(0;\tau_{\mathrm{N}},v_{\mathrm{D}}) + \|\xi\|^2_{L^2(\Omega)} + \|\mathcal{S}\,\mathrm{D}\,w\|^2_{L^2(\Omega)}\big).$$

This and the equality (3.31) in combination with the Cauchy-Schwarz and Young's inequality prove

$$\begin{aligned}&\|\sigma-\tau_{\mathrm{RT}}\|^2_{L^2(\Omega)} + \|\mathcal{S}\,\mathrm{D}(u-v_{\mathrm{C}})\|^2_{L^2(\Omega)}\\ &\quad\leq 2\,\big((1+C_{\mathrm{ell}})\,LS(f;\tau_{\mathrm{RT}},v_{\mathrm{C}}) + 2\,\|\mathcal{A}\xi-\mathcal{S}\,\mathrm{D}\,w\|^2_{L^2(\Omega)} + \|\xi\|^2_{L^2(\Omega)} + \|\mathcal{S}\,\mathrm{D}\,w\|^2_{L^2(\Omega)}\big).\end{aligned}$$

The triangle inequality and the estimates (3.28)–(3.30) conclude the proof of (3.26) with the positive generic constant

$$C_{\mathrm{LS1}} \coloneqq 2\max\big\{(1+C_{\mathrm{ell}}),\ (4C^2_{\mathcal{A}}+1)(1+C_{\mathrm{F}}^2)^2C^2_{\mathrm{N}},\ 5C^2_{\mathcal{S}}C^2_{\mathrm{D1}}\big\}.$$

Step 4. For the proof of the efficiency of the least-squares functional, the equality (3.31) provides

$$LS(f;\tau_{\mathrm{RT}},v_{\mathrm{C}}) \leq LS(0;\tau_{\mathrm{N}},v_{\mathrm{D}}) - 2\,(\mathcal{A}\tau_{\mathrm{RT}}-\mathcal{S}\,\mathrm{D}\,v_{\mathrm{C}},\mathcal{A}\xi-\mathcal{S}\,\mathrm{D}\,w)_{L^2(\Omega)}.$$

The boundedness (3.20) of the least-squares functional from Theorem 3.12 and the Cauchy-Schwarz inequality imply

$$\begin{aligned}LS(f;\tau_{\mathrm{RT}},v_{\mathrm{C}}) &\leq C_{\mathrm{bdd}}\,\big(\|\tau_{\mathrm{N}}\|^2_{L^2(\Omega)} + \|\mathcal{S}\,\mathrm{D}\,v_{\mathrm{D}}\|^2_{L^2(\Omega)}\big)\\ &\qquad + \|\mathcal{A}\tau_{\mathrm{RT}}-\mathcal{S}\,\mathrm{D}\,v_{\mathrm{C}}\|_{L^2(\Omega)}\|\mathcal{A}\xi-\mathcal{S}\,\mathrm{D}\,w\|_{L^2(\Omega)}.\end{aligned}$$

The triangle inequality and Young's inequality show

$$\begin{aligned}&LS(f;\tau_{\mathrm{RT}},v_{\mathrm{C}})\\ &\quad\leq 2C_{\mathrm{bdd}}\,\big(\|\sigma-\tau_{\mathrm{RT}}\|^2_{L^2(\Omega)} + \|\mathcal{S}\,\mathrm{D}(u-v_{\mathrm{C}})\|^2_{L^2(\Omega)} + \|\xi\|^2_{L^2(\Omega)} + \|\mathcal{S}\,\mathrm{D}\,w\|^2_{L^2(\Omega)}\big)\\ &\qquad + \frac{1}{2}\,\|\mathcal{A}\xi-\mathcal{S}\,\mathrm{D}\,w\|^2_{L^2(\Omega)} + \frac{1}{2}\,\|\mathcal{A}\tau_{\mathrm{RT}}-\mathcal{S}\,\mathrm{D}\,v_{\mathrm{C}}\|^2_{L^2(\Omega)}.\end{aligned}$$

The absorption of the last term, $\|\mathcal{A}\tau_{\mathrm{RT}}-\mathcal{S}\,\mathrm{D}\,v_{\mathrm{C}}\|^2_{L^2(\Omega)} \leq LS(f;\tau_{\mathrm{RT}},v_{\mathrm{C}})$, on the left-hand side yields

$$\begin{aligned}&LS(f;\tau_{\mathrm{RT}},v_{\mathrm{C}})\\ &\quad\leq 4C_{\mathrm{bdd}}\,\big(\|\sigma-\tau_{\mathrm{RT}}\|^2_{L^2(\Omega)} + \|\mathcal{S}\,\mathrm{D}(u-v_{\mathrm{C}})\|^2_{L^2(\Omega)} + \|\xi\|^2_{L^2(\Omega)} + \|\mathcal{S}\,\mathrm{D}\,w\|^2_{L^2(\Omega)}\big)\\ &\qquad + \|\mathcal{A}\xi-\mathcal{S}\,\mathrm{D}\,w\|^2_{L^2(\Omega)}.\end{aligned}$$

The estimates (3.28)–(3.30) conclude the proof of the efficiency (3.27) with the positive generic constant

$$C_{\mathrm{LS2}} \coloneqq \max\big\{4C_{\mathrm{bdd}},\ (4C_{\mathrm{bdd}}+2C^2_{\mathcal{A}})(1+C_{\mathrm{F}}^2)^2C^2_{\mathrm{N}},\ (2+4C_{\mathrm{bdd}})C^2_{\mathcal{S}}C^2_{\mathrm{D1}}\big\}.$$ □

3.6 Alternative a posteriori error estimator

Given the solution $(\sigma_{\mathrm{LS}}, u_{\mathrm{LS}})$ to the discrete equation (3.18) with respect to the triangulation $\mathcal{T}$, the residual contributions to the alternative error estimator on $T \in \mathcal{T}$ read

$$\begin{aligned}\eta_{\mathrm{res}}^2(\mathcal{T},T) \coloneqq{}& |T|^{2/3}\| \operatorname{div}(\mathcal{S}^*(\mathcal{A}\sigma_{\mathrm{LS}} - \mathcal{S}\,\mathrm{D}\,u_{\mathrm{LS}}))\|_{L^2(T)}^2 \\ &+ |T|^{2/3}\| \operatorname{curl}(\mathcal{A}^*(\mathcal{A}\sigma_{\mathrm{LS}} - \mathcal{S}\,\mathrm{D}\,u_{\mathrm{LS}}))\|_{L^2(T)}^2 \\ &+ |T|^{1/3} \sum_{F\in\mathcal{F}(T)\setminus\mathcal{F}(\Gamma_{\mathrm{D}})} \|[\mathcal{S}^*(\mathcal{A}\sigma_{\mathrm{LS}} - \mathcal{S}\,\mathrm{D}\,u_{\mathrm{LS}})]_F\ \nu_F\|_{L^2(F)}^2 \\ &+ |T|^{1/3} \sum_{F\in\mathcal{F}(T)\setminus\mathcal{F}(\Gamma_{\mathrm{N}})} \|\nu_F \times [\mathcal{A}^*(\mathcal{A}\sigma_{\mathrm{LS}} - \mathcal{S}\,\mathrm{D}\,u_{\mathrm{LS}})]_F\|_{L^2(F)}^2\end{aligned}$$

with tangential and normal jumps $[\nu \times \bullet]_F$ and $[\bullet\, \nu_F]_F$ along the faces $F \in \mathcal{F}$ from (2.13)–(2.14). Due to the assumptions (W6)–(W9), all these contributions are well-defined and bounded. The Dirichlet boundary data oscillations involve the surface gradient $\mathrm{D}\,u_{\mathrm{D}}$ from (2.4) applied to the boundary data u_{D}. Inhomogeneous boundary conditions lead to the oscillation contributions already defined in (3.25)

$$\begin{aligned}\eta_{\mathrm{osc}}^2(\mathcal{T},T) \coloneqq{}& |T|^{1/3} \sum_{F\in\mathcal{F}(T)\cap\mathcal{F}(\Gamma_{\mathrm{D}})} \|(1-\Pi_k)\,\mathrm{D}\,u_{\mathrm{D}}\|_{L^2(F)}^2 \\ &+ |T|^{1/3} \sum_{F\in\mathcal{F}(T)\cap\mathcal{F}(\Gamma_{\mathrm{N}})} \|(1-\Pi_k)\ t_{\mathrm{N}}\|_{L^2(F)}^2.\end{aligned} \tag{3.32}$$

For any subset $\mathcal{M} \subseteq \mathcal{T}$ of simplices, abbreviate $\eta_{\mathrm{res}}^2(\mathcal{T},\mathcal{M}) \coloneqq \sum_{T\in\mathcal{M}} \eta_{\mathrm{res}}^2(\mathcal{T},T)$ and $\eta_{\mathrm{osc}}^2(\mathcal{T},\mathcal{M}) \coloneqq \sum_{T\in\mathcal{M}} \eta_{\mathrm{osc}}^2(\mathcal{T},T)$. Their sum provides the alternative explicit a posteriori estimator for the ALSFEM algorithm from page 4

$$\eta^2(\mathcal{T},\mathcal{M}) \coloneqq \eta_{\mathrm{res}}^2(\mathcal{T},\mathcal{M}) + \eta_{\mathrm{osc}}^2(\mathcal{T},\mathcal{M}). \tag{3.33}$$

Moreover, for the full contribution on the triangulation $\mathcal{T}$, abbreviate $\eta^2(\mathcal{T}) \coloneqq \eta^2(\mathcal{T},\mathcal{T})$ and do so analogously for η_{res} and η_{osc}. The discrete reliability analysis in the Sections 4.2–4.3 below requires $(\sigma_{\mathrm{LS}}, u_{\mathrm{LS}})$ to solve the discrete equation (3.18) exactly. Hence, in contrast to the built-in estimator, adaptive algorithms driven by the alternative estimator η are obliged to employ an exact solution of the linear system.

Before the remaining part of this section is devoted to the proof of the efficiency of the estimator η, two additional quantities for the convergence analysis of the separate marking algorithm are introduced. The data approximation error $\mu^2(\mathcal{T}) \coloneqq \sum_{T\in\mathcal{T}} \mu^2(T)$ consists of, for $T \in \mathcal{T}$,

$$\mu^2(T) \coloneqq \|(1-\Pi_k)f\|_{L^2(T)}^2. \tag{3.34}$$

The data approximation solely concerns the volume data f. The boundary data approximation is controlled by the Dörfler marking and NVB in η_{osc}^2.

For any admissible triangulation $\mathcal{T} \in \mathbb{T}$ and its refinement $\widehat{\mathcal{T}} \in \mathbb{T}(\mathcal{T})$, the associated solutions $(\sigma_{\mathrm{LS}}, u_{\mathrm{LS}})$ and $(\widehat{\sigma}_{\mathrm{LS}}, \widehat{u}_{\mathrm{LS}})$ to (3.18) define the distance of the triangulations by

$$\delta^2(\widehat{\mathcal{T}}, \mathcal{T}) := \| \operatorname{div}(\widehat{\sigma}_{\mathrm{LS}} - \sigma_{\mathrm{LS}})\|^2_{L^2(\Omega)} + \|\mathcal{A}(\widehat{\sigma}_{\mathrm{LS}} - \sigma_{\mathrm{LS}}) - \mathcal{S}\,\mathrm{D}(\widehat{u}_{\mathrm{LS}} - u_{\mathrm{LS}})\|^2_{L^2(\Omega)}. \quad (3.35)$$

In accordance with the analysis presented in [37, Section 11], the distance function does not involve any boundary data oscillations. This relies on the following two facts. The strict locality of Π_k in the definitions of the oscillations $\operatorname{osc}(\mathrm{D}\, u_{\mathrm{D}}, \mathcal{F}(\Gamma_{\mathrm{D}}))$ and $\operatorname{osc}(t_{\mathrm{N}}, \mathcal{F}(\Gamma_{\mathrm{N}}))$ in (2.20) ensures that the corresponding terms vanish in the proof of the stability axiom in Theorem 4.1 below. Additionally, due to the orthogonality of the operator Π_k no terms like $\|(\widehat{\Pi}_k - \Pi_k)\,\mathrm{D}\, u_{\mathrm{D}}\|_{L^2(\Omega)}$ occur in the right-hand side of the reduction estimate in Theorem 4.2 below.

The following efficiency estimate for the error estimator η is not required in the axiomatic framework from [37, 40]. Nonetheless, it is a central result in the a posteriori analysis of FEMs and it is presented here to indicate the optimal rate approximation of the errors as well.

Theorem 3.18 (efficiency). *There exists a positive generic constant C_{eff} such that the residual contributions η_{res} to the a posteriori error estimator η satisfy*

$$\eta^2_{\mathrm{res}}(\mathcal{T}) \le C_{\mathrm{eff}}\, LS(f; \sigma_{\mathrm{LS}}, u_{\mathrm{LS}}). \quad (3.36)$$

The proof of Theorem 3.18 employs a modification of a result from [40, Lemma 5.2] involving the discrete trace inequalities (W8)–(W9) from Section 3.1.

Lemma 3.19 (discrete jump control). *Given the assumptions (W8) and (W9), there exists a positive generic constant C_{jc} such that any $\tau_{\mathrm{pw}} \in P_k(\mathcal{T}; \mathbb{R}^{3\times 3})$ and $v_{\mathrm{pw}} \in P_{k+1}(\mathcal{T}; \mathbb{R}^3)$ satisfy*

$$\sum_{T\in\mathcal{T}} |T|^{1/3} \sum_{F\in\mathcal{F}(T)} \big(\|[\mathcal{S}^*(\mathcal{A}\tau_{\mathrm{pw}} - \mathcal{S}\,\mathrm{D}\, v_{\mathrm{pw}})]_F\, \nu_F\|^2_{L^2(F)} + \|\nu_F \times [\mathcal{A}^*(\mathcal{A}\tau_{\mathrm{pw}} - \mathcal{S}\,\mathrm{D}\, v_{\mathrm{pw}})]_F\|^2_{L^2(F)} \big) \le C^2_{\mathrm{jc}}\, \|\mathcal{A}\tau_{\mathrm{pw}} - \mathcal{S}\,\mathrm{D}\, v_{\mathrm{pw}}\|^2_{L^2(\Omega)}.$$

The constant C_{jc} solely depends on the shape regularity of the triangulations in $\mathbb{T}$ and the generic constant C_{dti} from (W8)–(W9).

Proof. The discrete trace inequalities from (W8)–(W9) read

$$|T|^{1/6}\|(\mathcal{S}^*(\mathcal{A}\tau_{\mathrm{pw}} - \mathcal{S}\,\mathrm{D}\, v_{\mathrm{pw}}))|_T\, \nu_F\|_{L^2(F)} \le C_{\mathrm{dti}}\, \|\mathcal{A}\tau_{\mathrm{pw}} - \mathcal{S}\,\mathrm{D}\, v_{\mathrm{pw}}\|_{L^2(T)},$$
$$|T|^{1/6}\|\nu_F \times (\mathcal{A}^*(\mathcal{A}\tau_{\mathrm{pw}} - \mathcal{S}\,\mathrm{D}\, v_{\mathrm{pw}}))|_T\|_{L^2(F)} \le C_{\mathrm{dti}}\, \|\mathcal{A}\tau_{\mathrm{pw}} - \mathcal{S}\,\mathrm{D}\, v_{\mathrm{pw}}\|_{L^2(T)}.$$

These two estimate replace the first displayed equation in the proof of [40, Lemma 5.2]. The verbatim application of the proof therein establishes, for some positive generic

constant c_1,

$$\sum_{T\in\mathcal{T}} |T|^{1/3} \sum_{F\in\mathcal{F}(T)} \|[\mathcal{S}^*(\mathcal{A}\tau_{\mathrm{pw}} - \mathcal{S}\,\mathrm{D}\,v_{\mathrm{pw}})]_F\ \nu_F\|^2_{L^2(F)} \le c_1^2\,\|\mathcal{A}\tau_{\mathrm{pw}} - \mathcal{S}\,\mathrm{D}\,v_{\mathrm{pw}}\|^2_{L^2(\Omega)},$$
$$\sum_{T\in\mathcal{T}} |T|^{1/3} \sum_{F\in\mathcal{F}(T)} \|\nu_F \times [\mathcal{A}^*(\mathcal{A}\tau_{\mathrm{pw}} - \mathcal{S}\,\mathrm{D}\,v_{\mathrm{pw}})]_F\|^2_{L^2(F)} \le c_1^2\,\|\mathcal{A}\tau_{\mathrm{pw}} - \mathcal{S}\,\mathrm{D}\,v_{\mathrm{pw}}\|^2_{L^2(\Omega)}.$$

The sum of the two estimates concludes the proof with the constant $C_{\mathrm{jc}}^2 := 2c_1^2$. □

Proof of Theorem 3.18. Step 1. Abbreviate the discrete constitutive residual $\rho_{\mathrm{LS}} := \mathcal{A}\sigma_{\mathrm{LS}} - \mathcal{S}\,\mathrm{D}\,u_{\mathrm{LS}} \in L^2(\Omega;\mathbb{R}^{3\times3})$. Given any $T \in \mathcal{T}$, inverse estimates from the assumptions (W6)–(W7) and the boundedness of the adjoint operators $\mathcal{A}^*$ and $\mathcal{S}^*$ from (3.2) prove

$$|T|^{2/3}\|\operatorname{div}\mathcal{S}^*\rho_{\mathrm{LS}}\|^2_{L^2(T)} + |T|^{2/3}\|\operatorname{curl}\mathcal{A}^*\rho_{\mathrm{LS}}\|^2_{L^2(T)} \le C_{\mathrm{inv}}^2(C_{\mathcal{S}}^2 + C_{\mathcal{A}}^2)\,\|\rho_{\mathrm{LS}}\|^2_{L^2(T)}.$$

The sum over all $T \in \mathcal{T}$ concludes the estimate of the volume contributions in η_{res}.

Step 2. The estimate of the jump terms employs the discrete jump control from Lemma 3.19 to show

$$\sum_{T\in\mathcal{T}} |T|^{1/3} \sum_{F\in\mathcal{F}(T)} \big(\|[\mathcal{S}^*\rho_{\mathrm{LS}}]_F\ \nu_F\|^2_{L^2(F)} + \|\nu_F \times [\mathcal{A}^*\rho_{\mathrm{LS}}]_F\|^2_{L^2(F)}\big) \le C_{\mathrm{jc}}^2\,\|\rho_{\mathrm{LS}}\|^2_{L^2(\Omega)}.$$

This and the estimate $\|\rho_{\mathrm{LS}}\|^2_{L^2(\Omega)} \le LS(f;\sigma_{\mathrm{LS}},u_{\mathrm{LS}})$ complete the proof of the efficiency (3.36) with the positive generic constant $C_{\mathrm{eff}} := C_{\mathrm{inv}}^2(C_{\mathcal{S}}^2 + C_{\mathcal{A}}^2) + C_{\mathrm{jc}}^2$. □

4 Axioms of adaptivity

This chapter is devoted to the proofs of the axioms of adaptivity (A1)–(A4) and (QM) from the introductory Chapter 1. Section 4.1 is devoted to the stability (A1) and the reduction (A2). Section 4.2 presents the reliability of the alternative estimator η and its discrete reliability (A3). The comprehensive proof of the discrete reliability is given in Section 4.3. Some quasi-Pythagoras lemma establishes the quasi-orthogonality in Section 4.4. This chapter concludes with the proof of the quasi-monotonicity of $\eta + \mu$ in Section 4.5. Using [40, Theorem 2.1], these axioms establish the main result of this thesis, Theorem 1.1.

4.1 Stability and reduction

The proofs of the first two axioms employ techniques from the efficiency analysis in Section 3.6. Recall Notation 3 from page 22 for a regular triangulation $\mathcal{T} \in \mathbb{T}$ with admissible refinement $\widehat{\mathcal{T}} \in \mathbb{T}(\mathcal{T})$.

Theorem 4.1 (stability). *The a posteriori error estimator η and the distance δ satisfy the axiom* (A1)*: There exists a positive generic constant Λ_1 such that*

$$|\eta(\widehat{\mathcal{T}}, \widehat{\mathcal{T}} \cap \mathcal{T}) - \eta(\mathcal{T}, \widehat{\mathcal{T}} \cap \mathcal{T})| \leq \Lambda_1 \, \delta(\widehat{\mathcal{T}}, \mathcal{T}).$$

Proof. The proof follows the one of [40, Theorem 5.1]. Abbreviate the discrete constitutive residuals $\widehat{\rho}_{\mathrm{LS}} := \mathcal{A}\widehat{\sigma}_{\mathrm{LS}} - \mathcal{S}\,\mathrm{D}\,\widehat{u}_{\mathrm{LS}}$ and $\rho_{\mathrm{LS}} := \mathcal{A}\sigma_{\mathrm{LS}} - \mathcal{S}\,\mathrm{D}\,u_{\mathrm{LS}}$.

Step 1. Each of the terms $\eta(\widehat{\mathcal{T}}, \widehat{\mathcal{T}} \cap \mathcal{T})$ and $\eta(\mathcal{T}, \widehat{\mathcal{T}} \cap \mathcal{T})$ is the Euclidian norm $|\widehat{a}|$ and $|a|$ of some vector $\widehat{a}, a \in \mathbb{R}^m$ with $m := 10\,|\widehat{\mathcal{T}} \cap \mathcal{T}|$. The entries of $\widehat{a}$ consist of the square roots of the volume contributions, the edge contributions, and the boundary data oscillation terms from (3.33), for each $T \in \widehat{\mathcal{T}} \cap \mathcal{T}$,

$$\begin{aligned}
&|T|^{1/3} \| \operatorname{div}(\mathcal{S}^* \widehat{\rho}_{\mathrm{LS}}) \|_{L^2(T)}, && |T|^{1/3} \| \operatorname{curl}(\mathcal{A}^* \widehat{\rho}_{\mathrm{LS}}) \|_{L^2(T)}, \\
&|T|^{1/6} \| [\mathcal{S}^* \widehat{\rho}_{\mathrm{LS}}]_F \, \nu_F \|_{L^2(F)} && \text{for } F \in \mathcal{F}(T) \setminus \mathcal{F}(\Gamma_{\mathrm{D}}), \\
&|T|^{1/6} \| \nu_F \times [\mathcal{A}^* \widehat{\rho}_{\mathrm{LS}}]_F \|_{L^2(F)} && \text{for } F \in \mathcal{F}(T) \setminus \mathcal{F}(\Gamma_{\mathrm{N}}), \\
&|T|^{1/6} \| (1 - \widehat{\Pi}_k)\, \mathrm{D}\, u_{\mathrm{D}} \|_{L^2(F)} && \text{for } F \in \mathcal{F}(T) \cap \mathcal{F}(\Gamma_{\mathrm{D}}), \\
&|T|^{1/6} \| (1 - \widehat{\Pi}_k)\; t_{\mathrm{N}} \|_{L^2(F)} && \text{for } F \in \mathcal{F}(T) \cap \mathcal{F}(\Gamma_{\mathrm{N}}).
\end{aligned} \tag{4.1}$$

Analogously, the entries of a consist of the corresponding terms for ρ_{LS} and Π_k with

respect to $\mathcal{T}$. The reverse triangle inequality in $\mathbb{R}^m$ proves that

$$
\begin{aligned}
&(\eta(\widehat{\mathcal{T}},\widehat{\mathcal{T}}\cap\mathcal{T})-\eta(\mathcal{T},\widehat{\mathcal{T}}\cap\mathcal{T}))^2=(|\widehat{a}|-|a|)^2\le|\widehat{a}-a|^2\\
&=\sum_{T\in\widehat{\mathcal{T}}\cap\mathcal{T}}\Bigg[|T|^{2/3}\big(\|\operatorname{div}(\mathcal{S}^*\widehat{\rho}_{\mathrm{LS}})\|_{L^2(T)}-\|\operatorname{div}(\mathcal{S}^*\rho_{\mathrm{LS}})\|_{L^2(T)}\big)^2\\
&\quad+|T|^{2/3}\big(\|\operatorname{curl}(\mathcal{A}^*\widehat{\rho}_{\mathrm{LS}})\|_{L^2(T)}-\|\operatorname{curl}(\mathcal{A}^*\widehat{\rho}_{\mathrm{LS}})\|_{L^2(T)}\big)^2\\
&\quad+|T|^{1/3}\sum_{F\in\mathcal{F}(T)\setminus\mathcal{F}(\Gamma_{\mathrm{D}})}\big(\|[\mathcal{S}^*\widehat{\rho}_{\mathrm{LS}}]_F\,\nu_F\|_{L^2(F)}-\|[\mathcal{S}^*\rho_{\mathrm{LS}}]_F\,\nu_F\|_{L^2(F)}\big)^2\\
&\quad+|T|^{1/3}\sum_{F\in\mathcal{F}(T)\setminus\mathcal{F}(\Gamma_{\mathrm{N}})}\big(\|\nu_F\times[\mathcal{A}^*\widehat{\rho}_{\mathrm{LS}}]_F\|_{L^2(F)}-\|\nu_F\times[\mathcal{A}^*\rho_{\mathrm{LS}}]_F\|_{L^2(F)}\big)^2\\
&\quad+|T|^{1/3}\sum_{F\in\mathcal{F}(T)\cap\mathcal{F}(\Gamma_{\mathrm{D}})}\big(\|(1-\widehat{\Pi}_k)\,\mathrm{D}\,u_{\mathrm{D}}\|_{L^2(F)}-\|(1-\Pi_k)\,\mathrm{D}\,u_{\mathrm{D}}\|_{L^2(F)}\big)^2\\
&\quad+|T|^{1/3}\sum_{F\in\mathcal{F}(T)\cap\mathcal{F}(\Gamma_{\mathrm{N}})}\big(\|(1-\widehat{\Pi}_k)t_{\mathrm{N}}\|_{L^2(F)}-\|(1-\Pi_k)t_{\mathrm{N}}\|_{L^2(F)}\big)^2\Bigg].
\end{aligned}
$$

Step 2. For every $T\in\widehat{\mathcal{T}}\cap\mathcal{T}$, the reverse triangle inequality in $L^2(T)$ followed by the abstract inverse estimates (W6)–(W7) prove

$$
\begin{aligned}
&|T|^{2/3}\big(\|\operatorname{div}(\mathcal{S}^*\widehat{\rho}_{\mathrm{LS}})\|_{L^2(T)}-\|\operatorname{div}(\mathcal{S}^*\rho_{\mathrm{LS}})\|_{L^2(T)}\big)^2\\
&\quad\le|T|^{2/3}\|\operatorname{div}(\mathcal{S}^*(\widehat{\rho}_{\mathrm{LS}}-\rho_{\mathrm{LS}}))\|_{L^2(T)}^2\le C_{\mathrm{inv}}^2\|\mathcal{S}^*(\widehat{\rho}_{\mathrm{LS}}-\rho_{\mathrm{LS}})\|_{L^2(T)}^2
\end{aligned}
$$

and

$$
\begin{aligned}
&|T|^{2/3}\big(\|\operatorname{curl}(\mathcal{A}^*\widehat{\rho}_{\mathrm{LS}})\|_{L^2(T)}-\|\operatorname{curl}(\mathcal{A}^*\rho_{\mathrm{LS}})\|_{L^2(T)}\big)^2\\
&\quad\le|T|^{2/3}\|\operatorname{curl}(\mathcal{A}^*(\widehat{\rho}_{\mathrm{LS}}-\rho_{\mathrm{LS}}))\|_{L^2(T)}^2\le C_{\mathrm{inv}}^2\|\mathcal{A}^*(\widehat{\rho}_{\mathrm{LS}}-\rho_{\mathrm{LS}})\|_{L^2(T)}^2.
\end{aligned}
$$

The sum of these two estimates and the boundedness of the adjoint operators $\mathcal{A}^*$ and $\mathcal{S}^*$ from (3.2) yield

$$
\begin{aligned}
&|T|^{2/3}\big(\|\operatorname{div}(\mathcal{S}^*\widehat{\rho}_{\mathrm{LS}})\|_{L^2(T)}-\|\operatorname{div}(\mathcal{S}^*\rho_{\mathrm{LS}})\|_{L^2(T)}\big)^2\\
&\quad+|T|^{2/3}\big(\|\operatorname{curl}(\mathcal{A}^*\widehat{\rho}_{\mathrm{LS}})\|_{L^2(T)}-\|\operatorname{curl}(\mathcal{A}^*\rho_{\mathrm{LS}})\|_{L^2(T)}\big)^2\\
&\quad\le C_{\mathrm{inv}}^2(C_{\mathcal{S}}^2+C_{\mathcal{A}}^2)\,\|\widehat{\rho}_{\mathrm{LS}}-\rho_{\mathrm{LS}}\|_{L^2(T)}^2.
\end{aligned}
$$

Step 3. The reverse triangle inequality in $L^2(F)$ for every $F\in\mathcal{F}(T)$ and $T\in\widehat{\mathcal{T}}\cap\mathcal{T}$

plus the discrete jump control from Lemma 3.19 prove

$$\begin{aligned}
&\sum_{T\in\widehat{\mathcal{T}}\cap\mathcal{T}} |T|^{1/3} \Bigg[\sum_{F\in\mathcal{F}(T)\setminus\mathcal{F}(\Gamma_D)} \big(\|[\mathcal{S}^*\widehat{\rho}_{LS}]_F\,\nu_F\|_{L^2(F)} - \|[\mathcal{S}^*\rho_{LS}]_F\,\nu_F\|_{L^2(F)}\big)^2 \\
&\qquad + \sum_{F\in\mathcal{F}(T)\setminus\mathcal{F}(\Gamma_N)} \big(\|\nu_F\times[\mathcal{A}^*\widehat{\rho}_{LS}]_F\|_{L^2(F)} - \|\nu_F\times[\mathcal{A}^*\rho_{LS}]_F\|_{L^2(F)}\big)^2 \Bigg] \\
&\le \sum_{T\in\widehat{\mathcal{T}}\cap\mathcal{T}} |T|^{1/3} \sum_{F\in\mathcal{F}(T)} \big(\|[\mathcal{S}^*(\widehat{\rho}_{LS}-\rho_{LS})]_F\,\nu_F\|^2_{L^2(F)} + \|\nu_F\times[\mathcal{A}^*(\widehat{\rho}_{LS}-\rho_{LS})]_F\|^2_{L^2(F)}\big) \\
&\le C_{jc}^2\,\|\widehat{\rho}_{LS}-\rho_{LS}\|^2_{L^2(\Omega)}.
\end{aligned}$$

Step 4. For $T\in\mathcal{T}\cap\widehat{\mathcal{T}}$, the remaining contributions of the boundary data oscillations coincide

$$\begin{aligned}
\|(1-\widehat{\Pi}_k)\,\mathrm{D}\,u_D\|_{L^2(\partial T\cap\Gamma_D)} &= \|(1-\Pi_k)\,\mathrm{D}\,u_D\|_{L^2(\partial T\cap\Gamma_D)},\\
\|(1-\widehat{\Pi}_k)t_N\|_{L^2(\partial T\cap\Gamma_N)} &= \|(1-\Pi_k)t_N\|_{L^2(\partial T\cap\Gamma_N)}.
\end{aligned}$$

Step 5. The combination of all previous steps proves (A1) with

$$\Lambda_1 := \sqrt{C_{inv}^2(C_{\mathcal{S}}^2+C_{\mathcal{A}}^2)+C_{jc}^2}. \qquad \square$$

Theorem 4.2 (reduction). *The a posteriori error estimator η and the distance δ satisfy the axiom* (A2)*: There exist positive generic constants Λ_2 and $\rho_2<1$ such that*

$$\eta(\widehat{\mathcal{T}},\widehat{\mathcal{T}}\setminus\mathcal{T}) \le \rho_2\,\eta(\mathcal{T},\mathcal{T}\setminus\widehat{\mathcal{T}}) + \Lambda_2\,\delta(\widehat{\mathcal{T}},\mathcal{T}).$$

Proof. The proof follows the one of [40, Theorem 5.1]. Abbreviate the discrete constitutive residuals $\widehat{\rho}_{LS} := \mathcal{A}\widehat{\sigma}_{LS} - \mathcal{S}\,\mathrm{D}\,\widehat{u}_{LS}$ and $\rho_{LS} := \mathcal{A}\sigma_{LS} - \mathcal{S}\,\mathrm{D}\,u_{LS}$.

Step 1. Following the proof of Theorem 4.1, the term $\eta(\widehat{\mathcal{T}},\widehat{\mathcal{T}}\setminus\mathcal{T})$ is represented as the Euclidian norm $|\widehat{a}|$ of some vector $\widehat{a}\in\mathbb{R}^m$ the $m := 10\,|\widehat{\mathcal{T}}\setminus\mathcal{T}|$ entries according to (4.1) for each $T\in\widehat{\mathcal{T}}\setminus\mathcal{T}$. Additionally, let $a\in\mathbb{R}^m$ denote the vector with the identical entries but ρ_{LS} replacing $\widehat{\rho}_{LS}$. The triangle inequality in $\mathbb{R}^m$ proves that

$$\eta(\widehat{\mathcal{T}},\widehat{\mathcal{T}}\setminus\mathcal{T}) = |\widehat{a}| \le |a| + |\widehat{a}-a|.$$

Step 2. The reduction relies on the fact that each term is weighted with a corresponding power of the mesh-size $|T|$ being reduced at least by a factor 2, i.e., $|T|\le|K|/2$ for $K\in\mathcal{T}$ and $T\in\widehat{\mathcal{T}}(K)$. For every $K\in\mathcal{T}\setminus\widehat{\mathcal{T}}$, the sums of the associated volume terms satisfy

$$\begin{aligned}
\sum_{T\in\widehat{\mathcal{T}}(K)} |T|^{2/3}\|\operatorname{div}(\mathcal{S}^*\rho_{LS})\|^2_{L^2(T)} &\le |K|^{2/3}2^{-2/3}\|\operatorname{div}(\mathcal{S}^*\rho_{LS})\|^2_{L^2(K)},\\
\sum_{T\in\widehat{\mathcal{T}}(K)} |T|^{2/3}\|\operatorname{curl}(\mathcal{A}^*\rho_{LS})\|^2_{L^2(T)} &\le |K|^{2/3}2^{-2/3}\|\operatorname{curl}(\mathcal{A}^*\rho_{LS})\|^2_{L^2(K)}.
\end{aligned}$$

Since $\rho_{\mathrm{LS}} = \mathcal{A}\sigma_{\mathrm{LS}} - \mathcal{S}\,\mathrm{D}\,u_{\mathrm{LS}}$, the regularity assumption (3.1) guarantees that

$$\mathcal{S}^*\rho_{\mathrm{LS}} \in H(\mathrm{div}, \mathcal{T}; \mathbb{R}^{3\times 3}) \quad \text{and} \quad \mathcal{A}^*\rho_{\mathrm{LS}} \in H(\mathrm{curl}, \mathcal{T}; \mathbb{R}^{3\times 3}).$$

Hence, the normal jumps $[\mathcal{S}^*\rho_{\mathrm{LS}}]_F\, \nu_F = 0$ and the tangential jumps $\nu_F \times [\mathcal{A}^*\rho_{\mathrm{LS}}]_F = 0$ vanish on any interior face $F \in \widehat{\mathcal{F}}(K) \setminus \mathcal{F}(\partial K)$ inside of the coarse simplex $K \in \mathcal{T}$. Therefore, the sums of the face jumps fulfil

$$\begin{aligned}
&\sum_{T\in\widehat{\mathcal{T}}(K)} \sum_{F\in\mathcal{F}(T)\setminus\mathcal{F}(\Gamma_{\mathrm{D}})} |T|^{1/3} \|[\mathcal{S}^*\rho_{\mathrm{LS}}]_F\, \nu_F\|^2_{L^2(F)} \\
&\qquad\qquad \le \sum_{F\in\mathcal{F}(K)\setminus\mathcal{F}(\Gamma_{\mathrm{D}})} |K|^{1/3} 2^{-1/3} \|[\mathcal{S}^*\rho_{\mathrm{LS}}]_F\, \nu_F\|^2_{L^2(F)}, \\
&\sum_{T\in\widehat{\mathcal{T}}(K)} \sum_{F\in\mathcal{F}(T)\setminus\mathcal{F}(\Gamma_{\mathrm{N}})} |T|^{1/3} \|\nu_F \times [\mathcal{A}^*\rho_{\mathrm{LS}}]_F\|^2_{L^2(F)} \\
&\qquad\qquad \le \sum_{F\in\mathcal{F}(K)\setminus\mathcal{F}(\Gamma_{\mathrm{N}})} |K|^{1/3} 2^{-1/3} \|\nu_F \times [\mathcal{A}^*\rho_{\mathrm{LS}}]_F\|^2_{L^2(F)}.
\end{aligned}$$

Eventually, the sums of the boundary oscillations read

$$\begin{aligned}
&\sum_{T\in\widehat{\mathcal{T}}(K)} \sum_{F\in\mathcal{F}(T)\cap\mathcal{F}(\Gamma_{\mathrm{D}})} |T|^{1/3} \|(1-\Pi_k)\,\mathrm{D}\,u_{\mathrm{D}}\|^2_{L^2(F)} \\
&\qquad\qquad \le \sum_{F\in\mathcal{F}(K)\cap\mathcal{F}(\Gamma_{\mathrm{D}})} |K|^{1/3} 2^{-1/3} \|(1-\Pi_k)\,\mathrm{D}\,u_{\mathrm{D}}\|^2_{L^2(F)}, \\
&\sum_{T\in\widehat{\mathcal{T}}(K)} \sum_{F\in\mathcal{F}(T)\cap\mathcal{F}(\Gamma_{\mathrm{N}})} |T|^{1/3} \|(1-\Pi_k)\,t_{\mathrm{N}}\|^2_{L^2(F)} \\
&\qquad\qquad \le \sum_{F\in\mathcal{F}(K)\cap\mathcal{F}(\Gamma_{\mathrm{N}})} |K|^{1/3} 2^{-1/3} \|(1-\Pi_k)\,t_{\mathrm{N}}\|^2_{L^2(F)}.
\end{aligned}$$

The summation over all $K \in \mathcal{T}\setminus\widehat{\mathcal{T}}$ and the square root in the three previously displayed formulas yield

$$|a| \le 2^{-1/6}\,\eta(\mathcal{T}, \mathcal{T}\setminus\widehat{\mathcal{T}}).$$

Step 3. In order to estimate the term $|\widehat{a} - a|$ proceed analogously to the proof of Theorem 4.1. The reverse triangle inequality in $L^2(T)$, the abstract inverse estimates (W6)–(W7), and the boundedness of the adjoint operators $\mathcal{S}^*$ and $\mathcal{A}^*$ from (3.2) prove

$$\begin{aligned}
&\sum_{T\in\widehat{\mathcal{T}}\setminus\mathcal{T}} |T|^{2/3} \Big(\big(\|\,\mathrm{div}(\mathcal{S}^*\widehat{\rho}_{\mathrm{LS}})\|_{L^2(T)} - \|\,\mathrm{div}(\mathcal{S}^*\rho_{\mathrm{LS}})\|_{L^2(T)}\big)^2 \\
&\qquad\qquad + \big(\|\,\mathrm{curl}(\mathcal{A}^*\widehat{\rho}_{\mathrm{LS}})\|_{L^2(T)} - \|\,\mathrm{curl}(\mathcal{A}^*\rho_{\mathrm{LS}})\|_{L^2(T)}\big)^2 \Big) \\
&\quad \le C^2_{\mathrm{inv}}(C^2_{\mathcal{S}} + C^2_{\mathcal{A}})\, \|\widehat{\rho}_{\mathrm{LS}} - \rho_{\mathrm{LS}}\|^2_{L^2(\Omega)}.
\end{aligned}$$

The reverse triangle inequality in $L^2(F)$ for $F \in \mathcal{F}(T)$ and $T \in \widehat{\mathcal{T}} \setminus \mathcal{T}$ and the discrete jump control from Lemma 3.19 show

$$\begin{aligned}
&\sum_{T\in\widehat{\mathcal{T}}\setminus\mathcal{T}} |T|^{1/3} \left[\sum_{F\in\mathcal{F}(T)\setminus\mathcal{F}(\Gamma_D)} \big(\|[\mathcal{S}^*\widehat{\rho}_{LS}]_F\, \nu_F\|_{L^2(F)} - \|[\mathcal{S}^*\rho_{LS}]_F\, \nu_F\|_{L^2(F)}\big)^2 \right.\\
&\qquad\qquad \left. + \sum_{F\in\mathcal{F}(T)\setminus\mathcal{F}(\Gamma_N)} \big(\|\nu_F \times [\mathcal{A}^*\widehat{\rho}_{LS}]_F\|_{L^2(F)} - \|\nu_F \times [\mathcal{A}^*\rho_{LS}]_F\|_{L^2(F)}\big)^2 \right]\\
&\le \sum_{T\in\widehat{\mathcal{T}}\setminus\mathcal{T}} |T|^{1/3} \sum_{F\in\mathcal{F}(T)} \big(\|[\mathcal{S}^*(\widehat{\rho}_{LS}-\rho_{LS})]_F\, \nu_F\|^2_{L^2(F)} + \|\nu_F \times [\mathcal{A}^*(\widehat{\rho}_{LS}-\rho_{LS})]_F\|^2_{L^2(F)}\big)\\
&\le C_{jc}^2\, \|\widehat{\rho}_{LS}-\rho_{LS}\|^2_{L^2(\Omega)}.
\end{aligned}$$

The remaining contributions of the boundary data oscillations are bounded by the best-approximation property of the L^2 orthogonal projection Π_k, for $T \in \widehat{\mathcal{T}} \setminus \mathcal{T}$ and $F \in \mathcal{F}(T)$,

$$\begin{aligned}
\|(1-\widehat{\Pi}_k)\,\mathrm{D}\,u_D\|_{L^2(F\cap\Gamma_D)} &\le \|(1-\Pi_k)\,\mathrm{D}\,u_D\|_{L^2(F\cap\Gamma_D)},\\
\|(1-\widehat{\Pi}_k)\,t_N\|_{L^2(F\cap\Gamma_N)} &\le \|(1-\Pi_k)\,t_N\|_{L^2(F\cap\Gamma_N)}.
\end{aligned}$$

The three previously displayed formulas yield

$$|\widehat{a}-a| \le \sqrt{C_{inv}^2(C_{\mathcal{S}}^2+C_{\mathcal{A}}^2)+C_{jc}^2}\;\delta(\widehat{\mathcal{T}},\mathcal{T}).$$

Step 5. The combination of all previous steps concludes the proof of (A2) with the constants $\rho_2 := 2^{-1/6}$ and $\Lambda_2 := \Lambda_1$. □

4.2 Discrete reliability

The proof of the discrete reliability axiom (A3) is essentially based on the following Theorem 4.3. Since the proof is more extensive, it is postponed to its own Section 4.3 below. Before that, the reliability of the a posteriori error estimator and the axiom (A3) are deduced. Recall Notation 3 from page 22 for the refinement $\widehat{\mathcal{T}}$ of $\mathcal{T}$ and the notion of n-layers $\mathcal{R}_n$ around the refined simplices from Section 2.4.

Theorem 4.3 (discrete reliability). *Given the set*

$$\mathcal{R} := \mathcal{R}_3 \cup \big\{T\in\mathcal{T} \,:\, \exists F\in\mathcal{L}_5(\mathcal{F}\setminus\widehat{\mathcal{F}},\Gamma_D),\ F\subset T\big\} \subseteq \mathcal{R}_5, \tag{4.2}$$

there exist positive generic constants C_{drel} and $\widehat{C}_{drel}$ such that the a posteriori error estimator η and the distance δ satisfy

$$\delta^2(\widehat{\mathcal{T}},\mathcal{T}) \le C_{drel}\left(\eta^2(\mathcal{T},\mathcal{R})+\mu^2(\mathcal{T})\right) + \widehat{C}_{drel}\, LS(f;\widehat{\sigma}_{LS},\widehat{u}_{LS}). \tag{4.3}$$

The discrete reliability and the plain convergence of the LSFEM under uniform refinement imply reliability of the error estimator η in the following sense.

Corollary 4.4 (reliability). *For any admissible triangulation $\mathcal{T} \in \mathbb{T}$ with discrete solutions $(\sigma_{\mathrm{LS}}, u_{\mathrm{LS}}) \in \Sigma^k(\mathcal{T}) \times U^{k+1}(\mathcal{T})$ to* (3.18) *and the positive generic constant C_{drel} from Theorem 4.3, it holds that*

$$LS(f; \sigma_{\mathrm{LS}}, u_{\mathrm{LS}}) \leq C_{\mathrm{drel}} \left(\eta^2(\mathcal{T}) + \mu^2(\mathcal{T})\right). \tag{4.4}$$

Proof. Define the sequence $(\mathcal{T}_m : m \in \mathbb{N})$ of successive uniform one-level refinements $\mathcal{T}_m := \mathrm{refine}^{(m)}(\mathcal{T})$ with discrete solutions $(\sigma_m, u_m) \in \Sigma^k(\mathcal{T}_m) \times U^{k+1}(\mathcal{T}_m)$ to (3.18). This design ensures uniform convergence of the mesh-size $h_m := h_{\mathcal{T}_m}$ as $m \to \infty$,

$$\lim_{m\to\infty} \|h_m\|_{L^\infty(\Omega)} = 0.$$

The convergence of the LSFEM leads to

$$\begin{aligned}\lim_{m\to\infty} \delta^2(\mathcal{T}_m, \mathcal{T}) &= \lim_{m\to\infty} \Big(\|\operatorname{div}(\sigma_m - \sigma_{\mathrm{LS}})\|^2_{L^2(\Omega)} \\ &\qquad + \|\mathcal{A}(\sigma_m - \sigma_{\mathrm{LS}}) - \mathcal{S}\,\mathrm{D}(u_m - u_{\mathrm{LS}})\|^2_{L^2(\Omega)} \Big) \\ &= LS(f; \sigma_{\mathrm{LS}}, u_{\mathrm{LS}})\end{aligned}$$

and

$$\lim_{m\to\infty} LS(f; \sigma_m, u_m) = 0.$$

Theorem 4.3 implies, for every $m \in \mathbb{N}$,

$$\delta^2(\mathcal{T}_m, \mathcal{T}) \leq C_{\mathrm{drel}} \left(\eta^2(\mathcal{T}) + \mu^2(\mathcal{T})\right) + \widehat{C}_{\mathrm{drel}}\, LS(f; \sigma_m, u_m).$$

The combination of the three previously displayed formulas concludes the proof for $m \to \infty$. □

A combination of the discrete reliability from Theorem 4.3 and the reliability of the estimator results in the axiom (A3).

Corollary 4.5. *The a posteriori error estimator η and the distance δ satisfy the axiom* (A3)*: There exists a set $\mathcal{R} \subseteq \mathcal{T}$ with $|\mathcal{R}| \leq \Lambda_{\mathrm{ref}} |\mathcal{T} \setminus \widehat{\mathcal{T}}|$ and*

$$\delta^2(\widehat{\mathcal{T}}, \mathcal{T}) \leq \Lambda_3 \left(\eta^2(\mathcal{T}, \mathcal{R}) + \mu^2(\mathcal{T})\right) + \widehat{\Lambda}_3\, \eta^2(\widehat{\mathcal{T}}).$$

Proof. Since the set $\mathcal{R}$ from (4.2) satisfies $\mathcal{R} \subseteq \mathcal{R}_5$, the shape regularity of the triangulations $\mathcal{T} \in \mathbb{T}$ guarantees existence of a positive generic constant Λ_{ref} such that $|\mathcal{R}| \leq \Lambda_{\mathrm{ref}} |\mathcal{T} \setminus \widehat{\mathcal{T}}|$. The claim (A3) follows from the combination of (4.3) and (4.4) with respect to $\widehat{\mathcal{T}}$ reads

$$\delta(\widehat{\mathcal{T}}, \mathcal{T}) \leq C_{\mathrm{drel}} \left(\eta^2(\mathcal{T}, \mathcal{R}) + \mu^2(\mathcal{T})\right) + \widehat{C}_{\mathrm{drel}} C_{\mathrm{drel}} \left(\eta^2(\widehat{\mathcal{T}}) + \mu^2(\widehat{\mathcal{T}})\right).$$

The monotonicity $\mu(\widehat{\mathcal{T}}) \leq \mu(\mathcal{T})$ concludes the proof with the constants

$$\Lambda_3 := C_{\mathrm{drel}}(1 + \widehat{C}_{\mathrm{drel}}) \quad \text{and} \quad \widehat{\Lambda}_3 := \widehat{C}_{\mathrm{drel}} C_{\mathrm{drel}}.$$ □

4.3 Proof of discrete reliability

This section is devoted to the proof of Theorem 4.3. It is based on five lemmas and follows the ideas of [44, Section 5]. The proof departs with the construction of two intermediate functions $\widehat{\tau}_{\mathrm{RT}}$ and τ_{RT} in the following lemma.

Lemma 4.6. *There exists* $\widehat{\tau}_{\mathrm{RT}} \in RT_k(\widehat{\mathcal{T}};\mathbb{R}^{3\times3})$ *and* $\tau_{\mathrm{RT}} \in RT_k(\mathcal{T};\mathbb{R}^{3\times3})$ *with the Neumann boundary data*

$$\widehat{\tau}_{\mathrm{RT}}\nu = (\widehat{\Pi}_k - \Pi_k)t_{\mathrm{N}} \quad \textit{and} \quad \tau_{\mathrm{RT}}\nu = 0 \quad \textit{on } \Gamma_{\mathrm{N}} \tag{4.5}$$

and the divergences

$$\operatorname{div}\widehat{\tau}_{\mathrm{RT}} = (1-\Pi_k)\operatorname{div}(\widehat{\sigma}_{\mathrm{LS}} - \sigma_{\mathrm{LS}}) \quad \textit{and} \quad \operatorname{div}\tau_{\mathrm{RT}} = \Pi_k \operatorname{div}(\widehat{\sigma}_{\mathrm{LS}} - \sigma_{\mathrm{LS}}) \quad \textit{in } \Omega. \tag{4.6}$$

Furthermore, there exists a positive generic constant C_{stab} *such that*

$$\|\widehat{\tau}_{\mathrm{RT}}\|_{L^2(\Omega)} \le C_{\mathrm{stab}}\left(\|(1-\Pi_k)\operatorname{div}(\widehat{\sigma}_{\mathrm{LS}} - \sigma_{\mathrm{LS}})\|_{L^2(\Omega)} + \|(\widehat{\Pi}_k - \Pi_k)\widetilde{t}_{\mathrm{N}}\|_{H^{-1/2}(\partial\Omega)}\right), \tag{4.7}$$

$$\|\tau_{\mathrm{RT}}\|_{L^2(\Omega)} \le C_{\mathrm{stab}}\,\|\Pi_k \operatorname{div}(\widehat{\sigma}_{\mathrm{LS}} - \sigma_{\mathrm{LS}})\|_{L^2(\Omega)}. \tag{4.8}$$

Proof. Step 1. Let $w \in H^1(\Omega;\mathbb{R}^3)/\mathbb{R}^3$ solve the Neumann problem

$$(\mathrm{D}\, w, \mathrm{D}\, v)_{L^2(\Omega)} = -\big((1-\Pi_k)\operatorname{div}(\widehat{\sigma}_{\mathrm{LS}} - \sigma_{\mathrm{LS}}),\ v\big)_{L^2(\Omega)} \quad \text{for all } v \in H^1(\Omega;\mathbb{R}^3)/\mathbb{R}^3.$$

This problem is well-posed due to the compatibility condition

$$\int_\Omega (1-\Pi_k)\operatorname{div}(\widehat{\sigma}_{\mathrm{LS}} - \sigma_{\mathrm{LS}})\,\mathrm{d}x = 0.$$

The integration by parts shows that the weak derivative $\tau := \mathrm{D}\, w \in H(\operatorname{div},\Omega;\mathbb{R}^{3\times3})$ satisfies $\operatorname{div}\tau = (1-\Pi_k)\operatorname{div}(\widehat{\sigma}_{\mathrm{LS}} - \sigma_{\mathrm{LS}})$ in Ω and $\tau\nu = 0$ on $\partial\Omega$. The reduced elliptic regularity [54] of the Neumann problem ensures that $\tau \in H^{1/2+s}(\Omega;\mathbb{R}^{3\times3}) \cap H(\operatorname{div},\Omega;\mathbb{R}^{3\times3})$ for some regularity parameter $0 < s < 1/2$. Additionally, there exists some positive generic constant $c_1(s)$ such that

$$\|\tau\|_{H^{1/2+s}(\Omega)} \le c_1(s)\,\|(1-\Pi_k)\operatorname{div}(\widehat{\sigma}_{\mathrm{LS}} - \sigma_{\mathrm{LS}})\|_{L^2(\Omega)}. \tag{4.9}$$

Step 2. Let the componentwise integral

$$\alpha := \begin{pmatrix}\alpha_1\\ \alpha_2\\ \alpha_3\end{pmatrix} := \frac{1}{|\Gamma_{\mathrm{D}}|}\int_\Omega \operatorname{div}(\widehat{\sigma}_{\mathrm{LS}} - \sigma_{\mathrm{LS}})\,\mathrm{d}x = \frac{1}{|\Gamma_{\mathrm{D}}|}\int_\Omega \Pi_k \operatorname{div}(\widehat{\sigma}_{\mathrm{LS}} - \sigma_{\mathrm{LS}})\,\mathrm{d}x \in \mathbb{R}^3$$

define the piecewise constant boundary data $\alpha^*_{\mathrm{pw}} \in P_0(\mathcal{F}_0(\partial\Omega);\mathbb{R}^3)$ with respect to the initial triangulation $\mathcal{T}_0$ by

$$\alpha^*_{\mathrm{pw}} := \begin{cases} 0 & \text{on } \Gamma_{\mathrm{N}},\\ \alpha & \text{on } \Gamma_{\mathrm{D}}.\end{cases}$$

The Cauchy-Schwarz inequality shows, for the constant $c_2 \coloneqq |\Omega|^{1/2}/|\Gamma_D|$,

$$|\alpha_1| + |\alpha_2| + |\alpha_3| \leq \frac{1}{|\Gamma_D|} \|\Pi_k \operatorname{div}(\widehat{\sigma}_{LS} - \sigma_{LS})\|_{L^1(\Omega)} \leq c_2 \|\Pi_k \operatorname{div}(\widehat{\sigma}_{LS} - \sigma_{LS})\|_{L^2(\Omega)}. \quad (4.10)$$

Let $e_m \in \mathbb{R}^3$ for $m = 1, 2, 3$ denote the unit basis vectors and $(\psi_F : F \in \mathcal{F}_0)$ of $RT_0(\mathcal{T}_0)$ the canonical lowest-order Raviart-Thomas basis functions with

$$\fint_{F'} \psi_F \cdot \nu_{F'} \, da = \begin{cases} 1 & \text{if } F' = F, \\ 0 & \text{else.} \end{cases}$$

The tensor products $e_m \otimes \psi_F$ for $m = 1, 2, 3$ and $F \in \mathcal{F}_0$ form a basis of the matrix-valued Raviart-Thomas functions in $RT_0(\mathcal{T}_0; \mathbb{R}^{3\times 3})$. Define the discrete extension ζ^*_{RT} of the boundary data g^*_{pw} by

$$\zeta^*_{RT} \coloneqq \sum_{m=1}^{3} \sum_{F \in \mathcal{F}_0} a_{m,F} \, e_m \otimes \psi_F \in RT_0(\mathcal{T}_0; \mathbb{R}^{3\times 3})$$

with the coefficients, for $m = 1, 2, 3$ and $F \in \mathcal{F}_0$,

$$a_{m,F} \coloneqq \begin{cases} \alpha_m & \text{if } F \in \mathcal{F}_0(\Gamma_D), \\ 0 & \text{else.} \end{cases}$$

This extension satisfies $\zeta^*_{RT}\nu = \alpha^*_{pw}$ on $\partial\Omega$ and, in particular, $\zeta^*_{RT}\nu = 0$ on Γ_N. Furthermore, the triangle inequality proves

$$\|\zeta^*_{RT}\|_{H(\operatorname{div},\Omega)} \leq \big(|\alpha_1| + |\alpha_2| + |\alpha_3|\big) \sum_{F \in \mathcal{F}_0(\Gamma_D)} \|\psi_F\|_{H(\operatorname{div},\omega_F)}.$$

This and the estimate (4.10) establish

$$\|\zeta^*_{RT}\|_{H(\operatorname{div},\Omega)} \leq c_2 c_3 \, \|\Pi_k \operatorname{div}(\widehat{\sigma}_{LS} - \sigma_{LS})\|_{L^2(\Omega)} \quad (4.11)$$

with the constant $c_3 \coloneqq \sum_{F \in \mathcal{F}_0(\Gamma_D)} \|\psi_F\|_{H(\operatorname{div},\omega_F)}$ solely depending on the initial triangulation $\mathcal{T}_0$.

Step 3. For $f_{pw} \coloneqq \Pi_k \operatorname{div}(\widehat{\sigma}_{LS} - \sigma_{LS}) - \operatorname{div} \zeta^*_{RT} \in P_k(\mathcal{T}; \mathbb{R}^3)$, the Gauss divergence theorem implies

$$\begin{aligned} \int_\Omega f_{pw} \, dx &= \int_\Omega \operatorname{div}(\widehat{\sigma}_{LS} - \sigma_{LS}) \, dx - \int_\Omega \operatorname{div} \zeta^*_{RT} \, dx \\ &= \int_\Omega \operatorname{div}(\widehat{\sigma}_{LS} - \sigma_{LS}) \, dx - \int_{\partial\Omega} \alpha^*_{pw} \, da \\ &= \int_\Omega \operatorname{div}(\widehat{\sigma}_{LS} - \sigma_{LS}) \, dx - \int_{\Gamma_D} \alpha \, da = 0. \end{aligned}$$

Hence, the following Neumann problem is well-posed. Let $w^* \in H^1(\Omega;\mathbb{R}^3)/\mathbb{R}^3$ solve

$$(\mathrm{D}\, w^*, \mathrm{D}\, v)_{L^2(\Omega)} = -(f_{\mathrm{pw}}, v)_{L^2(\Omega)} \quad \text{for all } v \in H^1(\Omega;\mathbb{R}^3)/\mathbb{R}^3.$$

The integration by parts shows that the weak derivative $\tau^* := \mathrm{D}\, w^* \in H(\mathrm{div}, \Omega;\mathbb{R}^{3\times 3})$ satisfies $\mathrm{div}\, \tau^* = f_{\mathrm{pw}}$ in Ω and $\tau^* \nu = 0$ on $\partial\Omega$. An analog argument to Step 1 establishes the reduced elliptic regularity estimate

$$\|\tau^*\|_{H^{1/2+s}(\Omega)} \leq c_1(s)\, \|f_{\mathrm{pw}}\|_{L^2(\Omega)}.$$

By the definition of f_{pw}, this and (4.11) lead to

$$\|\tau^*\|_{H^{1/2+s}(\Omega)} \leq c_1(s)\, (1 + c_2 c_3)\, \|\Pi_k\, \mathrm{div}(\widehat{\sigma}_{\mathrm{LS}} - \sigma_{\mathrm{LS}})\|_{L^2(\Omega)}. \tag{4.12}$$

Step 4. The regularity $\tau, \tau^* \in H^{1/2+s}(\Omega;\mathbb{R}^{3\times 3}) \cap H(\mathrm{div}, \Omega;\mathbb{R}^{3\times 3})$ allows for the application of the Fortin interpolation operator $I_{\mathrm{F}} : L^p(\Omega;\mathbb{R}^{3\times 3}) \cap H(\mathrm{div}, \Omega;\mathbb{R}^{3\times 3}) \to RT_k(\mathcal{T};\mathbb{R}^{3\times 3})$ from [18, Example 2.5.3] for $p > 2$ in the three components. The approximation property of the Fortin interpolation operator from [83, Theorem 2.25] with some positive generic constant c_4 reads, for every $\xi \in H^{1/2+s}(\Omega;\mathbb{R}^{3\times 3}) \cap H(\mathrm{div}, \Omega;\mathbb{R}^{3\times 3})$,

$$\|\xi - I_{\mathrm{F}}\xi\|_{L^2(\Omega)} \leq c_4 h_{\max}^{1/2+s}\, \|\xi\|_{H^{1/2+s}(\Omega)}.$$

The triangle inequality and the uniform bound $h_{\max}^{1/2+s} \leq c_5$ prove the stability

$$\|I_{\mathrm{F}}\xi\|_{L^2(\Omega)} \leq (1 + c_4 c_5)\, \|\xi\|_{H^{1/2+s}(\Omega)}. \tag{4.13}$$

The identical estimate holds for the corresponding operator $\widehat{I}_{\mathrm{F}}$ with respect to the refinement $\widehat{\mathcal{T}}$.

Step 5. Lemma 3.9 provides a discrete divergence-free extension $\widehat{\xi}_{\mathrm{RT}} \in RT_k(\widehat{\mathcal{T}};\mathbb{R}^{3\times 3}) \cap H(\mathrm{div} = 0, \Omega;\mathbb{R}^{3\times 3})$ with $\widehat{\xi}_{\mathrm{RT}} = (\widehat{\Pi}_k - \Pi_k)\widetilde{t}_{\mathrm{N}}$ on $\partial\Omega$ and

$$\|\widehat{\xi}_{\mathrm{RT}}\|_{L^2(\Omega)} \leq C_{\mathrm{ext}}\, \|(\widehat{\Pi}_k - \Pi_k)\widetilde{t}_{\mathrm{N}}\|_{H^{-1/2}(\partial\Omega)}. \tag{4.14}$$

Step 6. Define the functions

$$\widehat{\tau}_{\mathrm{RT}} := \widehat{I}_{\mathrm{F}}\tau + \widehat{\xi}_{\mathrm{RT}} \in RT_k(\widehat{\mathcal{T}};\mathbb{R}^{3\times 3}) \quad \text{and} \quad \tau_{\mathrm{RT}} := I_{\mathrm{F}}\tau^* + \zeta^*_{\mathrm{RT}} \in RT_k(\mathcal{T};\mathbb{R}^{3\times 3}).$$

Since the Fortin interpolations $\widehat{I}_{\mathrm{F}}$ and I_{F} preserve polynomial boundary conditions, it holds that

$$\begin{aligned}
&\widehat{\tau}_{\mathrm{RT}}\nu = (\widehat{I}_{\mathrm{F}}\tau + \widehat{\xi}_{\mathrm{RT}})\nu = \widehat{\Pi}_k(\tau\nu) + \widehat{\xi}_{\mathrm{RT}}\nu = (\widehat{\Pi}_k - \Pi_k)\widetilde{t}_{\mathrm{N}} \quad \text{on } \Gamma_{\mathrm{N}},\\
&\tau_{\mathrm{RT}}\nu = (I_{\mathrm{F}}\tau^* + \zeta^*_{\mathrm{RT}})\nu = \widehat{\Pi}_k(\tau^*\nu) = 0 \quad \text{on } \Gamma_{\mathrm{N}}.
\end{aligned}$$

The commuting diagram property of $\widehat{I}_{\mathrm{F}}$ and I_{F} [18, Proposition 2.5.2] leads to

$$\begin{aligned}
&\mathrm{div}\, \widehat{\tau}_{\mathrm{RT}} = \mathrm{div}(\widehat{I}_{\mathrm{F}}\tau + \widehat{\xi}_{\mathrm{RT}}) = \widehat{\Pi}_k\, \mathrm{div}\, \tau = (1 - \Pi_k)\, \mathrm{div}(\widehat{\sigma}_{\mathrm{LS}} - \sigma_{\mathrm{LS}}),\\
&\mathrm{div}\, \tau_{\mathrm{RT}} = \mathrm{div}(I_{\mathrm{F}}\tau^* + \zeta^*_{\mathrm{RT}}) = \Pi_k\, \mathrm{div}\, \tau + \mathrm{div}\, \zeta^*_{\mathrm{RT}} = f_{\mathrm{pw}} + \mathrm{div}\, \zeta^*_{\mathrm{RT}} = \Pi_k\, \mathrm{div}(\widehat{\sigma}_{\mathrm{LS}} - \sigma_{\mathrm{LS}}).
\end{aligned}$$

The stability estimates (4.9), (4.12)–(4.14) establish

$$\begin{aligned}\|\widehat{\tau}_{\mathrm{RT}}\|_{L^2(\Omega)} &\leq \|\widehat{I}_{\mathrm{F}}\tau\|_{L^2(\Omega)} + \|\widehat{\xi}_{\mathrm{RT}}\|_{L^2(\Omega)}\\ &\leq c_1(s)\,(1+c_4c_5)\,\|(1-\Pi_k)\operatorname{div}(\widehat{\sigma}_{\mathrm{LS}}-\sigma_{\mathrm{LS}})\|_{L^2(\Omega)}\\ &\quad + C_{\mathrm{ext}}\,\|(\widehat{\Pi}_k-\Pi_k)\widetilde{t}_{\mathrm{N}}\|_{H^{-1/2}(\partial\Omega)},\\ \|\tau_{\mathrm{RT}}\|_{L^2(\Omega)} &\leq \|I_{\mathrm{F}}\tau^*\|_{L^2(\Omega)} + \|\zeta^*_{\mathrm{RT}}\|_{L^2(\Omega)}\\ &\leq c_1(s)\,(2+c_2c_3+c_4c_5)\;\|\Pi_k\operatorname{div}(\widehat{\sigma}_{\mathrm{LS}}-\sigma_{\mathrm{LS}})\|_{L^2(\Omega)}.\end{aligned}$$

This concludes the proof with the constant $C_{\mathrm{stab}} := \max\{c_1(s)\,(2+c_2c_3+c_4c_5), C_{\mathrm{ext}}\}$. □

These intermediate functions allow for the split of the left-hand side $\delta^2(\widehat{\mathcal{T}},\mathcal{T})$ from Theorem 4.3 in the following lemma.

Lemma 4.7. *There exist some $\widehat{w}_{\mathrm{C}} \in S^{k+1}(\widehat{\mathcal{T}};\mathbb{R}^3)$ and $\widehat{\beta}_{\mathrm{Ned}} \in N_k(\widehat{\mathcal{T}};\mathbb{R}^{3\times3})$ with the boundary data $\widehat{w}_{\mathrm{C}} = (\widehat{\mathcal{J}}^{k+1}_{\mathrm{D}} - \mathcal{J}^{k+1}_{\mathrm{D}})u_{\mathrm{D}}$ on Γ_{D} and $\nu\times\widehat{\beta}_{\mathrm{Ned}} = 0$ on Γ_{N} and the stability estimates*

$$\|\mathrm{D}\,\widehat{w}_{\mathrm{C}}\|_{L^2(\Omega)} \leq C_{\mathrm{OL}}C_{\mathrm{SZ}}\,\|(\widehat{\mathcal{J}}^{k+1}_{\mathrm{D}} - \mathcal{J}^{k+1}_{\mathrm{D}})u_{\mathrm{D}}\|_{H^{1/2}(\Gamma_{\mathrm{D}})}, \tag{4.15}$$

$$\|\widehat{\beta}_{\mathrm{Ned}}\|_{H(\mathrm{curl},\Omega)} \leq C_{\mathrm{Ned}}\,\|\widehat{\sigma}_{\mathrm{LS}} - \sigma_{\mathrm{LS}} - \widehat{\tau}_{\mathrm{RT}} - \tau_{\mathrm{RT}}\|_{H(\mathrm{div},\Omega)} \tag{4.16}$$

such that

$$\begin{aligned}\delta^2(\widehat{\mathcal{T}},\mathcal{T}) &= \|(1-\Pi_k)\operatorname{div}(\widehat{\sigma}_{\mathrm{LS}}-\sigma_{\mathrm{LS}})\|^2_{L^2(\Omega)}\\ &\quad + \big(\mathcal{A}(\widehat{\sigma}_{\mathrm{LS}}-\sigma_{\mathrm{LS}}) - \mathcal{S}\,\mathrm{D}(\widehat{u}_{\mathrm{LS}}-u_{\mathrm{LS}}),\ \mathcal{A}\widehat{\tau}_{\mathrm{RT}} - \mathcal{S}\,\mathrm{D}\,\widehat{w}_{\mathrm{C}}\big)_{L^2(\Omega)}\\ &\quad + \big(\mathcal{A}\sigma_{\mathrm{LS}} - \mathcal{S}\,\mathrm{D}\,u_{\mathrm{LS}},\ \mathcal{S}\,\mathrm{D}(\widehat{u}_{\mathrm{LS}}-u_{\mathrm{LS}}-\widehat{w}_{\mathrm{C}}) - \mathcal{A}\operatorname{curl}\widehat{\beta}_{\mathrm{Ned}}\big)_{L^2(\Omega)}.\end{aligned} \tag{4.17}$$

Proof. Step 1. Lemma 3.6 guarantees the existence of some discrete extension $\widehat{w}_{\mathrm{C}} \in S^{k+1}(\widehat{\mathcal{T}};\mathbb{R}^3)$ of the boundary approximation error with

$$\widehat{w}_{\mathrm{C}} = (\widehat{\mathcal{J}}^{k+1}_{\mathrm{D}} - \mathcal{J}^{k+1}_{\mathrm{D}})u_{\mathrm{D}} \quad\text{and}\quad \|\mathrm{D}\,\widehat{w}_{\mathrm{C}}\|_{L^2(\Omega)} \leq C_{\mathrm{OL}}C_{\mathrm{SZ}}\,\|(\widehat{\mathcal{J}}^{k+1}_{\mathrm{D}} - \mathcal{J}^{k+1}_{\mathrm{D}})u_{\mathrm{D}}\|_{H^{1/2}(\Gamma_{\mathrm{D}})}.$$

Since $\widehat{\rho}_{\mathrm{RT}} := \widehat{\sigma}_{\mathrm{LS}} - \sigma_{\mathrm{LS}} - \widehat{\tau}_{\mathrm{RT}} - \tau_{\mathrm{RT}} \in \Sigma^k_{\mathrm{N}}(\widehat{\mathcal{T}})$ is divergence-free, Theorem 2.8 provides the existence of some $\widehat{\beta}_{\mathrm{Ned}} \in N_k(\widehat{\mathcal{T}};\mathbb{R}^{3\times3})$ and $\rho^*_{\mathrm{RT}} \in \Sigma^k_{\mathrm{N}}(\mathcal{T}_0)$ satisfying $\widehat{\rho}_{\mathrm{RT}} - \rho^*_{\mathrm{RT}} = \operatorname{curl}\widehat{\beta}_{\mathrm{Ned}}$ and

$$\|\widehat{\beta}_{\mathrm{Ned}}\|_{H(\mathrm{curl},\Omega)} \leq C_{\mathrm{Ned}}\,\|\widehat{\rho}_{\mathrm{RT}}\|_{L^2(\Omega)}.$$

Additionally, it holds that $\nu\times\widehat{\beta}_{\mathrm{Ned}} = 0$ on Γ_{N} and $\operatorname{div}\rho^*_{\mathrm{RT}} = 0$ in Ω. This concludes the proof of (4.15)–(4.16).

Step 3. Since $\operatorname{div}\tau_{\mathrm{RT}} = \Pi_k\operatorname{div}(\widehat{\sigma}_{\mathrm{LS}}-\sigma_{\mathrm{LS}})$, the discrete equation (3.18) with respect to the triangulation $\mathcal{T}$ for the test functions $\tau_{\mathrm{LS}} = \tau_{\mathrm{RT}} \in \Sigma^k_{\mathrm{N}}(\mathcal{T})$ and $v_{\mathrm{LS}} \equiv 0$ shows

$$-\big(\Pi_k f + \operatorname{div}\sigma_{\mathrm{LS}},\ \operatorname{div}(\widehat{\sigma}_{\mathrm{LS}}-\sigma_{\mathrm{LS}})\big)_{L^2(\Omega)} = (\mathcal{A}\sigma_{\mathrm{LS}} - \mathcal{S}\,\mathrm{D}\,u_{\mathrm{LS}},\ \mathcal{A}\tau_{\mathrm{RT}})_{L^2(\Omega)}. \tag{4.18}$$

The boundary conditions (4.5) imply that $\tau_{\mathrm{LS}} = \widehat{\sigma}_{\mathrm{LS}} - \sigma_{\mathrm{LS}} - \widehat{\tau}_{\mathrm{RT}} \in \Sigma^k_{\mathrm{N}}(\widehat{\mathcal{T}})$ is an admissible test function. Moreover, the equalities (4.6) lead to

$$\operatorname{div}(\widehat{\sigma}_{\mathrm{LS}} - \sigma_{\mathrm{LS}} - \widehat{\tau}_{\mathrm{RT}}) = \Pi_k \operatorname{div}(\widehat{\sigma}_{\mathrm{LS}} - \sigma_{\mathrm{LS}}).$$

This and the discrete equation (3.18) with respect to the triangulation $\widehat{\mathcal{T}}$ with test functions τ_{LS} and $v_{\mathrm{LS}} = \widehat{u}_{\mathrm{LS}} - u_{\mathrm{LS}} - \widehat{w}_{\mathrm{C}} \in U^{k+1}_{\mathrm{D}}(\widehat{\mathcal{T}})$ prove that

$$\begin{aligned}\big(\mathcal{A}\widehat{\sigma}_{\mathrm{LS}} - \mathcal{S}\,\mathrm{D}\,\widehat{u}_{\mathrm{LS}},\ \mathcal{A}(\widehat{\sigma}_{\mathrm{LS}} - \sigma_{\mathrm{LS}} - \widehat{\tau}_{\mathrm{RT}}) - \mathrm{D}(\widehat{u}_{\mathrm{LS}} - u_{\mathrm{LS}} - \widehat{w}_{\mathrm{C}})\big)_{L^2(\Omega)}\\ = -\big(\widehat{\Pi}_k f + \operatorname{div}\widehat{\sigma}_{\mathrm{LS}},\ \Pi_k \operatorname{div}(\widehat{\sigma}_{\mathrm{LS}} - \sigma_{\mathrm{LS}})\big)_{L^2(\Omega)}.\end{aligned} \tag{4.19}$$

The homogeneous boundary conditions $\rho^*_{\mathrm{RT}}\nu = 0$ on Γ_{N} and the nestedness of the spaces $RT_k(\mathcal{T}_0;\mathbb{R}^{3\times3}) \subset RT_k(\mathcal{T};\mathbb{R}^{3\times3})$ make $\rho^*_{\mathrm{RT}} \in RT_k(\mathcal{T}_0;\mathbb{R}^{3\times3})$ an admissible test function with respect to $\mathcal{T}$. Since $\operatorname{div}\rho^*_{\mathrm{RT}} = 0$, the discrete equation (3.18) with $\tau_{\mathrm{LS}} = \rho^*_{\mathrm{RT}}$ and $v_{\mathrm{LS}} \equiv 0$ establishes

$$(\mathcal{A}\sigma_{\mathrm{LS}} - \mathcal{S}\,\mathrm{D}\,u_{\mathrm{LS}},\ \mathcal{A}\rho^*_{\mathrm{RT}})_{L^2(\Omega)} = 0. \tag{4.20}$$

Step 4. The orthogonality of the L^2 projection Π_k allows for the Pythagoras theorem

$$\|\operatorname{div}(\widehat{\sigma}_{\mathrm{LS}} - \sigma_{\mathrm{LS}})\|^2_{L^2(\Omega)} = \|(1-\Pi_k)\operatorname{div}(\widehat{\sigma}_{\mathrm{LS}} - \sigma_{\mathrm{LS}})\|^2_{L^2(\Omega)} + \|\Pi_k \operatorname{div}(\widehat{\sigma}_{\mathrm{LS}} - \sigma_{\mathrm{LS}})\|^2_{L^2(\Omega)}.$$

The addition and subtraction of the term $(\widehat{\Pi}_k f - \Pi_k f,\ \Pi_k \operatorname{div}(\widehat{\sigma}_{\mathrm{LS}} - \sigma_{\mathrm{LS}}))_{L^2(\Omega)} = 0$ and the projection property $\Pi_k = \Pi_k\widehat{\Pi}_k$ lead to

$$\begin{aligned}\|\operatorname{div}(\widehat{\sigma}_{\mathrm{LS}} - \sigma_{\mathrm{LS}})\|^2_{L^2(\Omega)} &= \|(1-\Pi_k)\operatorname{div}(\widehat{\sigma}_{\mathrm{LS}} - \sigma_{\mathrm{LS}})\|^2_{L^2(\Omega)}\\ &\quad + \big(\widehat{\Pi}_k f + \operatorname{div}\widehat{\sigma}_{\mathrm{LS}},\ \Pi_k \operatorname{div}(\widehat{\sigma}_{\mathrm{LS}} - \sigma_{\mathrm{LS}})\big)_{L^2(\Omega)}\\ &\quad - \big(\Pi_k f + \operatorname{div}\sigma_{\mathrm{LS}},\ \operatorname{div}(\widehat{\sigma}_{\mathrm{LS}} - \sigma_{\mathrm{LS}})\big)_{L^2(\Omega)}.\end{aligned} \tag{4.21}$$

The addition and subtraction of the terms

$$\begin{gathered}\big(\mathcal{A}(\widehat{\sigma}_{\mathrm{LS}} - \sigma_{\mathrm{LS}}) - \mathcal{S}\,\mathrm{D}(\widehat{u}_{\mathrm{LS}} - u_{\mathrm{LS}}),\ \mathcal{A}\widehat{\tau}_{\mathrm{RT}} - \mathcal{S}\,\mathrm{D}\,\widehat{w}_{\mathrm{C}}\big)_{L^2(\Omega)},\\ (\mathcal{A}\sigma_{\mathrm{LS}} - \mathcal{S}\,\mathrm{D}\,u_{\mathrm{LS}},\ \mathcal{A}\tau_{\mathrm{RT}})_{L^2(\Omega)}\end{gathered}$$

to and from the contribution $\|\mathcal{A}(\widehat{\sigma}_{\mathrm{LS}} - \sigma_{\mathrm{LS}}) - \mathcal{S}\,\mathrm{D}(\widehat{u}_{\mathrm{LS}} - u_{\mathrm{LS}})\|^2_{L^2(\Omega)}$ establishes the algebraic equality

$$\begin{aligned}&\|\mathcal{A}(\widehat{\sigma}_{\mathrm{LS}} - \sigma_{\mathrm{LS}}) - \mathcal{S}\,\mathrm{D}(\widehat{u}_{\mathrm{LS}} - u_{\mathrm{LS}})\|^2_{L^2(\Omega)}\\ &\quad= \big(\mathcal{A}\widehat{\sigma}_{\mathrm{LS}} - \mathcal{S}\,\mathrm{D}\,\widehat{u}_{\mathrm{LS}},\ \mathcal{A}(\widehat{\sigma}_{\mathrm{LS}} - \sigma_{\mathrm{LS}} - \widehat{\tau}_{\mathrm{RT}}) - \mathcal{S}\,\mathrm{D}(\widehat{u}_{\mathrm{LS}} - u_{\mathrm{LS}} - \widehat{w}_{\mathrm{C}})\big)_{L^2(\Omega)}\\ &\qquad- \big(\mathcal{A}\sigma_{\mathrm{LS}} - \mathcal{S}\,\mathrm{D}\,u_{\mathrm{LS}},\ \mathcal{A}\widehat{\rho}_{\mathrm{RT}} - \mathcal{S}\,\mathrm{D}(\widehat{u}_{\mathrm{LS}} - u_{\mathrm{LS}} - \widehat{w}_{\mathrm{C}})\big)_{L^2(\Omega)}\\ &\qquad- (\mathcal{A}\sigma_{\mathrm{LS}} - \mathcal{S}\,\mathrm{D}\,u_{\mathrm{LS}},\ \mathcal{A}\tau_{\mathrm{RT}})_{L^2(\Omega)}\\ &\qquad+ \big(\mathcal{A}(\widehat{\sigma}_{\mathrm{LS}} - \sigma_{\mathrm{LS}}) - \mathcal{S}\,\mathrm{D}(\widehat{u}_{\mathrm{LS}} - u_{\mathrm{LS}}),\ \mathcal{A}\widehat{\tau}_{\mathrm{RT}} - \mathcal{S}\,\mathrm{D}\,\widehat{w}_{\mathrm{C}}\big)_{L^2(\Omega)}.\end{aligned}$$

Using (4.18)–(4.20), the sum of the previously displayed formula and (4.21) reduces to

$$\begin{aligned}\delta^2(\widehat{\mathcal{T}},\mathcal{T}) &= \|(1-\Pi_k)\operatorname{div}(\widehat{\sigma}_{\mathrm{LS}}-\sigma_{\mathrm{LS}})\|^2_{L^2(\Omega)}\\ &\quad - \big(\mathcal{A}\sigma_{\mathrm{LS}}-\mathcal{S}\,\mathrm{D}\,u_{\mathrm{LS}},\ \mathcal{A}(\widehat{\rho}_{\mathrm{RT}}-\rho^*_{\mathrm{RT}})-\mathcal{S}\,\mathrm{D}(\widehat{u}_{\mathrm{LS}}-u_{\mathrm{LS}}-\widehat{w}_{\mathrm{C}})\big)_{L^2(\Omega)}\\ &\quad + \big(\mathcal{A}(\widehat{\sigma}_{\mathrm{LS}}-\sigma_{\mathrm{LS}})-\mathcal{S}\,\mathrm{D}(\widehat{u}_{\mathrm{LS}}-u_{\mathrm{LS}}),\ \mathcal{A}\widehat{\tau}_{\mathrm{RT}}-\mathcal{S}\,\mathrm{D}\,\widehat{w}_{\mathrm{C}}\big)_{L^2(\Omega)}.\end{aligned}$$

The replacement $\widehat{\rho}_{\mathrm{RT}}-\rho^*_{\mathrm{RT}}=\operatorname{curl}\widehat{\beta}_{\mathrm{Ned}}$ concludes the proof of (4.17). □

The following two lemmas employ the quasi-interpolation operators from Sections 2.6–2.7 to bound the terms on the right-hand side in (4.17).

Lemma 4.8. *There exists a positive generic constant C_{dr1} such that*

$$\begin{aligned}&\big(\mathcal{A}\sigma_{\mathrm{LS}}-\mathcal{S}\,\mathrm{D}\,u_{\mathrm{LS}},\ \mathcal{S}\,\mathrm{D}(\widehat{u}_{\mathrm{LS}}-u_{\mathrm{LS}}-\widehat{w}_{\mathrm{C}})\big)_{L^2(\Omega)}\\ &\le C_{\mathrm{dr1}}\,\|\,\mathrm{D}(\widehat{u}_{\mathrm{LS}}-u_{\mathrm{LS}}-\widehat{w}_{\mathrm{C}})\|_{L^2(\Omega)}\bigg(\sum_{T\in\mathcal{T}\setminus\widehat{\mathcal{T}}}\Big(|T|^{2/3}\,\|\operatorname{div}(\mathcal{S}^*(\mathcal{A}\sigma_{\mathrm{LS}}-\mathcal{S}\,\mathrm{D}\,u_{\mathrm{LS}}))\|^2_{L^2(T)}\\ &\qquad+\sum_{F\in\mathcal{F}(T)\setminus\mathcal{F}(\Gamma_{\mathrm{D}})}|T|^{1/3}\,\|[\mathcal{S}^*(\mathcal{A}\sigma_{\mathrm{LS}}-\mathcal{S}\,\mathrm{D}\,u_{\mathrm{LS}})]_F\,\nu_F\|^2_{L^2(F)}\Big)\bigg)^{1/2}.\end{aligned}$$

Proof. Step 1. For $\widehat{v}_{\mathrm{C}}:=\widehat{u}_{\mathrm{LS}}-u_{\mathrm{LS}}-\widehat{w}_{\mathrm{C}}\in U^{k+1}_{\mathrm{D}}(\widehat{\mathcal{T}})$, let $v_{\mathrm{C}}:=\mathcal{K}^{k+1}_{\mathrm{D}}\widehat{v}_{\mathrm{C}}\in U^{k+1}_{\mathrm{D}}(\mathcal{T})$ denote the Scott-Zhang quasi-interpolation of $\widehat{v}_{\mathrm{C}}\in U^{k+1}_{\mathrm{D}}(\widehat{\mathcal{T}})$ from Section 2.6 and set $\widehat{z}_{\mathrm{C}}:=\widehat{v}_{\mathrm{C}}-v_{\mathrm{C}}\in U^{k+1}_{\mathrm{D}}(\widehat{\mathcal{T}})$. Lemma 2.12 (h) asserts that $\widehat{z}_{\mathrm{C}}|_T=0$ vanishes on every unrefined simplex $T\in\widehat{\mathcal{T}}\cap\mathcal{T}$. The local stability and first-order approximation property of the operator $\mathcal{K}^{k+1}_{\mathrm{D}}$ from Lemma 2.12 (b) read

$$\|\,\mathrm{D}\,\widehat{z}_{\mathrm{C}}\|_{L^2(T)}+|T|^{-1/3}\|\widehat{z}_{\mathrm{C}}\|_{L^2(T)}\le C_{\mathrm{SZ}}\,\|\,\mathrm{D}\,\widehat{v}_{\mathrm{C}}\|_{L^2(\Omega_T)}. \tag{4.22}$$

A combination of this with the square root of the trace inequality (2.19) from Lemma 2.6 leads to

$$\begin{aligned}|T|^{-1/6}\|\widehat{z}_{\mathrm{C}}\|_{L^2(F)}&\le\sqrt{C_{\mathrm{tr}}}\,\big(\|\,\mathrm{D}\,\widehat{z}_{\mathrm{C}}\|_{L^2(T)}+|T|^{-1/3}\|\widehat{z}_{\mathrm{C}}\|_{L^2(T)}\big)\\ &\le\sqrt{C_{\mathrm{tr}}}C_{\mathrm{SZ}}\,\|\,\mathrm{D}\,\widehat{v}_{\mathrm{C}}\|_{L^2(\Omega_T)}.\end{aligned} \tag{4.23}$$

Step 2. Since $\mathcal{K}^{k+1}_{\mathrm{D}}$ preserves polynomial boundary conditions, $v_{\mathrm{C}}\in U^{k+1}_{\mathrm{D}}(\mathcal{T})$ is an admissible test function and the discrete equation (3.18) implies

$$(\mathcal{A}\sigma_{\mathrm{LS}}-\mathcal{S}\,\mathrm{D}\,u_{\mathrm{LS}},\mathcal{S}\,\mathrm{D}\,v_{\mathrm{C}})_{L^2(\Omega)}=0.$$

This and a piecewise integration by parts prove

$$\begin{aligned}(\mathcal{A}\sigma_{\mathrm{LS}}-\mathcal{S}\,\mathrm{D}\,u_{\mathrm{LS}},\mathcal{S}\,\mathrm{D}\,\widehat{v}_{\mathrm{C}})_{L^2(\Omega)}&=(\mathcal{A}\sigma_{\mathrm{LS}}-\mathcal{S}\,\mathrm{D}\,u_{\mathrm{LS}},\mathcal{S}\,\mathrm{D}\,\widehat{z}_{\mathrm{C}})_{L^2(\Omega)}\\ &=-\sum_{T\in\mathcal{T}\setminus\widehat{\mathcal{T}}}\bigg(\big(\widehat{z}_{\mathrm{C}},\ \operatorname{div}(\mathcal{S}^*(\mathcal{A}\sigma_{\mathrm{LS}}-\mathcal{S}\,\mathrm{D}\,u_{\mathrm{LS}}))\big)_{L^2(T)}\\ &\qquad+\sum_{F\in\mathcal{F}(T)\setminus\mathcal{F}(\Gamma_{\mathrm{D}})}\big(\widehat{z}_{\mathrm{C}},\ [\mathcal{S}^*(\mathcal{A}\sigma_{\mathrm{LS}}-\mathcal{S}\,\mathrm{D}\,u_{\mathrm{LS}})]_F\,\nu_F\big)_{L^2(F)}\bigg).\end{aligned} \tag{4.24}$$

Due to the regularity assumption (3.1), all terms in the previously displayed formula are well-defined.

Step 3. Given any $T \in \mathcal{T} \setminus \widehat{\mathcal{T}}$, a Cauchy-Schwarz inequality and the estimate (4.22) prove

$$\begin{aligned}
&\big(\widehat{z}_{\mathrm{C}},\ \operatorname{div}(\mathcal{S}^*(\mathcal{A}\sigma_{\mathrm{LS}} - \mathcal{S}\,\mathrm{D}\,u_{\mathrm{LS}}))\big)_{L^2(T)} \\
&\quad \le |T|^{-1/3}\|\widehat{z}_{\mathrm{C}}\|_{L^2(T)}|T|^{1/3}\|\operatorname{div}(\mathcal{S}^*(\mathcal{A}\sigma_{\mathrm{LS}} - \mathcal{S}\,\mathrm{D}\,u_{\mathrm{LS}}))\|_{L^2(T)} \\
&\quad \le C_{\mathrm{SZ}}\,\|\,\mathrm{D}\,\widehat{v}_{\mathrm{C}}\|_{L^2(\Omega_T)}|T|^{1/3}\|\operatorname{div}(\mathcal{S}^*(\mathcal{A}\sigma_{\mathrm{LS}} - \mathcal{S}\,\mathrm{D}\,u_{\mathrm{LS}}))\|_{L^2(T)}.
\end{aligned}$$

Given any $T \in \mathcal{T} \setminus \widehat{\mathcal{T}}$ with $F \in \mathcal{F}(T) \setminus \mathcal{F}(\Gamma_{\mathrm{D}})$, the combination of the Cauchy-Schwarz inequality and the estimate (4.23) shows

$$\begin{aligned}
&\big(\widehat{z}_{\mathrm{C}},\ [\mathcal{S}^*(\mathcal{A}\sigma_{\mathrm{LS}} - \mathcal{S}\,\mathrm{D}\,u_{\mathrm{LS}})]_F\,\nu_F\big)_{L^2(F)} \\
&\quad \le |T|^{-1/6}\|\widehat{z}_{\mathrm{C}}\|_{L^2(F)}|T|^{1/6}\|[\mathcal{S}^*(\mathcal{A}\sigma_{\mathrm{LS}} - \mathcal{S}\,\mathrm{D}\,u_{\mathrm{LS}})]_F\,\nu_F\|_{L^2(F)} \\
&\quad \le \sqrt{C_{\mathrm{tr}}}C_{\mathrm{SZ}}\,\|\,\mathrm{D}\,\widehat{v}_{\mathrm{C}}\|_{L^2(\Omega_T)}|T|^{1/6}\|[\mathcal{S}^*(\mathcal{A}\sigma_{\mathrm{LS}} - \mathcal{S}\,\mathrm{D}\,u_{\mathrm{LS}})]_F\,\nu_F\|_{L^2(F)}.
\end{aligned}$$

Step 4. The combination of the equality (4.24), the two displayed formulas from Step 3, the Cauchy-Schwarz inequality in $\mathbb{R}^m$ with

$$m = 5|\mathcal{T} \setminus \widehat{\mathcal{T}}| - \big|\{F \in \mathcal{F}(\Gamma_{\mathrm{D}})\ :\ \exists T \in \mathcal{T} \setminus \widehat{\mathcal{T}},\ F \in \mathcal{F}(T)\}\big|,$$

and a finite overlap of the patches Ω_T with the constant C_{OL} from (2.16) prove

$$\begin{aligned}
&\big(\mathcal{A}\sigma_{\mathrm{LS}} - \mathcal{S}\,\mathrm{D}\,u_{\mathrm{LS}},\ \mathcal{S}\,\mathrm{D}(\widehat{u}_{\mathrm{LS}} - u_{\mathrm{LS}} - \widehat{w}_{\mathrm{C}})\big)_{L^2(\Omega)} \\
&\le \max\{1, \sqrt{C_{\mathrm{tr}}}\}C_{\mathrm{SZ}}C_{\mathrm{OL}}\,\|\,\mathrm{D}\,\widehat{v}_{\mathrm{C}}\|_{L^2(\Omega)}\Bigg(\sum_{T\in\mathcal{T}\setminus\widehat{\mathcal{T}}}\Big(|T|^{2/3}\,\|\operatorname{div}(\mathcal{S}^*(\mathcal{A}\sigma_{\mathrm{LS}} - \mathcal{S}\,\mathrm{D}\,u_{\mathrm{LS}}))\|^2_{L^2(T)} \\
&\qquad + \sum_{F\in\mathcal{F}(T)\setminus\mathcal{F}(\Gamma_{\mathrm{D}})}|T|^{1/3}\,\|[\mathcal{S}^*(\mathcal{A}\sigma_{\mathrm{LS}} - \mathcal{S}\,\mathrm{D}\,u_{\mathrm{LS}})]_F\,\nu_F\|^2_{L^2(F)}\Big)\Bigg)^{1/2}.
\end{aligned}$$

This concludes the proof with the constant $C_{\mathrm{dr1}} := \max\{1, \sqrt{C_{\mathrm{tr}}}\}C_{\mathrm{SZ}}C_{\mathrm{OL}}$. □

Lemma 4.9. *There exists a positive generic constant C_{dr2} such that*

$$\begin{aligned}
&(\mathcal{A}\sigma_{\mathrm{LS}} - \mathcal{S}\,\mathrm{D}\,u_{\mathrm{LS}},\ \mathcal{A}\operatorname{curl}\widehat{\beta}_{\mathrm{Ned}})_{L^2(\Omega)} \\
&\quad \le C_{\mathrm{dr2}}\,\|\widehat{\beta}_{\mathrm{Ned}}\|_{H(\operatorname{curl},\Omega)}\Bigg(\sum_{T\in\mathcal{R}_3}\Big(|T|^{2/3}\,\|\operatorname{curl}(\mathcal{A}^*(\mathcal{A}\sigma_{\mathrm{LS}} - \mathcal{S}\,\mathrm{D}\,u_{\mathrm{LS}}))\|^2_{L^2(T)} \\
&\qquad + \sum_{F\in\mathcal{F}(T)\setminus\mathcal{F}(\Gamma_{\mathrm{N}})}|T|^{1/3}\,\|\nu_F \times [\mathcal{A}^*(\mathcal{A}\sigma_{\mathrm{LS}} - \mathcal{S}\,\mathrm{D}\,u_{\mathrm{LS}})]_F\|^2_{L^2(F)}\Big)\Bigg)^{1/2}.
\end{aligned}$$

Remark 4.10. The following proof is a correction of [27, Lemma 5.4]. Therein, it is not guaranteed that the construction of $\mathcal{I}_{\mathrm{N}}\widehat{\beta}_{\mathrm{N}}$ satisfies the required homogeneous tangential boundary conditions on Γ_{N}. Hence, the function $\operatorname{curl}(\mathcal{I}_{\mathrm{N}}\widehat{\beta}_{\mathrm{N}})$ may not be an admissible test function and the fourth displayed formula in the proof of [27, Lemma 5.4] fails. In this thesis, quasi-interpolation operators preserving partial homogeneous boundary conditions are employed as a remedy.

Proof of Lemma 4.9. Step 1. The local operator $Q_{\mathrm{Ned}} : B^k_{\mathrm{N}}(\widehat{\mathcal{T}};\mathbb{R}^{3\times 3}) \to B^k_{\mathrm{N}}(\mathcal{T};\mathbb{R}^{3\times 3})$ from Theorem 2.14 applied to the three components satisfies

$$\begin{aligned} &(1-Q_{\mathrm{Ned}})\widehat{\beta}_{\mathrm{Ned}} = 0 \text{ in every } T \in \mathcal{T}\setminus\mathcal{R}_2 \quad \text{and} \\ &\|(1-Q_{\mathrm{Ned}})\widehat{\beta}_{\mathrm{Ned}}\|_{H(\operatorname{curl},\Omega)} \le C_{\mathrm{qi}}\,\|\widehat{\beta}_{\mathrm{Ned}}\|_{H(\operatorname{curl},\Omega)}. \end{aligned} \tag{4.25}$$

Let $\mathcal{S}_{\mathrm{Ned}} : H_{\mathrm{N}}(\operatorname{curl},\Omega;\mathbb{R}^{3\times 3}) \to B^0_{\mathrm{N}}(\Omega;\mathbb{R}^{3\times 3})$ denote the componentwise application of the quasi-interpolation operator from Theorem 2.13. It allows for a regular split of the interpolation error into a function $z \in H^1_{\mathrm{N}}(\Omega;\mathbb{R}^{3\times 3})$ and a potential $\phi \in H^1_{\mathrm{N}}(\Omega;\mathbb{R}^3)$ such that

$$(1-\mathcal{S}_{\mathrm{Ned}})(1-Q_{\mathrm{Ned}})\widehat{\beta}_{\mathrm{Ned}} = z + \mathrm{D}\,\phi. \tag{4.26}$$

Moreover, the function z satisfies the local approximation error estimate, for every $T \in \mathcal{T}$ with mesh-size $h_T \equiv |T|^{1/3}$,

$$|T|^{-1/3}\|z\|_{L^2(T)} + \|\mathrm{D}\,z\|_{L^2(T)} \le C_{\mathrm{Sch}}\,\|\operatorname{curl}(1-Q_{\mathrm{Ned}})\widehat{\beta}_{\mathrm{Ned}}\|_{L^2(\Omega_T)}. \tag{4.27}$$

This and the square root of the trace inequality (2.19) from Lemma 2.6 lead to

$$\begin{aligned} |T|^{-1/6}\|z\|_{L^2(F)} &\le \sqrt{C_{\mathrm{tr}}}\,\big(|T|^{-1/3}\|z\|_{L^2(T)} + \|\mathrm{D}\,z\|_{L^2(T)}\big) \\ &\le \sqrt{C_{\mathrm{tr}}}C_{\mathrm{Sch}}\,\|\operatorname{curl}(1-Q_{\mathrm{Ned}})\widehat{\beta}_{\mathrm{Ned}}\|_{L^2(\Omega_T)}. \end{aligned} \tag{4.28}$$

Step 2. Since $\nu\times\widehat{\beta}_{\mathrm{Ned}} = 0$ on Γ_{N} and Q_{Ned} and $\mathcal{S}_{\mathrm{Ned}}$ preserve homogeneous boundary conditions, it holds $\nu\times Q_{\mathrm{Ned}}\widehat{\beta}_{\mathrm{Ned}} = 0$ and $\nu\times\mathcal{S}_{\mathrm{Ned}}(1-Q_{\mathrm{Ned}})\widehat{\beta}_{\mathrm{Ned}} = 0$ on Γ_{N}. Hence, $\operatorname{curl} Q_{\mathrm{Ned}}\widehat{\beta}_{\mathrm{Ned}} \in \Sigma^k_{\mathrm{N}}(\mathcal{T})$ and $\operatorname{curl}\mathcal{S}_{\mathrm{Ned}}(1-Q_{\mathrm{Ned}})\widehat{\beta}_{\mathrm{Ned}} \in \Sigma^k_{\mathrm{N}}(\mathcal{T})$ are admissible divergence-free test functions. The discrete equation (3.18) shows

$$\begin{aligned} &\big(\mathcal{A}\sigma_{\mathrm{LS}} - \mathcal{S}\,\mathrm{D}\,u_{\mathrm{LS}},\ \mathcal{A}\operatorname{curl}\widehat{\beta}_{\mathrm{Ned}}\big)_{L^2(\Omega)} \\ &\quad = \big(\mathcal{A}\sigma_{\mathrm{LS}} - \mathcal{S}\,\mathrm{D}\,u_{\mathrm{LS}},\ \mathcal{A}\operatorname{curl}(1-\mathcal{S}_{\mathrm{Ned}})(1-Q_{\mathrm{Ned}})\widehat{\beta}_{\mathrm{Ned}}\big)_{L^2(\Omega)}. \end{aligned}$$

A combination of the locality in (4.25) and the local estimate (4.27) prove that $z|_T = 0$ vanishes in every $T \in \mathcal{T}\setminus\mathcal{R}_3$ and, thus, $z|_F = 0$ on every $F \in \mathcal{F}(T)$. This and the split (4.26) lead to

$$\big(\mathcal{A}\sigma_{\mathrm{LS}} - \mathcal{S}\,\mathrm{D}\,u_{\mathrm{LS}},\ \mathcal{A}\operatorname{curl}\widehat{\beta}_{\mathrm{Ned}}\big)_{L^2(\Omega)} = \sum_{T\in\mathcal{R}_3}\big(\mathcal{A}\sigma_{\mathrm{LS}} - \mathcal{S}\,\mathrm{D}\,u_{\mathrm{LS}},\ \mathcal{A}\operatorname{curl} z\big)_{L^2(T)}.$$

Since $z = 0$ on Γ_{N}, a piecewise integration by parts shows that

$$\begin{aligned}
&\sum_{T\in\mathcal{R}_3} \big(\mathcal{A}\sigma_{\mathrm{LS}} - \mathcal{S}\,\mathrm{D}\,u_{\mathrm{LS}},\ \mathcal{A}\,\mathrm{curl}\,z\big)_{L^2(T)} \\
&\quad = \sum_{T\in\mathcal{R}_3} \Bigg(\big(z,\ \mathrm{curl}(\mathcal{A}^*(\mathcal{A}\sigma_{\mathrm{LS}} - \mathcal{S}\,\mathrm{D}\,u_{\mathrm{LS}}))\big)_{L^2(T)} \\
&\qquad\qquad + \sum_{F\in\mathcal{F}(T)\setminus\mathcal{F}(\Gamma_{\mathrm{N}})} \big(z,\ \nu_F \times [\mathcal{A}^*(\mathcal{A}\sigma_{\mathrm{LS}} - \mathcal{S}\,\mathrm{D}\,u_{\mathrm{LS}})]_F\big)_{L^2(F)} \Bigg).
\end{aligned} \tag{4.29}$$

Step 3. A Cauchy-Schwarz inequality and the estimate (4.27) prove, for every $T \in \mathcal{R}_3$,

$$\begin{aligned}
&\big(z,\ \mathrm{curl}(\mathcal{A}^*(\mathcal{A}\sigma_{\mathrm{LS}} - \mathcal{S}\,\mathrm{D}\,u_{\mathrm{LS}}))\big)_{L^2(T)} \\
&\quad \le |T|^{-1/3}\|z\|_{L^2(T)}\,|T|^{1/3}\|\,\mathrm{curl}(\mathcal{A}^*(\mathcal{A}\sigma_{\mathrm{LS}} - \mathcal{S}\,\mathrm{D}\,u_{\mathrm{LS}}))\|_{L^2(T)} \\
&\quad \le C_{\mathrm{Sch}}\,\|\,\mathrm{curl}(1 - \mathcal{Q}_{\mathrm{Ned}})\widehat{\beta}_{\mathrm{Ned}}\|_{L^2(\Omega_T)}\,|T|^{1/3}\|\,\mathrm{curl}(\mathcal{A}^*(\mathcal{A}\sigma_{\mathrm{LS}} - \mathcal{S}\,\mathrm{D}\,u_{\mathrm{LS}}))\|_{L^2(T)}.
\end{aligned}$$

Given any $T \in \mathcal{R}_3$ with $F \in \mathcal{F}(T) \setminus \mathcal{F}(\Gamma_{\mathrm{N}})$, a Cauchy-Schwarz inequality and the estimate (4.28) show

$$\begin{aligned}
&\big(z,\ \nu_F \times [\mathcal{A}^*(\mathcal{A}\sigma_{\mathrm{LS}} - \mathcal{S}\,\mathrm{D}\,u_{\mathrm{LS}})]_F\big)_{L^2(F)} \\
&\quad \le |T|^{-1/6}\|z\|_{L^2(F)}\,|T|^{1/6}\|\nu_{\mathcal{F}} \times [\mathcal{A}^*(\mathcal{A}\sigma_{\mathrm{LS}} - \mathcal{S}\,\mathrm{D}\,u_{\mathrm{LS}})\|_{L^2(F)} \\
&\quad \le \sqrt{C_{\mathrm{tr}}}C_{\mathrm{Sch}}\,\|\,\mathrm{curl}(1 - \mathcal{Q}_{\mathrm{Ned}})\widehat{\beta}_{\mathrm{Ned}}\|_{L^2(\Omega_T)}\,|T|^{1/6}\|\nu_F \times [\mathcal{A}^*(\mathcal{A}\sigma_{\mathrm{LS}} - \mathcal{S}\,\mathrm{D}\,u_{\mathrm{LS}})\|_{L^2(F)}.
\end{aligned}$$

Step 4. The two displayed formulas from Step 3 applied to the equality (4.29), the bounded overlap of the patches Ω_T with the positive generic constant C_{OL} from (2.16), and the stability estimate in (4.25) conclude the proof with the positive generic constant

$$C_{\mathrm{dr2}} := \max\big\{1, \sqrt{C_{\mathrm{tr}}}\big\}C_{\mathrm{Sch}}C_{\mathrm{qi}}C_{\mathrm{OL}}. \qquad \square$$

Lemma 4.11. *It holds that*

$$\begin{aligned}
&\big(\mathcal{A}(\widehat{\sigma}_{\mathrm{LS}} - \sigma_{\mathrm{LS}}) - \mathcal{S}\,\mathrm{D}(\widehat{u}_{\mathrm{LS}} - u_{\mathrm{LS}}),\ \mathcal{A}\widehat{\tau}_{\mathrm{RT}} - \mathcal{S}\,\mathrm{D}\,\widehat{w}_{\mathrm{C}}\big)_{L^2(\Omega)} \\
&\quad \le \max\{C_{\mathcal{A}}, C_{\mathcal{S}}\}\ \delta(\widehat{\mathcal{T}}, \mathcal{T})\ \big(\|\widehat{\tau}_{\mathrm{RT}}\|_{L^2(\Omega)} + \|\,\mathrm{D}\,\widehat{w}_{\mathrm{C}}\|_{L^2(\Omega)}\big).
\end{aligned}$$

Proof. The claim follows immediately from the Cauchy-Schwarz inequality, the triangle inequality, the boundedness of $\mathcal{A}$ in assumption (W1), and the boundedness of $\mathcal{S}$ in assumption (W4). $\square$

The combination of the four previous lemmas proves the discrete reliability.

Proof of Theorem 4.3. Step 1. Since $\widehat{\rho}_{\mathrm{RT}} := \widehat{\sigma}_{\mathrm{LS}} - \sigma_{\mathrm{LS}} - \widehat{\tau}_{\mathrm{RT}} - \tau_{\mathrm{RT}} \in \Sigma^k_{\mathrm{N}}(\widehat{\mathcal{T}})$ and $\widehat{v}_{\mathrm{C}} := \widehat{u}_{\mathrm{LS}} - u_{\mathrm{LS}} - \widehat{w}_{\mathrm{C}} \in U^{k+1}_{\mathrm{D}}(\widehat{\mathcal{T}})$ satisfy homogeneous boundary conditions, the abstract

Korn inequality (W5) and the ellipticity (3.21) of the least-squares functional from Theorem 3.12 establish

$$\|\widehat{\rho}_{\mathrm{RT}}\|^2_{L^2(\Omega)} + \|\,\mathrm{D}\,\widehat{v}_{\mathrm{C}}\|^2_{L^2(\Omega)} \leq \max\{1, C_{\mathrm{K}}^2\} C_{\mathrm{ell}}\, LS(0; \widehat{\rho}_{\mathrm{RT}}, \widehat{v}_{\mathrm{C}}). \tag{4.30}$$

Since $\operatorname{div} \widehat{\rho}_{\mathrm{RT}} = 0$, the triangle inequality and Young's inequality show

$$\begin{aligned} LS(0; \widehat{\rho}_{\mathrm{RT}}, \widehat{v}_{\mathrm{C}}) &= \|\mathcal{A}\widehat{\rho}_{\mathrm{RT}} - \mathcal{S}\,\mathrm{D}\,\widehat{v}_{\mathrm{C}}\|^2_{L^2(\Omega)} \\ &\leq 2\,\|\mathcal{A}(\widehat{\sigma}_{\mathrm{LS}} - \sigma_{\mathrm{LS}}) - \mathcal{S}\,\mathrm{D}(\widehat{u}_{\mathrm{LS}} - u_{\mathrm{LS}})\|^2_{L^2(\Omega)} \\ &\quad + 2\,\|\mathcal{A}\widehat{\tau}_{\mathrm{RT}}\|^2_{L^2(\Omega)} + 2\,\|\mathcal{A}\tau_{\mathrm{RT}}\|^2_{L^2(\Omega)} + 2\,\|\mathcal{S}\,\mathrm{D}\,\widehat{w}_{\mathrm{C}}\|^2_{L^2(\Omega)}. \end{aligned}$$

The boundedness of the operators $\mathcal{A}$ and $\mathcal{S}$ from the assumptions (W1) and (W4) and the stability estimates (4.7)–(4.8), (4.15) lead to

$$\begin{aligned} LS(0; \widehat{\rho}_{\mathrm{RT}}, \widehat{v}_{\mathrm{C}}) \leq{}& 2\,\|\mathcal{A}(\widehat{\sigma}_{\mathrm{LS}} - \sigma_{\mathrm{LS}}) - \mathcal{S}\,\mathrm{D}(\widehat{u}_{\mathrm{LS}} - u_{\mathrm{LS}})\|^2_{L^2(\Omega)} \\ &+ 4C_{\mathcal{A}}^2 C_{\mathrm{stab}}^2 \big(\|(1 - \Pi_k)\operatorname{div}(\widehat{\sigma}_{\mathrm{LS}} - \sigma_{\mathrm{LS}})\|^2_{L^2(\Omega)} + \|(\widehat{\Pi}_k - \Pi_k)\widetilde{t}_{\mathrm{N}}\|^2_{H^{-1/2}(\partial\Omega)}\big) \\ &+ 2C_{\mathcal{A}}^2 C_{\mathrm{stab}}^2\, \|\Pi_k \operatorname{div}(\widehat{\sigma}_{\mathrm{LS}} - \sigma_{\mathrm{LS}})\|^2_{L^2(\Omega)} \\ &+ 2C_{\mathcal{S}}^2 C_{\mathrm{OL}}^2 C_{\mathrm{SZ}}^2\, \|(\widehat{\mathcal{J}}_{\mathrm{D}}^{k+1} - \mathcal{J}_{\mathrm{D}}^{k+1})\|^2_{H^{1/2}(\Gamma_{\mathrm{D}})}. \end{aligned}$$

This and (4.30) prove

$$\begin{aligned} \|\widehat{\rho}_{\mathrm{RT}}\|^2_{L^2(\Omega)} + \|\,\mathrm{D}\,\widehat{v}_{\mathrm{C}}\|^2_{L^2(\Omega)} \leq c_1 \big(&\delta^2(\widehat{\mathcal{T}}, \mathcal{T}) + \|(\widehat{\Pi}_k - \Pi_k)\widetilde{t}_{\mathrm{N}}\|^2_{H^{-1/2}(\partial\Omega)} \\ &+ \|(\widehat{\mathcal{J}}_{\mathrm{D}}^{k+1} - \mathcal{J}_{\mathrm{D}}^{k+1})u_{\mathrm{D}}\|^2_{H^{1/2}(\Gamma_{\mathrm{D}})}\big) \end{aligned} \tag{4.31}$$

with the positive generic constant

$$c_1 := 2\max\{1, C_{\mathrm{K}}^2\} C_{\mathrm{ell}} \max\{1,\ 2C_{\mathcal{A}}^2 C_{\mathrm{stab}}^2,\ C_{\mathcal{S}}^2 C_{\mathrm{OL}}^2 C_{\mathrm{SZ}}^2\}.$$

Step 2. The split from the Lemma 4.7 and the estimates from the Lemmas 4.8–4.9 and 4.11 lead to

$$\begin{aligned} \delta^2(\widehat{\mathcal{T}}, \mathcal{T}) \leq{}& \|(1 - \Pi_k)\operatorname{div}(\widehat{\sigma}_{\mathrm{LS}} - \sigma_{\mathrm{LS}})\|^2_{L^2(\Omega)} \\ &+ c_2\,\delta(\widehat{\mathcal{T}}, \mathcal{T})\,\big(\|\widehat{\tau}_{\mathrm{RT}}\|_{L^2(\Omega)} + \|\,\mathrm{D}\,\widehat{w}_{\mathrm{C}}\|_{L^2(\Omega)}\big) \\ &+ c_3\,\big(\|\,\mathrm{D}\,\widehat{v}_{\mathrm{C}}\|_{L^2(\Omega)} + \|\widehat{\rho}_{\mathrm{RT}}\|_{L^2(\Omega)}\big)\,\eta_{\mathrm{res}}(\mathcal{T}, \mathcal{R}_3). \end{aligned}$$

with the positive generic constants

$$c_2 := \max\{C_{\mathcal{A}}, C_{\mathcal{S}}\} \quad \text{and} \quad c_3 := \max\{C_{\mathrm{dr1}}, C_{\mathrm{dr2}} C_{\mathrm{Ned}}\}.$$

Multiple applications of Young's inequality with parameter $\alpha > 0$ show

$$\begin{aligned} \delta^2(\widehat{\mathcal{T}}, \mathcal{T}) \leq{}& \|(1 - \Pi_k)\operatorname{div}(\widehat{\sigma}_{\mathrm{LS}} - \sigma_{\mathrm{LS}})\|^2_{L^2(\Omega)} + \frac{c_2}{2\alpha}\,\|\widehat{\tau}_{\mathrm{RT}}\|^2_{L^2(\Omega)} + \frac{c_2}{2\alpha}\,\|\,\mathrm{D}\,\widehat{w}_{\mathrm{C}}\|^2_{L^2(\Omega)} \\ &+ \alpha c_2\,\delta^2(\widehat{\mathcal{T}}, \mathcal{T}) + \alpha\frac{c_3}{2}\,\big(\|\,\mathrm{D}\,\widehat{v}_{\mathrm{C}}\|^2_{L^2(\Omega)} + \|\widehat{\rho}_{\mathrm{RT}}\|^2_{L^2(\Omega)}\big) + \frac{c_3}{\alpha}\,\eta^2_{\mathrm{res}}(\mathcal{T}, \mathcal{R}_3). \end{aligned}$$

The estimates (4.7)–(4.8), (4.15), and (4.31) prove

$$\begin{aligned}\delta^2(\widehat{\mathcal{T}},\mathcal{T}) \le{}& \Big(1+\frac{c_2C_{\mathrm{stab}}^2}{\alpha}\Big)\,\|(1-\Pi_k)\operatorname{div}(\widehat{\sigma}_{\mathrm{LS}}-\sigma_{\mathrm{LS}})\|_{L^2(\Omega)}^2\\ &+\Big(\frac{c_2C_{\mathrm{stab}}^2}{\alpha}+\alpha\frac{c_1c_3}{2}\Big)\,\|(\widehat{\Pi}_k-\Pi_k)\widetilde{t}_{\mathrm{N}}\|_{H^{-1/2}(\partial\Omega)}^2\\ &+\Big(\frac{c_2C_{\mathrm{OL}}^2C_{\mathrm{SZ}}^2}{2\alpha}+\alpha\frac{c_1c_3}{2}\Big)\,\|(\widehat{\mathcal{J}}_{\mathrm{D}}^{k+1}-\mathcal{J}_{\mathrm{D}}^{k+1})u_{\mathrm{D}}\|_{H^{1/2}(\Gamma_{\mathrm{D}})}^2\\ &+\frac{c_3}{\alpha}\,\eta_{\mathrm{res}}^2(\mathcal{T},\mathcal{R}_3)+\frac{\alpha}{2}(2c_2+c_1c_3)\,\delta^2(\widehat{\mathcal{T}},\mathcal{T}).\end{aligned}$$

The choice $\alpha := (2c_2+c_1c_3)^{-1}$ allows for an absorption of the term $\delta^2(\widehat{\mathcal{T}},\mathcal{T})$ on the left-hand side and results in

$$\begin{aligned}\delta^2(\widehat{\mathcal{T}},\mathcal{T}) \le{}& \Big(2+\frac{2c_2C_{\mathrm{stab}}^2}{\alpha}\Big)\,\|(1-\Pi_k)\operatorname{div}(\widehat{\sigma}_{\mathrm{LS}}-\sigma_{\mathrm{LS}})\|_{L^2(\Omega)}^2\\ &+\Big(\frac{2c_2C_{\mathrm{stab}}^2}{\alpha}+\alpha c_1c_3\Big)\,\|(\widehat{\Pi}_k-\Pi_k)\widetilde{t}_{\mathrm{N}}\|_{H^{-1/2}(\partial\Omega)}^2\\ &+\Big(\frac{c_2C_{\mathrm{OL}}^2C_{\mathrm{SZ}}^2}{\alpha}+\alpha c_1c_3\Big)\,\|(\widehat{\mathcal{J}}_{\mathrm{D}}^{k+1}-\mathcal{J}_{\mathrm{D}}^{k+1})u_{\mathrm{D}}\|_{H^{1/2}(\Gamma_{\mathrm{D}})}^2+\frac{2c_3}{\alpha}\,\eta_{\mathrm{res}}^2(\mathcal{T},\mathcal{R}_3).\end{aligned}$$

Lemma 3.8 and Corollary 3.11 imply

$$\begin{aligned}\delta^2(\widehat{\mathcal{T}},\mathcal{T}) \le{}& c_4\,\|(1-\Pi_k)\operatorname{div}(\widehat{\sigma}_{\mathrm{LS}}-\sigma_{\mathrm{LS}})\|_{L^2(\Omega)}^2+c_5\,\operatorname{osc}^2(t_{\mathrm{N}},\mathcal{F}(\Gamma_{\mathrm{N}})\setminus\widehat{\mathcal{F}}(\Gamma_{\mathrm{N}}))\\ &+c_6\,\operatorname{osc}^2(\mathrm{D}\,u_{\mathrm{D}},\mathcal{L}_5(\mathcal{F}\setminus\widehat{\mathcal{F}},\Gamma_{\mathrm{D}}))+c_7\,\eta_{\mathrm{res}}^2(\mathcal{T},\mathcal{R}_3)\end{aligned}$$

with the positive generic constants

$$\begin{aligned}c_4 &:= 2+2c_2C_{\mathrm{stab}}^2(2c_2+c_1c_3), & c_5 &:= C_{\mathrm{N}}^2\Big(2c_2C_{\mathrm{stab}}^2(2c_2+c_1c_3)+\frac{c_1c_3}{2c_2+c_1c_3}\Big),\\ c_6 &:= C_{\mathrm{D2}}\Big(c_2C_{\mathrm{OL}}^2C_{\mathrm{SZ}}^2(2c_2+c_1c_3)+\frac{c_1c_3}{2c_2+c_1c_3}\Big), & c_7 &:= 2c_3(2c_2+c_1c_3).\end{aligned}$$

The triangle inequality and Young's inequality in the estimate

$$\begin{aligned}\|(1-\Pi_k)\operatorname{div}(\widehat{\sigma}_{\mathrm{LS}}-\sigma_{\mathrm{LS}})\|_{L^2(\Omega)}^2 &= \|(1-\Pi_k)\operatorname{div}\widehat{\sigma}_{\mathrm{LS}}\|_{L^2(\Omega)}^2\\ &\le 2\,\|(1-\Pi_k)f\|_{L^2(\Omega)}^2+2\,LS(f;\widehat{\sigma}_{\mathrm{LS}},\widehat{u}_{\mathrm{LS}})\end{aligned}$$

conclude the proof of Theorem 4.3 with the positive generic constants

$$\widetilde{\Lambda}_3 := \max\{2c_4,c_5,c_6,c_7\} \quad\text{and}\quad \widehat{\Lambda}_3 := 2c_4. \qquad \square$$

4.4 Quasi-orthogonality

In the case of homogeneous boundary conditions, the variational formulation (3.18) provides a conforming discretisation. The Galerkin orthogonality immediately implies the quasi-orthogonality axiom (A4) [44, Theorem 4.1]. However, for triangulations $\mathcal{T}_j$ and $\mathcal{T}_{j+1}$, the (possibly) different boundary data approximations on the refined boundary faces $\mathcal{F}_j(\Gamma_X) \setminus \mathcal{F}_{j+1}(\Gamma_X)$ prevent the Galerkin orthogonality. The stable extensions of the approximation errors from the Sections 3.3–3.4 allow for a remedy in the proof of a quasi-Pythagoras Lemma 4.15 below. This result leads to the proof of a weakened version of the quasi-orthogonality axiom (A4) using a procedure from [37, the following Lemma 4.15 matches axiom (B3a) therein]. A standard result [40, Theorem 3.1] deduces (A4) and completes this chapter.

The Dirichlet data approximation error in the $H^{1/2}$ norm allows for an upper bound in terms of the boundary data oscillations on not less than five additional layers around the refined boundary faces in Lemma 3.8. This requires the notion of a modified mesh-size function $h(n)$ for $n \in \mathbb{N}_0$ being reduced by a factor $0 < \rho_{\mathrm{mms}}(n) < 1$ on the simplex $T \in \mathcal{T}$ if any simplex in the n-layer $\mathcal{L}_n(\{T\})$ is refined, cf. [62, Section 4.2] and [37, Section 8.7]. For $n = 0$, this coincides with the usual mesh-size function $h(0)|_T \equiv h_{\mathcal{T}}|_T \equiv |T|^{1/3}$ from (2.18).

Lemma 4.12 (modified mesh-size function). *For every $n \in \mathbb{N}_0$, there exist a piecewise constant modified mesh-size function $h(n) \in P_0(\mathcal{T})$, generic constants $C_{\mathrm{mms}}(n) \geq 1$, and $0 < \rho_{\mathrm{mms}}(n) < 1$ such that*

(i) $C_{\mathrm{mms}}(n)^{-1}\, h_{\mathcal{T}} \leq h(n) \leq h_{\mathcal{T}}$ *in* Ω,

(ii) $\widehat{h}(n)|_T \leq \rho_{\mathrm{mms}}(n)\, h(n)|_T$ *on every* $T \in \mathcal{R}_n = \mathcal{L}_n(\mathcal{T} \setminus \widehat{\mathcal{T}})$,

(iii) $\widehat{h}(n) \leq h(n)$ *in* Ω.

For $n = 0$, $h(0) \equiv h_{\mathcal{T}}$ satisfies (i)–(iii) with $C_{\mathrm{mms}} = 1$ and $\rho_{\mathrm{mms}} = 2^{-1/3}$.

Proof. The proof is given in [37, Proposition 8.6]. It relies on the shape regularity of triangulations in $\mathbb{T}$ ensuring that there exists a uniform upper bound c_1 with, for every $\mathcal{T} \in \mathbb{T}$,

$$\max\left\{|T|/|\widetilde{T}| \;:\; T, \widetilde{T} \in \mathcal{T} \text{ with } \operatorname{dist}(T, \widetilde{T}) = 0\right\} \leq c_1.$$

In particular, for every $T \in \mathcal{T}$ and $\widetilde{T} \in \mathcal{L}_n(\{T\})$,

$$c_2^{-1} \leq \frac{|T|}{|\widetilde{T}|} \leq c_2 \quad \text{and} \quad |\mathcal{L}_n(\{T\})| \leq c_3.$$

A successive definition over the one-level refinements from the initial triangulation $\mathcal{T}_0$ until $\mathcal{T}$ in $\mathbb{T}$ with a rescaling for the refined simplices leads to the mesh-size function $h(n)$. □

Using this notion of a mesh-size, define the modified boundary data oscillations, for $n \in \mathbb{N}_0$, $g \in L^2(\partial\Omega)$, and $\mathcal{M} \subseteq \mathcal{F}(\partial\Omega)$,

$$\operatorname{osc}_n^2(g, \mathcal{M}) := \sum_{F \in \mathcal{M}} \|h(n)^{1/2}(1 - \Pi_k)g\|_{L^2(F)}^2 \tag{4.32}$$

Thus, the oscillations osc_0 coincide with those defined in (2.20). The modified oscillations provide the following estimate for oscillations on n-layers.

Lemma 4.13. *Given any part $\Gamma_X \in \{\Gamma_D, \Gamma_N\}$ of the boundary $\partial\Omega$ and $n \in \mathbb{N}_0$, every $g \in L^2(\Gamma_D)$ satisfies*

$$\operatorname{osc}^2(g, \mathcal{L}_n(\mathcal{F} \setminus \widehat{\mathcal{F}}, \Gamma_X)) \leq C_{\operatorname{osc}}(n)\big(\operatorname{osc}_n^2(g, \mathcal{F}(\Gamma_X)) - \operatorname{osc}_n^2(g, \widehat{\mathcal{F}}(\Gamma_X))\big).$$

The constant $C_{\operatorname{osc}}(n)$ depends solely on the modified mesh-size function $h(n)$. In particular, it does not depend on the part Γ_X. For $n = 0$, $C_{\operatorname{osc}}(0) = 1$.

Remark 4.14. This result is included in the proof of [37, Proposition 11.1]. The estimate in the third displayed formula in [37, on page 1251] is false, because the equivalence of the modified mesh-size function from Lemma 4.12 (i) just allows for an upper bound $-C_{13}^{-1}\mu(\widehat{\mathcal{T}})^2$ therein. To provide a remedy in this thesis, the quasi-Pythagoras Lemma 4.15 is established for the modified oscillations osc_n. The equivalence from Lemma 4.12 (i) will be applied at the very end of the proof of Theorem 4.16.

Proof of Lemma 4.13. Recall the notion of the relative interior of boundary patches from (2.5). The estimates from Lemma 4.12 (ii)–(iii) approve, for the modified mesh-size function $h(n)$,

$$(1 - \rho_{\operatorname{mms}}(n))\, h(n) \leq h(n) - \widehat{h}(n) \quad \text{in } S_n := \operatorname{relint} \bigcup \mathcal{L}_n(\mathcal{T} \setminus \widehat{\mathcal{T}}). \tag{4.33}$$

On the boundary patch $\widetilde{S}_{X,n} := \operatorname{relint}(\bar{S}_n \cap \Gamma_X)$, the estimate (4.33) justifies

$$\begin{aligned}(1 - \rho_{\operatorname{mms}}(n))\, &\|h(n)^{1/2}(1 - \Pi_k)g\|_{L^2(\widetilde{S}_{X,n})}^2 \\ &\leq \|h(n)^{1/2}(1 - \Pi_k)g\|_{L^2(\widetilde{S}_{X,n})}^2 - \|\widehat{h}(n)^{1/2}(1 - \Pi_k)g\|_{L^2(\widetilde{S}_{X,n})}^2.\end{aligned}$$

The monotonicity (iii) shows for the remaining contributions

$$\|\widehat{h}(n)^{1/2}(1 - \Pi_k)g\|_{L^2(\Gamma_X \setminus \widetilde{S}_{X,n})}^2 \leq \|h(n)^{1/2}(1 - \Pi_k)g\|_{L^2(\Gamma_X \setminus \widetilde{S}_{X,n})}^2.$$

The combination of the two previously displayed formulas reads

$$\begin{aligned}(1 - \rho_{\operatorname{mms}}(n))\, &\|h(n)^{1/2}(1 - \Pi_k)g\|_{L^2(\Gamma_X)}^2 \\ &\leq \|h(n)^{1/2}(1 - \Pi_k)g\|_{L^2(\Gamma_X)}^2 - \|\widehat{h}(n)^{1/2}(1 - \Pi_k)g\|_{L^2(\Gamma_X)}^2.\end{aligned} \tag{4.34}$$

The piecewise polynomial L^2 orthogonal projection Π_k with respect to the faces $\mathcal{F}$ and the refined faces $\widehat{\mathcal{F}}$ satisfies

$$\|\widehat{h}(n)^{1/2}(1-\widehat{\Pi}_k)g\|^2_{L^2(\Gamma_X)} \leq \|\widehat{h}(n)^{1/2}(1-\Pi_k)g\|^2_{L^2(\Gamma_X)}.$$

This and (4.34) prove

$$\begin{aligned}(1-\rho_{\mathrm{mms}}(n))\,&\|h(n)^{1/2}(1-\Pi_k)g\|^2_{L^2(\widetilde{S}_{X,n})}\\ &\leq \|h(n)^{1/2}(1-\Pi_k)g\|^2_{L^2(\Gamma_X)} - \|\widehat{h}(n)^{1/2}(1-\widehat{\Pi}_k)g\|^2_{L^2(\Gamma_X)}.\end{aligned}$$

The equivalence (i) concludes the proof with the positive generic constant

$$C_{\mathrm{osc}}(n) := \frac{C_{\mathrm{mms}}(n)}{1-\rho_{\mathrm{mms}}(n)}.$$

For $n=0$, the orthogonality of Π_k immediately shows the result with $C_{\mathrm{osc}}(0)=1$. □

Given a regular triangulation $\mathcal{T}\in\mathbb{T}$ with admissible refinement $\widehat{\mathcal{T}}\in\mathbb{T}(\mathcal{T})$, recall Notation 3 from page 22. The following lemma involves the modified boundary data oscillations of the surface gradient $\mathrm{D}\,u_D$ from (2.4).

Lemma 4.15 (quasi-Pythagoras). *Abbreviate*

$$\widetilde{\eta}^2_{\mathrm{osc}}(\mathcal{T}) := \mathrm{osc}^2_5(\mathrm{D}\,u_D,\mathcal{F}(\Gamma_D)) + \mathrm{osc}^2(t_N,\mathcal{F}(\Gamma_N)) \tag{4.35}$$

and do so analogously for $\widehat{\mathcal{T}}$. There exists a positive generic constant C_{QP} such that every $\alpha>0$ satisfies

$$\begin{aligned}\delta^2(\widehat{\mathcal{T}},\mathcal{T}) \leq{}& (1+\alpha)\,LS(f;\sigma_{LS},u_{LS}) - (1-\alpha)\,LS(f;\widehat{\sigma}_{LS},\widehat{u}_{LS})\\ &+\frac{C_{\mathrm{QP}}}{\alpha}\,\big(\widetilde{\eta}^2_{\mathrm{osc}}(\mathcal{T}) - \widetilde{\eta}^2_{\mathrm{osc}}(\widehat{\mathcal{T}})\big).\end{aligned} \tag{4.36}$$

The constant C_{QP} does not depend on α.

Proof. Step 1. Lemma 3.6 guarantees the existence of a discrete extension $\widehat{w}_C\in S^{k+1}(\widehat{\mathcal{T}};R^3)$ with $\widehat{w}_C=(\widehat{\mathcal{J}}^{k+1}_D-\mathcal{J}^{k+1}_D)u_D$ on Γ_D and

$$\|\mathrm{D}\,\widehat{w}_C\|_{L^2(\Omega)} \leq C_{\mathrm{OL}}C_{\mathrm{SZ}}\,\|(\widehat{\mathcal{J}}^{k+1}_D-\mathcal{J}^{k+1}_D)u_D\|_{H^{1/2}(\Gamma_D)}.$$

Lemma 3.8 justifies the estimate

$$\|\mathrm{D}\,\widehat{w}_C\|^2_{L^2(\Omega)} \leq C^2_{\mathrm{OL}}C^2_{\mathrm{SZ}}C_{\mathrm{D2}}\,\mathrm{osc}^2(\mathrm{D}\,u_D,\mathcal{L}_5(\mathcal{F}\setminus\widehat{\mathcal{F}},\Gamma_D)).$$

Eventually, Lemma 4.13 for $n=5$ and $\Gamma_X=\Gamma_D$ accomplishes

$$\|\mathrm{D}\,\widehat{w}_C\|^2_{L^2(\Omega)} \leq C^2_{\mathrm{OL}}C^2_{\mathrm{SZ}}C_{\mathrm{D2}}C_{\mathrm{osc}}(5)\,\big(\mathrm{osc}^2_5(\mathrm{D}\,u_D,\mathcal{F}(\Gamma_D)) - \mathrm{osc}^2_5(\mathrm{D}\,u_D,\widehat{\mathcal{F}}(\Gamma_D))\big). \tag{4.37}$$

Moreover, Lemma 3.9 provides some discrete extension $\widehat{\xi}_{\mathrm{RT}} \in RT_k(\widehat{\mathcal{T}};\mathbb{R}^{3\times 3})$ with $\operatorname{div}\widehat{\xi}_{\mathrm{RT}} = 0$ in Ω and $\widehat{\xi}_{\mathrm{RT}} = (\widehat{\Pi}_k - \Pi_k)t_{\mathrm{N}}$ on Γ_{N}. It satisfies the stability estimate

$$\|\widehat{\xi}_{\mathrm{RT}}\|_{L^2(\Omega)} \leq C_{\mathrm{ext}}\,\|(\widehat{\Pi}_k - \Pi_k)t_{\mathrm{N}}\|_{H^{-1/2}(\partial\Omega)}.$$

This and Corollary 3.11 establish

$$\|\widehat{\xi}_{\mathrm{RT}}\|^2_{L^2(\Omega)} \leq C^2_{\mathrm{ext}}C^2_{\mathrm{N}}\ \operatorname{osc}^2(t_{\mathrm{N}},\mathcal{F}(\Gamma_{\mathrm{N}})\setminus\widehat{\mathcal{F}}(\Gamma_{\mathrm{N}})).$$

Since the oscillation term in this formula coincides with the modified oscillation $\operatorname{osc}_0^2(t_{\mathrm{N}},\mathcal{F}(\Gamma_{\mathrm{N}})\setminus\widehat{\mathcal{F}}(\Gamma_{\mathrm{N}}))$, Lemma 4.13 for $n=0$ and $\Gamma_{\mathrm{X}}=\Gamma_{\mathrm{N}}$ applies with $C_{\mathrm{osc}}(0)=1$. Consequently,

$$\|\widehat{\xi}_{\mathrm{RT}}\|^2_{L^2(\Omega)} \leq C^2_{\mathrm{ext}}C^2_{\mathrm{N}}\left(\operatorname{osc}^2(t_{\mathrm{N}},\mathcal{F}(\Gamma_{\mathrm{N}})) - \operatorname{osc}^2(t_{\mathrm{N}},\widehat{\mathcal{F}}(\Gamma_{\mathrm{N}}))\right). \tag{4.38}$$

Step 2. Abbreviate the exact minimiser $X := (\sigma,u)$ and the solutions $X_{\mathrm{LS}} := (\sigma_{\mathrm{LS}},u_{\mathrm{LS}})$ and $\widehat{X}_{\mathrm{LS}} := (\widehat{\sigma}_{\mathrm{LS}},\widehat{u}_{\mathrm{LS}})$ to the discrete equations (3.18) with respect to the triangulations $\mathcal{T}$ and $\widehat{\mathcal{T}}$. The weak solution satisfies the two equations $-\operatorname{div}\sigma = f$ and $\mathcal{A}\sigma = \mathcal{S}\,\mathrm{D}\,u$ exactly and, thus, $\operatorname{div}\widehat{\xi}_{\mathrm{RT}} = 0$ shows

$$\mathcal{B}(X-\widehat{X}_{\mathrm{LS}};(\widehat{\xi}_{\mathrm{RT}},\widehat{w}_{\mathrm{C}})) = -\big(\mathcal{A}\widehat{\sigma}_{\mathrm{LS}} - \mathcal{S}\,\mathrm{D}\,\widehat{u}_{\mathrm{LS}},\ \mathcal{A}\widehat{\xi}_{\mathrm{RT}} - \mathcal{S}\,\mathrm{D}\,\widehat{w}_{\mathrm{C}}\big)_{L^2(\Omega)}.$$

The Cauchy-Schwarz and the triangle inequality combined with the boundedness of $\mathcal{A}$ and $\mathcal{S}$ from the assumptions (W1) and (W4) verify

$$\mathcal{B}(X-\widehat{X}_{\mathrm{LS}};(\widehat{\xi}_{\mathrm{RT}},\widehat{w}_{\mathrm{C}})) \leq \|\mathcal{A}\widehat{\sigma}_{\mathrm{LS}} - \mathcal{S}\,\mathrm{D}\,\widehat{u}_{\mathrm{LS}}\|_{L^2(\Omega)}\Big(C_{\mathcal{A}}\,\|\widehat{\xi}_{\mathrm{RT}}\|_{L^2(\Omega)} + C_{\mathcal{S}}\,\|\,\mathrm{D}\,\widehat{w}_{\mathrm{C}}\|_{L^2(\Omega)}\Big).$$

Young's inequality with parameter $\alpha/2>0$ shows

$$\mathcal{B}(X-\widehat{X}_{\mathrm{LS}};(\widehat{\xi}_{\mathrm{RT}},\widehat{w}_{\mathrm{C}})) \leq \frac{\alpha}{2}\,LS(f;\widehat{\sigma}_{\mathrm{LS}},\widehat{u}_{\mathrm{LS}}) + \frac{C^2_{\mathcal{S}}}{\alpha}\,\|\,\mathrm{D}\,\widehat{w}_{\mathrm{C}}\|^2_{L^2(\Omega)} + \frac{C^2_{\mathcal{A}}}{\alpha}\,\|\widehat{\xi}_{\mathrm{RT}}\|^2_{L^2(\Omega)}.$$

This and the estimates (4.37)–(4.38) from Step 1 prove

$$\mathcal{B}(X-\widehat{X}_{\mathrm{LS}};(\widehat{\xi}_{\mathrm{RT}},\widehat{w}_{\mathrm{C}})) \leq \frac{\alpha}{2}\,LS(f;\widehat{\sigma}_{\mathrm{LS}},\widehat{u}_{\mathrm{LS}}) + \frac{C_{\mathrm{QP}}}{2\alpha}\left(\widetilde{\eta}^2_{\mathrm{osc}}(\mathcal{T}) - \widetilde{\eta}^2_{\mathrm{osc}}(\widehat{\mathcal{T}})\right) \tag{4.39}$$

with the positive generic constant

$$C_{\mathrm{QP}} := 2\max\left\{C^2_{\mathcal{S}}C^2_{\mathrm{OL}}C^2_{\mathrm{SZ}}C_{\mathrm{D2}}C_{\mathrm{osc}}(5),\ C^2_{\mathcal{A}}C^2_{\mathrm{ext}}C^2_{\mathrm{N}}\right\}.$$

Step 3. The boundary data extensions $\widehat{w}_{\mathrm{C}}$ and $\widehat{\xi}_{\mathrm{RT}}$ from Step 1 allow for the construction of an admissible test function $\widehat{X}_{\mathrm{LS}} - X_{\mathrm{LS}} - (\widehat{\xi}_{\mathrm{RT}},\widehat{w}_{\mathrm{C}}) \in \Sigma^k_{\mathrm{N}}(\widehat{\mathcal{T}})\times U^{k+1}_{\mathrm{D}}(\widehat{\mathcal{T}})$. Therefore, the Galerkin orthogonality of the variational formulation (3.18) reads

$$\mathcal{B}(X-\widehat{X}_{\mathrm{LS}};\widehat{X}_{\mathrm{LS}} - X_{\mathrm{LS}} - (\widehat{\xi}_{\mathrm{RT}},\widehat{w}_{\mathrm{C}})) = 0. \tag{4.40}$$

This and the binomial formula for the symmetric bilinear form $\mathcal{B}$ show

$$\begin{aligned}\mathcal{B}(X - X_{\mathrm{LS}}; X - X_{\mathrm{LS}}) &= \mathcal{B}((X - \widehat{X}_{\mathrm{LS}}) + (\widehat{X}_{\mathrm{LS}} - X_{\mathrm{LS}}); (X - \widehat{X}_{\mathrm{LS}}) + (\widehat{X}_{\mathrm{LS}} - X_{\mathrm{LS}})) \\ &= \mathcal{B}(X - \widehat{X}_{\mathrm{LS}}; X - \widehat{X}_{\mathrm{LS}}) + \mathcal{B}(\widehat{X}_{\mathrm{LS}} - X_{\mathrm{LS}}; \widehat{X}_{\mathrm{LS}} - X_{\mathrm{LS}}) \\ &\quad + 2\mathcal{B}(X - \widehat{X}_{\mathrm{LS}}; (\widehat{\xi}_{\mathrm{RT}}, \widehat{w}_{\mathrm{C}})).\end{aligned}$$

A rearrangement of this formula in terms of the least-squares functional and the application of the estimate (4.39) conclude the proof. □

Theorem 4.16 (quasi-orthogonality with $\varepsilon > 0$). *The output triangulations $(\mathcal{T}_\ell : \ell \in \mathbb{N}_0)$ of the adaptive algorithm ALSFEM from page 4 satisfy axiom* (A4$_\varepsilon$)*: For every $\varepsilon > 0$ there exists a positive generic constant $\widetilde{\Lambda}_4(\varepsilon)$ such that, for every $m, n \in \mathbb{N}_0$,*

$$\sum_{\ell=m}^{m+n} \delta^2(\mathcal{T}_{\ell+1}, \mathcal{T}_\ell) \le \widetilde{\Lambda}_4(\varepsilon) \left(\eta^2(\mathcal{T}_m) + \mu^2(\mathcal{T}_m)\right) + \varepsilon \sum_{\ell=m}^{m+n} \left(\eta^2(\mathcal{T}_\ell) + \mu^2(\mathcal{T}_\ell)\right). \tag{A4$_\varepsilon$}$$

This weakened version of the quasi-orthogonality axiom (A4) allows for the immediate conclusion of (A4) in presence of the axioms (A1)–(A2) by [40, Theorem 3.1].

Corollary 4.17. *Given the positive generic constants Λ_{12} and $\rho_{12} < 1$ from [40, Theorem 4.1], the axioms* (A1)–(A2) *and* (A4$_\varepsilon$) *with $0 < \varepsilon < (1 - \rho_{12})/\Lambda_{12}$ imply quasi-orthogonality* (A4) *with the positive generic constant*

$$\Lambda_4 := \widetilde{\Lambda}_4(\varepsilon) + \varepsilon(1 + \Lambda_{12}\widetilde{\Lambda}_4(\varepsilon))/(1 - \rho_{12} - \varepsilon\Lambda_{12}).$$

Proof of Theorem 4.16. The proof of (A4$_\varepsilon$) proceeds as the one for [37, Lemma 3.7]. It is displayed here in detail because of the presence of oscillations with the modified mesh-size in Lemma 4.15 and the slightly different distance δ in this thesis (cf. [37, Section 2.2]). The point of departure is the quasi-Pythagoras Lemma 4.15 being applied to the output triangulations $(\mathcal{T}_\ell : \ell \in \mathbb{N}_0)$ of the adaptive algorithm ALSFEM. This reads, for every $\ell \in \mathbb{N}_0$ and $\alpha > 0$,

$$\begin{aligned}\delta^2(\mathcal{T}_{\ell+1}, \mathcal{T}_\ell) &\le (1 + \alpha)\, LS(f; \sigma_\ell, u_\ell) - (1 - \alpha)\, LS(f; \sigma_{\ell+1}, u_{\ell+1}) \\ &\quad + \frac{C_{\mathrm{QP}}}{\alpha} \left(\widetilde{\eta}^2_{\mathrm{osc}}(\mathcal{T}_\ell) - \widetilde{\eta}^2_{\mathrm{osc}}(\mathcal{T}_{\ell+1})\right).\end{aligned}$$

This is equivalent to

$$\begin{aligned}&\delta^2(\mathcal{T}_{\ell+1}, \mathcal{T}_\ell) - 2\alpha\, LS(f; \sigma_{\ell+1}, u_{\ell+1}) \\ &\quad \le (1 - \alpha) \left(LS(f; \sigma_\ell, u_\ell) - LS(f; \sigma_{\ell+1}, u_{\ell+1})\right) + \frac{C_{\mathrm{QP}}}{\alpha} \left(\widetilde{\eta}^2_{\mathrm{osc}}(\mathcal{T}_\ell) - \widetilde{\eta}^2_{\mathrm{osc}}(\mathcal{T}_{\ell+1})\right).\end{aligned}$$

The telescoping sum over $\ell = m, \dots, m + n$ leads to

$$\sum_{\ell=m}^{m+n} \left(\delta^2(\mathcal{T}_{\ell+1}, \mathcal{T}_\ell) - 2\alpha\, LS(f; \sigma_{\ell+1}, u_{\ell+1})\right) \le (1 - \alpha)\, LS(f; \sigma_m, u_m) + \frac{C_{\mathrm{QP}}}{\alpha}\, \widetilde{\eta}^2_{\mathrm{osc}}(\mathcal{T}_m).$$

The equivalence of the modified mesh-size function from Lemma 4.12 (i) ensures that $\widetilde{\eta}^2_{\mathrm{osc}}(\mathcal{T}_m) \leq \eta^2_{\mathrm{osc}}(\mathcal{T}_m)$. Consequently, the reliability (4.4) from Corollary 4.4 shows

$$\sum_{\ell=m}^{m+n} \delta^2(\mathcal{T}_{\ell+1}, \mathcal{T}_\ell) \leq \left((1-\alpha)\widetilde{\Lambda}_3 + \frac{C_{\mathrm{QP}}}{\alpha}\right)\left(\eta^2(\mathcal{T}_m) + \mu^2(\mathcal{T}_m)\right) + 2\alpha\widetilde{\Lambda}_3 \sum_{\ell=m}^{m+n}\left(\eta^2(\mathcal{T}_\ell) + \mu^2(\mathcal{T}_\ell)\right).$$

Given any $\varepsilon > 0$ and $\widetilde{\Lambda}_4(\varepsilon) := (1-\alpha)\widetilde{\Lambda}_3 + C_{\mathrm{QP}}/\alpha$ with $\alpha := \varepsilon/(2\widetilde{\Lambda}_3)$, this is the assertion (A4$_\varepsilon$). □

4.5 Quasi-monotonicity

The analysis in [40, Section 3.2] shows that the quasi-monotonicity (QM) can be deduced from the axioms (A1)–(A3) if $(\Lambda_1^2 + \Lambda_2^2)\widehat{\Lambda}_3 < 1$ is sufficiently small [40, Theorem 3.2]. For the ALSFEM algorithm at hand, this is not guaranteed in general. Thus, axiom (QM) has to be established explicitly as follows. The least-squares functional *LS* is minimised over nested discrete space in the case of homogeneous boundary conditions. This provides its strict monotonicity. In the presence of inhomogeneous boundary conditions, the quasi-Pythagoras Lemma 4.15 allows for quasi-monotonicity of the least-squares functional plus the modified oscillations. In combination with the efficiency and the reliability of the alternative a posteriori error estimator, it implements (QM). Recall Notation 3 from page 22 for regular triangulation $\mathcal{T} \in \mathbb{T}$ and its admissible refinement $\widehat{\mathcal{T}} \in \mathbb{T}(\mathcal{T})$.

Theorem 4.18 (quasi-monotonicity of $\eta + \mu$). *The a posteriori error estimator η and the data approximation error μ satisfy the axiom* (QM)*: There exists a positive generic constant Λ_7 such that, for any $\mathcal{T} \in \mathbb{T}$ with admissible refinement $\widehat{\mathcal{T}} \in \mathbb{T}(\mathcal{T})$,*

$$\eta(\widehat{\mathcal{T}}) + \mu(\widehat{\mathcal{T}}) \leq \Lambda_7 \left(\eta(\mathcal{T}) + \mu(\mathcal{T})\right)$$

Proof. Step 1. The modified mesh-size function $h(5) \in P_0(\mathcal{T})$ from Lemma 4.12 satisfies the equivalence, for $C_{\mathrm{mms}}(5) \geq 1$,

$$C_{\mathrm{mms}}^{-1}(5)\, h_{\mathcal{T}} \leq h(5) \leq h_{\mathcal{T}} \quad \text{a.e. in } \Omega.$$

For the oscillations from (2.20) and the modified oscillations from (4.32), this shows

$$C_{\mathrm{mms}}(5)^{-1}\ \mathrm{osc}^2(\mathrm{D}\, u_{\mathrm{D}}, \mathcal{F}(\Gamma_{\mathrm{D}})) \leq \mathrm{osc}_5^2(\mathrm{D}\, u_{\mathrm{D}}, \mathcal{F}(\Gamma_{\mathrm{D}})) \leq \mathrm{osc}^2(\mathrm{D}\, u_{\mathrm{D}}, \mathcal{F}(\Gamma_{\mathrm{D}})).$$

In particular, for η_{osc} from (3.32) and $\widetilde{\eta}_{\mathrm{osc}}$ from (4.35),

$$C_{\mathrm{mms}}^{-1}(5)\, \eta^2_{\mathrm{osc}}(\mathcal{T}) \leq \widetilde{\eta}^2_{\mathrm{osc}}(\mathcal{T}) \leq \eta^2_{\mathrm{osc}}(\mathcal{T}). \tag{4.41}$$

An analogous estimate holds with respect to the refinement $\widehat{\mathcal{T}}$.

Step 2. A rearrangement of the quasi-Pythagoras estimate (4.36) from Lemma 4.15 reads, for every $\alpha > 0$,

$$\begin{aligned}(1-\alpha)\, LS(f;\widehat{\sigma}_{\mathrm{LS}},\widehat{u}_{\mathrm{LS}}) + \frac{C_{\mathrm{QP}}}{\alpha}\,\widetilde{\eta}^2_{\mathrm{osc}}(\widehat{\mathcal{T}}) + \delta^2(\widehat{\mathcal{T}},\mathcal{T})\\ \leq (1+\alpha)\, LS(f;\sigma_{\mathrm{LS}},u_{\mathrm{LS}}) + \frac{C_{\mathrm{QP}}}{\alpha}\,\widetilde{\eta}^2_{\mathrm{osc}}(\mathcal{T}).\end{aligned}$$

Under the assumption $0 < \alpha < 1$, this shows

$$LS(f;\widehat{\sigma}_{\mathrm{LS}},\widehat{u}_{\mathrm{LS}}) + \widetilde{\eta}^2_{\mathrm{osc}}(\widehat{\mathcal{T}}) \leq c_1(\alpha)\,\big(LS(f;\sigma_{\mathrm{LS}},u_{\mathrm{LS}}) + \widetilde{\eta}^2_{\mathrm{osc}}(\mathcal{T})\big) \tag{4.42}$$

with the positive generic constant

$$c_1(\alpha) := \frac{\max\{1+\alpha, C_{\mathrm{QP}}/\alpha\}}{\min\{1-\alpha, C_{\mathrm{QP}}/\alpha\}}\,.$$

Step 3. Since $\mu^2(\widehat{\mathcal{T}}) \leq LS(f,\widehat{\sigma}_{\mathrm{LS}},\widehat{u}_{\mathrm{LS}})$, the efficiency from Theorem 3.18 with respect to $\widehat{\mathcal{T}}$ implies

$$\eta^2(\widehat{\mathcal{T}}) + \mu^2(\widehat{\mathcal{T}}) \leq (1+C_{\mathrm{eff}})\,\big(LS(f;\widehat{\sigma}_{\mathrm{LS}},\widehat{u}_{\mathrm{LS}}) + \eta^2_{\mathrm{osc}}(\widehat{\mathcal{T}})\big).$$

The estimates (4.41)–(4.42) verify

$$\eta^2(\widehat{\mathcal{T}}) + \mu^2(\widehat{\mathcal{T}}) \leq (1+C_{\mathrm{eff}})C_{\mathrm{mms}}(5)c_1(\alpha)\,\big(LS(f;\sigma_{\mathrm{LS}},u_{\mathrm{LS}}) + \widetilde{\eta}^2_{\mathrm{osc}}(\mathcal{T})\big).$$

The estimate (4.41) and the reliability from Corollary 4.4 establish

$$\eta^2(\widehat{\mathcal{T}}) + \mu^2(\widehat{\mathcal{T}}) \leq (1+C_{\mathrm{eff}})C_{\mathrm{mms}}(5)c_1(\alpha)(1+\widetilde{\Lambda}_3)\,\big(\eta^2(\mathcal{T}) + \mu^2(\mathcal{T})\big).$$

The square root of this estimate plus standard estimates conclude the proof with the generic constant

$$\Lambda_7 := \sqrt{2(1+C_{\mathrm{eff}})C_{\mathrm{mms}}(5)c_1(\alpha)(1+\widetilde{\Lambda}_3)}.$$ □

5 Numerical experiments

The following three sections present numerical experiments with a MATLAB/Octave implementation of the lowest-order LSFEM from (3.18). Since the typical benchmark problems in fluid and solid mechanics solely involve constant volume forces $f \in P_0(\Omega;\mathbb{R}^3)$, the data approximation error $\|f - \Pi_0 f\|_{L^2(\Omega)}$ does not appear. Accordingly, the code is restricted to a collective marking strategy (Case A in ALSFEM). The implementation is based on the in-house software package AFEM [43]. However, it is completely rewritten to improve the performance and to facilitate the generalisation to various choices of the operators $\mathcal{A}$ and $\mathcal{S}$ in the model problem (3.3). The usage and implementation is presented in detail in the Appendix A. If not stated otherwise, the adaptive computations are driven by the alternative a posteriori error estimator η with a bulk parameter of $\theta = 0.3$.

Due to the large number of simplices in the adaptively refined meshes, their plots solely present the triangulation of the surface $\mathcal{F}(\partial\Omega)$. In every convergence history plot, the results for uniform refinement are displayed with dashed lines and grey markers and for adaptive refinement with solid lines and colourful markers. Every error or estimator term has a unique colour and marker as depicted in Figure 5.1.

The regularity of the exact solution σ and u to (3.3) in the notion of Besov spaces as well as the polynomial degree of the approximation determine the optimal convergence rate s in Theorem 1.1. For a detailed discussion of this rate, the reader is referred to [14, Section 9] and [48, Section 5.1] and the references therein. For the lowest-order discretisation in 3D, the expected optimal convergence rate is 1/3.

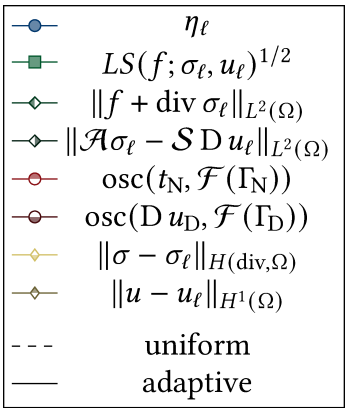

Figure 5.1: Overview of the involved error and estimator terms.

5.1 Poisson model problem

This section presents numerical experiments for two benchmark problems of the scalar-valued version of the model problem (3.3) with $\mathcal{A} = \mathcal{S} = \mathrm{id}$.

5.1.1 Fichera cube

The Fichera cube [63] is given by $\Omega = (-1,1)^3 \setminus [0,1]^3$. Let $f \equiv 1$ be constant and suppose homogeneous Dirichlet boundary conditions $u_D \equiv 0 \in H^1(\Gamma_D)$ on the full boundary $\Gamma_D := \partial\Omega$. Consequently, no data approximation terms appear in this example.

The adaptive algorithm creates meshes with the expected increased refinement along the reentrant edges as depicted in Figure 5.2a. The convergence history plot in Figure 5.3a reveals the optimal convergence rate of $1/3$ for the alternative estimator η_ℓ as well as for the built-in estimator $LS(f;\sigma_\ell,u_\ell)^{1/2}$. Due to the reduced Sobolev regularity of the exact solution on this non-convex domain, the computation with uniform refinement attains a slightly suboptimal rate of about 0.28. The comparison of the estimator contributions in Figure 5.3a confirms the higher order of convergence of the equilibrium residual $\|\Pi_0 f + \operatorname{div}\sigma_\ell\|_{L^2(\Omega)}$ from [45, Theorem 3.1], for the mesh-size $h_\ell := h_{\mathcal{T}_\ell}$,

$$\|\Pi_0 f + \operatorname{div}\sigma_\ell\|_{L^2(\Omega)} \le C_{\mathrm{hoc}}\,\|h_\ell\|^s_{L^\infty(\Omega)}\|\sigma_\ell - \nabla u_\ell\|_{L^2(\Omega)}. \tag{5.1}$$

Even in the case of adaptive mesh-refinement, where the maximal mesh-size does not necessarily converge $\|h_\ell\|^s_{L^\infty(\Omega)} \to 0$ as $\ell \to \infty$, the residual $\|\Pi_0 f + \operatorname{div}\sigma_\ell\|_{L^2(\Omega)}$ is of higher order.

5.1.2 Two bricks domain

This section considers a domain consisting of two bricks laying on top of each other

$$\Omega := \big((-1,0)\times(-1,1)\times(-1,0)\big) \cup \big((-1,0)\times(0,1)\times 0\big) \cup \big((-1,1)\times(0,1)\times(0,1)\big)$$

with Dirichlet boundary $\Gamma_D := \partial\Omega$. Let $f \equiv 1$ and $u_D \equiv 0$ be constant. The domain Ω is no Lipschitz domain in the sense of Assumption 1 in Section 2.3 because the boundary around the origin $(0,0,0)^\top$ does not allow for a representation as a graph [82, Figure 2 (iii) on page 91]. However, it belongs to the class of weakly Lipschitz domains [78, Section 2 and Theorem 4.1]. Thus, the analysis in this thesis does not apply to Ω.

Nonetheless, the convergence plot in Figure 5.5 indicates the optimal convergence rate of $1/3$ from about 3 000 degrees of freedom. Similar to the benchmark from the previous Section 5.1.1, uniform refinement results in a slightly suboptimal convergence rate. Also, the adaptive refinement focuses on the two reentrant edges as depicted in Figure 5.4.

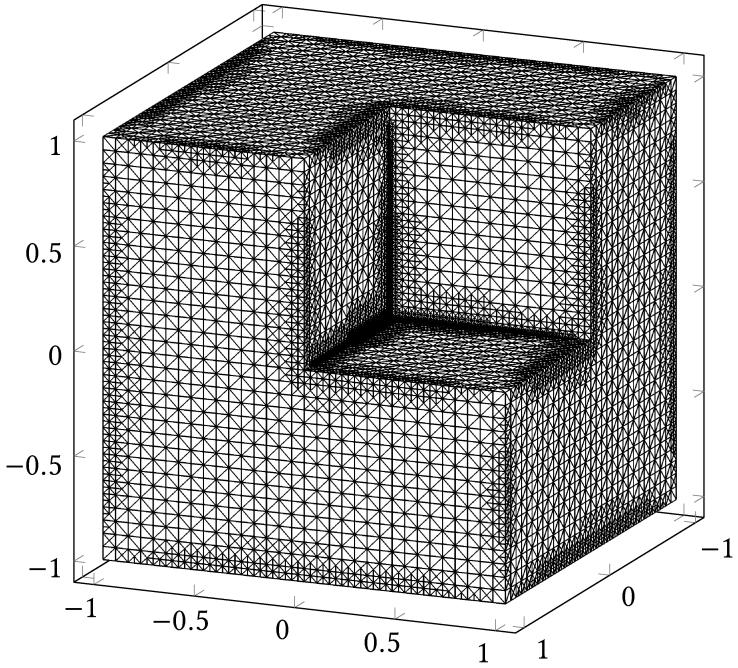

(a) Triangulation $\mathcal{T}_\ell$

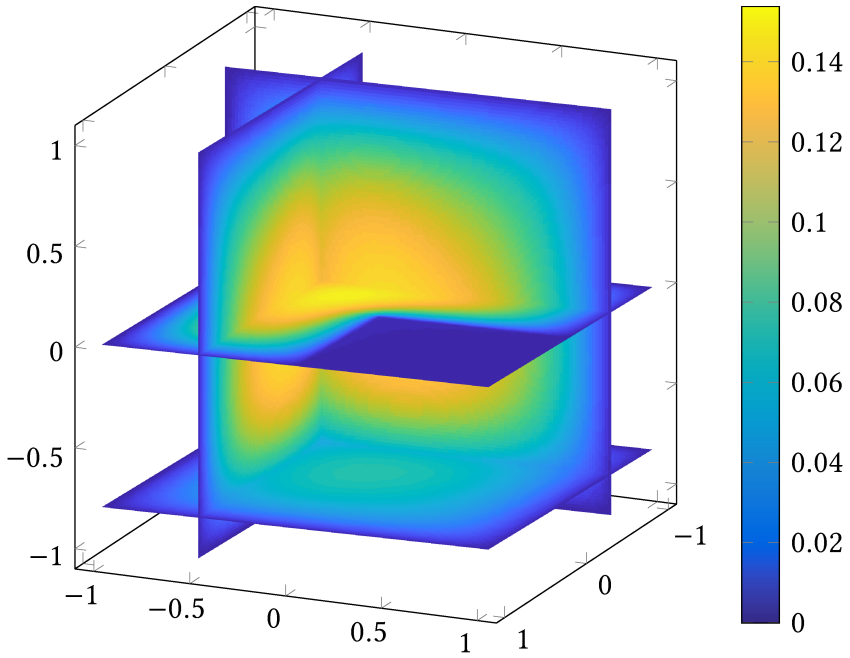

(b) Solution u_ℓ

Figure 5.2: Adaptively refined mesh $\mathcal{T}_\ell$ in (a) for $\ell = 33$ of the Fichera cube from Subsection 5.1.1 composed of 479 940 simplices and the corresponding solution u_ℓ in (b). The colour represents the value of the solution u_ℓ along the given slices.

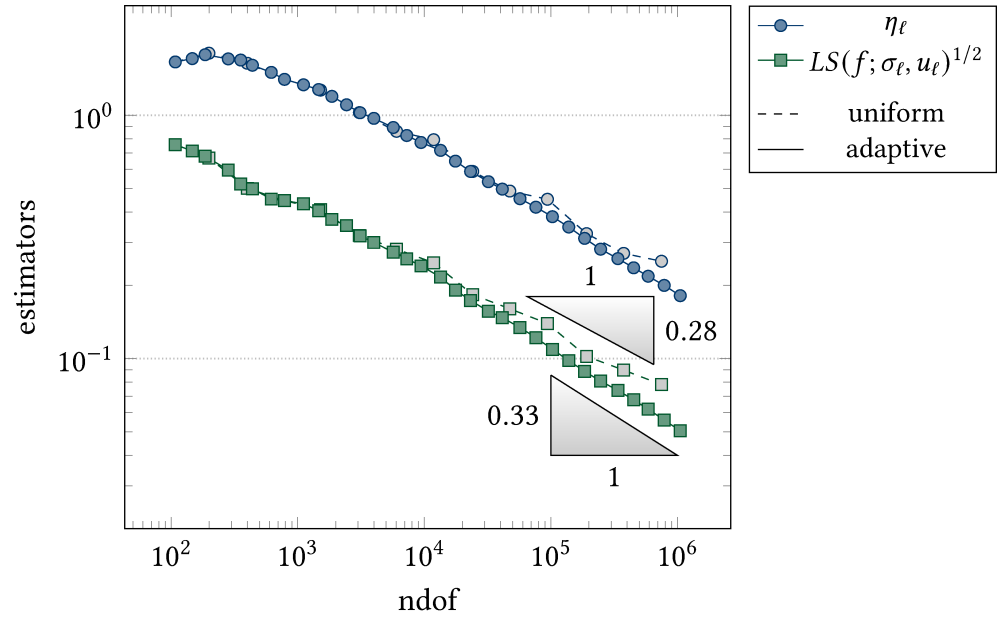

(a) Comparison of uniform and adaptive refinement

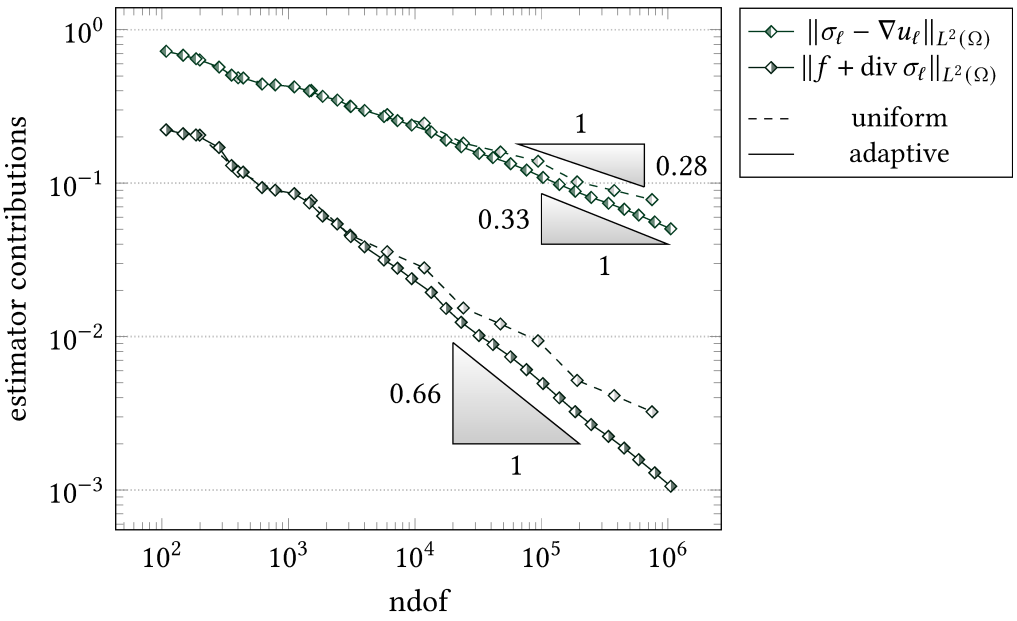

(b) Comparison of contributions to the least-squares functional

Figure 5.3: Convergence history plots for the Fichera cube benchmark of the Poisson model problem from Subsection 5.1.1.

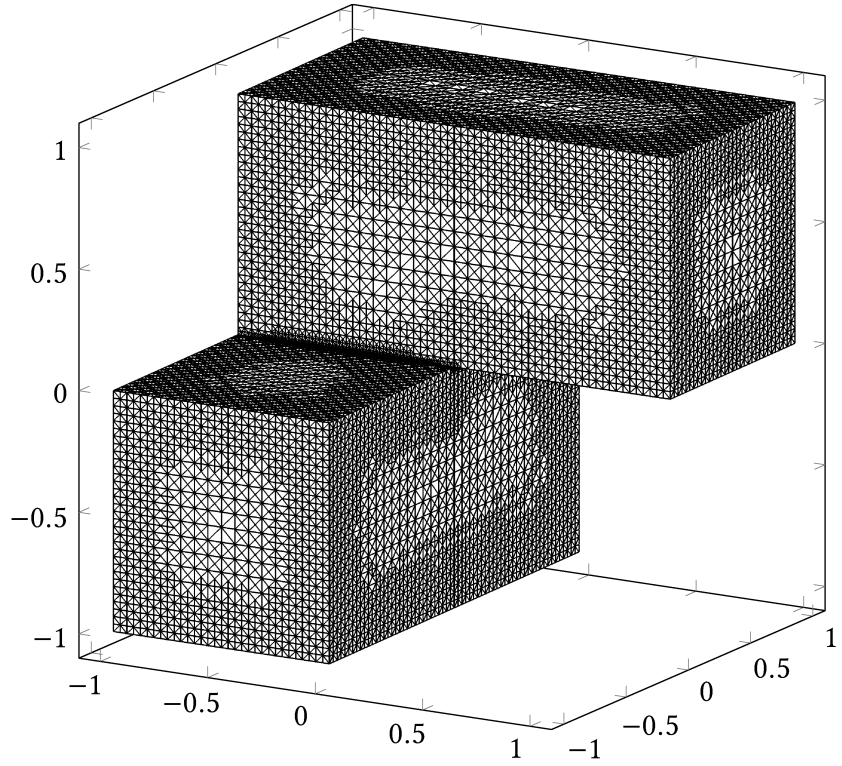

Figure 5.4: Adaptively refined mesh $\mathcal{T}_\ell$ for $\ell = 35$ of the two bricks domain from Subsection 5.1.2 composed of 569 736 simplices.

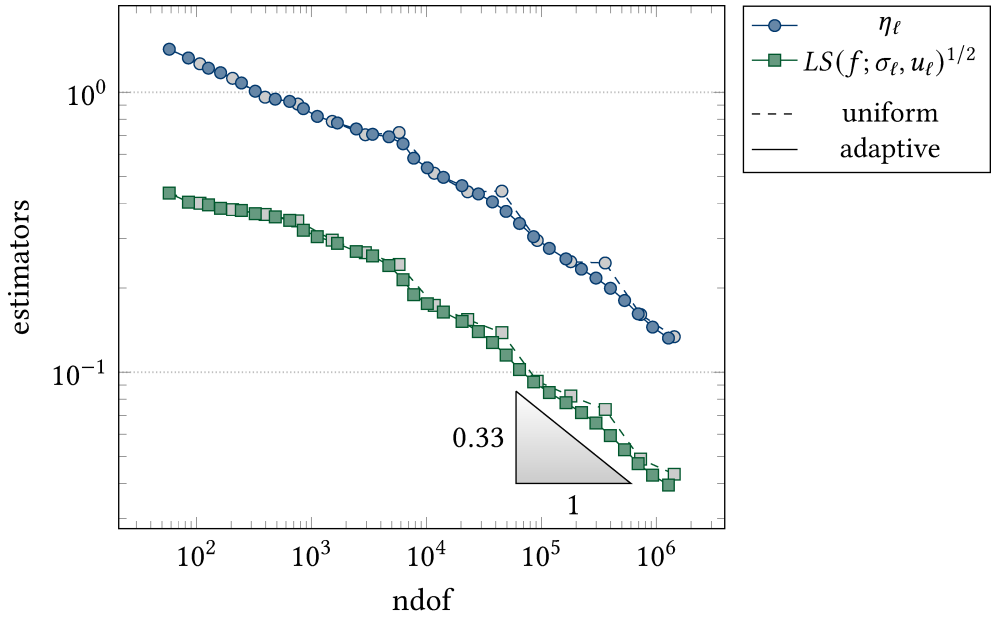

Figure 5.5: Convergence history plot for the two bricks benchmark of the Poisson model problem from Subsection 5.1.2.

5.2 Stokes problem

This section investigates the laminar flow of a Newtonian fluid modelled by the Stokes equations.

5.2.1 Hagen-Poiseuille flow

This subsection considers the flow in the unit cube $\Omega := (0,1)^3$. For vanishing right-hand side $f \equiv 0$, the exact solution $u \in P_2(\Omega;\mathbb{R}^3)$ and $p \in P_1(\Omega)$ reads

$$u(x) = (4x_2(x_2-1),0,0)^\top \quad \text{and} \quad p(x) = 8x_1 - 4$$

and prescribes the inhomogeneous Dirichlet boundary conditions.

Figure 5.6a displays the convergence history plot for the adaptive and uniform mesh-refinement. Due to the smooth solution u, both refinement schemes lead to the optimal rate of $1/3$ from the very beginning of the computation at about 200 degrees of freedom. The first four levels do not sufficiently resolve the boundary data and the residual terms in the alternative estimator η as well as the least-squares functional LS exhibit some pre-asymptotic behaviour. Due to the inhomogeneous boundary conditions, the discrete spaces $U^{k+1}(\mathcal{T})$ are not nested and the least-squares functional is not necessarily monotonically decreasing. The Dirichlet data approximation term $\operatorname{osc}(\mathrm{D}\, u_\mathrm{D}, \mathcal{F}(\Gamma_\mathrm{D}))$ is of higher order. The known exact solution allows for a comparison of the estimators and the errors. Figure 5.6b confirms their theoretically proven equivalence from the Theorems 3.16, 3.18, and Corollary 4.4.

5.2.2 Backward facing step

This standard example describes the flow in a pipe with bottleneck. The right-hand side $f \equiv 0$ vanishes on the domain

$$\Omega := \big((-1,1)\times(-2,8)\times(-1,1)\big) \setminus \big([-1,1]\times[-2,0]\times[-1,0]\big).$$

The inhomogeneous Dirichlet boundary data are prescribed by

$$u_\mathrm{D}(x) := \begin{cases} (0, 1/10\,(x_1+1)(x_1-1)x_3(x_3-1),0)^\top & \text{if } x_2 = -2, \\ (0, 1/80\,(x_1+1)(x_1-1)(x_3+1)(x_3-1),0)^\top & \text{if } x_2 = 8, \\ 0 & \text{otherwise.} \end{cases}$$

The polynomial in- and outflow are scaled such that the compatibility condition

$$\int_{\partial\Omega} u_\mathrm{D}\cdot\nu \,\mathrm{d}a = 0$$

following from the side condition $\operatorname{div} u = 0$ is satisfied. In order to sufficiently resolve the boundary data on the initial triangulation, three uniform refinements are carried out before the start of the adaptive algorithm.

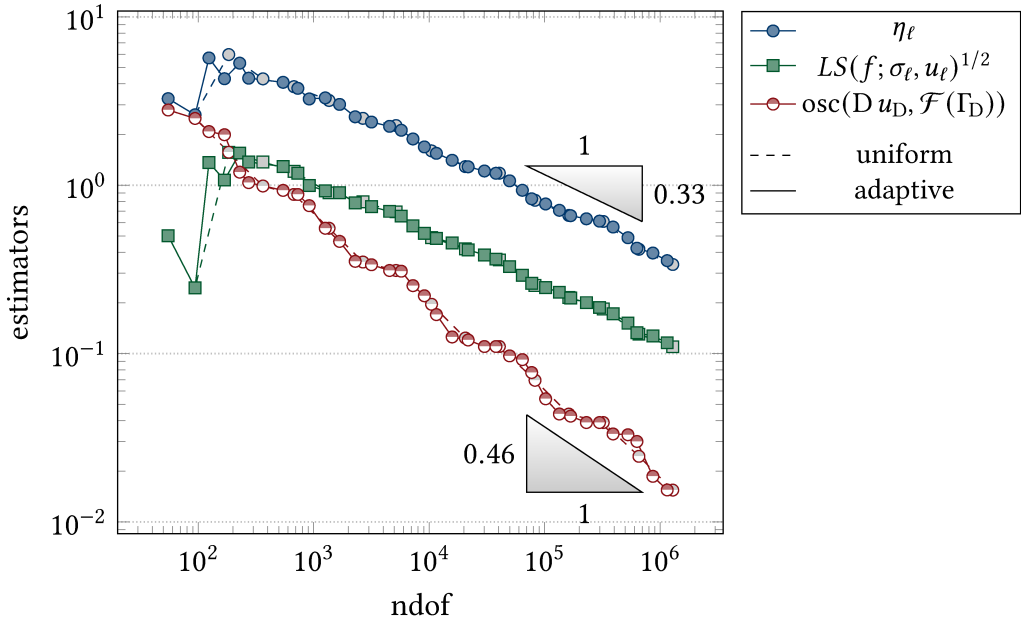

(a) Comparison of uniform and adaptive refinement

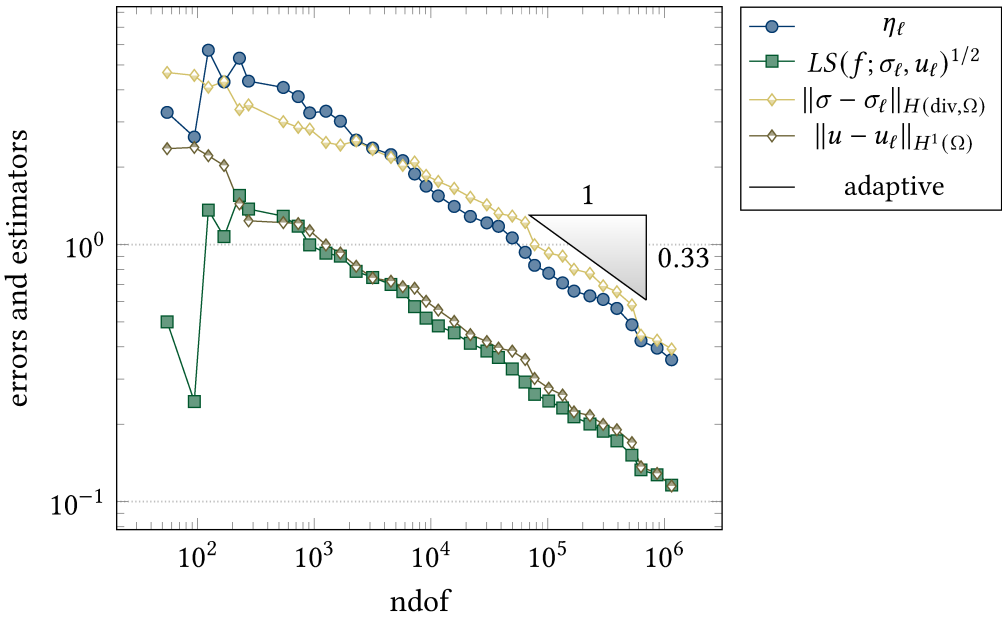

(b) Comparison of exact errors and error estimators

Figure 5.6: Convergence history plot for the Hagen-Poiseuille benchmark of the Stokes equations from Subsection 5.2.1.

Contrasting the expected behaviour, the convergence plot in Figure 5.7a does not confirm optimal convergence rates. Since the alternative and the built-in error estimators exhibit a slightly different rate of convergence, it is reasonable to suspect this to be some pre-asymptotic behaviour. Indeed, the triangulation plot in Figure 5.8a shows that the refinement solely focuses on the boundary parts with inhomogeneous data at $x_2 = 2$ and $x_2 = 8$ and almost no refinement happens for $x \in \Omega$ with $1 < x_2 < 4$. This part of the triangulation is to coarse to sufficiently resolve the solution. In particular, the singularity along the reentrant edge has not been detected even on the finest level of the computation. This prevents the observation of an asymptotic behaviour even for relatively small bulk parameters $\theta \ll 1$ in Figure 5.7b.

5.3 Linear elasticity problem

This section presents two benchmark problems for the linear elasticity problem. If not stated otherwise, the implementation employs the Young's modulus $E = 200$ and the Poisson ratio $\nu = 0.25$ to provide the Lamé parameters according to

$$\mu := \frac{E}{2(1+\nu)} \quad \text{and} \quad \lambda := \frac{E\nu}{(1+\nu)(1-2\nu)} \quad \text{for } 0 < E,\ 0 < \nu < 0.5.$$

The following sections include plots of the deformed domain $(\mathrm{id} + \alpha u_\ell)(\Omega)$ for some scaling factor $\alpha > 0$. Due to the small values of the displacement u_ℓ, a scaling factor $10 < \alpha < 100$ is employed.

5.3.1 Uniaxial tension test

This benchmark is modelled on a standard experiment from material science for the determination of isotropic material parameters. Therefore, a rod or flat block is clamped into a universal testing machine and a tension force in one direction applies to it. By symmetry, it suffices to consider the lower half of the specimen.

For the numerical simulation, let $\Omega := (0,1)^3$ denote the unit cube with the Dirichlet boundary $\Gamma_\mathrm{D} = [0,1]^2 \times 0$ at the bottom and the remaining Neumann boundary $\Gamma_\mathrm{N} := \partial\Omega \setminus \Gamma_\mathrm{D}$. At the Dirichlet boundary, the specimen is clamped such that $u_\mathrm{D} \equiv 0$. A constant force t_N applies to the top

$$t_\mathrm{N}(x) := \begin{cases} (0,0,1) & \text{if } x_3 = 1, \\ 0 & \text{else.} \end{cases}$$

Along the interface Γ_I between the Dirichlet boundary Γ_D and the Neumann boundary Γ_N, the unknown exact solution u is less regular. This causes the adaptive algorithm to generate meshes with increased refinement along Γ_I as depicted in Figure 5.9. Figure 5.10 approves that the resulting convergence rate of the adaptive scheme is optimal. However, uniform refinement leads to a suboptimal rate of about 0.2.

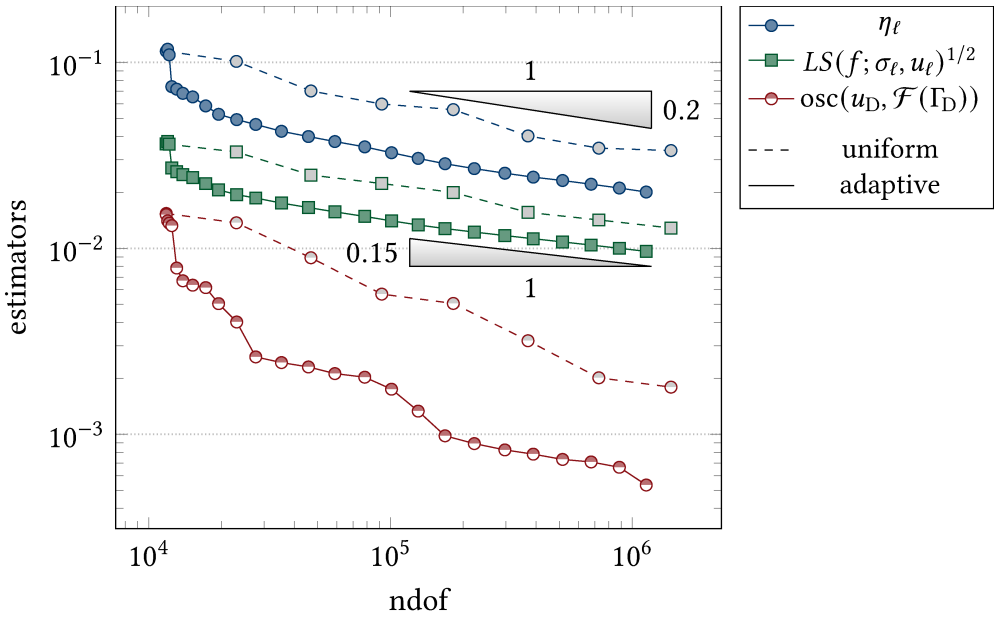

(a) Comparison of uniform and adaptive refinement

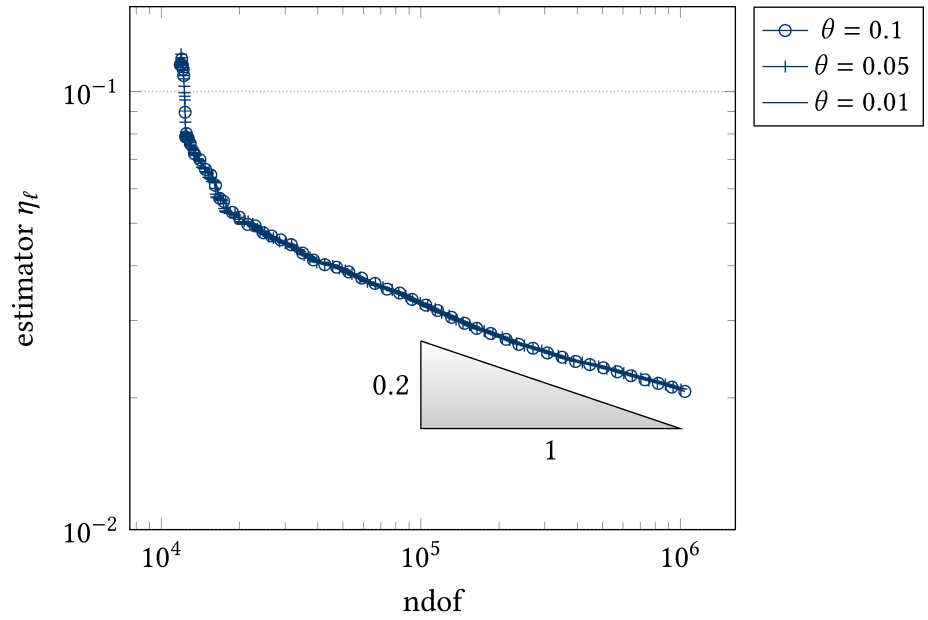

(b) Comparison of small bulk parameters $\theta \ll 0$

Figure 5.7: Convergence history plots for the backward facing step benchmark of the Stokes equations from Subsection 5.2.2.

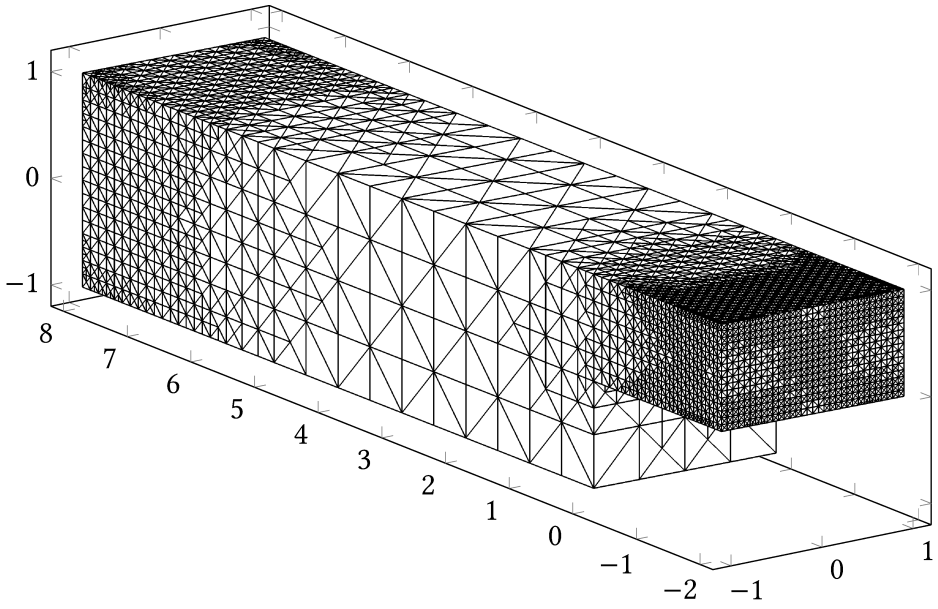

(a) Triangulation $\mathcal{T}_\ell$

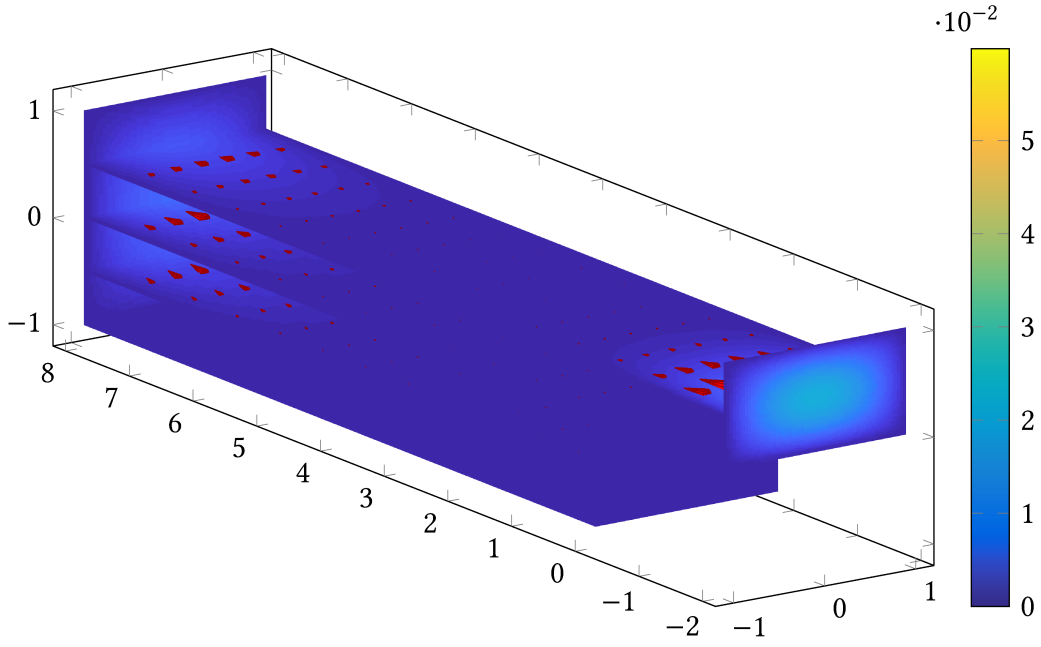

(b) Solution u_ℓ

Figure 5.8: Adaptively refined mesh $\mathcal{T}_\ell$ (a) for $\ell = 25$ of the backward facing step domain from Subsection 5.2.2 composed of 173 036 simplices and the corresponding solution u_ℓ (b). The color indicates the length of the velocity vector field $|u_\ell|$.

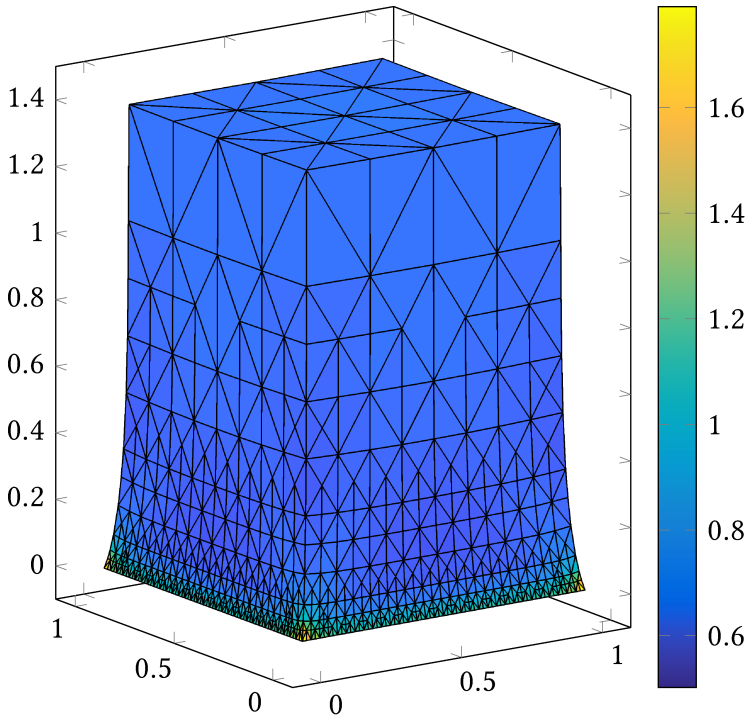

Figure 5.9: Deformation of the adaptively refined mesh $\mathcal{T}_\ell$ for $\ell = 25$ from the uniaxial tension test from Subsection 5.3.1 composed of 20 976 simplices. The deformation is scaled by the factor $\alpha = 80$. The colour indicates the piecewise constant approximation of the von Mises stress $|\operatorname{dev} \sigma_\ell|$.

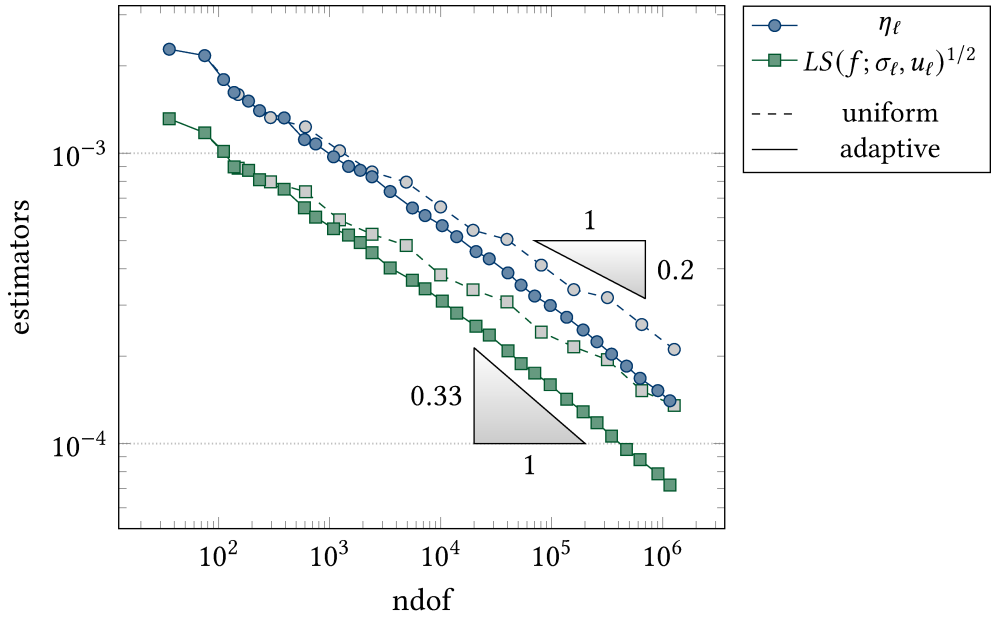

Figure 5.10: Convergence history plot for the uniaxial tension benchmark of the linear elasticity problem from Subsection 5.3.1.

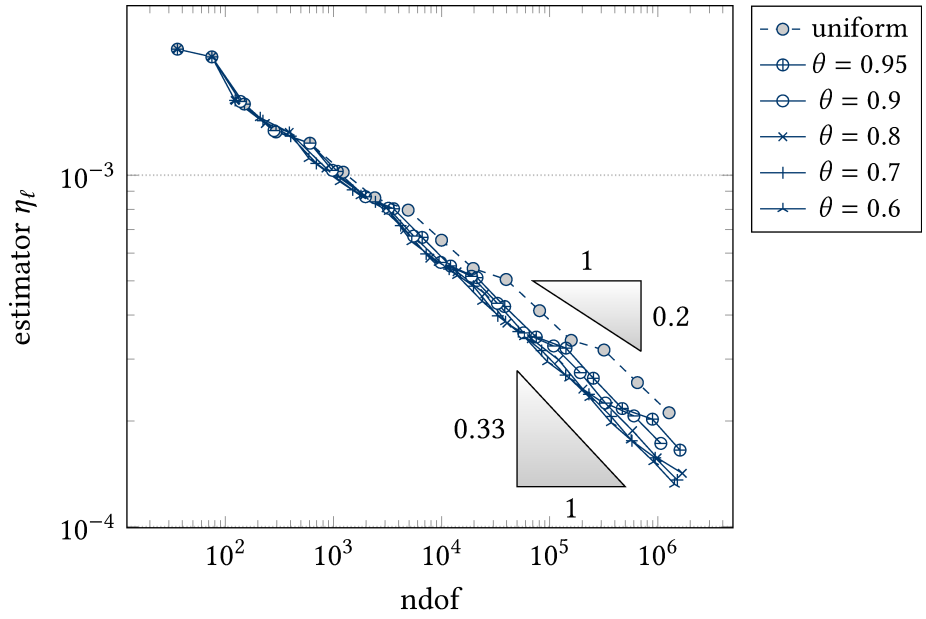

Figure 5.11: Comparison of the values of the alternative a posteriori error estimator η_ℓ for various choices of the bulk parameter θ in the uniaxial tension benchmark for the linear elasticity problem from Subsection 5.3.1.

A theoretical analysis of the upper bound θ_0 of the bulk parameter in Theorem 1.1 in [42, Section 6] establishes $\theta_0 \geq 2.6 \times 10^{-6}$ in the case of the Courant FEM for the 2D Poisson model problem with an underlying triangulation into right isosceles triangles. In practice, moderate choices of $0.3 \leq \theta \leq 0.5$ usually lead to optimal rates while avoiding too many solution steps. Indeed, a closer investigation of the influence of the bulk parameter θ for the ALSFEM algorithm shows that the optimal rate of $1/3$ is already attained for about $\theta \leq 0.8$ in Figure 5.11.

For the modelling of (nearly) incompressible material, the Poisson ratio ν tends to 0.5 and, correspondingly, the Lamé parameter λ tends to ∞. Due to the λ independence of the generic constants in Lemma 3.4, the LSFEM is robust with respect to large λ [34]. Figure 5.12 confirms this robustness.

Given some right-hand side $f \in L^2(\Omega)$, let $\widetilde{\sigma}_f$ and $\widetilde{u}_f$ solve the model problem with Neumann boundary data $\Pi_0 t_{\mathrm{N}}$ replacing t_{N} and vanishing Dirichlet boundary data $u_{\mathrm{D}} \equiv 0$. Define the quantities

$$
\begin{aligned}
e_1(\mathcal{T}, f) &:= \inf \left\{ \|\mathbb{C}^{-1}(\widetilde{\sigma}_f - \tau_{\mathrm{RT}})\|_{L^2(\Omega)} \ : \ \tau_{\mathrm{RT}} \in \Sigma^0(\mathcal{T}) \text{ with } \Pi_0 f + \operatorname{div} \tau_{\mathrm{RT}} = 0 \right\}, \\
e_2(\mathcal{T}, f) &:= \inf \left\{ |\varepsilon(\widetilde{u}_f - v_{\mathrm{C}})\|_{L^2(\Omega)} \ : \ v_{\mathrm{C}} \in U^1(\mathcal{T}) \right\}, \\
\bar{e}_m &:= \sup \left\{ e_m(\mathcal{T}, f) \ : \ f \in L^2(\Omega; \mathbb{R}^3) \text{ with } \|f\|_{L^2(\Omega)} = 1 \right\} \text{ for } m = 1, 2.
\end{aligned}
$$

Employing the analysis from [22], the higher-order convergence of the equilibrium residual similar to (5.1) can be established in the context of linear elasticity [27, The-

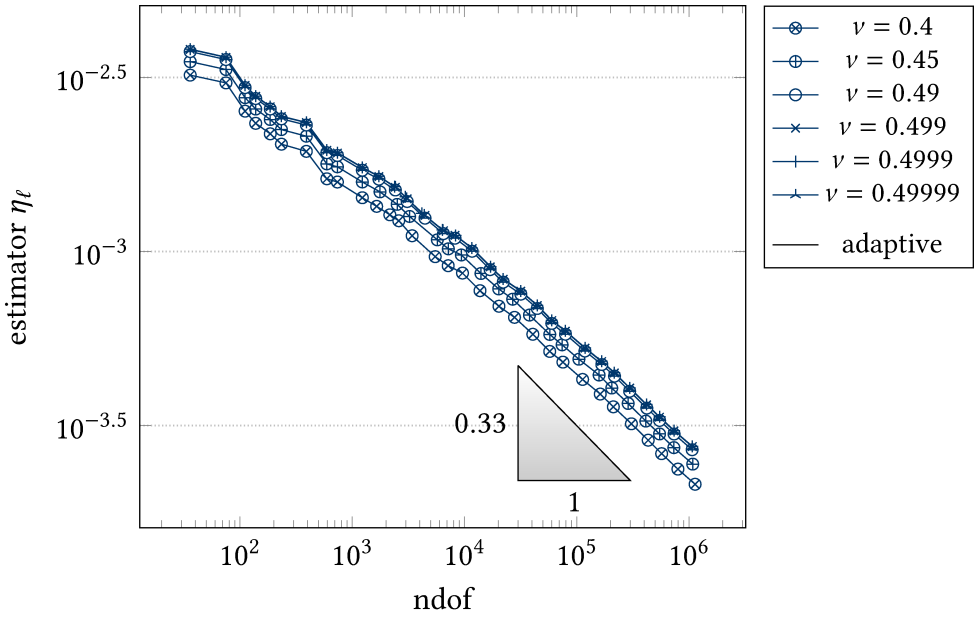

Figure 5.12: Comparison of the values of the alternative a posteriori error estimator η_ℓ for various choices of the Poisson ratio ν in the uniaxial tension benchmark for the linear elasticity problem from Subsection 5.3.1.

orem 3.3]

$$\|\Pi_0 f + \operatorname{div} \sigma_{\mathrm{LS}}\|_{L^2(\Omega)} \leq \widetilde{C}_{\mathrm{hoc}} \left(\bar{e}_1(\mathcal{T}) + \bar{e}_2(\mathcal{T})\right) LS(f; \sigma_{\mathrm{LS}}, u_{\mathrm{LS}})^{1/2}.$$

Undisplayed numerical experiments confirm this higher-order convergence in the case of uniform and adaptive mesh-refinement.

5.3.2 Cook membrane

Let $f \equiv 0 \in L^2(\Omega; \mathbb{R}^3)$ on the Cook's membrane [53]

$$\Omega := \left\{x \in \mathbb{R}^3 \ : \ (x_1, x_2) \in \operatorname{conv}\{(0,0), (48,44), (48,60), (0,44)\} \text{ and } x_3 \in [0,10]\right\}.$$

Its boundary $\partial\Omega$ is split into the Dirichlet part $\Gamma_{\mathrm{D}} := \{0\} \times [0,44] \times [0,10]$ with homogeneous boundary data $u_{\mathrm{D}} \equiv 0$ and the remaining Neumann part $\Gamma_{\mathrm{N}} := \partial\Omega \setminus \Gamma_{\mathrm{D}}$ with constant vertical shear load on the right-hand side $x_1 = 48$

$$t_{\mathrm{N}}(x) := \begin{cases} (0,0,1)^\top & \text{if } x \in \{48\} \times [44,60] \times [0,10], \\ 0 & \text{else.} \end{cases}$$

Six uniform refinements of the initial mesh are carried out before the adaptive algorithm.

The convergence history plot in Figure 5.14 exhibits suboptimal behaviour of the estimators for the whole computation from 300 to 10^6 degrees of freedom. The value of

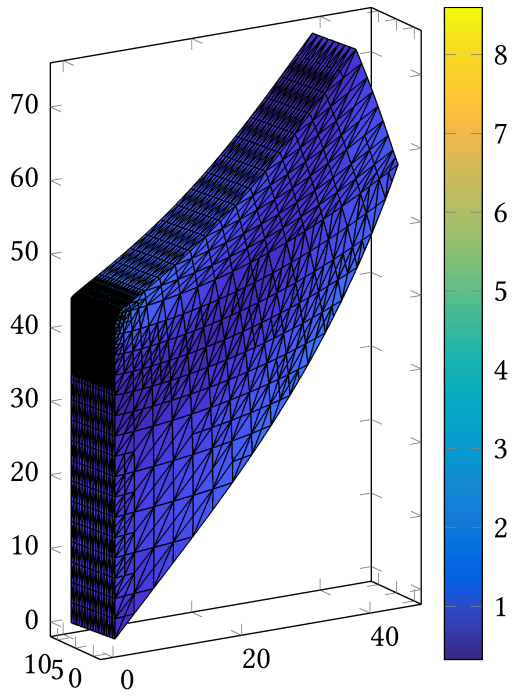

Figure 5.13: Deformation plot of the Cook membrane from Subsection 5.3.2 composed of 74 474 simplices ($\ell = 21$). The deformation is scaled by the factor $\alpha = 10$. The colour indicates the piecewise constant approximation of the von Mises stress $|\operatorname{dev} \sigma_\ell|$.

the alternative estimator η_ℓ increases until 10^5 degrees of freedom and, subsequently, improves up to a rate of convergence of about 0.2 on the finest level of the computation. Due to the exact approximation of the piecewise constant boundary conditions, the discrete spaces $\Sigma^k(\mathcal{T})$ and $U^{k+1}(\mathcal{T})$ are nested. Accordingly, the least-squares functional decreases monotonically. The convergence rate of about 0.25 from about 2×10^5 degrees of freedom remains suboptimal. Undisplayed numerical experiments with the bulk parameters $\theta = 0.1, 0.05, 0.01$ lead to the same rate for the alternative and the built-in estimator.

This pre-asymptotic behaviour indicates an insufficient resolution of the boundary singularity. Figure 5.13 presents the triangulation and the deformation at the beginning of the reduction of the estimator at about 4×10^5 degrees of freedom (marked by a red circle in Figure 5.14). It reveals a slightly increased refinement along the interface Γ_I between Γ_D and Γ_N. However, most of the (boundary) simplices are of equal size. On the finest level of the computation, the triangulation remains to coarse to optimally resolve the singularity.

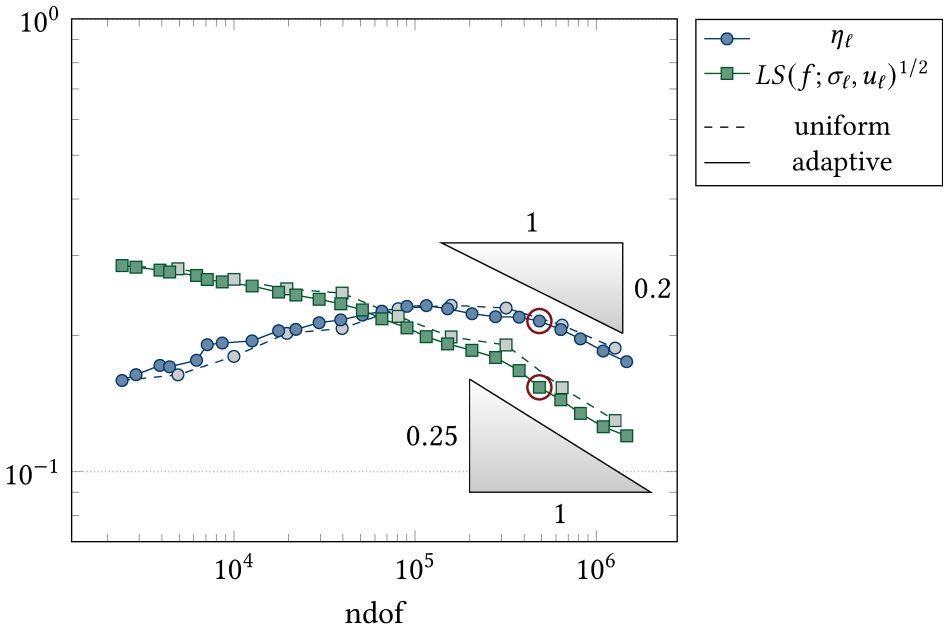

Figure 5.14: Convergence history plot for the Cook membrane benchmark of the linear elasticity problem from Subsection 5.3.2. The red circle marks the computation on the triangulation from Figure 5.13.

6 Conclusion and outlook

This thesis established the convergence of an adaptive LSFEM for three model problems with optimal rates. Therefore, an alternative a posteriori error estimator has been presented and employed in an adaptive refinement algorithm with a separate marking strategy. The proof adheres to the axiomatic framework from [37, 40] and employs techniques for the analysis of inhomogeneous Dirichlet boundary conditions in 3D from [4]. Recent results on quasi-interpolation operators preserving partial homogeneous boundary conditions [93, 77] and a discrete regular decomposition for arbitrary polynomial degree [70] laid the foundations for a local and stable quasi-interpolation operator Q_{Ned} for Nédélec functions in Theorem 2.14. Following [106], this operator may enable the proof of optimal convergence rates of adaptive algorithms for Nédélec finite element discretisations with mixed boundary conditions.

The reliability and the efficiency of the alternative estimator η from Corollary 4.4 and Theorem 3.18 provide optimal rate approximation in terms of the least-squares functional reading

$$\begin{aligned}
&\sup_{\ell\in\mathbb{N}} \big(|\mathcal{T}_\ell| - |\mathcal{T}_0| + 1\big)^s \big(LS(f;\sigma_\ell,u_\ell) + \operatorname{osc}^2(\mathrm{D}\, u_{\mathrm{D}}, \mathcal{F}_\ell(\Gamma_{\mathrm{D}})) + \operatorname{osc}^2(t_{\mathrm{N}}, \mathcal{F}_\ell(\Gamma_{\mathrm{N}}))\big)^{1/2} \\
&\quad \le C_{\mathrm{opt2}} \sup_{N\in\mathbb{N}} (N+1)^s \min_{\mathcal{T}\in\mathbb{T}(N)} \min_{(\tau_{\mathrm{LS}},v_{\mathrm{LS}})\in\Sigma^k(\mathcal{T})\times U^{k+1}(\mathcal{T})} \\
&\qquad \big(LS(f;\tau_{\mathrm{LS}},v_{\mathrm{LS}}) + \operatorname{osc}^2(\mathrm{D}\, u_{\mathrm{D}}, \mathcal{F}(\Gamma_{\mathrm{D}})) + \operatorname{osc}^2(t_{\mathrm{N}}, \mathcal{F}(\Gamma_{\mathrm{N}}))\big)^{1/2}.
\end{aligned}$$

Additionally, the a posteriori estimates for the least-squares functional from Theorem 3.16 lead to the analogous result in terms of the errors in

$$\begin{aligned}
&\sup_{\ell\in\mathbb{N}} \big(|\mathcal{T}_\ell| - |\mathcal{T}_0| + 1\big)^s \big(\|\sigma-\sigma_\ell\|^2_{L^2(\Omega)} + \|\mathcal{S}\,\mathrm{D}(u-u_\ell)\|^2_{L^2(\Omega)} + \operatorname{osc}^2(\mathrm{D}\, u_{\mathrm{D}}, \mathcal{F}_\ell(\Gamma_{\mathrm{D}})) \\
&\qquad\qquad + \operatorname{osc}^2(t_{\mathrm{N}}, \mathcal{F}_\ell(\Gamma_{\mathrm{N}}))\big)^{1/2} \\
&\quad \le C_{\mathrm{opt3}} \sup_{N\in\mathbb{N}} (N+1)^s \min_{\mathcal{T}\in\mathbb{T}(N)} \min_{(\tau_{\mathrm{RT}},v_{\mathrm{C}})\in\Sigma^k(\mathcal{T})\times U^{k+1}(\mathcal{T})} \\
&\qquad \big(\|\sigma-\tau_{\mathrm{RT}}\|^2_{L^2(\Omega)} + \|\mathcal{S}\,\mathrm{D}(u-v_{\mathrm{C}})\|^2_{L^2(\Omega)} + \operatorname{osc}^2(\mathrm{D}\, u_{\mathrm{D}}, \mathcal{F}(\Gamma_{\mathrm{D}})) + \operatorname{osc}^2(t_{\mathrm{N}}, \mathcal{F}(\Gamma_{\mathrm{N}}))\big)^{1/2}.
\end{aligned}$$

Several numerical experiments confirm the optimal convergence rates in terms of the alternative a posteriori error estimator, of the least-squares functional, and the errors. A benchmark with known exact solution validates the implementation and underlines the equivalence of the error estimators and the exact errors. For the benchmarks where the uniform refinement converges suboptimally, the adaptive algorithm leads to the

optimal rate of convergence. Two benchmarks suffered from a large pre-asymptotic regime.

Further research on the convergence analysis with rates may consider adaptive algorithms based on any of the numerous least-squares formulations including, but not restricted to, the examples given in Section 3.2. Beyond that, some least-squares approaches impose the boundary conditions in a weak sense [21] or minimise the least-squares functional under side conditions, for instance, to enforce local mass conservation [50]. Likewise, the convergence of adaptive LSFEMs for nonlinear problems such as in [97] is an open question. Fairly general assumptions on the operators $\mathcal{A}$ and $\mathcal{S}$ in the model problem (3.3) in Section 3.1 allow for a well-posed least-squares formulation even in the nonlinear case. Although, the convergence analysis in the remaining parts of the thesis essentially relied on the linearity of $\mathcal{A}$ and $\mathcal{S}$, this may provide a starting point for further research on nonlinear LSFEMs.

The novel discontinuous Petrov-Galerkin (dPG) method [55, 56, 108, 57, 36] has been described as a weighted least-squares method [35, 68, 103, 102]. This connection has been exploited to establish optimal convergence rates for the lowest-order dPG method applied to the 2D Poisson model problem [68]. The techniques presented in this thesis may provide additional tools to treat higher polynomial degrees in three spatial dimensions as well.

In spite of the presence of a built-in error estimator, the least-squares methods as well as the dPG methods require an adaptive mesh-refinement by some alternative estimator in the proof of optimal convergence rates. A further development of the axiomatic framework to apply for estimators without any prefactors in terms of the mesh-size may be a challenging but rewarding goal for future research.

A The octAFEM3D software package

The MATLAB/Octave software package `octAFEM3D` is based on the unpublished in-house software package AFEM [43]. However, it is completely rewritten to improve the performance of the code and to enable a straightforward generalisation to model problems of the form (3.3). In particular, the adaptive mesh-refinement in three dimensions suffered from an inefficient implementation and is replaced by object-oriented approach.

Except for the two classes `Node.m` and `Simplex.m` based on the code from [104], the software is provided under the terms of the GNU General Public License as published by the Free Software Foundation, either version 3 or (at your option) any later version.

Figure A.2 at the end of this chapter lists all included files of the software package.

A.1 Purpose

The software package allows for the solution of the three partial differential equations given by the model problems in three spatial dimensions

- Poisson model problem,
- Stokes equations,
- linear elasticity problem.

The problems are solved using the lowest-order least-squares finite element method (LSFEM) with adaptive mesh-refinement employing a collective marking strategy (Case A in ALSFEM algorithm on page 4).

The adaptive mesh-refinement is realised by an object-oriented implementation of the triangulation of tagged simplices and the three-dimensional NVB following [104]. The approximation of Dirichlet boundary data employs the Scott-Zhang quasi-interpolation operator from Section 3.3 and the L^2 orthogonal projection from Section 3.4 for the Neumann data. The solution of the symmetric and positive definite system matrix utilises MATLAB's highly optimised `mldivide` function (backslash operator).

The software package is developed and tested for MATLAB version 9.6.0.1072779 (R2019a). The included functions generating plots of discrete solutions utilise MATLAB's PDE toolbox. Every other component, most notably the LSFEM solver and the

alternative a posteriori error estimation, are compatible to Octave version 5.1.0 as well. The usage of MATLAB's parallelisation toolbox may provide significant improvements of the performance. The `parfor` loop is utilised for costly integrations on each of the large number of tetrahedrons or faces of the triangulation or for the transformation of the basis functions from the reference domain to all simplices of the triangulation.

A.2 Usage

First of all, initialise the software package with the command

```
poolobj = initAFEM3D(nWorkers)
```

The script adds the current folder to the path recursively and enables logging to a new file in the folder `./logs`. The argument `nWorkers` is optional and starts the parallel computing toolbox with the specified number of workers if called in MATLAB. The parallel pool object is returned for later usage. Octave does not support automatic parallel computing yet. After the initialisation, numerical experiments can be conducted in three steps.

Step 1. Load one of the benchmark problems from the folder `./benchmarks`.

```
B = Poisson_Brick()
```

The benchmark problem can be adjusted by directly modifying the fields of `B`.

```
B.theta = 0.7
B.minNdof = 1e5
```

Section A.3 below presents all available fields.

Step 2. The adaptive algorithm is started by

```
S = AFEMRunLS(B, 'my_experiment')
```

Several information is printed during runtime. The structure array `S` contains the initial information from the benchmark `B` and the output for each level of the adaptive computation such as the coefficients of the discrete solutions and error and estimator values. Section A.4 below presents a complete overview of the included data. The structure array `S` is automatically saved as a `.mat`-file in a subfolder in `./results`. The name of the subfolder consists of the model problem and the name of the benchmark problem. The file name depends on the choice of adaptive or uniform refinement, the break condition by `B.minNdof`, and the identifier `'my_experiment'` specified above.

Step 3. The results of the experiment can be displayed using the command

```
AFEMPlot(S, './results')
```

This generates a figure containing a convergence history plot and an additional plot for runtime in seconds and conditional number of the system matrix. The plot allows for a quick check of the adaptive computation. If called from MATLAB, a triangulation

and a solution plot is created as well. This makes use of MATLAB's PDE toolbox. The generated plot is saved automatically to the folder specified by the second argument.

Additionally, the command

```
AFEMData(S, './results')
```

produces a text file containing a tabulator-separated list of the computed estimator and error values as well as other information such as the runtime and an estimated conditional number of the linear system.

For more information of the usage of each function, use the help function for the main routine

```
help AFEMRunLS
```

or other included functions.

A.3 Benchmark problems

The benchmark problems can be created using the command

```
B = BENCHMARK()
```

where `BENCHMARK` is one of the following functions

- `LinearElasticity_CookMembrane`
- `LinearElasticity_UniaxialTension`
- `Poisson_Brick`
- `Poisson_FicheraCube`
- `Stokes_BackwardFacingStep`
- `Stokes_HagenPouisseuille`

The structure array `B` contains the following fields

- `problem (string)` – name of the model problem
- `name (string)` – name of the benchmark
- `minNdof (int)` – minimal number of degrees of freedom as break condition
- `theta (float)` – bulk parameter for the Dörfler marking
- `refinementIndicator (string)` – one of the strings `'eta'`, `'etaRes'`, `'LS'` specifying the refinement indicator

- `computeCondition (boolean)` – determines whether to estimate the conditional number of the linear system of equations
- `c4n (array)` – coordinates of the nodes of the initial triangulation
- `n4e (array)` – numbers of the nodes of each simplex of the initial triangulation
- `tag4e (array)` – refinement tag of each simplex of the initial triangulation
- `onDirichlet`, `onNeumann (function handles)` – provide boolean values for a list of nodes whether the node belongs to the Dirichlet or Neumann boundary
- `normal (function handle)` – provides the normal vector for arguments `x` on the boundary of the domain
- `lambda`, `mu (float)` – Lamé parameter determining the material in the case of the linear elasticity problem
- `f (function handle)` – right-hand side f
- `degreeF (integer)` – degree specifying the accuracy for the quadrature of the right-hand side f
- `u4Db (function handle)` – Dirichlet boundary data u_{D}
- `degreeU (integer)` – degree specifying the accuracy for the quadrature of the Dirichlet boundary data u_{D}
- `t4Nb (function handle)` – Neumann boundary data t_{N}
- `degreeT (integer)` – degree specifying the accuracy for the quadrature of the Neumann boundary data t_{N}
- `exactKnown (boolean)` – specifies whether an exact solution to this problem is known
- `sigmaExact`, `uExact`, `gradUExact (function handles)` – exact solution and its derivatives (optional)

The benchmarks include the initial triangulation for the following six domains. The information can be created using the command

```
[c4n, n4e, tag4e, onDirichlet, onNeumann, normal] = DOMAIN()
```

where `DOMAIN` is one of the following functions

- `Brick`
- `BackwardFacingStep`

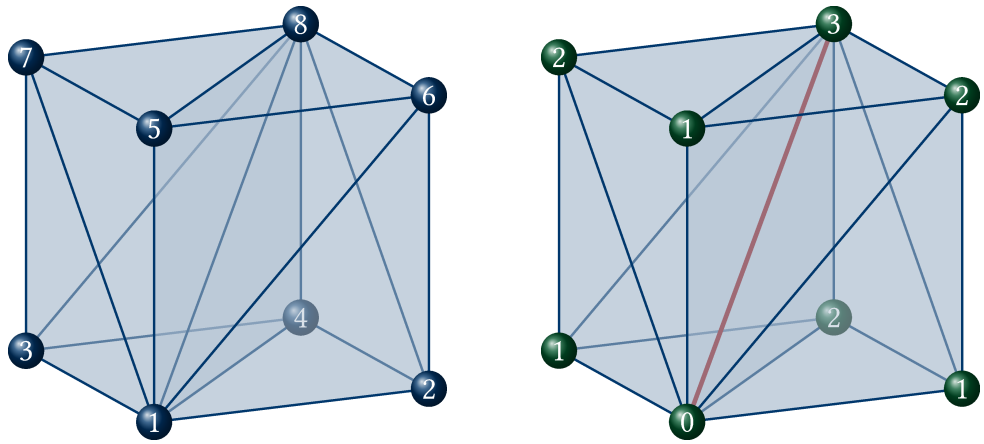

(a) Triangulation with global node numbers **(b)** Triangulation with local node numbers

Figure A.1: Initial triangulation of the unit cube into six simplices of equal volume.

- `CookMembrane`
- `Cube`
- `CubeNb`
- `FicheraCube`

The data structure `c4n` contains an array where each line represents a node of the triangulation. Each row of `n4e` contains a list of four node numbers forming a simplex of the triangulation. The argument `tag4e` is used for the initialisation of the tags of a tagged simplex in the sense of Section 2.4. For the initial triangulation, this usually contains a list of zeros. The function handles `onDirichlet` and `onNeumann` return boolean values determining whether a given node belongs to the respective part of the boundary, for instance,

```
isOnDirichletBoundary = onDirichlet([0 0 0])
```

Figure A.1 and Table A.3 present the initial triangulation of the unit cube with the data structures `c4n` and `n4e`. Any other initial triangulation in this software package is composed of triangulations of cubes with the same triangulation (up to rotations).

A.4 Main routine `AFEMRunLS`

The structure array `S` contains the initial information from `B` and the following additional fields.

- `method (string)` – contains the string `LS` specifying the employed solver

c4n		
0	0	0
1	0	0
0	1	0
1	1	0
0	0	1
1	0	1
0	1	1
1	1	1

n4e			
1	2	4	8
1	3	4	8
1	2	6	8
1	5	6	8
1	3	7	8
1	5	7	8

Table A.1: Data structure for initial triangulation of the unit cube.

- `identifier (string)` – the identifier from the second argument to the function
- `level (cell array)` – list of structure arrays containing the following information for each level of the computation
  - `c4n (array)` – coordinates of the nodes
  - `n4e (array)` – numbers of the nodes of each simplex
  - `tag4e (array)` – refinement tag of each simplex
  - `ndof (integer)` – number of degrees of freedom
  - `condition (float)` – estimated conditional number of the linear system of equations
  - `refinementTime (float)` – elapsed time for the refinement routine (in seconds)
  - `setupTime (float)` – elapsed time for the computation and assembling of the stiffness matrix (in seconds)
  - `solutionTime (float)` – elapsed time for the solution of the linear system of equations (in seconds)
  - `estimatorTime (float)` – elapsed time for the computation of the alternative error estimator η_ℓ (in seconds)
  - `u (array)` – coefficients of the solution u_ℓ
  - `sigma (array)` – coefficients of the solution σ_ℓ
  - `eta (float)` – value of the alternative error estimator η_ℓ

– `etaVol (float)` – volume contribution

$$\eta_{\mathrm{vol},\ell} \coloneqq \Bigg(\sum_{T\in\mathcal{T}_\ell} |T|^{2/3} \big(\| \operatorname{div}(\mathcal{S}^*(\mathcal{A}\sigma_\ell - \mathcal{S}\,\mathrm{D}\,u_\ell))\|^2_{L^2(T)} + \| \operatorname{curl}(\mathcal{A}^*(\mathcal{A}\sigma_\ell - \mathcal{S}\,\mathrm{D}\,u_\ell))\|^2_{L^2(T)} \big) \Bigg)^{1/2}$$

to the alternative error estimator η_ℓ

– `etaJump (float)` – jump contribution

$$\eta_{\mathrm{jump},\ell} \coloneqq \Bigg(\sum_{T\in\mathcal{T}_\ell} |T|^{1/3} \Big(\sum_{F\in\mathcal{F}_\ell(T)\setminus\mathcal{F}_\ell(\Gamma_\mathrm{D})} \|[\mathcal{S}^*(\mathcal{A}\sigma_\ell - \mathcal{S}\,\mathrm{D}\,u_\ell)]_F\ \nu_F\|^2_{L^2(F)} + \sum_{F\in\mathcal{F}_\ell(T)\setminus\mathcal{F}_\ell(\Gamma_\mathrm{N})} \|\nu_F \times [\mathcal{A}^*(\mathcal{A}\sigma_\ell - \mathcal{S}\,\mathrm{D}\,u_\ell)]_F\|^2_{L^2(F)} \Big) \Bigg)^{1/2}$$

to the alternative error estimator η_ℓ

– `oscDb (float)` – value of the Dirichlet data oscillations $\operatorname{osc}(\mathrm{D}\,u_\mathrm{D}, \mathcal{F}(\Gamma_\mathrm{D}))$

– `oscNb (float)` – value of the Neumann data oscillations $\operatorname{osc}(t_\mathrm{N}, \mathcal{F}(\Gamma_\mathrm{N}))$

– `res (float)` – square root of the value of the least-squares functional $LS(f;\sigma_\ell,u_\ell)^{1/2}$

– `resDiv (float)` – contribution $\|f + \operatorname{div}\sigma_\ell\|_{L^2(\Omega)}$ to the least-squares functional $LS(f;\sigma_\ell,u_\ell)^{1/2}$

– `resL2`, `resDev`, `resMat (float)` – contribution $\|\mathcal{A}\sigma_\ell - \mathcal{S}\,\mathrm{D}\,u_\ell\|_{L^2(\Omega)}$ to the least-squares functional $LS(f;\sigma_\ell,u_\ell)^{1/2}$ for one of the three model problems

– `errSigma (float)` – exact error contribution $\|\sigma - \sigma_\ell\|_{H(\mathrm{div},\Omega)}$ (if available)

– `errU (float)` – exact error contribution $\|u - u_\ell\|_{H^1(\Omega)}$ (if available)

A.5 `Triangulation` and `MeshData` classes

The object-oriented representation of triangulations is realised by two main classes. The `Triangulation` class implements the set of `Simplex` and `Node` objects from [104].

Given a list of coordinates `c4n` and a list of node numbers `n4e` specifying the simplices of a triangulation, a new object can be created using

```
T = Triangulation(c4n, n4e, tag4e)
```

The argument `tag4e` is used for the initialisation of the tags of a tagged simplex in the sense of Section 2.4 and usually contains a list of zeros. Any initial triangulation must be reflected in the sense of [104] meaning that, if a node z has the local node number

$k \in \{1, \ldots, 4\}$ in some simplex, z has the same local number k in every other simplex containing z. The domains from Section A.3 take care of this requirement.

For a refinement step with closure execute

```
T.refine(marked)
```

The optional argument `marked` contains a list of numbers of simplices to refine as given by the Dörfler marking with the function call

```
marked = markBulk(eta4e, theta)
```

If the argument `marked` is omitted in `T.refine()`, one step of uniform refinement is carried out. In order to obtain the geometric information, execute

```
c4n = T.c4n
n4e = T.n4e
tag4e = T.tag4e
```

Due to the complicated graph structure of the simplices, the `Triangulation` objects include an explicit destructor function

```
T.delete()
```

These data structures and the function handles from the domain functions in Section A.3 allow for the generation of a `MeshData` object

```
M = MeshData(c4n, n4e, onDirichlet, onNeumann)
```

This object provides any kind of geometric information required in this software package such as `M.n4f` or `M.NbFaces`. For a complete overview of all available data structures, use MATLAB's `doc` function

```
doc MeshData
```

or refer to the documented list of properties within the `MeshData` class.

A.6 Quadrature

The function `Quadrature` provides Gauss points and weights for the numerical quadrature on the 1D, 2D, or 3D reference simplex

```
[GaussPoints, weights] = Quadrature(dim, degree)
```

The argument `dim` specifies the dimension of the reference simplex and `degree` determines that the computed quadrature rule is exact up this partial polynomial degree.

The function includes the local function `computeGaussLegendre` from the AFEM package [43] for the computation of Gauss points on the unit interval. The main function computes the tensor product and transforms the resulting Gauss points from the unit cube to the reference simplex.

The function `integrate` allows for an easy-to-use wrapper for the integration of norms. It computes the sum over every component for vector- or matrix-valued functions and the output is always a vector of the length of the number $|\mathcal{T}|$ of simplices or the number $|\mathcal{F}|$ of faces. The following example shows an example usage to compute the L^2 norm of the scalar-valued discrete $u_C \in S^1(\mathcal{T})$ given by the coefficients `u` on a triangulation $\mathcal{T}$ given by the `MeshData` object `M`.

```
[GP, W] = Quadrature(3, 2)
valU4e = S1Element.evaluate(M, u, GP)
int4e = integrate(valU4e.^2, W, M.vol4e)
normU = sqrt(sum(int4e))
```

In order to compute an approximation of the L^2 norm of $u \in L^2(\Omega)$ given by a function handle `uExact`, proceed as follows.

```
degreeU = 5
[GP, W] = Quadrature(3, degreeU)
valUExact4e = M.evaluateFunction(uExact, GP)
int4e = integrate(valUExact4e.^2, W, M.vol4e)
normU = sqrt(sum(int4e))
```

A.7 Finite element classes

The following three static classes `P0FaceElement`, `RT0Element`, and `S1Element` form the core of this implementation. They provide the following functions for the evaluation of the corresponding finite element basis functions or discrete functions given by the associated coefficients.

```
val4e = RT0Element.evaluateBasis(M, xref, nComp)
div4e = RT0Element.evaluateBasisDivergences(M, xref, nComp)
grads4e = RT0Element.evaluateBasisGradients(M, xref)
valSigma4e = RT0Element.evaluate(M, sigma, xref)
divSigma4e = RT0Element.evaluateDivergence(M, sigma, xref)
gradSigma4e = RT0Element.evaluateGradient(M, sigma, xref)
jumpSigma4f = ...
    RT0Element.evaluateJump(M, sigma, GP4ePlus, GP4eMinus)
```

```
val4e = S1Element.evaluateBasis(xref, nComp, nElem)
grads4e = S1Element.evaluateBasisGradients(M, xref, nComp)
valU4e = S1Element.evaluate(M, u, xref)
gradU4e = S1Element.evaluateGradient(M, u, xref)
jumpGradU4f = ...
    S1Element.evaluateGradientJump(M, u, GP4ePlus, GP4eMinus)
```

Dimension	Size	Meaning
1	`nComp`	components of the function (3 for $RT_0(\mathcal{T};\mathbb{R}^{3\times3})$)
2	1 or 3	components of the basis function (3 for RT_0)
3	`nBasis`	basis functions of the element (4 for RT_0)
4	`nElem`/`nFaces`	number of simplex or face
5	`nXref`	given points on the reference simplex for evaluation

Table A.2: Meaning of the dimensions of five-dimensional arrays returned by the point evaluations of the finite element classes in Section A.7.

The arguments read

- `M (MeshData)` – object providing geometric information
- `xref (array)` – list of points on the reference simplex, where the corresponding discrete function should be evaluated
- `nComp (integer)` – number of components of the discrete functions
- `GP4ePlus`, `GP4eMinus (arrays)` – Gauss points on the each face transformed to the corresponding point on the reference simplex for evaluation of the jumps; provided by the function `[GP4ePlus, GP4eMinus] = M.GaussPoints4jumps(GP2D)`

Given some point on the reference simplex, these functions provide a data structure that contains the evaluation of this point transformed to each of the simplices or faces of the triangulation. The returned values are five-dimensional arrays where each dimension has a specific meaning as displayed in Table A.2.

The class `P0FaceElement` provides the Π_0 projection from Section 3.4 on a given set of faces.

```
f0 = P0FaceElement.projection(M, fun, degree, faces)
```

This returns an array `f0` of the piecewise integral means of each component of the function. The arguments read

- `M (MeshData)` – object providing the geometric information
- `fun (function handle)` – function to project
- `degree (integer)` – determining the exactness of the employed quadrature rule
- `faces (array)` – numbers of the faces on which the function should be approximated, e.g., `M.NbFaces`

The same arguments allow for the computation of face oscillations from 2.20.

```
[osc, osc4f] = ...
    P0FaceElement.oscillation(M, fun, degree, faces)
```

The output variable `osc4f` contains the corresponding squared contribution on each of the faces.

The class `S1Element` also realises the computation of the Scott-Zhang quasi-interpolation operator for the approximation of the Dirichlet boundary data from Section 3.3.

```
u = S1Element.ScottZhang(M, fun, degree, interpNodes)
```

This provides an array `u` containing the coefficients of the S^1 function for each component. The arguments read

- `M (MeshData)` – object providing the geometric information
- `fun (function handle)` – function to interpolate
- `degree (integer)` – determining the exactness of the employed quadrature rule
- `interpNodes (array)` – numbers of the nodes in which the function should be interpolated, e.g., `M.DbNodes`

In order to compute the H^1 error of a Courant function $u_C \in S^1(\mathcal{T};\mathbb{R}^m)$ given by its coefficients `u` and a function $u \in H^1(\Omega;\mathbb{R}^m)$ given by the function handle `uExact`, utilise

```
[errL2, errL24e, errGrad, errGrad4e, errtime] = ...
    S1Element.error(M, u, uExact, gradUExact, degreeU)
```

The integer m refers to the number of components `nComp` in Table A.2. The variable `errtime` contains the elapsed time in seconds.

An analog function allows for the computation of the $H(\mathrm{div})$ error of a Raviart-Thomas function $\sigma_{RT} \in RT_0(\mathcal{T};\mathbb{R}^{m\times 3})$ given by its coefficients `sigma` and a function $\sigma \in H(\mathrm{div},\Omega;\mathbb{R}^{m\times 3})$ given by the function handle `sigmaExact`.

```
[errL2, errL24e, errDiv, errDiv4e, errtime] = ...
    RT0Element.error(M, sigma, sigmaExact, divSigmaExact, ...
                     degreeSigma)
```

A.8 ALSFEM functions

The solution of the LSFEM for the respective model problem is computed by the functions

```
[sigma, u, res4e, ndof, resDiv, resMat, condition, ...
    setupTime, solutionTime] = solveLinearElasticityLS(B, M)

[sigma, u, res4e, ndof, resDiv, resL2, condition, ...
    setupTime, solutionTime] = solvePoissonLS(B, M)

[sigma, u, res4e, ndof, resDiv, resDev, condition, ...
    setupTime, solutionTime] = solveStokesLS(B, M)
```

The arguments read

- `B (structure array)` – contains the benchmark information from Section A.3
- `M (MeshData)` – object providing the geometric information from Section A.5

The output consists of

- `sigma (array)` – coefficients of the solution σ_ℓ
- `u (array)` – coefficients of the solution u_ℓ
- `res4e (array)` – contribution $\|f + \operatorname{div}\sigma_\ell\|^2_{L^2(T)} + \|\mathcal{A}\sigma_\ell - \mathcal{S}\,\mathrm{D}\,u_\ell\|^2_{L^2(T)}$ to the least-squares functional $LS(f;\sigma_\ell,u_\ell)$ on each simplex T
- `ndof (integer)` – number of degrees of freedom
- `resDiv (float)` – contribution $\|f + \operatorname{div}\sigma_\ell\|_{L^2(\Omega)}$ to the least-squares functional $LS(f;\sigma_\ell,u_\ell)^{1/2}$
- `resMat / resL2 / resDev (float)` – contribution $\|\mathcal{A}\sigma_\ell - \mathcal{S}\,\mathrm{D}\,u_\ell\|_{L^2(\Omega)}$ to the least-squares functional $LS(f;\sigma_\ell,u_\ell)^{1/2}$ for one of the three model problems
- `condition (float)` – estimated conditional number of the linear system of equations
- `setupTime (float)` – elapsed time for the computation and assembling of the stiffness matrix (in seconds)
- `solutionTime (float)` – elapsed time for the solution of the linear system of equations (in seconds)

For the evaluation of the element-wise contributions to the alternative a posteriori error estimator utilise the functions

```
[eta, eta4e, estimatorTime, etaVol, etaJump, oscDb, oscNb, ...
    etaVol4e, etaJump4e, oscDb4e, oscNb4e] = ...
        estimateLinearElasticityLS(B, M, sigma, u)

[eta, eta4e, estimatorTime, etaVol, etaJump, oscDb, oscNb, ...
    etaVol4e, etaJump4e, oscDb4e, oscNb4e] = ...
        estimatePoissonLS(B, M, sigma, u)

[eta, eta4e, estimatorTime, etaVol, etaJump, oscDb, ...
    etaVol4e, etaJump4e, oscDb4e] = ...
        estimateStokesLS(B, M, sigma, u)
```

The additional arguments are the coefficients `sigma` and `u` from the `solve` functions above. The output variables read

- `eta (float)` – value of the alternative error estimator η_ℓ
- `eta4e (array)` – contribution $\eta_\ell^2(T)$ to the alternative error estimator η_ℓ on each simplex T
- `estimatorTime (float)` – elapsed time for the computation of the alternative error estimator η_ℓ (in seconds)
- `etaVol (float)` – volume contribution $\eta_{\mathrm{vol},\ell}$ to the alternative error estimator η_ℓ
- `etaJump (float)` – jump contribution $\eta_{\mathrm{jump},\ell}$ to the alternative error estimator η_ℓ
- `oscDb (float)` – value of the Dirichlet data oscillations $\operatorname{osc}(\mathrm{D}\, u_\mathrm{D}, \mathcal{F}(\Gamma_\mathrm{D}))$
- `oscNb (float)` – value of the Neumann data oscillations $\operatorname{osc}(t_\mathrm{N}, \mathcal{F}(\Gamma_\mathrm{N}))$
- `etaVol4e (array)` – contribution $\eta_{\mathrm{vol},\ell}^2(T)$ to the volume terms $\eta_{\mathrm{vol},\ell}$ on each simplex T
- `etaJump4e (array)` – contribution $\eta_{\mathrm{jump},\ell}^2(T)$ to the jump terms $\eta_{\mathrm{jump},\ell}$ on each simplex T
- `oscDb4e (array)` – contribution $|T|^{1/3}\|(1-\Pi_0)\,\mathrm{D}\, u_\mathrm{D}\|_{L^2(\partial T\cap\Gamma_\mathrm{D})}$ to the Dirichlet data oscillations $\operatorname{osc}(\mathrm{D}\, u_\mathrm{D}, \mathcal{F}(\Gamma_\mathrm{D}))$
- `oscNb4e (array)` – contribution $|T|^{1/3}\|(1-\Pi_0)t_\mathrm{N}\|_{L^2(\partial T\cap\Gamma_\mathrm{N})}$ to the Neumann data oscillations $\operatorname{osc}(t_\mathrm{N}, \mathcal{F}(\Gamma_\mathrm{N}))$

A.9 Plot functions

Several functions are included to display the computed results

- `plotConvergence(ndof4lvl, error4lvl, name)` – plots the errors of successive computations with respect to the numbers of degrees of freedom (ndof) in a double logarithmic scale; the optional `name` will be displayed in a legend
- `plotSurface(c4n, n4fBdr)` – draws a triangulation of the surface of a three-dimensional domain
- `plotDeformedDomain(c4n, n4fBdr, u4n, scaling)` – plots a deformed domain for the displacement `u4n` in the nodes; the displacement is scaled with the optional multiplicative factor `scaling`

The following functions are solely available in MATLAB

- `coneP1(c4n, u)` – draws an S^1 vector field using cones
- `plotTriangulation(c4n, n4e)` – plots the simplices of a triangulation
- `quiverP1(c4n, u)` – draws an S^1 vector field using arrows in the nodes of the triangulation
- `scatterP1(c4n, u)` – draws the values of an S^1 function in the nodes of the triangulation
- `sliceP1(c4n, u)` – draws the values of an S^1 function along slices through the domain
- `streamsliceP1(c4n, u)` – draws streamlines of an S^1 vector field along slices through the domain

The corresponding arguments read

- `ndof4lvl (array)` – number of degrees of freedom for each level of the adaptive computation
- `error4lvl (array)` – error value for each level of the adaptive computation
- `name (string)` – legend entry
- `c4n (array)` – coordinates of the nodes
- `n4fBdr (array)` – numbers of the nodes forming the boundary faces
- `u4n (array)` – displacement in each node
- `scaling (float)` – scaling factor for the displacement
- `n4e (array)` – numbers of the nodes of each simplex
- `u (array)` – coefficients of the solution u_ℓ

Figure A.2: List of files included in the octAFEM3D software package. The functions written in blue are taken from the software package AFEM [43]. The functions written in red are taken from [104].

Bibliography

[1] J. H. Adler, T. A. Manteuffel, S. F. McCormick, J. W. Nolting, J. W. Ruge, and L. Tang. Efficiency based adaptive local refinement for first-order system least-squares formulations. *SIAM J. Sci. Comput.*, 33(1):1–24, 2011.

[2] M. Ainsworth, J. Guzmán, and F.-J. Sayas. Discrete extension operators for mixed finite element spaces on locally refined meshes. *Math. Comp.*, 85(302):2639–2650, 2016.

[3] C. Amrouche, C. Bernardi, M. Dauge, and V. Girault. Vector potentials in three-dimensional non-smooth domains. *Math. Methods Appl. Sci.*, 21(9):823–864, 1998.

[4] M. Aurada, M. Feischl, J. Kemetmüller, M. Page, and D. Praetorius. Each $H^{1/2}$-stable projection yields convergence and quasi-optimality of adaptive FEM with inhomogeneous Dirichlet data in $\mathbb{R}^d$. *ESAIM Math. Model. Numer. Anal.*, 47(4):1207–1235, 2013.

[5] I. Babuška, A. Miller, and M. Vogelius. Adaptive methods and error estimation for elliptic problems of structural mechanics. In: *Adaptive computational methods for partial differential equations (College Park, Md., 1983)*, pages 57–73. SIAM, Philadelphia, PA, 1983.

[6] I. Babuška and W. C. Rheinboldt. Error estimates for adaptive finite element computations. *SIAM J. Numer. Anal.*, 15(4):736–754, 1978.

[7] S. Bartels, C. Carstensen, and G. Dolzmann. Inhomogeneous Dirichlet conditions in a priori and a posteriori finite element error analysis. *Numer. Math.*, 99(1):1–24, 2004.

[8] S. Bauer, P. Neff, D. Pauly, and G. Starke. Dev-Div- and DevSym-DevCurl-inequalities for incompatible square tensor fields with mixed boundary conditions. *ESAIM Control Optim. Calc. Var.*, 22(1):112–133, 2016.

[9] S. Bauer, D. Pauly, and M. Schomburg. The Maxwell compactness property in bounded weak Lipschitz domains with mixed boundary conditions. *SIAM J. Math. Anal.*, 48(4):2912–2943, 2016.

[10] M. Bebendorf. A note on the Poincaré inequality for convex domains. *Z. Anal. Anwendungen*, 22(4):751–756, 2003.

[11] R. Becker and S. Mao. An optimally convergent adaptive mixed finite element method. *Numer. Math.*, 111(1):35–54, 2008.

[12] M. Berndt, T. A. Manteuffel, and S. F. McCormick. Local error estimates and adaptive refinement for first-order system least squares (FOSLS). In: vol. 6, number Dec. Pages 35–43. 1997. Special issue on multilevel methods (Copper Mountain, CO, 1997).

[13] F. Bertrand, Z. Cai, and E. Y. Park. Least-squares methods for elasticity and Stokes equations with weakly imposed symmetry. *Comput. Methods Appl. Math.*, 19(3):415–430, 2019.

[14] P. Binev, W. Dahmen, and R. DeVore. Adaptive finite element methods with convergence rates. *Numer. Math.*, 97(2):219–268, 2004.

[15] P. Binev and R. DeVore. Fast computation in adaptive tree approximation. *Numer. Math.*, 97(2):193–217, 2004.

[16] P. B. Bochev and M. D. Gunzburger. Least-squares methods for the velocity-pressure-stress formulation of the Stokes equations. *Comput. Methods Appl. Mech. Engrg.*, 126(3-4):267–287, 1995.

[17] P. B. Bochev and M. D. Gunzburger. *Least-squares finite element methods*, vol. 166 of *Applied Mathematical Sciences*. Springer, New York, 2009, pages xxii+660.

[18] D. Boffi, F. Brezzi, and M. Fortin. *Mixed finite element methods and applications*, vol. 44 of *Springer Series in Computational Mathematics*. Springer, Heidelberg, 2013, pages xiv+685.

[19] D. Braess. *Finite elements*. Cambridge University Press, Cambridge, third edition, 2007, pages xviii+365. Theory, fast solvers, and applications in elasticity theory.

[20] J. H. Bramble and A. H. Schatz. Least squares methods for 2*m*th order elliptic boundary-value problems. *Math. Comp.*, 25:1–32, 1971.

[21] J. H. Bramble and A. H. Schatz. Rayleigh-Ritz-Galerkin methods for Dirichlet's problem using subspaces without boundary conditions. *Comm. Pure Appl. Math.*, 23:653–675, 1970.

[22] J. Brandts, Y. Chen, and J. Yang. A note on least-squares mixed finite elements in relation to standard and mixed finite elements. *IMA J. Numer. Anal.*, 26(4):779–789, 2006.

[23] S. C. Brenner and L. R. Scott. *The mathematical theory of finite element methods*, vol. 15 of *Texts in Applied Mathematics*. Springer, New York, third edition, 2008, pages xviii+397.

[24] H. Brezis. *Functional analysis, Sobolev spaces and partial differential equations*. Universitext. Springer, New York, 2011, pages xiv+599.

[25] P. Bringmann and C. Carstensen. *h*-adaptive least-squares finite element methods for the 2D Stokes equations of any order with optimal convergence rates. *Comput. Math. Appl.*, 74(8):1923–1939, 2017.

[26] P. Bringmann and C. Carstensen. An adaptive least-squares FEM for the Stokes equations with optimal convergence rates. *Numer. Math.*, 135(2):459–492, 2017.

[27] P. Bringmann, C. Carstensen, and G. Starke. An adaptive least-squares FEM for linear elasticity with optimal convergence rates. *SIAM J. Numer. Anal.*, 56(1):428–447, 2018.

[28] A. Buffa, M. Costabel, and D. Sheen. On traces for $\mathbf{H}(\mathbf{curl}, \Omega)$ in Lipschitz domains. *J. Math. Anal. Appl.*, 276(2):845–867, 2002.

[29] Z. Cai, T. A. Manteuffel, and S. F. McCormick. First-order system least squares for the Stokes equations, with application to linear elasticity. *SIAM J. Numer. Anal.*, 34(5):1727–1741, 1997.

[30] Z. Cai, V. Carey, J. Ku, and E.-J. Park. Asymptotically exact a posteriori error estimators for first-order div least-squares methods in local and global L_2 norm. *Comput. Math. Appl.*, 70(4):648–659, 2015.

[31] Z. Cai, J. Korsawe, and G. Starke. An adaptive least squares mixed finite element method for the stress-displacement formulation of linear elasticity. *Numer. Methods Partial Differential Equations*, 21(1):132–148, 2005.

[32] Z. Cai, B. Lee, and P. Wang. Least-squares methods for incompressible Newtonian fluid flow: linear stationary problems. *SIAM J. Numer. Anal.*, 42(2):843–859, 2004.

[33] Z. Cai and G. Starke. First-order system least squares for the stress-displacement formulation: linear elasticity. *SIAM J. Numer. Anal.*, 41(2):715–730, 2003.

[34] Z. Cai and G. Starke. Least-squares methods for linear elasticity. *SIAM J. Numer. Anal.*, 42(2):826–842, 2004.

[35] C. Carstensen, P. Bringmann, F. Hellwig, and P. Wriggers. Nonlinear discontinuous Petrov-Galerkin methods. *Numer. Math.*, 139(3):529–561, 2018.

[36] C. Carstensen, L. Demkowicz, and J. Gopalakrishnan. Breaking spaces and forms for the DPG method and applications including Maxwell equations. *Comput. Math. Appl.*, 72(3):494–522, 2016.

[37] C. Carstensen, M. Feischl, M. Page, and D. Praetorius. Axioms of adaptivity. *Comput. Math. Appl.*, 67(6):1195–1253, 2014.

[38] C. Carstensen, D. Gallistl, and M. Schedensack. L^2 best approximation of the elastic stress in the Arnold-Winther FEM. *IMA J. Numer. Anal.*, 36(3):1096–1119, 2016.

[39] C. Carstensen, M. Maischak, and E. P. Stephan. A posteriori error estimate and h-adaptive algorithm on surfaces for Symm's integral equation. *Numer. Math.*, 90(2):197–213, 2001.

[40] C. Carstensen and H. Rabus. Axioms of adaptivity with separate marking for data resolution. *SIAM J. Numer. Anal.*, 55(6):2644–2665, 2017.

[41] C. Carstensen. Collective marking for adaptive least-squares finite element methods with optimal rates. *Math. Comp.*, 89(321):89–103, 2020.

[42] C. Carstensen and F. Hellwig. Constants in discrete Poincaré and Friedrichs inequalities and discrete quasi-interpolation. *Comput. Methods Appl. Math.*, 18(3):433–450, 2018.

[43] C. Carstensen and Numerical Analysis Group. AFEM. Unpublished MATLAB software package, 2009.

[44] C. Carstensen and E.-J. Park. Convergence and optimality of adaptive least squares finite element methods. *SIAM J. Numer. Anal.*, 53(1):43–62, 2015.

[45] C. Carstensen, E.-J. Park, and P. Bringmann. Convergence of natural adaptive least squares finite element methods. *Numer. Math.*, 136(4):1097–1115, 2017.

[46] C. Carstensen and H. Rabus. An optimal adaptive mixed finite element method. *Math. Comp.*, 80(274):649–667, 2011.

[47] C. Carstensen and J. Storn. Asymptotic exactness of the least-squares finite element residual. *SIAM J. Numer. Anal.*, 56(4):2008–2028, 2018.

[48] J. M. Cascon, C. Kreuzer, R. H. Nochetto, and K. G. Siebert. Quasi-optimal convergence rate for an adaptive finite element method. *SIAM J. Numer. Anal.*, 46(5):2524–2550, 2008.

[49] S. N. Chandler-Wilde, I. G. Graham, S. Langdon, and E. A. Spence. Numerical-asymptotic boundary integral methods in high-frequency acoustic scattering. *Acta Numer.*, 21:89–305, 2012.

[50] C. L. Chang and J. J. Nelson. Least-squares finite element method for the Stokes problem with zero residual of mass conservation. *SIAM J. Numer. Anal.*, 34(2):480–489, 1997.

[51] P. G. Ciarlet. *The finite element method for elliptic problems*. North-Holland Publishing Co., Amsterdam-New York-Oxford, 1978, pages xix+530. Studies in Mathematics and its Applications, Vol. 4.

[52] P. G. Ciarlet. *Mathematical elasticity. Vol. I*, vol. 20 of *Studies in Mathematics and its Applications*. North-Holland Publishing Co., Amsterdam, 1988, pages xlii+451. Three-dimensional elasticity.

[53] R. D. Cook. Improved two-dimensional finite element. *J. Struct. Div.-ASCE*, 100(9):1851–1863, 1974.

[54] M. Dauge. Neumann and mixed problems on curvilinear polyhedra. *Integral Equations Operator Theory*, 15(2):227–261, 1992.

[55] L. Demkowicz and J. Gopalakrishnan. A class of discontinuous Petrov-Galerkin methods. Part I: the transport equation. *Comput. Methods Appl. Mech. Engrg.*, 199(23-24):1558–1572, 2010.

[56] L. Demkowicz and J. Gopalakrishnan. A class of discontinuous Petrov-Galerkin methods. II. Optimal test functions. *Numer. Methods Partial Differential Equations*, 27(1):70–105, 2011.

[57] L. Demkowicz, J. Gopalakrishnan, and A. H. Niemi. A class of discontinuous Petrov-Galerkin methods. Part III: Adaptivity. *Appl. Numer. Math.*, 62(4):396–427, 2012.

[58] D. A. Di Pietro and A. Ern. *Mathematical aspects of discontinuous Galerkin methods*, vol. 69 of *Mathématiques & Applications (Berlin) [Mathematics & Applications]*. Springer, Heidelberg, 2012, pages xviii+384.

[59] W. Dörfler. A convergent adaptive algorithm for Poisson's equation. *SIAM J. Numer. Anal.*, 33(3):1106–1124, 1996.

[60] A. Ern and J.-L. Guermond. *Theory and practice of finite elements*, vol. 159 of *Applied Mathematical Sciences*. Springer-Verlag, New York, 2004, pages xiv+524.

[61] L. C. Evans and R. F. Gariepy. *Measure theory and fine properties of functions*. Textbooks in Mathematics. CRC Press, Boca Raton, FL, revised edition, 2015, pages xiv+299.

[62] M. Feischl, T. Führer, M. Karkulik, J. M. Melenk, and D. Praetorius. Quasi-optimal convergence rates for adaptive boundary element methods with data approximation, part I: weakly-singular integral equation. *Calcolo*, 51(4):531–562, 2014.

[63] G. Fichera. *Numerical and quantitative analysis*, vol. 3 of *Surveys and Reference Works in Mathematics*. Pitman (Advanced Publishing Program), Boston, Mass.-London, 1978, pages x+208. Translated from the Italian by Sandro Graffi.

[64] D. Gallistl, M. Schedensack, and R. P. Stevenson. A remark on newest vertex bisection in any space dimension. *Comput. Methods Appl. Math.*, 14(3):317–320, 2014.

[65] V. Girault and P.-A. Raviart. *Finite element methods for Navier-Stokes equations*, vol. 5 of *Springer Series in Computational Mathematics*. Springer-Verlag, Berlin, 1986, pages x+374. Theory and algorithms.

[66] V. Gol'dshtein, I. Mitrea, and M. Mitrea. Hodge decompositions with mixed boundary conditions and applications to partial differential equations on Lipschitz manifolds. *J. Math. Sci. (N.Y.)*, 172(3):347–400, 2011. Problems in mathematical analysis. No. 52.

[67] J. Gopalakrishnan and W. Qiu. Partial expansion of a Lipschitz domain and some applications. *Front. Math. China*, 7(2):249–272, 2012.

[68] F. Hellwig. Adaptive Discontinuous Petrov-Galerkin Finite-Element-Methods. *PhD thesis*, 2018. Humboldt-Universität zu Berlin.

[69] R. Hiptmair. Finite elements in computational electromagnetism. *Acta Numer.*, 11:237–339, 2002.

[70] R. Hiptmair and C. Pechstein. Discrete Regular Decompositions of Tetrahedral Discrete 1-Forms. Technical report 2017-47, Seminar for Applied Mathematics, ETH Zürich, Switzerland, 2017.

[71] D. C. Jespersen. A least squares decomposition method for solving elliptic equations. *Math. Comp.*, 31(140):873–880, 1977.

[72] B.-N. Jiang and C. L. Chang. Least-squares finite elements for the Stokes problem. *Comput. Methods Appl. Mech. Engrg.*, 78(3):297–311, 1990.

[73] F. Jochmann. Regularity of weak solutions of Maxwell's equations with mixed boundary-conditions. *Math. Methods Appl. Sci.*, 22(14):1255–1274, 1999.

[74] M. Karkulik, G. Of, and D. Praetorius. Convergence of adaptive 3D BEM for weakly singular integral equations based on isotropic mesh-refinement. *Numer. Methods Partial Differential Equations*, 29(6):2081–2106, 2013.

[75] S. D. Kim, T. A. Manteuffel, and S. F. McCormick. First-order system least squares (FOSLS) for spatial linear elasticity: pure traction. *SIAM J. Numer. Anal.*, 38(5):1454–1482, 2000.

[76] J. Ku and E.-J. Park. A posteriori error estimators for the first-order least-squares finite element method. *J. Comput. Appl. Math.*, 235(1):293–300, 2010.

[77] M. W. Licht. Smoothed projections and mixed boundary conditions. *Math. Comp.*, 88(316):607–635, 2019.

[78] M. W. Licht. Smoothed projections over weakly Lipschitz domains. *Math. Comp.*, 88(315):179–210, 2019.

[79] J.-L. Lions and E. Magenes. *Non-homogeneous boundary value problems and applications. Vol. I.* Springer-Verlag, New York-Heidelberg, 1972, pages xvi+357. Translated from the French by P. Kenneth, Die Grundlehren der mathematischen Wissenschaften, Band 181.

[80] P. P. Lynn and S. K. Arya. Use of the least squares criterion in the finite element formulation. *Internat. J. Numer. Methods Engrg.*, 6:75–88, 1973.

[81] J. M. Maubach. Local bisection refinement for n-simplicial grids generated by reflection. *SIAM J. Sci. Comput.*, 16(1):210–227, 1995.

[82] W. McLean. *Strongly elliptic systems and boundary integral equations*. Cambridge University Press, Cambridge, 2000, pages xiv+357.

[83] P. Monk. *Finite element methods for Maxwell's equations*. Numerical Mathematics and Scientific Computation. Oxford University Press, New York, 2003, pages xiv+450.

[84] P. Morin, R. H. Nochetto, and K. G. Siebert. Data oscillation and convergence of adaptive FEM. *SIAM J. Numer. Anal.*, 38(2):466–488, 2000.

[85] J. Nečas. *Direct methods in the theory of elliptic equations*. Springer Monographs in Mathematics. Springer, Heidelberg, 2012, pages xvi+372. Translated from the 1967 French original by Gerard Tronel and Alois Kufner, Editorial coordination and preface by Šárka Nečasová and a contribution by Christian G. Simader.

[86] J.-C. Nédélec. Mixed finite elements in $\mathbf{R}^3$. *Numer. Math.*, 35(3):315–341, 1980.

[87] J.-C. Nédélec. Éléments finis mixtes incompressibles pour l'équation de Stokes dans $\mathbf{R}^3$. *Numer. Math.*, 39(1):97–112, 1982.

[88] L. E. Payne and H. F. Weinberger. An optimal Poincaré inequality for convex domains. *Arch. Rational Mech. Anal.*, 5:286–292 (1960), 1960.

[89] A. I. Pehlivanov, G. F. Carey, and R. D. Lazarov. Least-squares mixed finite elements for second-order elliptic problems. *SIAM J. Numer. Anal.*, 31(5):1368–1377, 1994.

[90] H. Rabus. On the quasi-optimal convergence of adaptive nonconforming finite element methods in three examples. *PhD thesis*, 2014. Humboldt-Universität zu Berlin.

[91] P.-A. Raviart and J. M. Thomas. A mixed finite element method for 2nd order elliptic problems. In:*Mathematical aspects of finite element methods (Proc. Conf., Consiglio Naz. delle Ricerche (C.N.R.), Rome, 1975)*, 292–315. Lecture Notes in Math., Vol. 606, 1977.

[92] R. Sacchi and A. Veeser. Locally efficient and reliable a posteriori error estimators for Dirichlet problems. *Math. Models Methods Appl. Sci.*, 16(3):319–346, 2006.

[93] J. Schöberl. A posteriori error estimates for Maxwell equations. *Math. Comp.*, 77(262):633–649, 2008.

[94] A. Schwarz, J. Schröder, and G. Starke. A modified least-squares mixed finite element with improved momentum balance. *Internat. J. Numer. Methods Engrg.*, 81(3):286–306, 2010.

[95] A. Schwarz, K. Steeger, and J. Schröder. Weighted overconstrained least-squares mixed finite elements for static and dynamic problems in quasi-incompressible elasticity. *Comput. Mech.*, 54(3):603–612, 2014.

[96] L. R. Scott and S. Zhang. Finite element interpolation of nonsmooth functions satisfying boundary conditions. *Math. Comp.*, 54(190):483–493, 1990.

[97] G. Starke. An adaptive least-squares mixed finite element method for elastoplasticity. *SIAM J. Numer. Anal.*, 45(1):371–388, 2007.

[98] G. Starke, A. Schwarz, and J. Schröder. Analysis of a modified first-order system least squares method for linear elasticity with improved momentum balance. *SIAM J. Numer. Anal.*, 49(3):1006–1022, 2011.

[99] E. M. Stein. *Singular integrals and differentiability properties of functions*. Princeton Mathematical Series, No. 30. Princeton University Press, Princeton, N.J., 1970, pages xiv+290.

[100] R. Stevenson. Optimality of a standard adaptive finite element method. *Found. Comput. Math.*, 7(2):245–269, 2007.

[101] R. Stevenson. The completion of locally refined simplicial partitions created by bisection. *Math. Comp.*, 77(261):227–241, 2008.

[102] J. Storn. On a relation of discontinuous Petrov-Galerkin and least-squares finite element methods. Submitted, 2019.

[103] J. Storn. Topics in Least-Squares and Discontinuous Petrov-Galerkin Finite Element Analysis. *PhD thesis*, 2019. Humboldt-Universität zu Berlin.

[104] C. T. Traxler. An algorithm for adaptive mesh refinement in n dimensions. *Computing*, 59(2):115–137, 1997.

[105] R. Verfürth. A posteriori error estimators for the Stokes equations. *Numer. Math.*, 55(3):309–325, 1989.

[106] L. Zhong, L. Chen, S. Shu, G. Wittum, and J. Xu. Convergence and optimality of adaptive edge FEMs for time-harmonic Maxwell equations. *Math. Comp.*, 81(278):623–642, 2012.

[107] O. C. Zienkiewicz and J. Z. Zhu. A simple error estimator and adaptive procedure for practical engineering analysis. *Internat. J. Numer. Methods Engrg.*, 24(2):337–357, 1987.

[108] J. Zitelli, I. Muga, L. Demkowicz, J. Gopalakrishnan, D. Pardo, and V. M. Calo. A class of discontinuous Petrov-Galerkin methods. Part IV: the optimal test norm and time-harmonic wave propagation in 1D. *J. Comput. Phys.*, 230(7):2406–2432, 2011.

List of Figures

Selbständigkeitserklärung

Ich erkläre, dass ich die Dissertation selbstständig und nur unter Verwendung der von mir gemäß §7 Abs. 3 der Promotionsordnung der Mathematisch-Naturwissenschaftlichen Fakultät, veröffentlicht im Amtlichen Mitteilungsblatt der Humboldt-Universität zu Berlin Nr. 42/2018 am 11.07.2018 angegebenen Hilfsmittel angefertigt habe.

Philipp Bringmann, Berlin, 01. Oktober 2019